ELEC 5606
Phase-Locked Loops
And
Receiver Synchronizers

Lecture Notes

Jim Wight
Department of Electronics
Carleton University

Phase-Locked Loops

1. Working Principles

Application List (Motivation)

- Tracking Filter
- Frequency Demodulation
- Phase Demodulation
- Phase Modulation
- Frequency Synthesis
- Carrier Recovery
- Clock Recovery

- a PLL is a device in which the phase of a frequency modulated oscillator is obliged to follow that of an input signal.

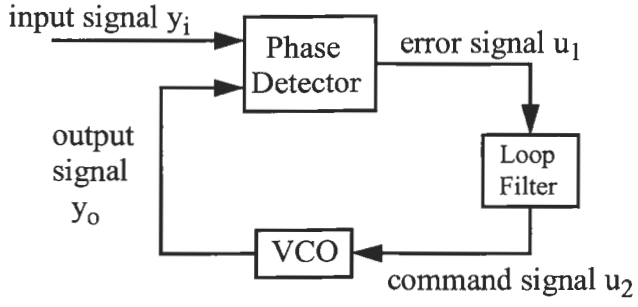

note: u_1 is a function of the phase difference between the two applied signals.

operation

- suppose the loop is unlocked and

$$y_i(t) = A\cos(\omega_i t + \theta_i)$$

$$y_o(t) = B\cos(\omega_o t + \phi_o)$$

- in general, $\omega_i \neq \omega_o$

- If the phase detector has a sinusoidal characteristic

$$u_1 = K_1 \cos[(\omega_i - \omega_o)t + \theta_i - \phi_o] \qquad -(1)$$

note: $u_1(t)$ is a sinusoid of freq. equal to the difference between ω_i and ω_o.

- at a given instant, u_2 is applied to the VCO input.

- If $\omega_i - \omega_o$ does not exceed a certain value, then after a certain time, y_o will become synchronous with y_i.

$$y_o(t) = B\cos(\omega_i t + \psi_o)$$

- in other words

$$\phi_o = (\omega_i - \omega_o)t + \psi_o \qquad -(2)$$

- and the phase detector output (error) signal becomes DC.

$$u_1 = K_1\cos(\theta_i - \psi_o) \qquad -(3)$$

The loop filters are always LPF

- consequently, the command signal is:

$$u_2 = u_1 = K_1\cos(\theta_i - \psi_o)$$

- Now the VCO instantaneous freq., ω_{inst} is a linear function of the command signal near the central freq. ω_o

$$\omega_{inst} = \frac{d}{dt}(\omega_o t + \phi_o) = \omega_o + K_3 u_2$$

$$\therefore \quad \frac{d\phi}{dt} = K_3 u_2 \qquad -(4)$$

Note: K_3 is called the modulation sensitivity and has units of (rad/sec/volt).

- inserting (2) and (3) into (4) gives:

$$\omega_i - \omega_o = K_1 K_3\cos(\theta_i - \psi_o)$$

or

$$\psi_o = \theta_i - \cos^{-1}\left(\frac{\omega_i - \omega_o}{K_1 K_3}\right) \qquad -(5)$$

$$u_1 = \frac{\omega_i - \omega_o}{K_3} \qquad -(6)$$

Recapitulate

- After the loop has locked onto y_i, the signals y_i and y_o have the same frequency ω_i but a difference in phase $(\theta_i - \psi_o)$ given by (5).

- This difference in phase produces in the phase detector output a DC component that passes the LPF and is supplied to the VCO modulation input.

$$u_2 = u_1 = \frac{\omega_i - \omega_o}{K_3}$$

- from this equation we see that by means of the DC signal u_2, the VCO frequency changes from ω_o to ω_i.

$$\begin{aligned} \omega_{inst} &= \omega_o + K_3 u_2 \\ &= \omega_o + \omega_i - \omega_o \\ &= \omega_i \end{aligned}$$

Note: if the initial frequency difference $\omega_i - \omega_o \ll K_1 K_3$ then (5) becomes:

$$\theta_i - \psi_o \approx \cos^{-1}(0) \approx \pm\pi/2$$

- consequently, the VCO is near phase quadrature with the input signal for small $\omega_i - \omega_o$.

- Hence, we usually use the new notation, θ_o where:

$$\theta_o = \psi_o \pm \pi/2$$

$\cos(\alpha \pm 90) = \pm \sin(\alpha)$

so that

$$u_1 = K_1 \cos(\theta_i - \psi_o) = K_1 \sin(\theta_i - \theta_o)$$

K_1 represents the phase detector sensitivity (V/rad).

- using θ_o in place of ψ_o yields (5) in the form:

$$\theta_i - \theta_o = \sin^{-1}\left(\frac{\omega_i - \omega_o}{K_1 K_3}\right) \qquad -(7)$$

- (7) lets us see some of the conditions for which the loop functions.

- consider a loop in lock, for which we gradually deviate ω_i from the VCO freq. ω_o.

- When $\left|\frac{\omega_i - \omega_o}{K_1 K_3}\right| > 1$, a solution for θ_o can no longer be found from (7).

- Hence, the loop falls out of lock, and the VCO frequency returns to ω_o.

- Here the phase detector is no longer able to produce a DC component necessary to maintain synchronism.

- for phase detectors of the sinusoidal type, the limits within which synchronization is possible range from:

$$(\omega_o - K) \text{ to } (\omega_o + K) \text{ where } K = K_1 K_3$$

- The range for ω_i is dependent on the type of phase detector used.

- Example p.7, Blanchard.

2. Loop Components

- 3 elements of PLL are
  - phase detectors
  - loop filters
  - VCO

1 -Phase Detectors

- 2 categories
  - sinusoidal signal phase detectors
  - square signal phase detectors

  (Here the sq. signal may be the original signal or produced by hard limiting)

- when the signals are sinusoidal, the phase detector can be a 2 or 4 diode bridge (or an analog multiplier if the frequency response allows it) and the phase detector has a sinusoidal characteristic.

- when the waveform is square, diode bridges or logic circuits can be used and the phase detector has a triangular characteristic $(0, \pi)$ or a sawtooth characteristic $(0, 2\pi)$.

Two Diode Phase Detector(Only second circuit will be discussed here)

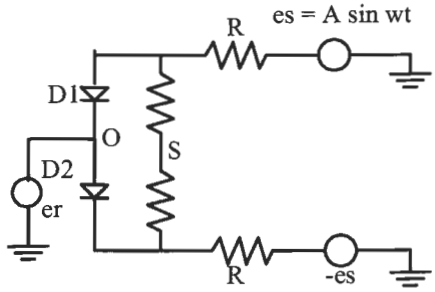

Circuit No. 1

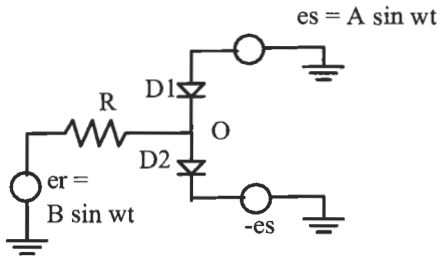

Circuit No. 2

- here internal resistance of e_s and $-e_s$ is assumed zero, and diode on-resistance is ρ.

- calculate the voltage at O

- there are 4 cases

Case I D1 and D2 do not conduct

$$e_s < v_o, \qquad -e_s > v_o$$

$$\text{then } v_o = e_r$$

and the conditions become

$$e_s < e_r, \qquad -e_s > e_r$$

Case 2 D1 conducts, D2 does not conduct

$$e_s \geq v_o, \qquad -e_s > v_o$$

$$\therefore \quad v_o = \frac{Re_s + \rho e_r}{R + \rho}$$

and the conditions become

$$e_s \geq e_r, \qquad -e_s > \frac{\rho}{2R + \rho} e_r$$

Case 3 D1 does not conduct, D2 conducts
similar to Case 2

$$e_s < \frac{\rho}{2R + \rho} e_r, \qquad -e_s \leq e_r$$

Case 4 D1 and D2 conduct

$$e_s \geq v_o, \qquad -e_s \leq v_o$$
$$\therefore \quad v_o = \frac{\rho e_r}{2R + \rho}$$

and the conditions become

$$e_s \geq \frac{\rho}{2R + \rho} e_r, \qquad -e_s \leq \frac{\rho}{2R + \rho} e_r$$

- if $\rho \ll R$, the four cases can be summarized in the table:

Case	Diode D1	Diode D2	Limit Conditions	v_O
(1)	No conduct	No conduct	$e_R > e_S$ and $e_R < -e_S$	e_R
(2)	Conducting	No conduct	$e_R \leq e_S$ and $-e_S > 0$	e_S
(3)	No conduct	Conducting	$e_S < 0$ and $e_R \geq -e_S$	$-e_S$
(4)	Conducting	Conducting	$e_S \geq 0$ (and $-e_S \leq 0$)	0

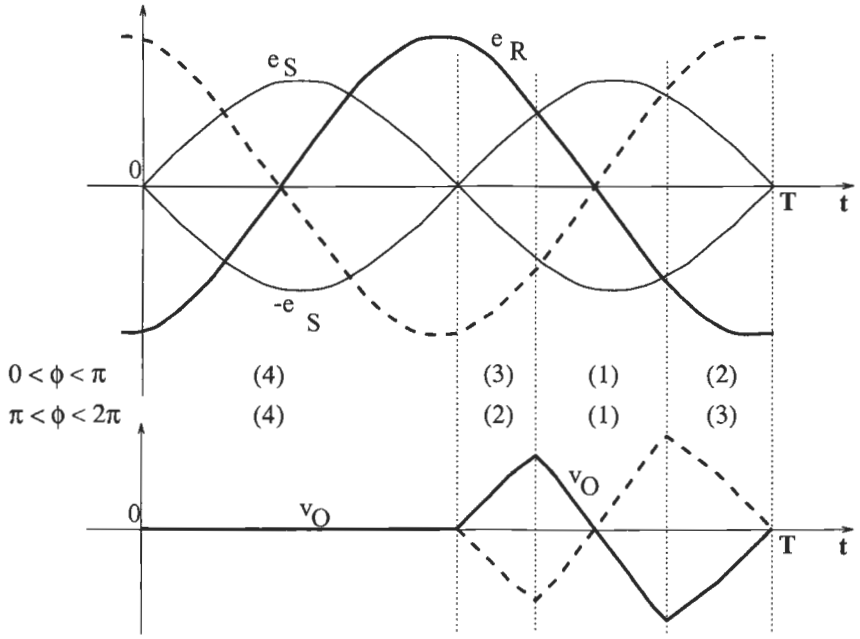

FIGURE 2.6. Limit conditions for the D1 and D2 diode conduction and waveforms in the second type phase detector.

- Unbroken lines in the fig. represent $0 < \phi < \pi$

- broken lines represent $\pi < \phi < 2\pi$

- the signal at O is a complicated function of time but put through a LPF and the DC component extracted, we have for:

Case I A = B

$$\overline{v_o} = \begin{cases} -\frac{\sqrt{2}}{\pi} A \cos\left(\frac{\phi}{2} + \frac{\pi}{4}\right), & 0 < \phi < \pi \\ \frac{\sqrt{2}}{\pi} A \cos\left(\frac{\phi}{2} - \frac{\pi}{4}\right), & \pi < \phi < 2\pi \end{cases}$$

Case II $A \ll B$

Here we get

$$\overline{v_o} = -\frac{A}{\pi} \cos\phi$$

Note: these results are identical within the sign for the DC from the first circuit (shown in Blanchard).

Advantages of the second circuit over the first

- here R is in series with the generator required to produce high amplitude signals (e_r).

- the impedance of e_s and $-e_s$ must be small but this is not too difficult for low amplitude signals.

- amplitude at O for second cct is far smaller than amplitude at S of first cct. Consequently it is easier to use a buffer amplifier to extract signal at O.

Four Diode Phase Detector

- The waveform v_o from last cct had half its period when $v_o = 0$.

- If over this time slot, we substituted a signal identical with the part which is not null, we would obtain a waveform which more closely approximately a sinusoid of twice the applied frequency.

- This behaviour would be closer to that of an analog multiplier.

Note: since potential at A and A' are independent of conduction conditions of diodes, the LHS and RHS of the cct are independent.

- now the LHS is identical to previous cct.

- also, RHS is same as LHS except for direction of diodes

- the four cases are shown in the diagram:

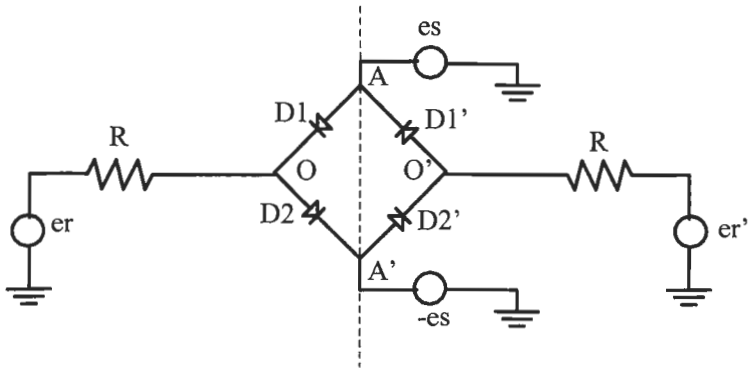

Ring Modulator

Diode D1'	Diode D2'	Limit Conditions	$v_{O'}$
No conduct	No conduct	$e_R < e_S$ and $e_R > -e_S$	e_R
Conducting	No conduct	$e_R \geq e_S$ and $-e_S < 0$	e_S
No conduct	Conducting	$e_S > 0$ and $e_R \leq -e_S$	$-e_S$
Conducting	Conducting	$e_S \leq 0$ (and $-e_S \geq 0$)	0

The limit conditions for the diodes D1 and D2 and for vo are given in the Table of Figure 2.6.

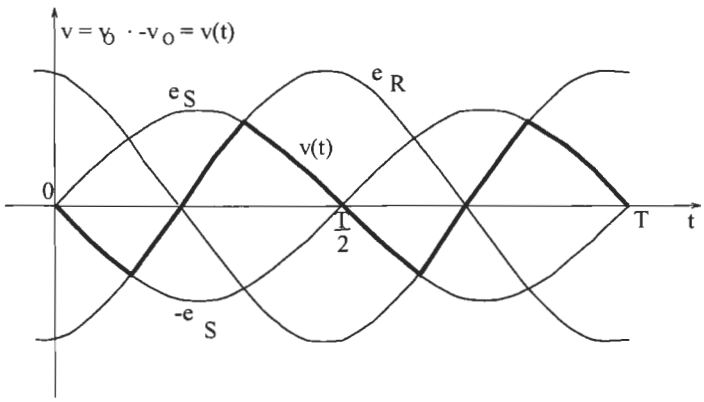

FIGURE 2.6. Limit conditions for the D1' and D2' diode conduction and waveforms in a four-diode phase detector (before filtering)..

- we get the above fig. if e_s and e_r are sinusoids.

Note: $v(t)$ has a period $T/2$ and consequently has no spectrum component freq. of e_s and e_r.

- the DC component is

$$\overline{v} = \overline{v_o}' - \overline{v_o}, \quad \text{but} \quad \overline{v_o}' = -\overline{v_o}$$

$$\therefore \quad \overline{v} = -2\overline{v_o}$$

Note: twice the amplitude compared to 2 diode detector

- also $\overline{v} = \frac{2A}{\pi}\cos\phi, \quad B \gg A$

- the 4 diode produces the signal shown for $B \gg A$.

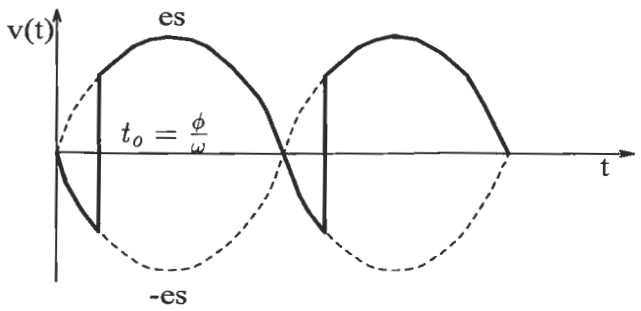

Note: this is identical as output from the following cct:

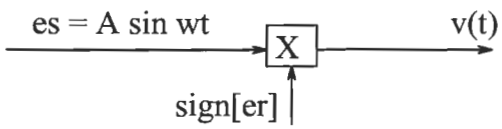

Analog Multiplier

- the above diode detectors have difficulties with

  -perfect diodes do not exist, at high freq, the diodes have spurious cap effects, diodes are not perfect matches

  - generators - do not supply perfect sine wave, internal impedance must be low

  - difficult to obtain e_s and $-e_s$ in phase opposition with equal amplitude

- alternative is to use analog multiplier (when freq. is not too high) such as Gilbert Cell.

- Note: recall difficulty of design for large dynamic range of inputs.

Linear Phase Detectors - Triangle Characteristics

Note: the previous phase detectors had sinusoid or truncated sinusoid characteristics.

- desirable to have linear characteristics (const. slope) over certain interval of phase.

- easy to construct if signals are sq. waves or can be transformed to sq. waves.

- consider the 4 diode detector. We have seen that if e_r is square and its amplitude exceeds e_s, we get

$$v(t) = e_s \text{ sign}[e_r]$$

- if e_s is also sq. wave $\Longrightarrow e_s = A \text{ sign}[e_s]$

$$v(t) = A \text{ sign}[e_s] \text{ sign}[e_r]$$

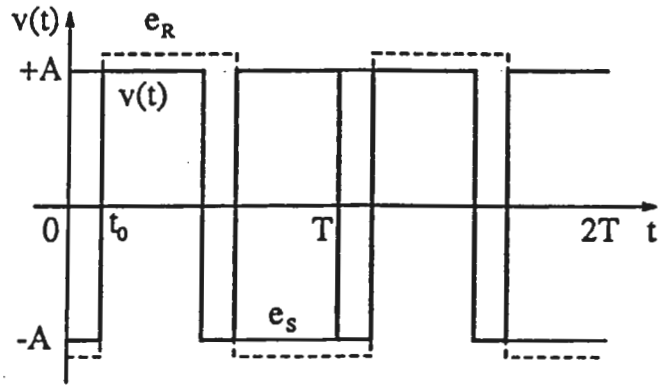

- we can use the term phase difference for the quantity $\phi = \omega t_o$ where t_o is the delay of e_r compared to e_s.

- to find the DC term for $v(t)$

$$\overline{v}(t) = \frac{1}{T}\int_0^T v(t)dt$$

$$\overline{v}(t) = \begin{cases} \frac{2A}{\pi}\left(\frac{\pi}{2} - \phi\right) ; & 0 < \phi < \pi \\ \frac{2A}{\pi}\left(\phi - \frac{3\pi}{2}\right) ; & \pi < \phi < 2\pi \end{cases}$$

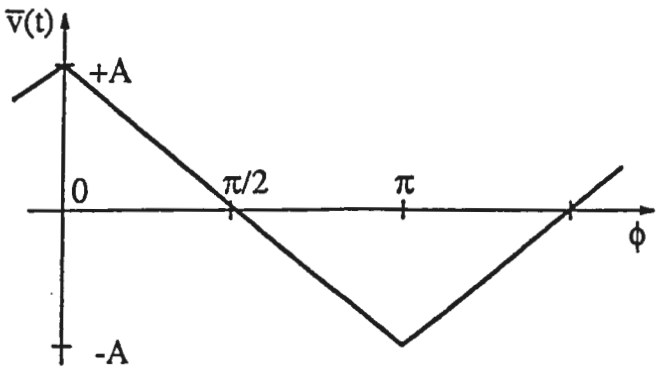

The detector sensitivity is

$$K_1 = \frac{2A}{\pi}$$

An easier method than the 4 diode detector is to use logic circuits. let

$e_s = +A \implies e_s$ is 1

$e_s = -A \implies e_s$ is 0

$e_{fR} = +B \implies e_r$ is 1

$e_{fR} = -B \implies e_r$ is 0

Desired truth table is

e_S	e_R	e_0
0	0	1
0	1	0
1	0	0
1	1	1

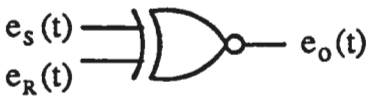

Note: $\overline{v_o}(t)$ must be extracted from $v_o(t)$ by LPF

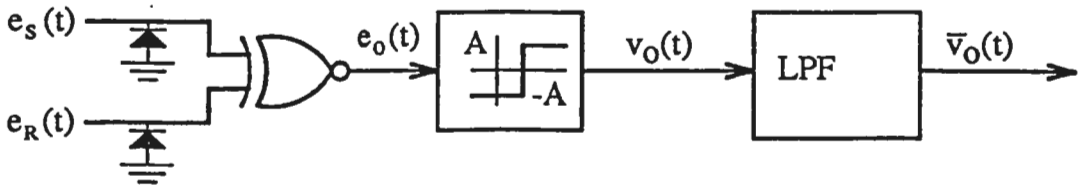

Note: also easy to obtain linear phase comparator characteristic over interval $(0, \pi)$ by using an AND cct - even though the operation sign$[e_s]$ sign$[e_r]$ does not take place.

- the AND cct phase detector has half the sensitivity of the EX-OR cct and is centered about $-A/2$ rather than zero.

Linear Phase Detector - Sawtooth Characteristic

$$\overline{v} = \frac{1}{T}\int_0^T v(t)dt = \frac{A}{\pi}(\phi - \pi)$$

$$\therefore \; K_1 = \frac{A}{\pi}$$

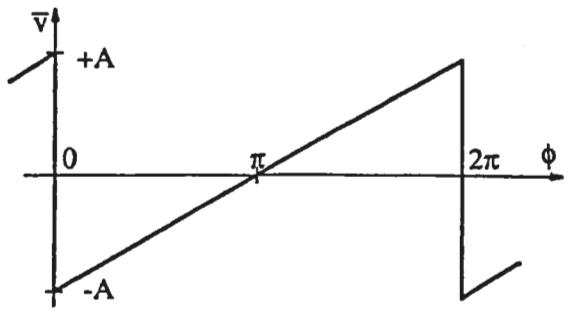

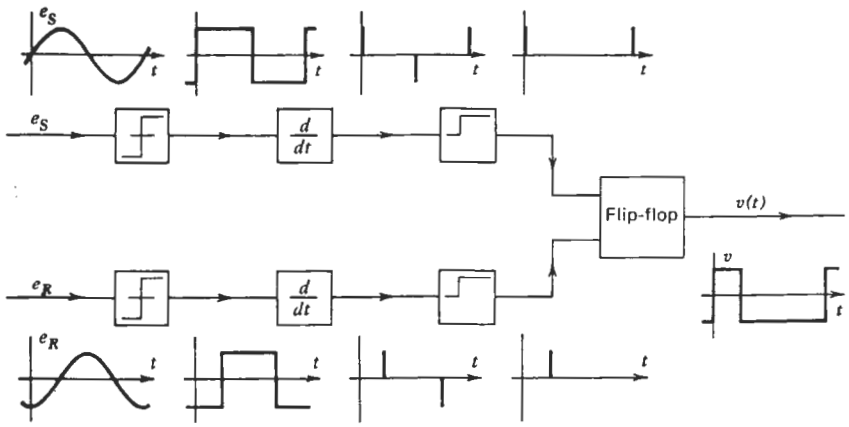

FIGURE 2.16. Circuits and waveforms in a linear over $(0, 2\pi)$ phase detector.

Frequency Modulated Oscillator (Voltage-Controlled Oscillator - VCO)

required properties

- good central freq. stability

- high modulation sensitivity, K_3 (rad/sec/V). These 2 conditions are contradictory and to achieve good stability, often an opamp amplifier must be introduced before the VCO.

- wide frequency deviation, at least $\pm K$ in order to operate over the whole synchronization range of the loop.

- 5% to 10% tolerance on linearity of K_3.

- modulation bandwidth usually does not have to be wide (except for frequency demodulation applications).

- fast enough settling time

Technologies

- for applications up to 3 MHz where central freq stability is not stringent, can use astable multivibrator. Here freq is adjusted by controlling the cap charging current. (Note: output is sq. wave)

- can also use oscillators which are freq. adjusted by resistor or cap variation in feedback as Wien Bridge, RC phase shift oscillator. Can replace resistor by FET.

- can use LC oscillators where freq. is adjusted with a voltage-controlled capacitor (composed of the cap of a reverse biased semiconductor junction) called a varactor. Such ccts are the Hartley and Clapp oscillators.

- for freq. between 300 MHz and 90 GHz, the feedback circuits are replaced by resonant lines tuned with varactor diodes and the transistor replaced with:

Bipolar	up to 6 GHz
FETs	up to 24 GHz
IMPATT	up to 90 GHz
GUNN	up to 90 GHz

can also use tube technology here with:

Reflex Klystron	
Magnetron	up to $\approx$ 25 GHz
BWO	

Quartz Stabilized Oscillator (VCXO)

- when a high degree of stability is required, use VCXO

- the series resonant freq. can be controlled to some extent by a varactor in series with the XTAL.

- systems most often used are Clapp Oscillator with XTAL and varactor (+ linearization elements) comprising the feedback cct.

- the quartz crystals are usually AT-cut crystals oscillating at fundamental freq. (1 MHz $<$ f $<$ 30 MHz).

- to extend this frequency range upwards we use freq. multipliers composed of SRDs, varactor diodes

- to extend this freq. range downwards, we use flip flop dividers.

Example p. 35 Blanchard

construct : 100 MHz PLL
: synchronization range $\pm$ 10 KHz
: VCO stability required to result in phase error $<$ 0.1 rad
: phase detector has $K_1 = 1$ V/rad

Find characteristics of VCO

1) make synchronization range equal to loop gain

$$K = K_1 K_3 = 2\pi \times 10^4 \text{ rad/sec}$$

$$\therefore K_3 = 2\pi \times 10^4 \text{ rad/sec/V}$$

$$= 10 \text{ kHz/V}$$

2) find Δf_0 (central freq. drift) such that corresponding phase error < 0.1 rad. We have:

$$\Delta\phi = \sin^{-1}\frac{2\pi\Delta f_0}{K} = 0.1 \text{ rad}$$

$$\therefore \Delta f = 10^3 \text{Hz}$$

3) find required stability

$$\frac{\Delta f_0}{f_0} = \frac{10^3}{100 \times 10^6} = 10^{-5} \text{ (this requires XTAL)}$$

4) use a 20 MHz VCXO with a multiplier chain of 5.

Loop Filters

- the transfer function of the LPFs have considerable influence on the properties of the loop.

- we use one of 2 filters most often (these are 1 passive or 1 active LPF)

- in some cases a passive LPF is followed by an opamp gain stage just to boost the loop gain.

I First-Order Loop

Filter has transfer function:

$$F(j\omega) = 1$$

(no filter)

II Second-Order Loop -Filter I

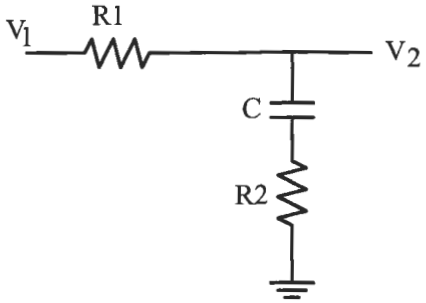

$$F(j\omega) = \frac{1 + j\omega R_2 C}{1 + j\omega(R_1 + R_2)C} = \frac{1 + j\omega\tau_2}{1 + j\omega\tau_1} \qquad \tau_2 = R_2 C \qquad \tau_1 = (R_1 + R_2)C$$

- here we have 2 parameters, τ_1 and τ_2 which will contribute to the behaviour of the loop. We will see that this allows an independent choice of the 2 essential properties of a second-order loop - natural freq. and damping factor.

- technological limitations on cap values for very low natural freq. We will see that

$$\omega_n^2 = \frac{K}{\tau_1}$$

consequently, if ω_n is small and K is high, then τ_1 is very large ($\approx$ 100 sec).

III Second-Order Loop -Filter II

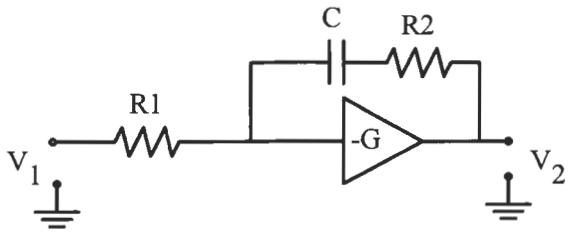

here

$$F(j\omega) = -G\frac{1 + j\omega R_2 C}{1 + j\omega(R_1 + GR_1 + R_2)C} = -G\frac{1 + j\omega\tau_2}{1 + j\omega\tau_1}$$

where $\tau_2 = R_2 C$ $\tau_1 = (R_1 + GR_1 + R_2)C$

Note: loop gain K is enhanced by G, $K = K_1 K_3 G$.

a) if $K_1 K_3$ is not adequate, we can use the active filter to increase the loop gain. The natural freq. ω_n will be found as:

$$\omega_n^2 = \frac{K}{\tau_1} = \frac{K_1 K_3 G}{(R_1 + GR_1 + R_2)C}$$

if G is large,

$$\omega_n^2 \approx \frac{K_1 K_3}{R_1 C}$$

Note: for a given $K_1 K_3$ value, we require the same value for $R_1 C$ to obtain a specified ω_n as for Filter I. Consequently, we have resolved loop gain problem but not low ω_n requirement.

b) if $K_1 K_3$ is adequate, but to obtain ω_n the necessary $R_1 C$ value cannot be realized with passive filter then active filter with gain G can be used but the product $K_1 K_3 G$ will have to be divided by G with a potentiometer to keep $K = K_1 K_3$.

$$\therefore \omega_n^2 = \frac{K}{\tau_1} = \frac{K_1 K_3}{(R_1 + GR_1 + R_2)C} \approx \frac{K_1 K_3}{(R_1 C)G}$$

ω_n is easily obtained since R_1C is now multiplied by G.

Note: the transfer function for the active filter is:

$$F(j\omega) = -G\frac{1+j\omega\tau_2}{1+j\omega\tau_1}$$

- we have seen that most phase detectors have alternating positive and negative slopes. We will see that of the two possible operating points of equal absolute value for sensitivities, only one will be stable. The neg. sign in the transfer function for the filter will change the stable operating point and the VCO will lead rather than lag. In general we are not really interested ..

Note: if the phase detector is sawtooth, then the sign of K_1 or K_2 must be changed to preserve stability.

Note: If G is very high, and ω is not too small (application a) then:

$$F(j\omega) \approx -G\frac{1+j\omega\tau_2}{1+j\omega GR_1C} \approx -G\frac{1+j\omega\tau_2}{j\omega GR_1C}$$

ignoring the negative sign gives:

$$F(j\omega) \approx \frac{1+j\omega\tau_2}{j\omega\tau_1'} \qquad \tau_2 = R_2C, \qquad \tau_1' = R_1C$$

This approximation will simplify certain calculations. A loop filter which satisfied this exactly would have infinite gain at DC - Consequently the approx is not good for some applications. (Example pp. 41).

Other Loop Filters

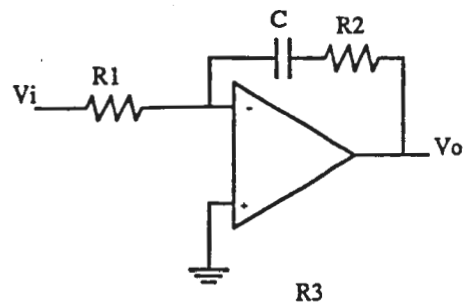

$$\frac{v_o}{v_i} = -\frac{1+sCR_2}{sCR_1}$$

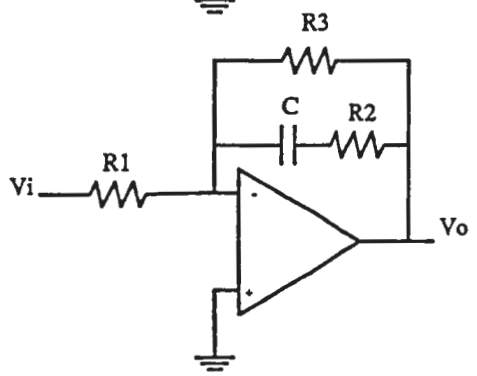

$$\frac{v_o}{v_i} = -\frac{R_3}{R_1}\frac{1+sCR_2}{1+sC(R_2+R_3)} \approx -\frac{R_3}{R_1}\frac{1+sCR_2}{sCR_3} = -\frac{1+sCR_2}{sCR_1}$$

3. General Equations

- we have stated that after acquisition, the VCO signal y_o and the input signal y_i are in synchronism but have a phase difference.

- we will consider the case where a modulation or disturbance is applied to the input signal phase. To do this we must write equations to describe the operation of the loop.

- However, the phase detector characteristic is nonlinear and periodic $\Longrightarrow$ complicates the mathematical description.

- We will assume the PLL operates properly $\Longrightarrow$ the difference in phase between y_o and y_i is slight $\Longrightarrow$ approximate phase detector characteristic by a linear characteristic.

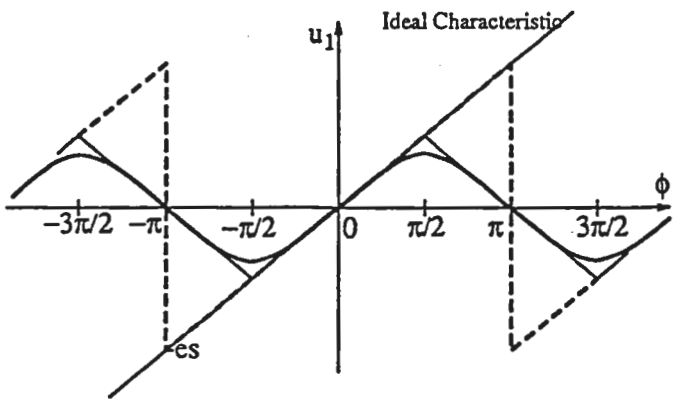

Gen Time Domain Equations for loops with Sinusoidal Char. for Phase Detector

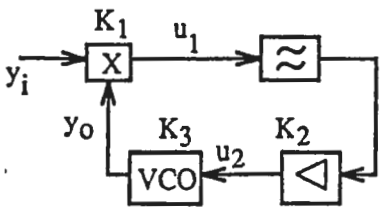

$$y_i(t) = A\sin[\omega t + \phi_i(t)]$$

$$y_o(t) = B\cos[\omega t + \phi_o(t)]$$

Note: y_i and y_o may be at different freq. the difference being included in $\phi_i(t) - \phi_o(t)$

For phase Detector

$$u_1 = K_1 \sin[\phi_i(t) - \phi_o(t)] \qquad -(1)$$

For loop filter let $F(j\omega)$ be the transfer function.

$$\text{then} \qquad f(t) = \int_{-\infty}^{\infty} F(j2\pi f)e^{j2\pi ft}df$$

$$\therefore \quad u_2(t) = K_2 u_1(t) * f(t) \qquad -(2)$$

$$= K_2 \int_{-\infty}^{\infty} u_1(\tau) f(t-\tau) d\tau$$

For VCO

$$\frac{d\phi_o}{dt} = K_3 u_2(t) \qquad -(3)$$

combine (1), (2), and (3)

$$\frac{d\phi_o}{dt} = K_1 K_2 K_3 \{\sin[\phi_i(t) - \phi_o(t)] * f(t)\} \qquad -(4)$$

Note: this is very complicated.

General Linearized Equations

assume $\phi_i(t) - \phi_o(t) < 1/2$ rad

$$\therefore \sin[\phi_i(t) - \phi_o(t)] \approx \phi_i(t) - \phi_o(t)$$

equation (4) becomes:

$$\frac{d\phi_o}{dt} = K[\phi_i(t) - \phi_o(t)] * f(t) \qquad -(5)$$

$$\text{let} \qquad \phi_i(t) \; \leftarrow \mathcal{F} \rightarrow \; \Phi_i(j\omega)$$

$$\text{and} \qquad \phi_o(t) \; \leftarrow \mathcal{F} \rightarrow \; \Phi_o(j\omega)$$

then (5) becomes:

$$j\omega \Phi_o(j\omega) = K[\Phi_i(j\omega) - \Phi_o(j\omega)] F(j\omega)$$

$$\text{or} \qquad \frac{\Phi_o(j\omega)}{\Phi_i(j\omega)} = \frac{KF(j\omega)}{(j\omega + KF(j\omega)} = H(j\omega) \qquad -(6)$$

Note: $H(j\omega)$ is the linearized transfer function of a PLL. The instantaneous phase error is:

$$\phi(t) = \phi_i(t) - \phi_o(t)$$

$$\therefore \qquad \Phi(j\omega) = [\Phi_i(j\omega) - \Phi_o(j\omega)]$$

$$\therefore \qquad \frac{\Phi(j\omega)}{\Phi_i(j\omega)} = \frac{j\omega}{(j\omega + KF(j\omega)} = 1 - H(j\omega) \qquad -(7)$$

Linearized Equations for First-Order Loop

- PLL is first-order when it has no loop filter.

$$\text{here} \qquad H(j\omega) = \frac{K}{j\omega + K} \qquad -(10)$$

- and the phase error function is:

$$\frac{\Phi}{\Phi_i} = 1 - H(j\omega) = \frac{j\omega}{j\omega + K} \qquad -(11)$$

- from the transfer and error functions, it is easy to find the time domain equations for loop operation. Rewriting (10) in the s domain:

$$(s + K)\Phi_o(s) = K\Phi_i(s)$$

which gives in the time domain:

$$\frac{d\phi_o}{dt} + K\phi_o(t) = K\phi_i(t) \qquad -(12)$$

similarly, (11) gives:

$$\frac{d\phi}{dt} + K\phi(t) = \frac{d\phi_i(t)}{dt}$$

Note: these are first order linear diff eqn. hence the loop is called first order. Note: if we didn't assume $\phi(t)$ to be small (and consequently that the phase detector characteristic is linear) we would have in place of (12)

$$\frac{d\phi_o}{dt} = K\sin[\phi_i(t) - \phi_o(t)] \qquad -(12b)$$

- this is a nonlinear first order diff eqn. which we will need to determine acquisition time for loops.

Linearized Equations for Second-Order Loop

Here $F(j\omega) = \dfrac{1 + j\omega\tau_2}{j\omega\tau_1} \quad \tau_1 = R_1C, \quad \tau_2 = R_2C$

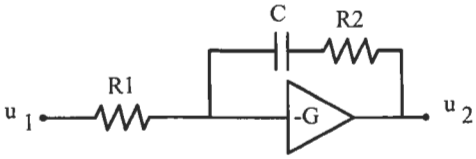

where $G \rightarrow \infty$ so that actual transfer function approximates above equation

Insert $F(j\omega)$ into (6) and (7).

$$H(j\omega) = \frac{K + j\omega K\tau_2}{K - \omega^2\tau_1 + j\omega\tau_2} \qquad -(13)$$

$$1 - H(j\omega) = \frac{-\omega^2\tau_1}{K - \omega^2\tau_1 + j\omega\tau_2} \qquad -(14)$$

these lead to the time-domain equations

$$\tau_1 \frac{d^2\phi_o}{dt^2} + K\tau_2 \frac{d\phi_o}{dt} + K\phi_o(t) = K\tau_2 \frac{d\phi_i}{dt} + K\phi_i(t) \qquad -(17)$$

$$\tau_1 \frac{d^2\phi}{dt^2} + K\tau_2 \frac{d\phi}{dt} + K\phi(t) = \tau_1 \frac{d^2\phi_i}{dt^2} \qquad -(18)$$

Note: these equations are second-order linear diff equations. Hence the loop is called second order.

b) One-Pole LPF with phase-lead correction

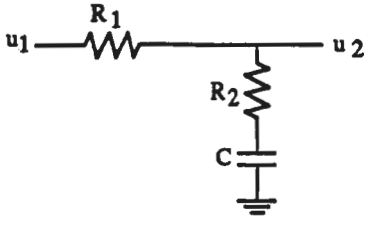

Here

$$F(j\omega) = \frac{1 + j\omega\tau_2}{1 + j\omega\tau_1} \quad \tau_1 = (R_1 + R_2)C, \quad \tau_2 = R_2C$$

Insert above into (6) and (7):

$$H(j\omega) = \frac{K + j\omega K\tau_2}{K - \omega^2\tau_1 + j\omega(1 + K\tau_2)} \qquad -(25)$$

$$1 - H(j\omega) = \frac{-\omega^2\tau_1 + j\omega}{K - \omega^2\tau_1 + j\omega(1 + K\tau_2)} \qquad -(26)$$

From above we can obtain the time-domain equations as:

$$\tau_1 \frac{d^2\phi_o}{dt^2} + (1 + K\tau_2)\frac{d\phi_o}{dt} + K\phi_o(t) = K\tau_2 \frac{d\phi_i}{dt} + K\phi_i(t) \qquad -(29)$$

$$\tau_1 \frac{d^2\phi}{dt^2} + (1 + K\tau_2)\frac{d\phi}{dt} + K\phi(t) = \tau_1 \frac{d^2\phi_i}{dt^2} + \frac{d\phi_i}{dt} \qquad -(30)$$

General Time-Domain Equations for Second-Order Loop with Sinusoidal Phase Detector

The above equations are only valid if $\phi(t) = \phi_i(t) - \phi_o(t) < 1/2$ rad.

a) Integrator with phase-lead correction

now filter equation is:

$$F(s) = \frac{u_2}{u_1} = \frac{1 + \tau_2 s}{\tau_1 s}$$

consequently

$$\tau_1 \frac{du_2}{dt} = u_1 + \tau_2 \frac{du_1}{dt}$$

Making allowances for an amplifier of gain K_2

$$\tau_1 \frac{du_2}{dt} = K_2 \left[u_1 + \tau_2 \frac{du_1}{dt} \right] \qquad -(31)$$

Now phase detector equation is:

$$u_1(t) = K_1 \sin[\phi_i(t) - \phi_o(t)] \qquad -(32a)$$

$$\therefore \quad \frac{du_1}{dt} = K_1 \cos[\phi_i(t) - \phi_o(t)] \left[\frac{d\phi_i}{dt} - \frac{d\phi_o}{dt} \right] \qquad -(32b)$$

and VCO equation is:

$$\frac{d\phi_o}{dt} = K_3 u_2(t) \qquad -(32c)$$

$$\therefore \quad \frac{d^2\phi_o}{dt^2} = K_3 \frac{du_2}{dt} \qquad -(32d)$$

put (32) into (31) gives:

$$\tau_1 \frac{d^2\phi_o}{dt^2} = K \sin[\phi_i(t) - \phi_o(t)] + K\tau_2 \cos[\phi_i(t) - \phi_o(t)] \left[\frac{d\phi_i}{dt} - \frac{d\phi_o}{dt} \right] \qquad -(33)$$

similarly for the instantaneous phase error, $\phi(t)$

$$\tau_1 \frac{d^2\phi}{dt^2} + K\tau_2[\cos\phi]\frac{d\phi}{dt} + K \sin\phi = \tau_1 \frac{d^2\phi_i}{dt^2} \qquad -(34)$$

Note: the above 2 equations are second order nonlinear differential equations which cannot be solved analytically.

b) One pole LPF with Phase-Lead Correction

Again we obtain second-order nonlinear diff equations (p 55 Blanchard)

Parameters of a Second-Order Loop

-In general, the denominator of a second-order transfer function is formulated:

$$s^2 + 2\zeta\omega_n s + \omega_n^2$$

- consequently we substitute the time constants τ_1 and τ_2 for the natural frequency ω_n and the damping factor ζ.

a) Integrator with Phase-Lead Correction

here we have:

$$\omega_n^2 = \frac{K}{\tau_1} \qquad -(41)$$

$$2\zeta\omega_n = \frac{K\tau_2}{\tau_1} \qquad -(42)$$

and consequently, using (13)

$$H(j\omega) = \frac{\omega_n^2 + j2\zeta\omega_n\omega}{\omega^2 + 2\zeta\omega_n\omega + \omega_n^2} \qquad -(43)$$

$$\text{and} \qquad 1 - H(j\omega) = \frac{-\omega^2}{\omega_n^2 - \omega^2 + j2\zeta\omega_n\omega} \qquad -(44)$$

b) <u>One-Pole LPF with Phase-Lead Correction</u>

here we have:

$$\omega_n^2 = \frac{K}{\tau_1} \qquad -(52a)$$

$$2\zeta\omega_n = \frac{1 + K\tau_2}{\tau_1} \qquad -(52b)$$

and consequently,

$$H(j\omega) = \frac{\omega_n^2 + j\left(2\zeta\omega_n - \frac{\omega_n^2}{K}\right)\omega}{\omega_n^2 - \omega^2 + j2\zeta\omega_n\omega} \qquad -(53)$$

$$1 - H(j\omega) = \frac{-\omega^2 + j\left(\frac{\omega_n^2}{K}\right)\omega}{\omega_n^2 - \omega^2 + j2\zeta\omega_n\omega} \qquad -(54)$$

Note: if we compare (42) with (52), we see that the former is a good approx of the latter when $K\tau_2 \gg 1$. However this does not mean that an integrator with phase lead correction is equivalent to a one pole LPF with phase lead correction since (44) and (54) are equivalent only if

$$\frac{\omega_n^2}{K} \ll 1$$

$\therefore$ for both filters to act equivalently we must have

$$K\tau_2 \gg 1 \qquad \text{and} \qquad \frac{\omega_n^2}{K} \ll 1$$

Note: Of the 3 parameters K, τ_1 and τ_2, the loop gain is likely to vary most (since the phase detector sensitivity is dependent on amplitude A of the VCO).

- Now from equations (41) to (54), ω_n and ζ depend on K.

- If we use subscript $_o$ to designate the values of ω_n and ζ when VCO signal is equal to A_o, we have the following variations:

$$K = K_o\frac{A}{A_o} \qquad \left(\text{since} \quad K = K_1(A)K_2K_3 = K'A, \quad \text{and} \quad K_o = K'A_o\right)$$

$$\omega_n = \omega_{no}\sqrt{\frac{A}{A_o}} \qquad \left(\text{since} \quad \omega_n^2 = \frac{K_o}{\tau_1}\frac{A}{A_o}, \quad \text{and} \quad \omega_{no}^2 = \frac{K_o}{\tau_1}\right)$$

a) for Integrator with phase-lead correction:

$$2\zeta\omega_{no}\sqrt{\frac{A}{A_o}} = K_o\frac{A}{A_o}\frac{\tau_2}{\tau_1} \qquad \left(\text{from} \quad 2\zeta\omega_n = K\frac{\tau_2}{\tau_1}\right)$$

or

$$\zeta = \zeta_o\sqrt{\frac{A}{A_o}} \qquad \left(\text{solve above for} \quad \zeta = \frac{K_o}{2\omega_{no}}\frac{\tau_2}{\tau_1}\sqrt{\frac{A}{A_o}}, \quad \text{substitute} \quad 2\omega_{no}\zeta_o = K_o\frac{\tau_2}{\tau_1}\right)$$

b) for One-Pole LPF with phase-lead correction:

$$2\zeta\omega_{no}\sqrt{\frac{A}{A_o}} = \frac{1 + K_o(A/A_o)\tau_2}{\tau_1}$$

or

$$\zeta = \frac{1 + K_o(A/A_o)\tau_2}{2\sqrt{K_o(A/A_o)\tau_1}} \approx \zeta_o\sqrt{\frac{A}{A_o}} \qquad \text{for} \quad K_o\frac{A}{A_o}\tau_2 \gg 1$$

4. Phase-Locked Loop Stability

- we shall investigate stability of loops by means of Bode Diagrams.

- we shall use the linear approximation for the phase detector. Consequently, the conditions for stability which we will obtain do not guarantee stability.

- The open-loop transfer function is:

$$G(j\omega) = K_1 K_2 F(j\omega)\frac{K_3}{j\omega} = K\frac{F(j\omega)}{j\omega}$$

where $F(j\omega)$ is the filter transfer function.

First-Order Loops

$$\text{here} \qquad F(j\omega) = 1, \qquad \text{and} \qquad G(j\omega) = \frac{K}{j\omega}$$

plot G in dB $\Longrightarrow G = 20\log|G(j\omega)|$

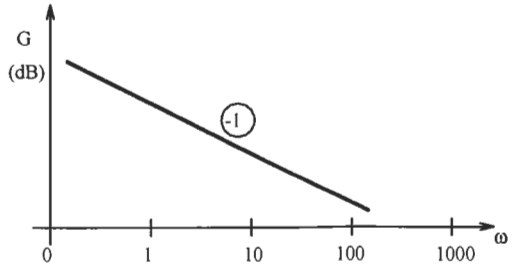

plot phase of G in rads

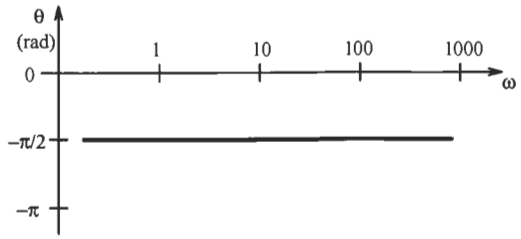

this loop is unconditionally stable

- however, we haven't considered unwanted phase shifts which are unavoidable due to phase detector and VCO

a) -phase detector output is always filtered to remove the 2ω term and the ω term. The phase detector filter is a one-pole LPF. Consequently, K_1 must be replaced with $\frac{K_1}{1+j\omega\tau}$

b) -VCO - For all realizable VCOs, there is always large frequency offsets for which the impedance is high for the modulation and low for the frequency to be modulated.

-Thus the modulation sees the equivalent of a LPF, and K_3 must be replaced with $\frac{K_3}{1+j\omega\tau'}$

Consequently, the open-loop transfer function becomes:

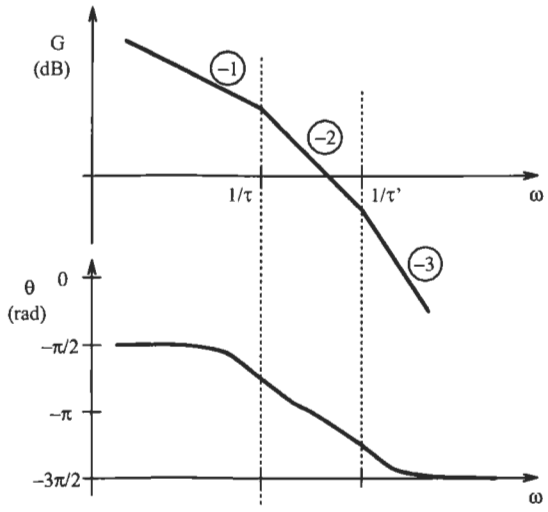

$$G(j\omega) = \frac{K}{j\omega(1+j\omega\tau)(1+j\omega\tau')}$$

- Since asymptotic phase shift is $3\pi/2$, loop is no longer unconditionally stable.

- Here the phase shift is $-\pi$ for $G < 1$. Loop oscillates.

- To stabilize loop, must reduce the loop K.

Second-Order Loop (with perfect integrator)

Here

$$F(j\omega) = \frac{1}{j\omega}$$

and

$$G(j\omega) = \frac{K}{(j\omega)^2}$$

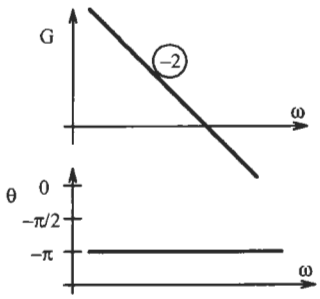

- since $\theta = -\pi$ independent of ω, the loop is unstable and will oscillate at a frequency determined by the closed loop transfer function.

Second-Order Loop (integrator with phase lead correction)

$$F(j\omega) = \frac{1+j\omega\tau_2}{j\omega\tau_1}$$

$$G(j\omega) = \frac{K(1+j\omega\tau_2)}{\tau_1(j\omega)^2}$$

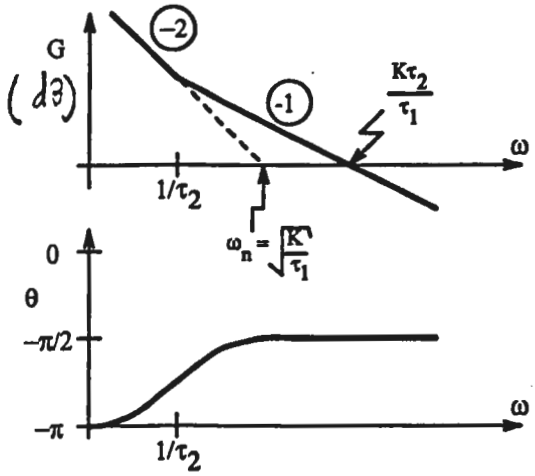

- Here entire phase curve is $> -\pi$
- note: if $1/\tau_2 < \omega_n$, then the phase shift is between $-\pi/2$ and $-3\pi/4$ when G = 0. dB
- this is good stability.
- the condition $1/\tau_2 < \omega_n$ can be written as

$$\omega_n \tau_2 > 1$$

but $2\zeta\omega_n = \dfrac{K\tau_2}{\tau_1}$

equivalently: $\omega_n \tau_2 = 2\zeta$

- consequently, the condition is

$$\zeta > 1/2$$

and the greater the damping, the greater the safety margin.

- if we include the spurious time constants τ and τ' we see that for the loop to stay stable, these constants cannot introduce additional phase shift greater than $\pi/4$ for frequencies for which $G = 0$. dB

- since for second-order loops we usually want ω_n small and consequently frequency for $G = 0$ dB is also small $\Longrightarrow$ we can often ignore τ and τ'.

Second-Order Loop (LPF with phase-lead correction)

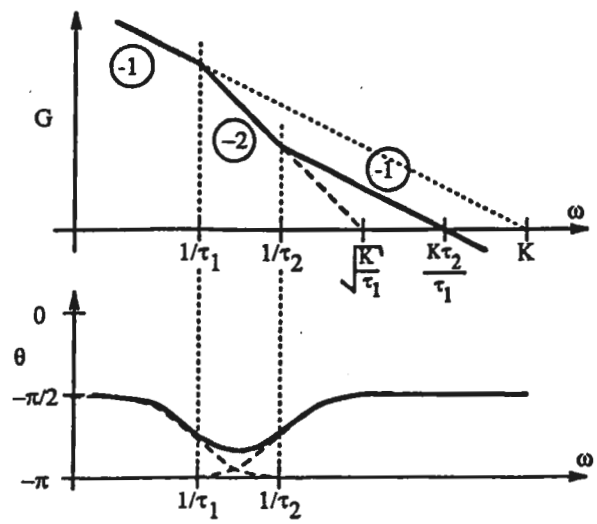

here

$$F(j\omega) = \frac{1 + j\omega\tau_2}{1 + j\omega\tau_1}$$

$$G(j\omega) = \frac{K(1 + j\omega\tau_2)}{j\omega(1 + j\omega\tau_1)}$$

- Note: phase safety margin is about $\pi/2$
- This allows us to use phase detectors and VCOs with small modulation bandwidths without compromising loop stability (inexpensive).

- Note: for a given τ_1, the safety margin increases with τ_2. For a predetermined ω_n, K, and τ_1, equation (52) shows that increasing τ_2 means increasing ζ.

- Consequently we are free to choose a satisfactory ζ whatever the ω_n selected.

- Note: if τ_1 is very large, or τ_2 is small, θ can get very close to $-\pi$ at $\omega = 1/\sqrt{\tau_1\tau_2}$. This corresponds to a low loop damping factor. Loop can go unstable due to parasitics τ and τ'

Superior-Order Loops

- Loops of order grater than 2 are not usually used.

- However, to allow for a high spurious time constant, we must consider a second-order loop as a third order loop.

- we must analyze 2 cases

a)

$$F(j\omega) = \frac{1}{j\omega}\frac{1}{1+j\omega\tau}$$

- this corresponds to an integrator followed by a LPF

- this gives

$$G(j\omega) = \frac{K}{(j\omega)^2(1+j\omega\tau)}$$

- in the above cct, phase shift is never equal to $-\pi$

- However, a loop of this type is unstable!

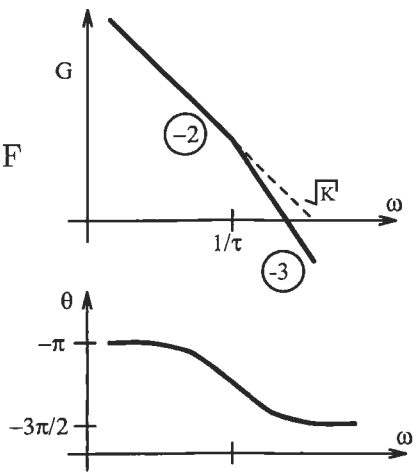

b)

$$F(j\omega) = \frac{(1+j\omega\tau_2)^2}{(j\omega\tau_1)^2}$$

consequently

$$G(j\omega) = \frac{K(1+j\omega\tau_2)^2}{\tau_1^2(j\omega)^3}$$

- In above cct, gain is $\gg 1$ for ω where $\theta = -\pi$

- However a loop of this type can be stable!

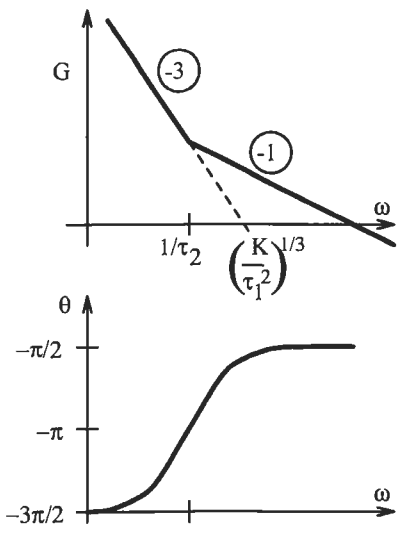

- To determine whether the closed loop response is stable we must use another method for the above ccts.

- recall equation (8)

$$H(s) = \frac{\Phi_o(s)}{\Phi_i(s)} = \frac{KF(s)}{s + KF(s)}$$

Note: if the transfer function poles contain positive real parts, the time domain solution will have positive real exponentials and the solution blows up.

- Consequently, we can determine stability by determining poles with positive real parts.

Root Locus Method

- represent in the complex plane the $H(s)$ denominator root locus as the open loop gain K varies. If the locus cuts the imaginary axis the loop is unstable for these values of K.

- we will do this graphically.

a) here

$$H(s) = \frac{N(s)}{D(s)}$$

$$\text{with} \qquad D(s) = \tau s^3 + s^2 + K$$

We want to determine the real part of the solution to:

$$D(s) = 0$$

$$\therefore \quad \tau(\sigma + j\omega)^3 + (\sigma + j\omega)^2 + K = 0 \qquad -(1)$$

- this complex equation is equivalent to the simultaneous solution of the following 2 equations.

$$\tau\sigma^3 - 3\tau\sigma\omega^2 + \sigma^2 - \omega^2 + K = 0 \qquad -(2)$$

$$3\tau\sigma^2\omega - \tau\omega^3 + 2\sigma\omega = 0 \qquad -(3)$$

The solutions to the second equation are:

$$\omega = 0$$

$$\omega^2 = 3\sigma^2 + \frac{2}{\tau}\sigma$$

For the first solution, sub into (2)

$$\tau\sigma^3 + \sigma^2 + K = 0$$

This has no positive σ solutions since τ and K are positive.

For the second solution, sub into (2)

$$8\tau\sigma^3 + 8\sigma^2 + \frac{2}{\tau}\sigma - K = 0 \qquad -(4)$$

Now the LHS is an increasing function of σ for σ positive. Now for $\sigma = 0$, the LHS of (4) is:

$$\text{LHS} = -K$$

For $\sigma \to \infty$, the LHS of (4) is

$$\text{LHS} \to +\infty$$

consequently the loop is unstable!

b) here

$$H(s) = \frac{N(s)}{D(s)}$$

$$\text{with} \qquad D(s) = \tau_1^2 s^3 + K\tau_2^2 s^2 + 2K\tau_2 s + K$$

We want to determine the real part of the solution to:

$$D(s) = 0$$

$$\therefore \quad \tau_1^2(\sigma + j\omega)^3 + K\tau_2^2(\sigma + j\omega)^2 + 2K\tau_2(\sigma + j\omega) + K = 0 \qquad -(5)$$

- this complex equation is equivalent to the simultaneous solution of the following 2 equations.

$$\tau_1^2\sigma^3 - 3\tau_1^2\sigma\omega^2 + K\tau_2^2\sigma^2 - K\tau_2^2\omega^2 + 2K\tau_2\sigma + K = 0 \qquad -(6)$$

$$3\tau_1^2\sigma^2\omega - \tau_1^2\omega^3 + 2K\tau_2^2\sigma\omega + 2K\tau_2\omega = 0 \qquad -(7)$$

The solutions to the second equation are:

$$\omega = 0$$

$$\omega^2 = 3\sigma^2 + 2K\frac{\tau_2^2}{\tau_1^2}\sigma + 2K\frac{\tau_2}{\tau_1^2}$$

For the first solution, sub into (6)

$$\tau_1^2\sigma^3 + K\tau_2^2\sigma^2 + 2K\tau_2\sigma + K = 0$$

This has no positive σ solutions since τ_1, τ_2, and K are positive.

For the second solution, sub into (6)

$$8\tau_1^2\sigma^3 + 8K\tau_2^2\sigma^2 + \left(4K\tau_2 + 2K^2\frac{\tau_2^4}{\tau_1^2}\right)\sigma + 2K^2\frac{\tau_2^3}{\tau_1^2} - K = 0$$

Now the LHS is an increasing function of σ for σ positive. For $\sigma = 0$:

$$\text{LHS} = 2K^2\frac{\tau_2^3}{\tau_1^2} - K$$

For $\sigma \to \infty$:

$$\text{LHS} \to +\infty$$

consequently the equation $D(s)$ possesses a positive σ root iff

$$2K^2\frac{\tau_2^3}{\tau_1^2} - K < 0$$

or

$$K < \frac{1}{2}\left(\frac{\tau_1^2}{\tau_2^3}\right)$$

and the loop will be unstable.

- to keep the loop stable, we must therefore make:

$$K \geq \frac{1}{2}\left(\frac{\tau_1^2}{\tau_2^3}\right)$$

5. Linear Behavior

- we will analyze the PLL response to modulations and disturbances under linear conditions

- we will assume the loop is in lock with a null phase error

- will assume the phase error will be low enough to verify hypothesis of linearity. If various disturbances or modulations are simultaneously applied, the total phase error calculated by superposition must remain small.

- linearity applies to
  - phase detector
  - amplifier (avoid saturation)
  - VCO characteristic and amplitude consistency

Transient Response

- here we assume loop is in lock at $t = 0$ with null phase error. Therefore

$$\left.\begin{aligned} y_i(t) &= A\sin\omega t \\ y_o(t) &= B\cos\omega t \end{aligned}\right\} t < 0$$

- when $t \geq 0$, the signals become

$$y_i(t) = A\sin(\omega t + \phi_i(t))$$

$$y_o(t) = B\cos(\omega t + \phi_o(t))$$

- here $\phi_o(t)$ is loop response to excitation $\phi_i(t)$

- also $\phi(t) = \phi_i(t) - \phi_o(t)$ is the loop error.

Phase Step Response

- here $\phi_i(t) = \theta\Upsilon(t)$ where $\Upsilon(t)$ is the unit step function at time $t = 0$ and θ is the size of the phase step.

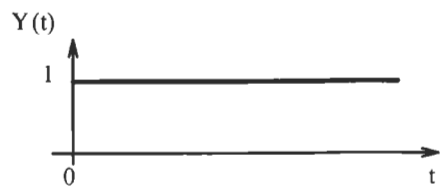

- consequently

$$\Phi_i(s) = \frac{\theta}{s}$$

- now the loop phase error is, from eqn (3.9)

$$\frac{\Phi(s)}{\Phi_i(s)} = 1 - H(s)$$

$$\therefore \qquad \Phi(s) = [1 - H(s)]\,\frac{\theta}{s} \qquad -(5.1)$$

First Order Loop

- the error function in (5.1) becomes:

$$\Phi(s) = \frac{\theta}{s + K}$$

- using the final value theorem

$$\lim_{t\to\infty} \phi(t) = \lim_{s\to 0} s\Phi(s)$$

- as $s \to 0$, $s\Phi(s) \to 0 \implies$ no steady state phase error.

Second-Order Loop - Integrator with phase lead

- here

$$F(s) = \frac{1 + \tau_2 s}{\tau_1 s}$$

- and

$$\Phi(s) = \frac{\tau_1 s\theta}{\tau_1 s^2 + K\tau_2 s + K}$$

- or

$$\Phi(s) = \frac{s\theta}{s^2 + 2\zeta\omega_n s + \omega_n^2}$$

Taking inverse transform gives eqn. (5.3) below:

$$\begin{aligned}
&\zeta > 1 \qquad \phi(t) = \theta e^{-\zeta\omega_n t}\left[\cosh\left(\omega_n\sqrt{\zeta^2-1}\;t\right) - \frac{\zeta}{\sqrt{\zeta^2-1}}\sinh\left(\omega_n\sqrt{\zeta^2-1}\;t\right)\right] \\
&\zeta = 1 \qquad \phi(t) = \theta e^{-\omega_n t}\,(1 - \omega_n t) \qquad -(5.3) \\
&\zeta < 1 \qquad \phi(t) = \theta e^{-\zeta\omega_n t}\left[\cos\left(\omega_n\sqrt{1-\zeta^2}\;t\right) - \frac{\zeta}{\sqrt{1-\zeta^2}}\sin\left(\omega_n\sqrt{1-\zeta^2}\;t\right)\right]
\end{aligned}$$

- See Fig 5-1, 5-2 Blanchard, reproduced on the next page.

- Note : max. phase error is θ and occurs at $t = 0$

: consequently the curves are valid only if $\theta < 1/2$ rad for sine detector,

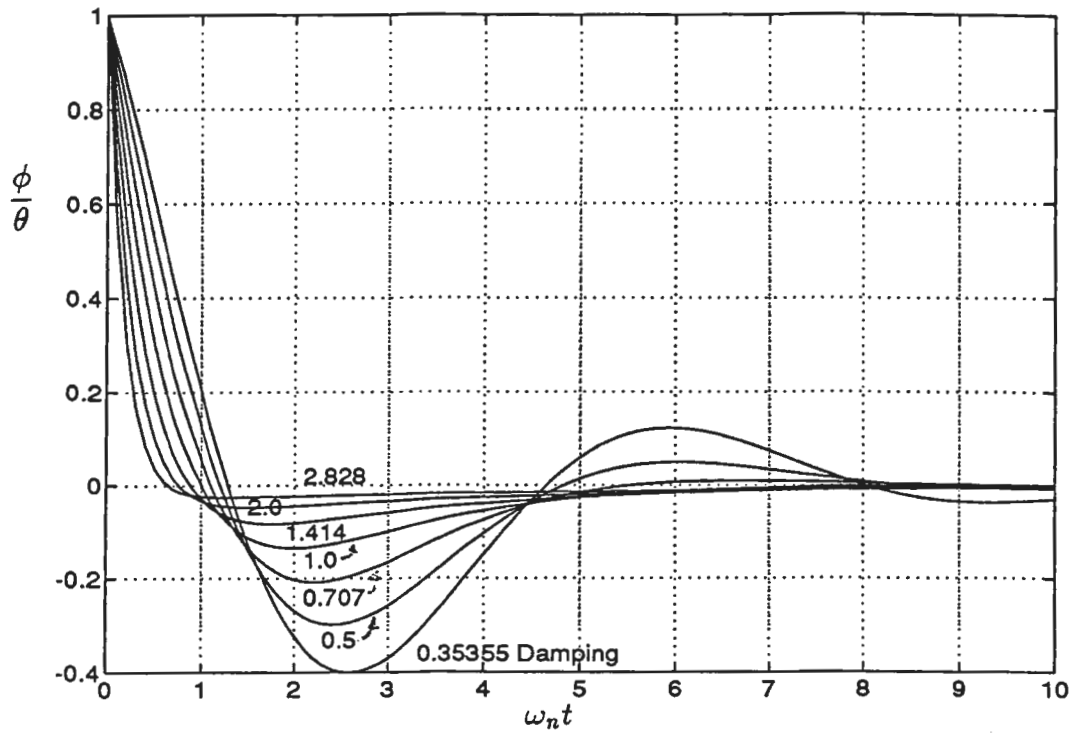

Figure 5.1. Phase error of a second-order loop (with $[F(s) = (1 + s\tau_2 s/\tau_1 s)]$) for a phase step of the input signal.

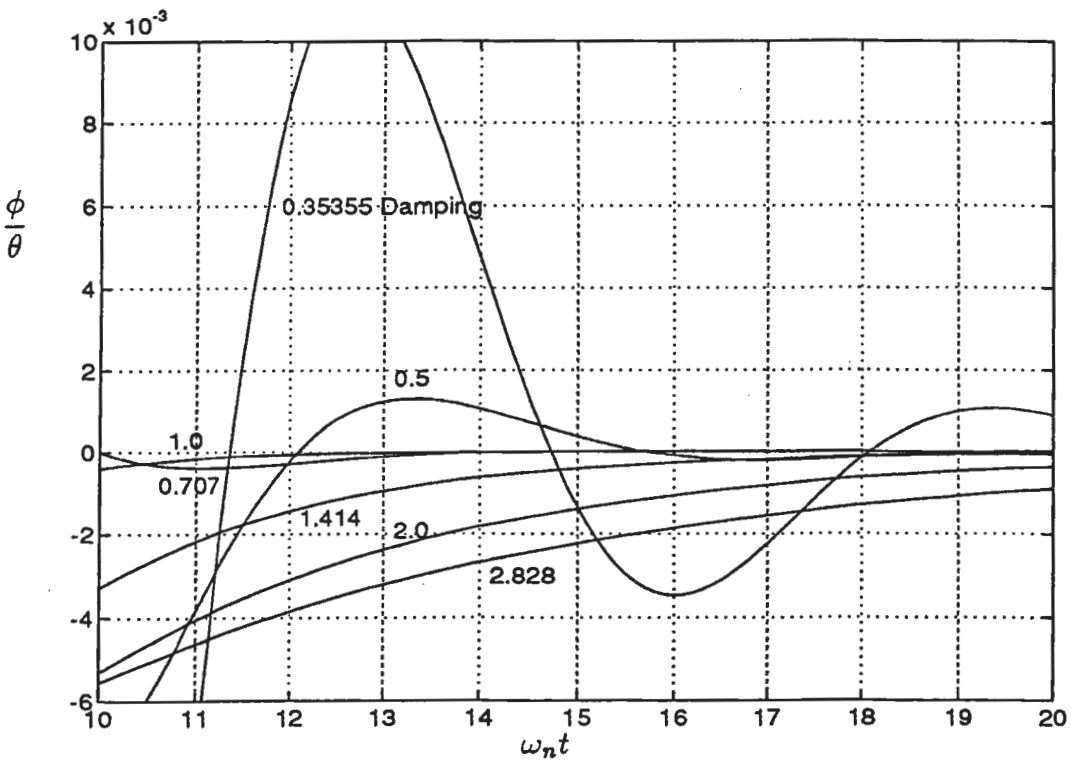

Figure 5.2. Tail of the phase error of a second-order loop (with $[F(s) = (1 + s\tau_2 s/\tau_1 s)]$) for a phase step of the input signal.

if $\theta < \pi/2$ for triangle detector,

if $\theta < \pi$ for sawtooth detector.

: choice of $\zeta = 1$ gives fastest elimination of loop error.

Second-Order loop - LPF with phase-lead correction

- here the error function is:

$$\Phi(s) = \frac{\left(s + \frac{\omega_n^2}{K}\right)\theta}{s^2 + 2\zeta\omega_n s + \omega_n^2}$$

- taking the reciprocal transform gives eqn. (5.5) Blanchard.

-Note: in eqn. 5.5, $\zeta \gg \omega_n/K$ generally. Consequently, eqn. 5.5 can be approximated with eqn. 5.3 and phase error curves in Fig. 5.1 and 5.2 can be used.

-Note: comparing Fig. 5.1 (for integrator with phase lead) and Fig 5.3 (for simple LPF) we see that the correction network results in much faster response to final condition. Therefore the phase correction not only improves stability, but also loop response rate.

5.2 Frequency Step Response

- here

$$\phi_i(t) = \Delta\omega t \Upsilon(t)$$

or

$$\Phi_i(s) = \frac{\Delta\omega}{s^2}$$

Consequently, phase error is

$$\Phi(s) = [1 - H(s)]\frac{\Delta\omega}{s^2}$$

First-Order Loops

here

$$\Phi = \frac{\Delta\omega}{s(s+K)}$$

The inverse Laplace Transform gives:

$$\phi(t) = \frac{\Delta\omega}{K}\left(1 - e^{-Kt}\right)$$

Note: steady state error is $\frac{\Delta\omega}{K}$, which is the phase error obtained at start of notes for an offset in frequency of ω_i and with respect to VCO central frequency.

Second-Order loop - Integrator with phase-lead correction

$$\Phi(s) = \frac{\Delta\omega}{s^2 + 2\zeta\omega_n s + \omega_n^2}$$

this yields

$$\begin{aligned}
\zeta > 1 \qquad & \phi(t) = \frac{\Delta\omega}{\omega_n} e^{-\zeta\omega_n t} \quad \frac{\sinh\left(\omega_n\sqrt{\zeta^2 - 1}\, t\right)}{\sqrt{\zeta^2 - 1}} \\
\zeta = 1 \qquad & \phi(t) = \frac{\Delta\omega}{\omega_n} e^{-\omega_n t} \quad \omega_n t \qquad\qquad -(5.8) \\
\zeta < 1 \qquad & \phi(t) = \frac{\Delta\omega}{\omega_n} e^{-\zeta\omega_n t} \quad \frac{\sin\left(\omega_n\sqrt{1 - \zeta^2}\, t\right)}{\sqrt{1 - \zeta^2}}
\end{aligned}$$

- curves for $\left[\frac{\omega_n}{\Delta\omega}\right] \phi(t)$ are given in Fig. 5.4 and 5.5 Blanchard.

-Note: - max. phase error increases as ζ decreases.

- steady state error is null - as predicted by final value theorem.

- again, $\zeta = 1$ gives fastest elimination of loop error.

- Example - page 92.

Second-Order loop - LPF with phase-lead correction

- here

$$\Phi(s) = \frac{\Delta\omega}{s^2 + 2\zeta\omega_n s + \omega_n^2} + \frac{\omega_n^2}{K} \frac{\Delta\omega}{s\left(s^2 + 2\zeta\omega_n s + \omega_n^2\right)}$$

- this gives eqn. 5.10 Blanchard for $\phi(t)$.

- From this eqn. the steady state error is $\frac{\Delta\omega}{K}$

- When K is large, the error is small

- When K is made large, the eqn. (5.10) closely approximates (5.8) and hence the curves of Fig. 5.4 and 5.5 can be used for the LPF with phase lead correction as well as for the integrator with phase lead correction.

Note: the steady state error for a LPF (without correction) is

$$\frac{2\zeta\Delta\omega}{\omega_n} = \frac{\Delta\omega}{K}$$

as above.

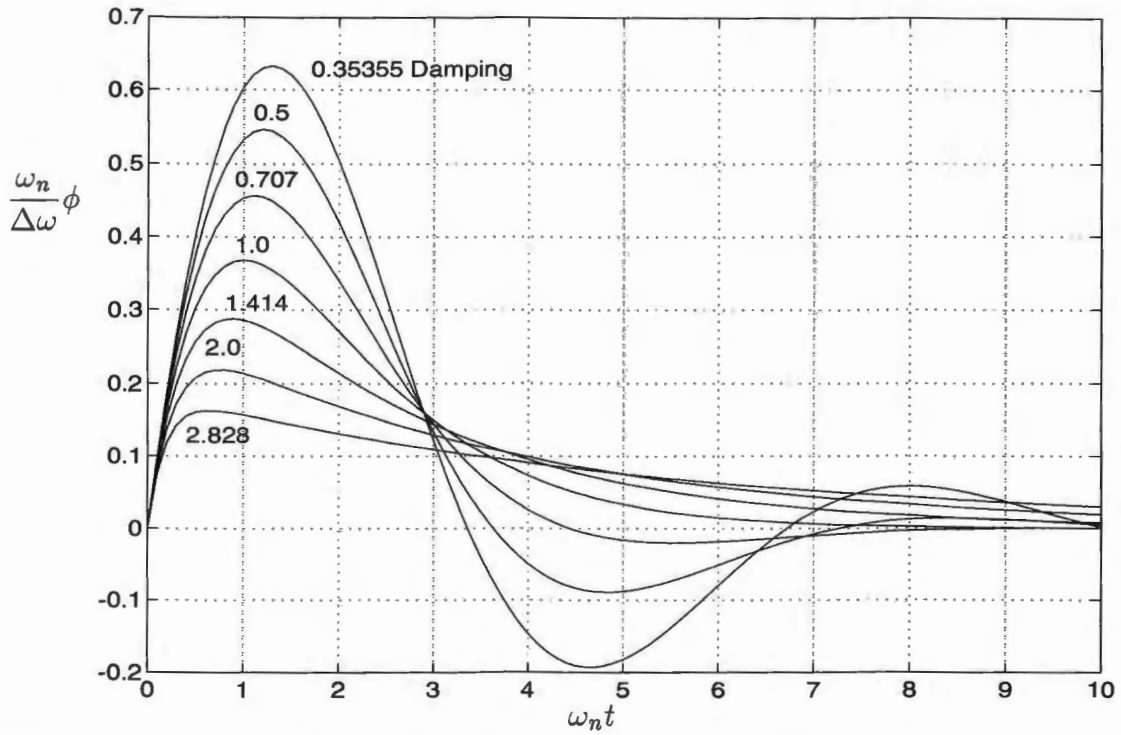

Figure 5.4. Phase error of a second-order loop (with $[F(s) = (1 + \tau_2 s/\tau_1 s)]$) for a frequency step of the input signal.

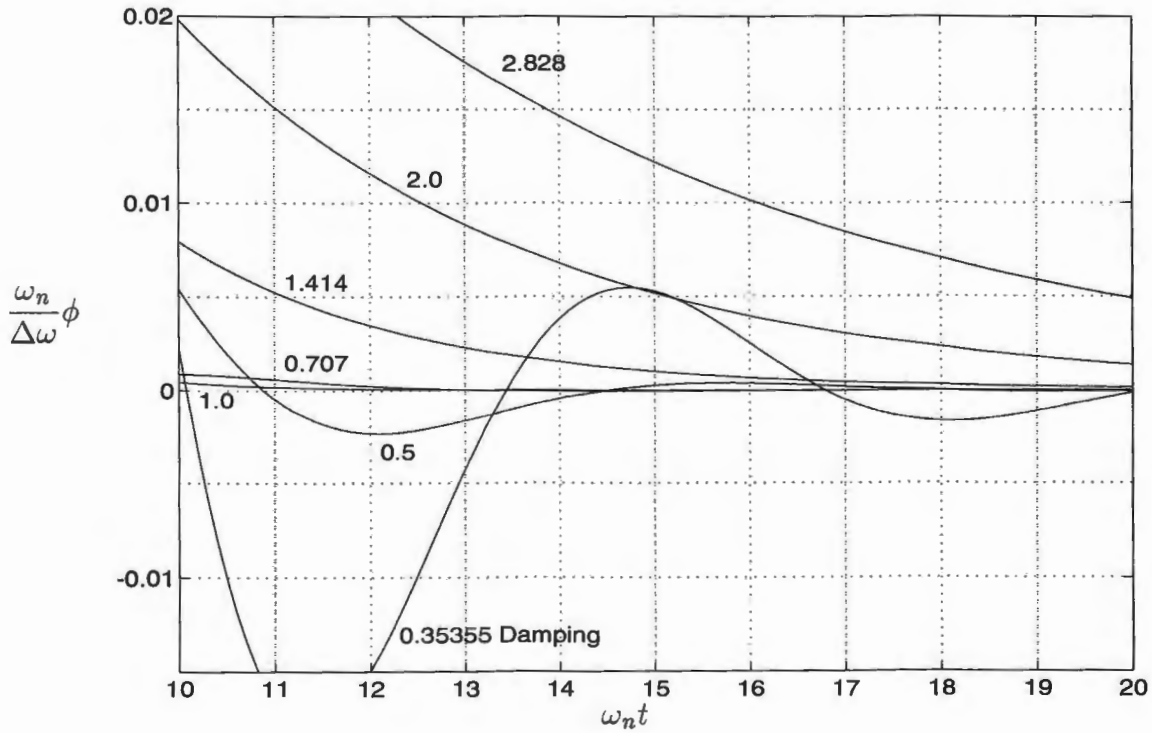

Figure 5.5. Tail of the phase error of a second-order loop (with $[F(s) = (1 + \tau_2 s/\tau_1 s)]$) for a frequency step of the input signal.

- if we try to reduce the error by increasing K, we end up with a low value for ζ. Small values of ζ imply relative instability in the loop. We do not have this problem for LPF with phase lead correction.

5.3 Linear Frequency Variation

$$f_{i_{inst}} = f + Rt\Upsilon(t)$$

$$\therefore \quad \phi_i(t) = 2\pi R \frac{t^2}{2} \Upsilon(t) = \mathcal{R} \frac{t^2}{2} \Upsilon(t)$$

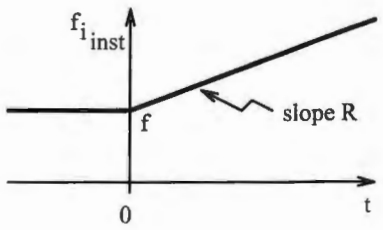

where $\mathcal{R} = 2\pi R$ in rad /sec^2.

Taking the Laplace transform:

$$\Phi(s) = [1 - H(s)]\frac{\mathcal{R}}{s^3}$$

First-Order Loop

$$\Phi(s) = \frac{\mathcal{R}}{s^2(s+K)}$$

$$\therefore \quad \phi(t) = \frac{\mathcal{R}t}{K} - \frac{\mathcal{R}}{K^2}\left[1 - e^{-Kt}\right]$$

Note: steady state phase error consists of a constant tracking error $-\frac{\mathcal{R}}{K^2}$, and a term increasing with time. This corresponds to a steady state frequency error of $\Delta\omega = \mathcal{R}t$.

- This freq. error will cause the loop to work outside the linear domain, and when $\phi(t) > \pi/2$ the loop falls out of lock.

Second-Order Loop (Integrator with phase lead)

$$\Phi(s) = \frac{\mathcal{R}}{s\left(s^2 + 2\zeta\omega_n s + \omega_n^2\right)}$$

the curves representing $\left[\frac{\omega_n^2}{\mathcal{R}}\right]\phi(t)$ are given in Fig. 5-7.

- There is a steady state phase error $\frac{\mathcal{R}}{\omega_n^2}$

- There is no time dependent error!

- if $\frac{\mathcal{R}}{\omega_n^2}$ is small, and if ζ is large enough to limit overshoot, then the loop stays in lock.

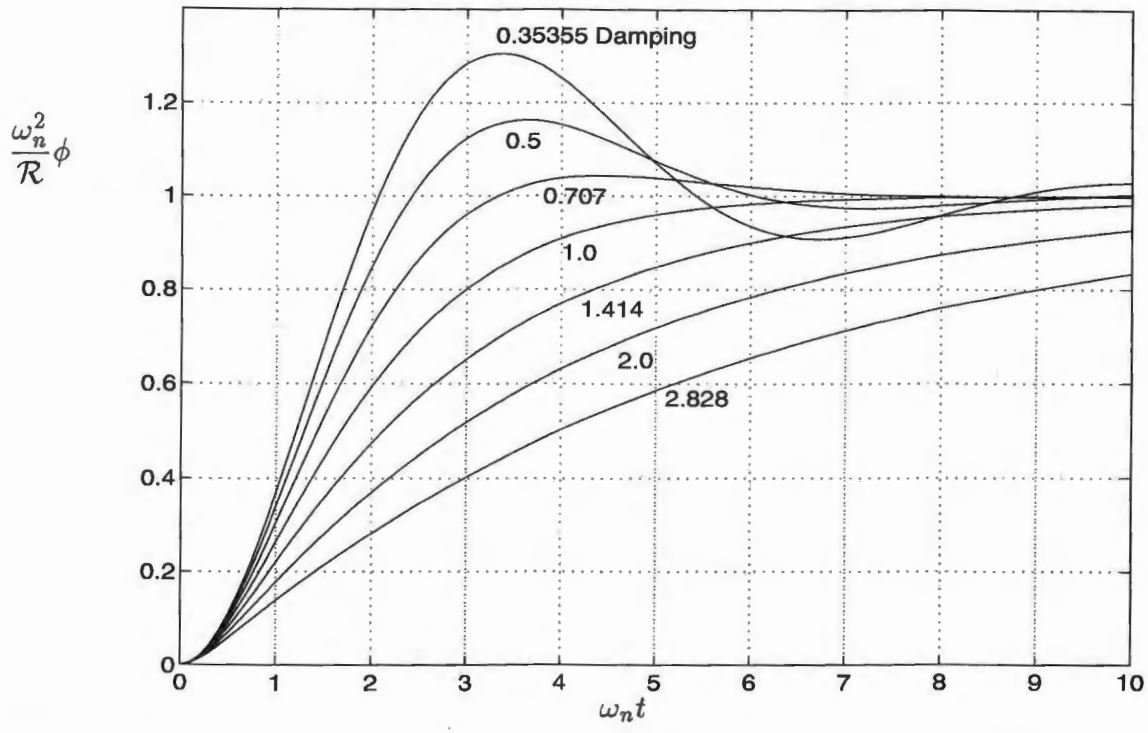

Figure 5.7. Phase error of a second-order loop (with $[F(s) = (1 + \tau_2 s/\tau_1 s)]$) for a linearly varying frequency of the input signal.

- However, recall that the transfer function we are using for the filter, $\frac{1+\tau_2 s}{\tau_1 s}$ is physically unrealizable.

Second-Order Loop (LPF with phase lead)

- the phase error eqn. are given by eqn. 5.15

- If K is very high, the expression 5.15 is identical to that for the integrator with phase lead correction as long as $\frac{\mathcal{R}t}{K}$ remains small $\Rightarrow$ curve of Fig. 5.7.

- However, the term $\frac{\mathcal{R}t}{K}$ can cause the phase detector to operate outside the linear zone even for large K $\Rightarrow$ loop falls out of lock.

- For a given ω_n and ζ, we can choose K much larger than if we used just a LPF (without phase lead correction). This means that for a given ramp freq. R, the VCO will stay in synchronism for much longer.

- Example p. 101.

Summary of Conditions

for LPF with phase lead to approximate Integrator with phase lead

phase step	$\frac{\omega_n}{K} \ll \zeta$
freq. step	$K \gg 1$
freq. ramp	$K \gg 1$ $\frac{\mathcal{R}}{K} t \ll 1$

6. Sinusoidal Operating Conditions

- Here we will designate the transfer function as:

$$\frac{\Phi_o(j\Omega)}{\Phi_i(j\Omega)} = H(j\Omega)$$

and the error function as

$$\frac{\Phi(j\Omega)}{\Phi_i(j\Omega)} = 1 - H(j\Omega)$$

where $\Omega = 2\pi f$ = modulation angular frequency.

- we will also let $\omega = 2\pi f$ designate the input signal angular frequency and the VCO central frequency.

Sinusoidal Phase Modulation

$$y_i(t) = A\sin\left[\omega t + m_i \sin(\Omega t + \Theta_i)\right]$$

- the modulation index, m_i is assumed to be small enough for phase error resulting from

$$\phi_i(t) = m_i \sin(\Omega t + \Theta_i)$$

to be small $\Rightarrow$ phase detector characteristic is linear

- The steady state VCO output signal phase, ϕ_o is also sinusoidal

$$\phi_o(t) = m_o \sin(\Omega t + \Theta_o)$$

- The steady state error is

$$\phi(t) = m \sin(\Omega t + \Theta)$$

- m_o, Θ_o, m, and Θ can be found from the transfer function 3.6 and error function 3.7.

that is:

$$\begin{aligned} m_o &= m_i \text{ Mag } [H(j\Omega)] \\ \Theta_o &= \Theta_i + \text{ Arg } [H(j\Omega)] \end{aligned} \qquad -(6.1)$$

$$\begin{aligned} m &= m_i \text{ Mag } [1 - H(j\Omega)] \\ \Theta &= \Theta_i + \text{ Arg } [1 - H(j\Omega)] \end{aligned} \qquad -(6.2)$$

- we will use the various expressions for $H(j\Omega)$ corresponding to the different loops to find the VCO modulation signal and phase error signal.

First-Order Loop

- Here

$$H(j\Omega) = \frac{K}{K + j\Omega}$$

sub into (6.1) to get

$$\left.\begin{aligned} m_o &= \frac{K}{\sqrt{K^2 + \Omega^2}} m_i \\ \Theta_o &= \Theta_i - \tan^{-1}\frac{\Omega}{K} \end{aligned}\right\} - (6.3)$$

The VCO phase modulating signal is thus:

$$\phi_o(t) = \frac{K m_i}{\sqrt{K^2 + \Omega^2}} \sin\left[\Omega t + \Theta_i - \tan^{-1}\frac{\Omega}{K}\right]$$

For the error signal, sub in (6.2)

$$\begin{aligned} m &= \frac{\Omega}{\sqrt{K^2 + \Omega^2}} m_i \\ \Theta &= \Theta_i + \frac{\pi}{2} - \tan^{-1}\frac{\Omega}{K} \end{aligned}$$

The error signal is:

$$\phi(t) = \frac{\Omega m_i}{\sqrt{K^2 + \Omega^2}} \sin\left[\Omega t + \Theta_i + \frac{\pi}{2} - \tan^{-1}\frac{\Omega}{K}\right]$$

Note: the first-order loop acts as a one pole LPF with time constant $\tau = 1/K$ with respect to the modulation $\phi_i(t)$ (of input $y_i(t)$) and the modulation $\phi_o(t)$ (of the VCO).

: as regards the error signal, its loop looks like a phase demodulator followed by a a one pole HPF of time constant $\tau = 1/K$.

Note: in fig 6.1, no part of the real loop provides access to the modulation signal ϕ_i and ϕ_o.

: in Fig 6.2, although there is no direct access to $\phi_i(t)$, there is a signal proportional to ϕ. This is $u_1 = K_1\phi$.

Note: from the analysis of transient conditions, the loop K must be high to reduce static errors and transients

- consequently, the filtering of the modulation transfer from input to VCO is minimal (Fig 6.1).

- Also the phase demodulation application is poor since all frequency modulation components below $K/2\pi$ Hz are cutoff (Fig 6.2).

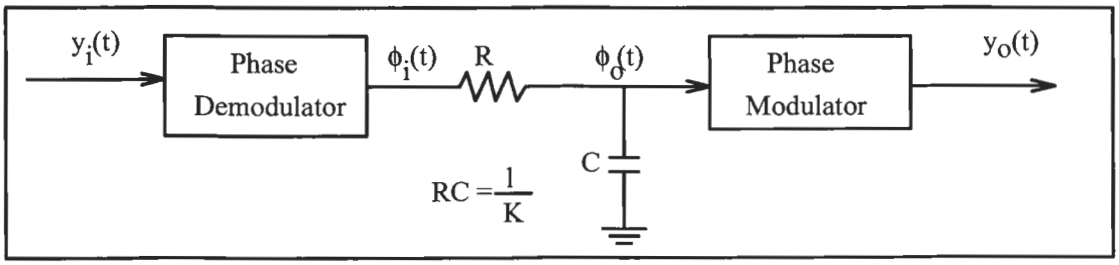

Figure 6.1. Model of a first-order loop for input signal modulation and VCO signal modulation.

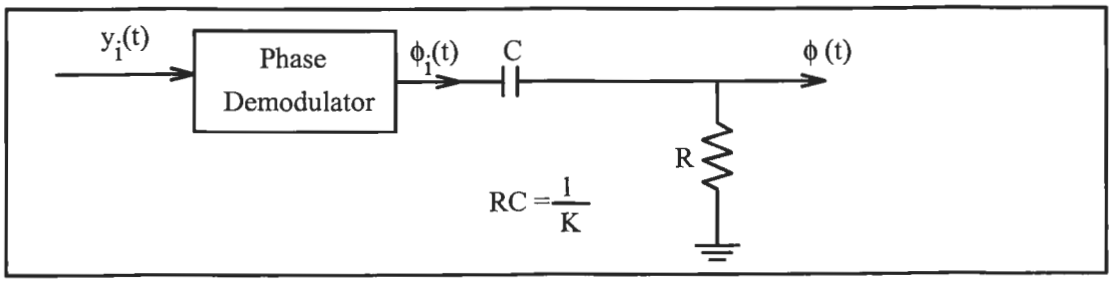

Figure 6.2. Model of a first-order loop for input signal modulation and phase error in the loop.

Second-Order Loop (Integrator with phase-lead correction)

Sub the expression for $H(j\Omega)$ into eqn. (6.1).

$$H(j\Omega) = \frac{\omega_n^2 + j2\zeta\omega_n\Omega}{\omega_n^2 - \Omega^2 + j2\zeta\omega_n\Omega}$$

yields

$$m_o = m_i \sqrt{\frac{\omega_n^4 + 4\zeta^2\omega_n^2\Omega^2}{\left(\omega_n^2 - \Omega^2\right)^2 + 4\zeta^2\omega_n^2\Omega^2}} \qquad -(6.5)$$

$$\Theta_o = \Theta_i + \tan^{-1}\left(2\zeta\frac{\Omega}{\omega_n}\right) - \tan^{-1}\left(\frac{2\zeta\omega_n\Omega}{\omega_n^2 - \Omega^2}\right)$$

- These curves are plotted in Fig. 6.3 and 6.4, Blanchard where $x = \Omega/\omega_n$.

- For the error signal we have:

$$m = m_i \frac{x^2}{\sqrt{\left(1 - x^2\right)^2 + 4\zeta^2 x^2}} \qquad -(6.6)$$

$$\Theta = \Theta_i + \pi - \tan^{-1}\frac{2\zeta x}{1 - x^2}$$

These are given in Fig 6.5 and 6.6.

- Note: loop gain K has no influence on above expressions.

- We have two possible applications

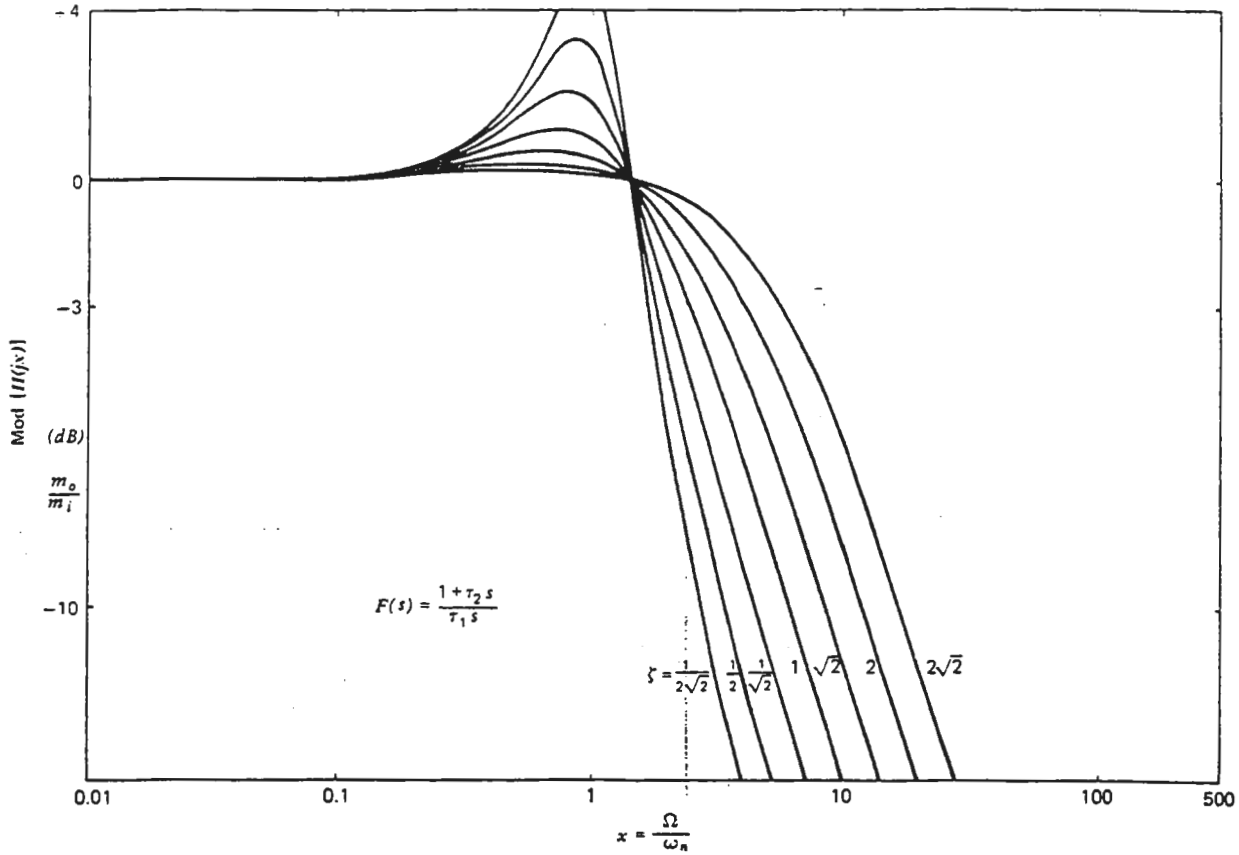

FIGURE 6.3. Transfer function of a second-order loop with $F(s)=(1+\tau_2 s)/(\tau_1 s)$: amplitude-frequency characteristic.

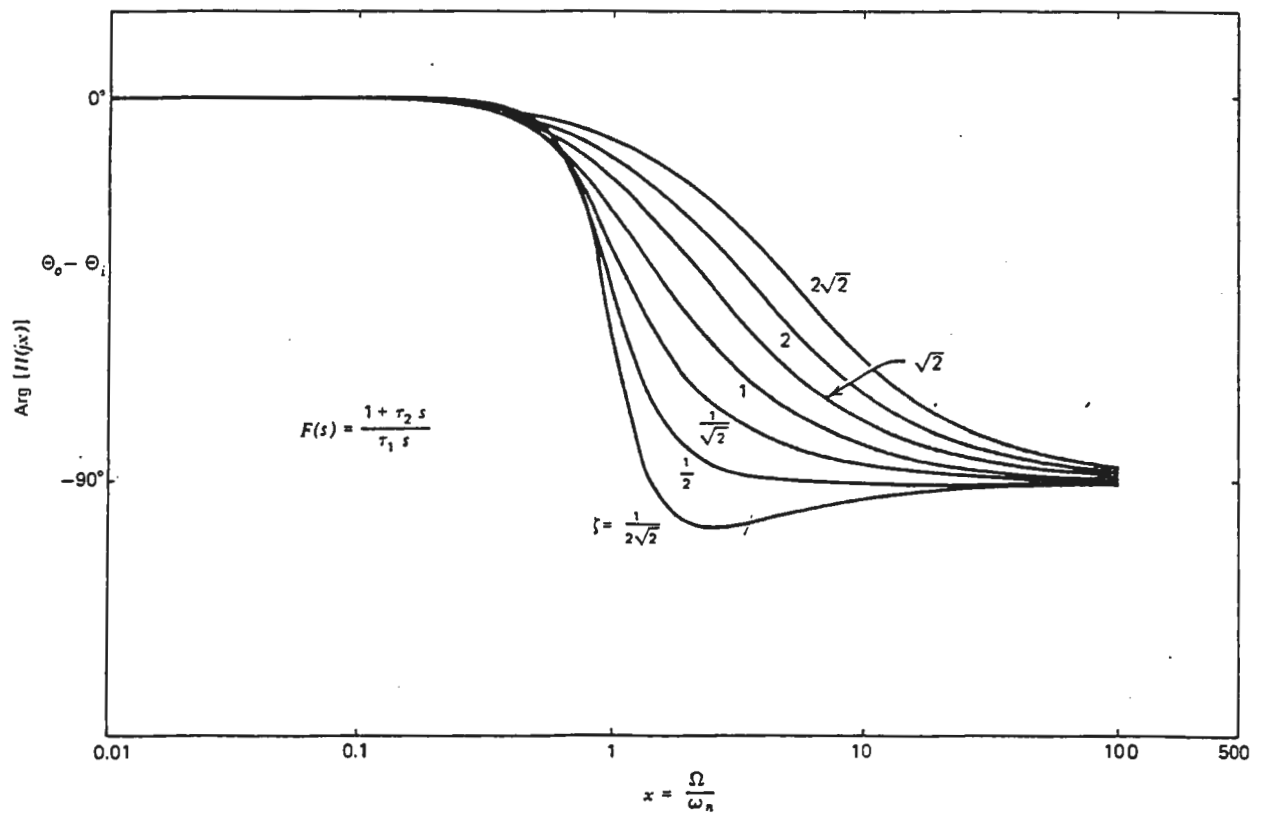

FIGURE 6.4. Transfer function of a second-order loop with $F(s)=(1+\tau_2 s)/(\tau_1 s)$: phase-frequency characteristic.

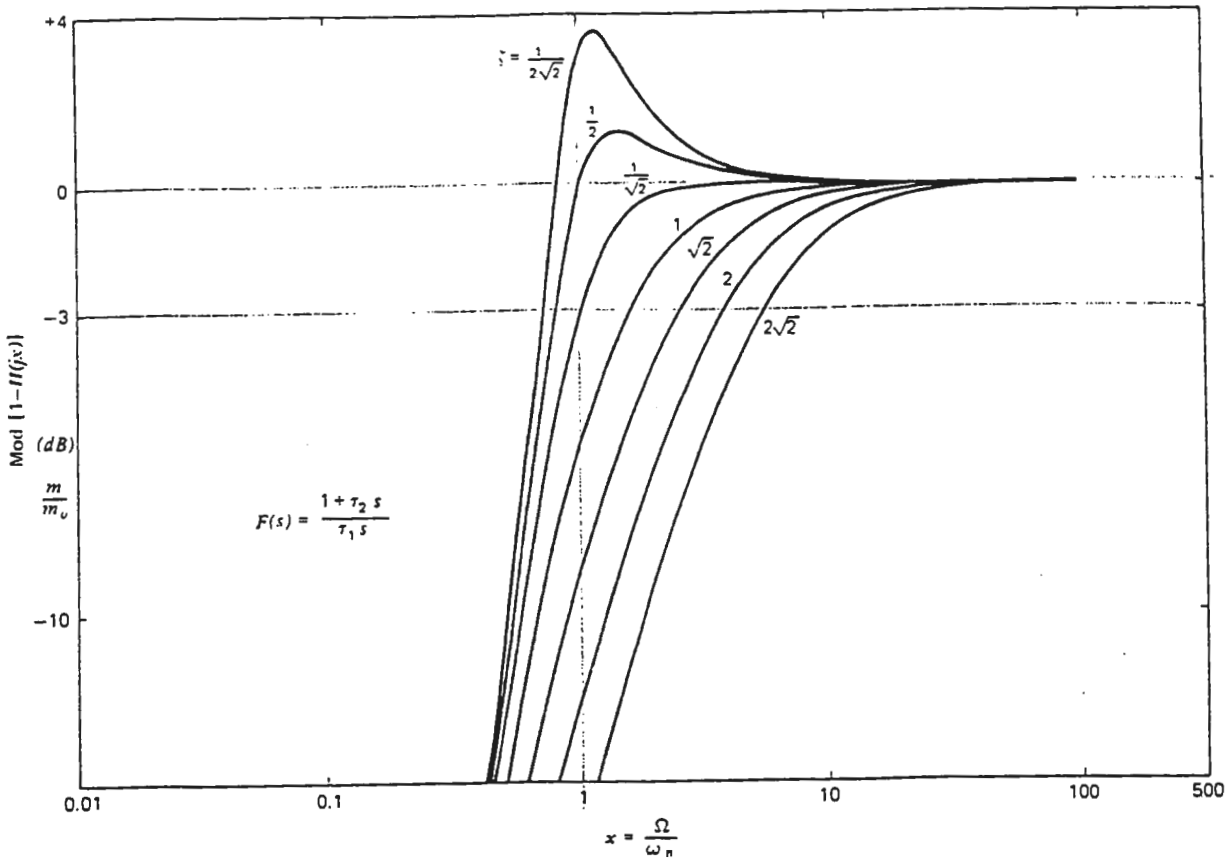

FIGURE 6.5. Error function of a second-order loop with $F(s)=(1+\tau_2 s)/(\tau_1 s)$: amplitude-frequency characteristic.

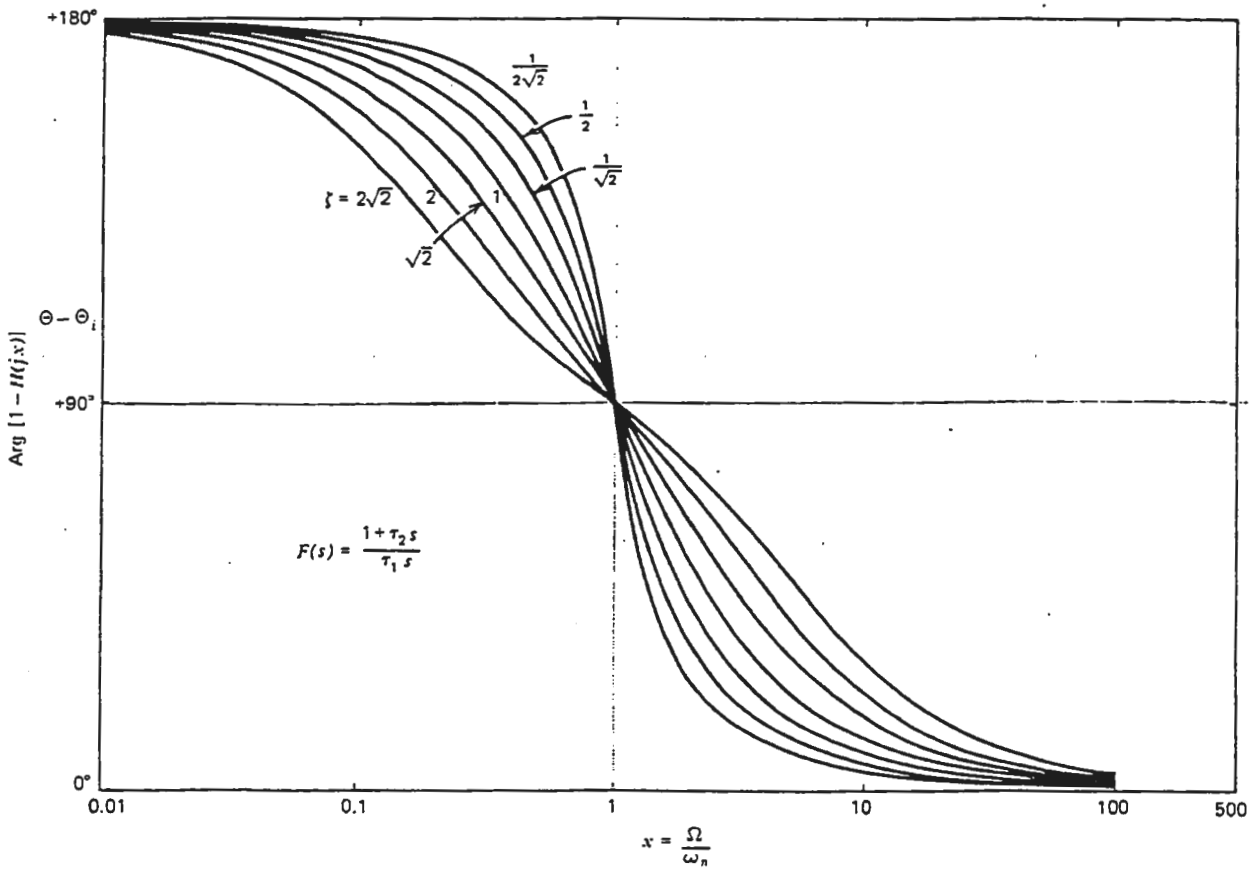

FIGURE 6.6. Error function of a second-order loop with $F(s)=(1+\tau_2 s)/(\tau_1 s)$: phase-frequency characteristic.

- narrow band LPF filtering of modulation

- demodulation of input signal so as to lose only fraction of modulation spectrum while maintaining small phase error in case of VCO drift.

- Note - From curves of Fig. 6.3 (modulation transferred from input to VCO), the amplitude characteristics all exceed 0 dB for $x < 1$

- The max value of overshoot increases for lower damping factor.

- All curves cut 0 dB at $x = \sqrt{2}$.

- Neg. slope after $x = \sqrt{2}$ increases as ζ ~~increases~~ decreases

- asymptotic slope is -1 for $x \to \infty$

- From curves of Fig 6.5 (error signal), the error signal is a reliable image of input modulation for $x > 1$.

- This is especially true for $\sqrt{2}/2 < \zeta < 1$.

- the low frequencies are attenuated $\Rightarrow$ loop acts as a phase demod followed by HPF with slope $= +2$ as $x \to 0$.

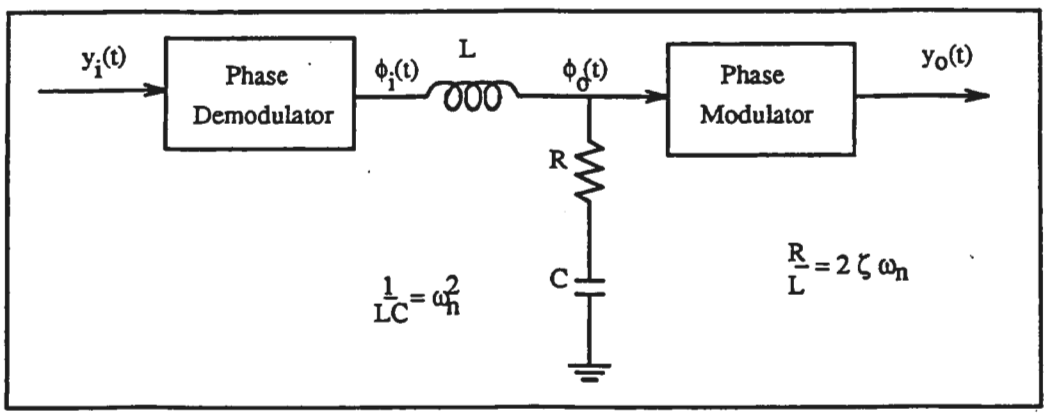

Figure 6.7. Model of a second-order loop [with int. + ph. lead] for input signal and VCO signal Modulations

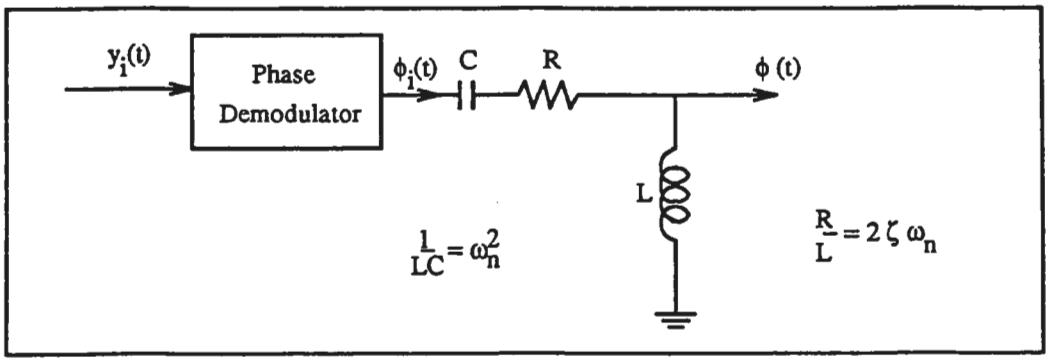

Figure 6.8. Model of a second-order loop [with int. + ph. lead] working as an input signal phase demodulator.

Second-Order Loop (LPF with phase-lead correction)

The signal modulating the VCO has:

$$m_o = m_i \sqrt{\frac{1+\left(2\zeta - \frac{\omega_n}{K}\right)^2 x^2}{(1-x^2)^2 + 4\zeta^2 x^2}} \qquad -(6.9)$$

$$\Theta_o = \Theta_i + \tan^{-1}\left(2\zeta - \frac{\omega_n}{K}\right) x - \tan^{-1}\left(\frac{2\zeta x}{1-x^2}\right)$$

The error signal (demodulated signal) has:

$$m = m_i \sqrt{\frac{x^4 + (\omega_n^2/K^2)\, x^2}{(1-x^2)^2 + 4\zeta^2 x^2}} \qquad -(6.10)$$

$$\Theta = \Theta_i + \pi - \tan^{-1}\left(\frac{\omega_n}{Kx}\right) - \tan^{-1}\left(\frac{2\zeta x}{1-x^2}\right)$$

where $x = \Omega/\omega_n$.

- generally $K \gg \omega_n$ and consequently (6.9) and (6.10) approximate (6.5) and (6.6). Consequently, curves 6.3 to 6.6 can also be used for this loop.

Note: for the error signal, the approximation of using curves 6.5 and 6.6 is not good for low frequencies ($x \to 0$).

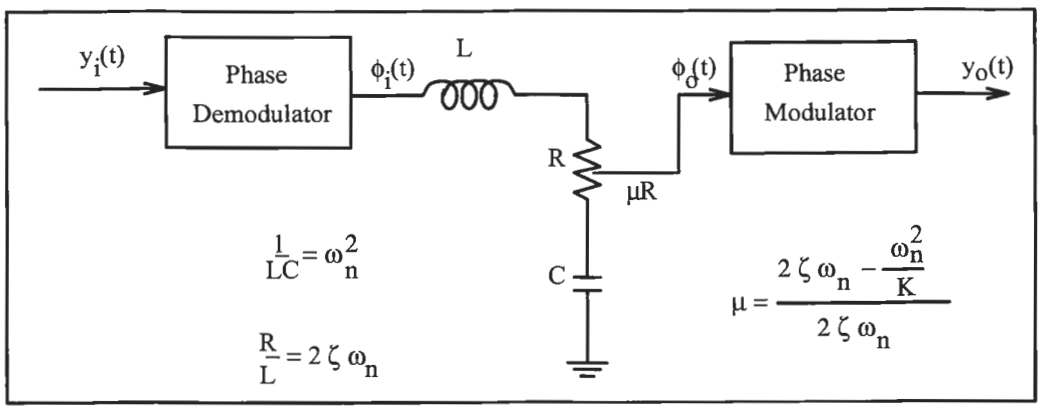

Figure 6.13. Model of a second-order loop [with LPF + ph. lead] for input signal and VCO signal Modulations

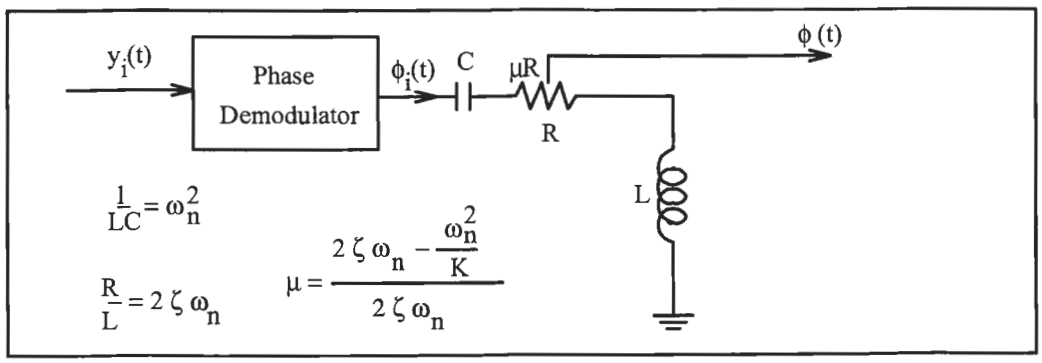

Figure 6.14. Model of a second-order loop [with LPF + ph. lead] working as a phase demodulator.

- We have the following general conclusions for second-order loops:

- if Ω is lower than ω_n, the input signal modulation is transferred to the VCO signal with minimal attenuation and phase shift. The phase error stays low even if input modulation index goes beyond phase detector linear zone.

- if Ω is higher than ω_n, the input is <u>not</u> transferred to VCO output. The loop error is a good duplicate of the input signal modulation (phase demodulation operation). However if loop phase error is to be kept low for phase comparator to remain in linear zone, m_i must be below:

$$\begin{cases} \pi/4 & \text{for sin detector} \\ \pi/2 & \text{for triangle detector} \\ \pi & \text{for sawtooth detector} \end{cases}$$

6.2 Establishment of Steady-State Conditions

- the above expressions are valid only for steady state conditions

- we will find how the loop responds when

$$\phi_i(t) = m_i \sin \Omega t \Upsilon(t)$$

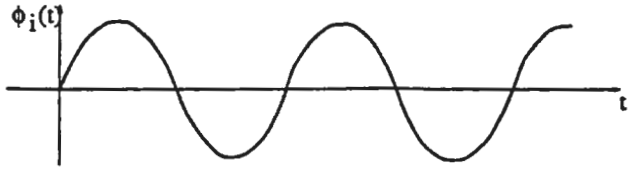

- 2 methods
  - first is to solve differential eqn.
  - second is to use Laplace transforms

- we have

$$\Phi_i(s) = m_i \frac{\Omega}{s^2 + \Omega^2}$$

- the loop phase error is then given by eqn (3.9)

$$\Phi(s) = m_i \frac{\Omega}{s^2 + \Omega^2} [1 - H(s)]$$

- Now for second order loop with integrator and phase lead correction:

$$F(s) = \frac{1 + \tau_2 s}{\tau_1 s}$$

$$\Phi(s) = m_i \frac{\Omega s^2}{(s^2 + \Omega^2)(s^2 + 2\zeta\omega_n s + \omega_n^2)}$$

- Taking the reciprocal transform gives

$$o(t) = \phi_p(t) + \phi_T(t)$$

where

$\phi_p(t)$ = steady state response

$\phi_T(t)$ = transient response

- the expression is given page 120 Blanchard

- The transient term has 2 parts - the first is the loop response to a freq. step $m_i\Omega$

- Note: when the modulation $\phi_i(t) = m_i \sin \Omega t \Upsilon(t)$ is applied, the loop does undergo an instantaneous freq. change

$$\left.\frac{d\phi_i}{dt}\right|_{t=0} = m_i\Omega$$

The second transient part represents the signal required to change $\phi(t)$ from its null value at $t = 0$ to the steady state value as shown. This term is negligible if $\Omega \ll \omega_n$.

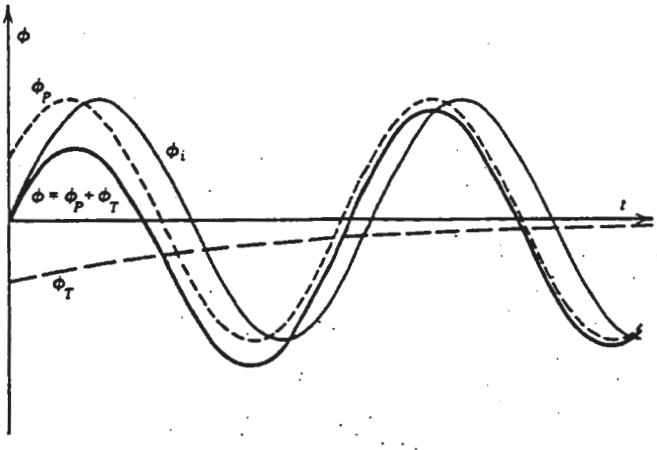

FIGURE 6.15. Transient response of a second-order loop to a sinusoidal phase modulation of the input signal.

6.3 Sinusoidal Frequency Modulation

- here

$$f_{i_{inst}} = f + \Delta f_i \cos(\Omega t + \Theta_i) \qquad -(6.11)$$

- consequently

$$y_i(t) = A \sin\left[\omega t + \frac{2\pi\Delta f_i}{\Omega} \sin(\Omega t + \Theta_i)\right]$$

- Therefore, the modulation can be interpreted as a phase modulation $\phi_i(t)$ where:

$$\phi_i(t) = \frac{2\pi\Delta f_i}{\Omega} \sin(\Omega t + \Theta_i)$$

$$= \frac{\Delta\omega_i}{\Omega} \sin(\Omega t + \Theta_i)$$

- Note: difference between freq. mod. and phase mod. is that the modulation index:

$$m_i = \frac{\Delta\omega_i}{\Omega} \qquad -(6.12)$$

is not independent of Ω.

- Providing we remain in the linear domain, the VCO output signal $y_o(t)$ is:

$$y_o(t) = B\cos\left[\omega t + m_o \sin(\Omega t + \Theta_o)\right]$$

where m_o and Θ_o are related to m_i and Θ_i by eqn (6.12). $G_c(s)$ and m_i is given by 6

- Consequently

$$y_o(t) = B\cos\left[\omega t + \frac{\Delta\omega_i}{\Omega}\text{Mod}\,[H(j\Omega)]\sin\left(\Omega t + \Theta_i + \text{Arg}[H(j\Omega)]\right)\right]$$

- the instantaneous freq. of the VCO is then:

$$f_{o_{inst}} = f + \Delta f_i\ \text{Mod}[H(j\Omega)]\cos\left(\Omega t + \Theta_i + \text{Arg}[H(j\Omega)]\right)$$

Comparing with (6.11) we see that

$$f_{o_{inst}} = f + \Delta f_o \cos(\Omega t + \Theta_o)$$

where

$$\left.\begin{aligned}\Delta f_o &= \Delta f_i \text{Mod}[H(j\Omega)]\\ \Theta_o &= \Theta_i + \text{Arg}[H(j\Omega)]\end{aligned}\right\} \qquad -(6.14)$$

Note: the curves of $\frac{\Delta f_o}{\Delta f_i}$ and the curves of $\Theta_o - \Theta_i$ versus $\frac{\Omega}{\omega_n}$ are identical to the curves representing $\frac{m_o}{m_i}$ and $\Theta_o - \Theta_i$ obtained for phase modulation. Therefore, we use curves 6.3 and 6.4.

Note: we can also use the models for the loops on pages 6-3 and 6-4 if we replace the phase demod and phase mod blocks with freq demod and freq mod.

- For the error signal we have

$$\phi(t) = \Delta\phi \sin(\Omega t + \Theta) \qquad -(6.15)$$

where

$$\left.\begin{aligned}\Delta\phi &= m_i \text{Mod}[1 - H(j\Omega)] = \frac{\Delta\omega_i}{\Omega}\text{Mod}[1 - H(j\Omega)]\\ \Theta &= \Theta_i + \text{Arg}[1 - H(j\Omega)]\end{aligned}\right\} \qquad -(6.16)$$

Note: -Here the curves giving the phase difference between the error signal and the input signal (viewed as a phase mod) remain unchanged and we use Fig. 6.6.

- However, the case for error signal amplitude $\Delta\phi$ is different and is analyzed for each type of loop.

- $\Delta\phi$ is very important in order to check the linearity hypothesis on which the analyses are based.

First-Order Loop

- here

$$\Delta\phi = \frac{\Delta\omega_i}{\sqrt{K^2+\Omega^2}} \qquad -(6.17)$$

a) - if $\Omega \ll K$

$$\Delta\phi \approx \frac{\Delta\omega_i}{K}$$

- here the linearity condition requires the input signal angular freq deviation, $\Delta\omega_i$ to remain below K.

b) if $\Omega \gg K$

$$\Delta\phi \approx \frac{\Delta\omega_i}{\Omega} = m_i$$

- here linearity condition requires input signal phase mod index, m_i to remain small.

Second-Order Loop - Integrator with phase lead correction

- Here

$$\begin{aligned}\Delta\phi &= \Delta\omega_i \frac{\Omega}{\sqrt{(\omega_n^2-\Omega^2)^2+4\zeta^2\omega_n^2\Omega^2}} \\ &= \frac{\Delta\omega_i}{\omega_n}\frac{x}{\sqrt{(1-x^2)^2+4\zeta^2x^2}}\end{aligned} \qquad -(6.18)$$

- curves for $\Delta\phi\left[\frac{\omega_n}{\omega_i}\right]$ are given in Fig 6.16 Blanchard.

- Note: curves are symmetrical wrt $x = 1$ on a log scale, the error signal max. amplitude occurs at $x = 1$ and is:

$$\Delta\phi_M = \frac{\Delta\omega_i}{2\zeta\omega_n}$$

- The values for x for which we get a 3 dB attenuation in $\Delta\phi$ are:

$$x' = \sqrt{\zeta^2+1}+\zeta$$
$$x'' = \sqrt{\zeta^2+1}-\zeta$$

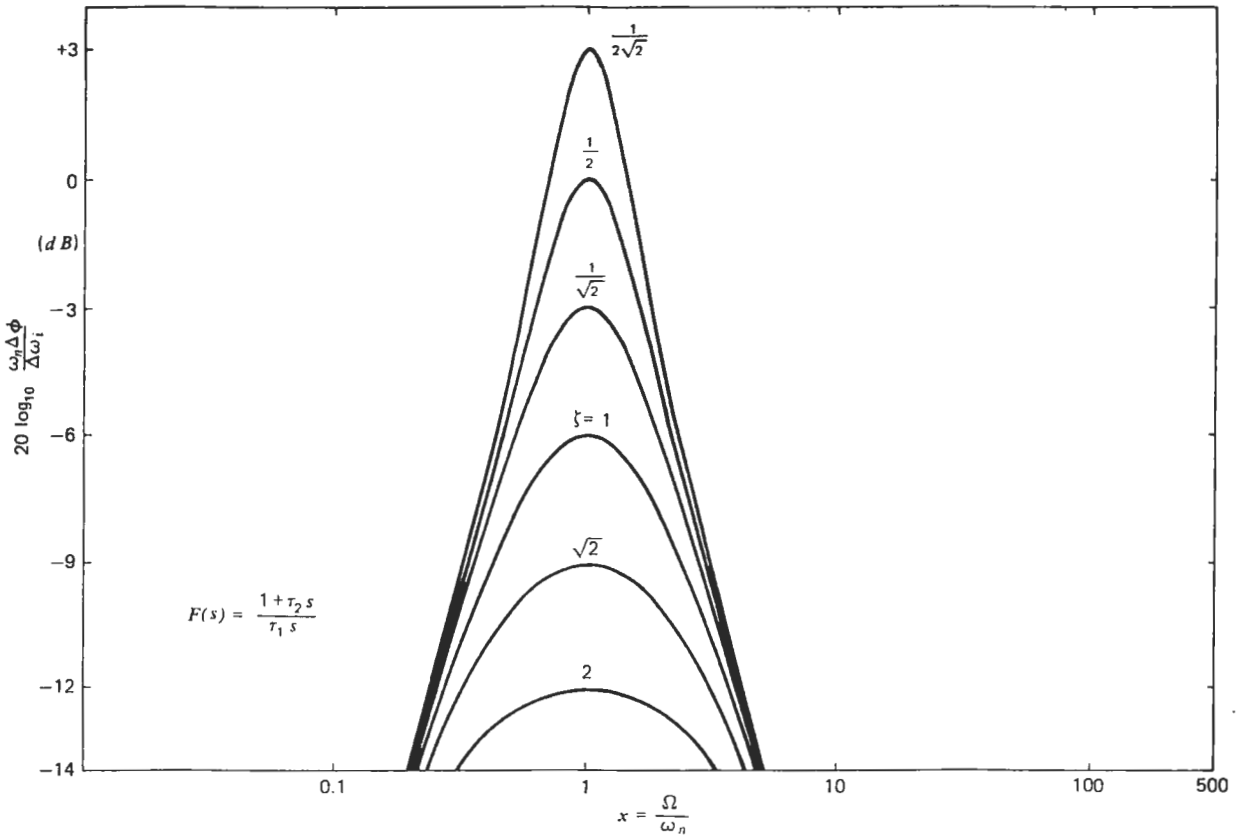

FIGURE 6.16. Amplitude-frequency characteristic of the phase error of a second-order loop $[F(s)=(1+\tau_2 s)/(\tau_1 s)]$ for a sinusoidal frequency modulation of the input signal.

Note:

$$x'x'' = 1 \qquad \text{and} \qquad x' - x'' = 2\zeta$$

- This result lets us find experimentally the ω_n and ζ of a loop of this type, just by exciting the loop with a signal which is frequency modulated at Ω (variable).

- The frequency deviation is set low so that:

$$\frac{2\pi\Delta f_i}{2\hat{\zeta}\hat{\omega}_n} < 1/2 \quad \text{rad}$$

where $\hat{\zeta}$ and $\hat{\omega}_n$ are the estimated values of ζ and ω_n.

- measure the two angular freqs, Ω' and Ω'' corresponding to -3 dB of the max value (use scope or AC voltmeter)

- Example page 127.

Second-Order Loop - LPF with phase lead correction

- Here

$$\Delta\phi = \frac{\Delta\omega_i}{\omega_n}\sqrt{\frac{x^2+\omega_n^2/K^2}{(1-x^2)^2+4\zeta^2x^2}} \qquad -(6.20)$$

- again when $K \gg \omega_n$, the results are approximately the same as for the integrator with phase-lead correction and Fig 6.16 can be used.

- However, the symmetry in Fig 6.16 around $x = 1$ is only approximate since as $x \to 0$, $\Delta\phi$ does not approach 0 but $\Delta\omega_i/K$.

Phase-Locked Loop as a Discriminator

We will see that we can pick up a signal in the loop which under certain conditions is a good duplicate of the input signal modulation.

- if we take the first order loop error signal and multiply it by K_1 we get $u_1(t)$.

$$\begin{aligned} u_1(t) &= \frac{K_1\Delta\omega_i}{\sqrt{K^2+\Omega^2}}\sin\left(\Omega t+\Theta_i+\frac{\pi}{2}-\tan^{-1}\frac{\Omega}{K}\right) \\ &= \Delta u_1\cos\left(\Omega t+\Theta_i-\tan^{-1}\frac{\Omega}{K}\right) \end{aligned}$$

compare this with eqn (6.11) (rewritten below)

$$f_{i_{inst}} = f + \Delta f_i\cos(\Omega t+\Theta_i) \qquad -(6.11)$$

- We see that $u_1(t)$ is a duplicate of the modulating signal differing only by a constant and a low pass filtering with $\tau = 1/K$.

- this is the same as a discriminator with slope K_D followed by the LPF

$$K_D = \lim_{\Omega\to 0}\frac{\Delta u_1}{\Delta f_i} = \frac{2\pi K_1}{K} = \frac{2\pi}{K_3} \quad \text{in V/Hz if } K_3 \text{ in (rad/sec/V)}$$

$$= \frac{1}{K_3} \qquad \text{in V/Hz if } K_3 \text{ in (Hz/V)}$$

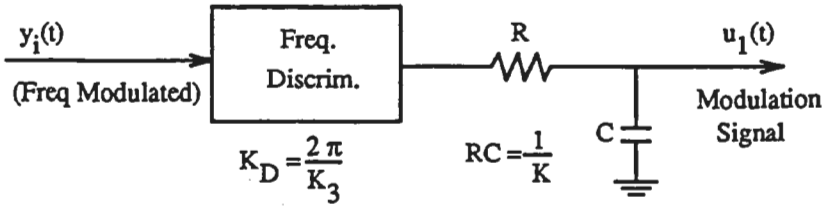

Note: discriminator slope is independent of K_1 and inversely dependent on VCO sensitivity.

Second-Order Loop - Integrator with phase lead correction or LPF with phase lead correction

- Fig. 6.16 shows that the phase detector output voltage cannot be used as a discriminator output signal.

- However, we saw (Sect 6.3) that the VCO freq. modulation is a duplicate of the input freq. modulation accounting for $H(j\Omega)$.

- Now the VCO modulation is proportional to u_2

- Therefore, the VCO command signal u_2 can be used as the discriminator output.

- input signal modulation is $\Delta f_i \cos(\Omega t + \Theta_i)$ then the VCO modulation is $\Delta f_o \cos(\Omega t + \Theta_o)$ where Δf_o and Θ_o are related to Δf_i and Θ_i by (6.14) .

- Now

$$\Delta f_o = \frac{K_3}{2\pi}\Delta u_2$$

$$\therefore \quad u_2(t) = \Delta u_2 \cos(\Omega t + \Theta_o)$$

with

$$\Delta u_2 = \frac{2\pi \Delta f_i}{K_3}\text{MOD}[H(j\Omega)]$$

The loop acts as a discriminator with slope:

$$K_D = \lim_{\Omega \to 0} \frac{\Delta u_2}{\Delta f_i} = \frac{2\pi}{K_3} \quad \text{in V/Hz where } K_3 \text{ is in (rad/sec/V)}$$

Note: For Integrator with correction and for LPF with correction (and with K large) Fig. 6.3 response curves all have overshoot in the discriminator bandwidth and asymptotic slope of -6 dB/octave.

- If we want to avoid this overshoot and obtain a stronger filtering at higher frequencies, we include a supplemental filtering of $u_2(t)$ to obtain $u_2'(t)$ where:

$$\frac{u_2'(j\Omega)}{u_2(j\Omega)} = \frac{1}{1 + j\Omega\tau_2}$$

or

$$\text{MOD}\left[\frac{u_2'(j\Omega)}{u_2(j\Omega)}\right] = \frac{1}{\sqrt{1 + \Omega^2\tau_2^2}} = \frac{1}{\sqrt{1 + \omega_n^2\tau_2^2\frac{\Omega^2}{\omega_n^2}}} = \frac{1}{\sqrt{1 + 4\zeta^2 x^2}}$$

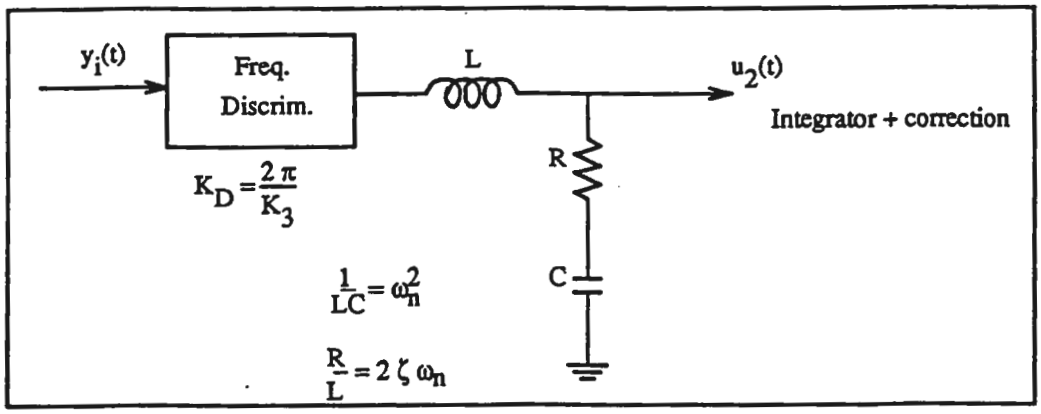

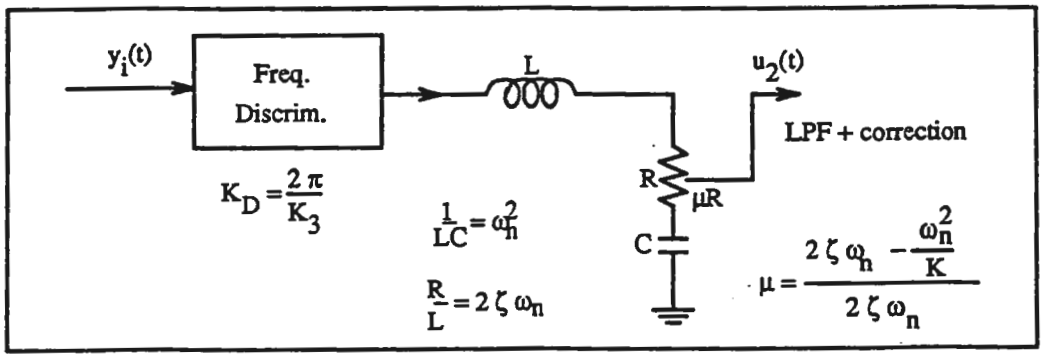

since

$$\omega_n \tau_2 = 2\zeta$$

- This means:

$$\frac{\Delta u_2'}{\Delta f_i} = \frac{2\pi}{K_3} \frac{1}{\sqrt{(1-x^2)^2 + 4\zeta^2 x^2}}$$

- This characteristic is given in Fig 6.9 (with $\frac{m_o}{m_i}$ replaced by $\frac{\Delta u_2'}{\Delta f_i}\left[\frac{K_3}{2\pi}\right]$).

-Note : there is no bandwidth overshoot if $\zeta \geq \sqrt{2}/2$

: asymptotic slope = -12 dB /octave.

: this signal $u_2'(t)$ can also be obtained by taking the signal between R_2 and C for a LPF with phase-lead correction.

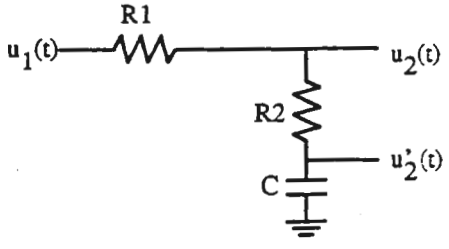

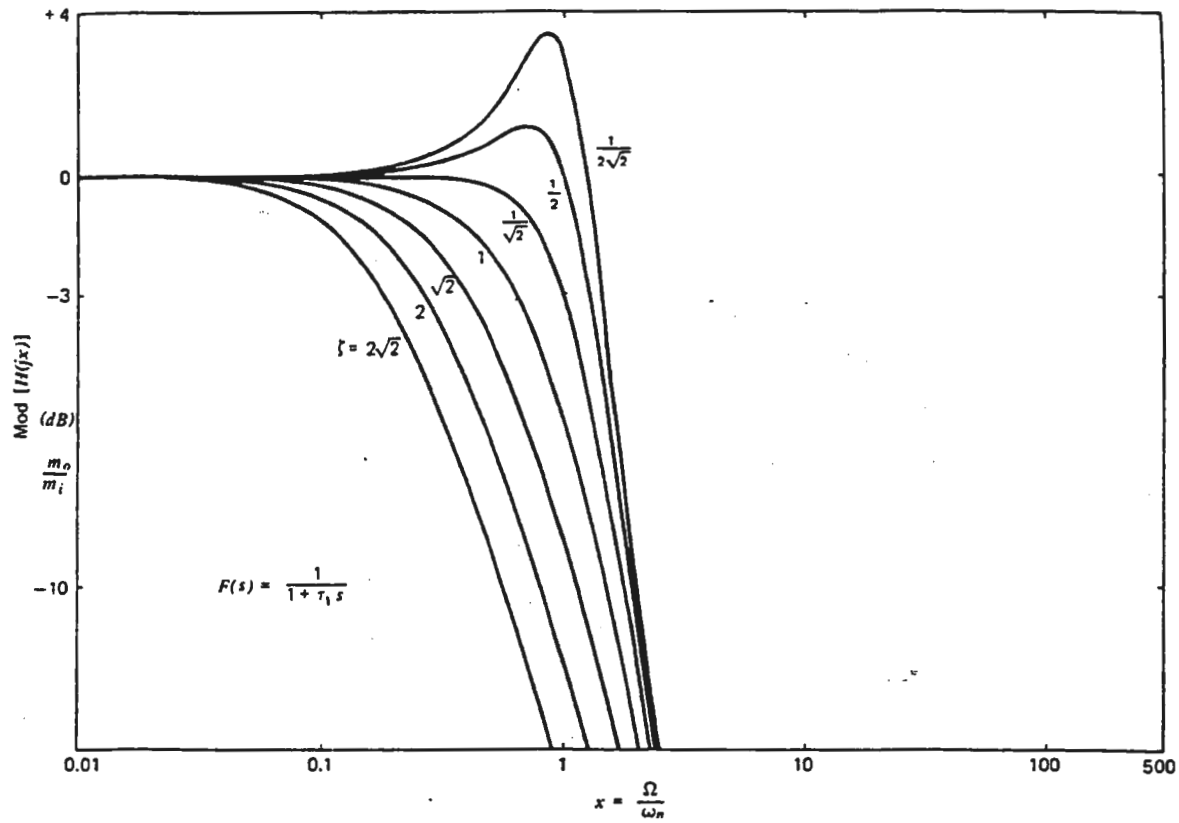

FIGURE 6.9. Transfer function of a second-order loop with $F(s) = 1/(1+\tau_1 s)$: amplitude-frequency characteristic.

Second-Order Loop - LPF

- Here

$$F(s) = \frac{1}{1+\tau_1 s}$$

The error signal is given by 6.19

$$\Delta\phi = \Delta\omega_i \frac{2\zeta}{\omega_n} \sqrt{\frac{1+\frac{x^2}{4\zeta^2}}{(1-x^2)^2+4\zeta^2 x^2}} \qquad -(6.19)$$

- Here $\frac{\omega_n}{2\zeta} = K$ and $\Delta u_1 = K_1 \Delta\phi$ tends toward $\frac{\Delta\omega_i}{K_3}$ for low mod frequencies.

- Discriminator slope:

$$K_D = \frac{2\pi}{K_3}$$

- change variables in above equation: let $\tau_1 = \alpha/K$ then:

$$\omega_n = \sqrt{\frac{K}{\tau_1}} = \frac{K}{\sqrt{\alpha}} \qquad \text{and} \qquad 2\zeta\omega_n = \frac{1}{\tau_1} \quad \Rightarrow \quad \zeta = \frac{1}{2\sqrt{\alpha}}$$

- Consequently:

$$\Delta\phi = \frac{\Delta\omega_i}{K}\sqrt{\frac{1+\alpha^2\frac{\Omega^2}{K^2}}{\left(1-\alpha\frac{\Omega^2}{K^2}\right)^2+\frac{\Omega^2}{K^2}}}$$

- This is plotted in Fig. 6.19, Blanchard.

- Note: All curves have the same value as $\Omega \to 0$, consequently the discriminator slope is independent of τ_1 for low Ω.

- Note: For $\alpha = 0$, $\tau = 0$ and the loop is a first-order loop.

- Example page 137.

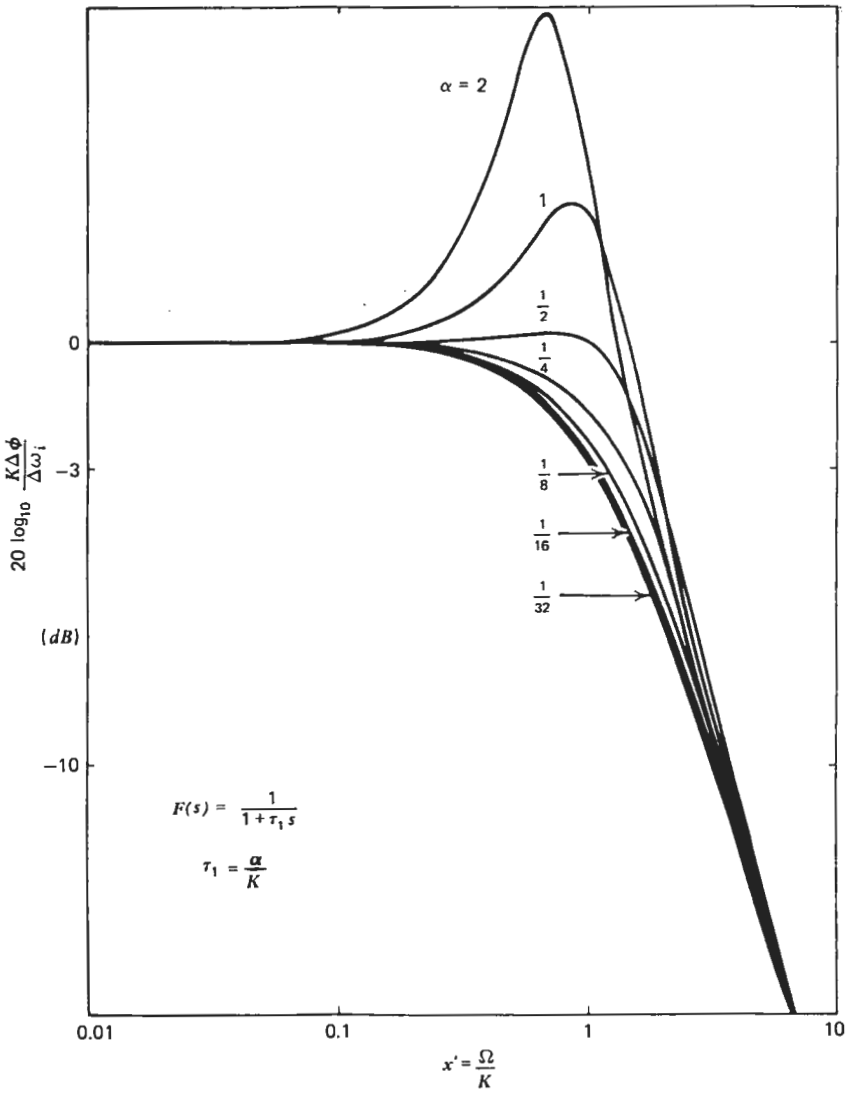

FIGURE 6.19. Amplitude-frequency characteristic of a second-order loop with $F(s)=1/(1+\tau_1 s)$ working as a frequency demodulator (the error signal being the output signal).

10. Natural Acquisition of Input Signal

- we have previously disregarded the phase detector nonlinearity by assuming the phase error to be small

- this led to linear diff eqn which are easy to handle in Laplace Transform Domain for low order loops

- this above assumption implies VCO synchronism

- However, when the signal actually arrives at the loop input, an unknown phase difference exists between the input and the VCO signals ⇒ linear approx is not valid

- We have to use the real characteristic of the VCO ⇒ nonlinear dif eqn.

- To simplify matters, we will deal only with an unmodulated input signal, without additive noise, and employ a sinusoidal phase detector.

- the operating principles are not too different for the other types of phase detectors.

Signal Acquisition by a First-Order Loop

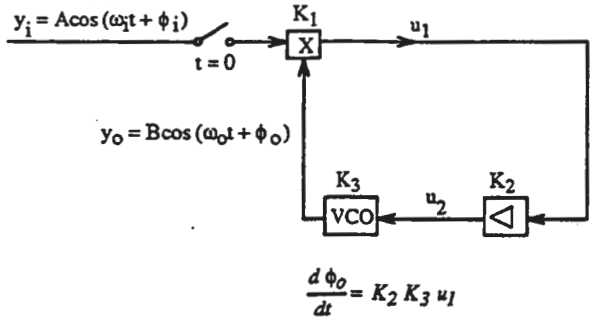

FIGURE 10.1 First-order phase-locked loop.

we have

$$\frac{d\phi_o}{dt} = K_2 K_3 u_1(t)$$

$$\phi_o = K_2 K_3 \int u_1(t)dt + C$$

- now for $t < 0$, $u_1 = 0$ and $\phi_o = C$.

- we will now assume $C = 0$ without limitations

- for $t \geq 0$

$$u_1(t) = K_1 \cos[(\omega_i - \omega_o)t + \theta_i - \phi_o(t)]$$

and

$$\frac{d\phi_o(t)}{dt} = K_1 K_2 K_3 \cos[(\omega_i - \omega_o)t + \theta_i - \phi_o(t)] \qquad -(1)$$

let

$$K = K_1 K_2 K_3$$

$$\Omega_o = \omega_i - \omega_o$$

$$\phi(t) = \Omega_o t + \theta_i - \phi_o(t)$$

implying:

$$\frac{d\phi}{dt} = \Omega_o - \frac{d\phi_o}{dt}$$

Then eqn (1) becomes

$$\frac{d\phi}{dt} = \Omega_o - K\cos\phi(t)$$

or

$$dt = \frac{d\phi}{\Omega_o - K\cos\phi} \qquad -(2)$$

Phase Acquisition

- assume the highly unlikely case where $\Omega_o = 0$

- eqn. (2) becomes

$$\frac{d\phi}{\cos\phi} = -K\,dt$$

integrate

$$\frac{1}{2}\ln\left[\frac{1+\sin\phi}{1-\sin\phi}\right] = -K(t - t_o)$$

or

$$\frac{1+\sin\phi}{1-\sin\phi} = e^{-2Kt}e^{+2Kt_o}$$

- to determine the integration constant t_o, we state that at $t = 0$, ϕ is equal to θ_i

- hence

$$\sin\phi = \frac{(1+\sin\theta_i)e^{-2Kt} - (1-\sin\theta_i)}{(1+\sin\theta_i)e^{-2Kt} + (1-\sin\theta_i)} \qquad -(3)$$

- now when $t \to \infty$ we have:

$$\sin\phi \to -1 \quad ; \quad \phi \to -\pi/2 \quad \text{if} \quad K > 0$$

$$\sin\phi \to +1 \quad ; \quad \phi \to \pi/2 \quad \text{if} \quad K < 0$$

- to find the direction of the variation of $\sin\phi$ between $t = 0$ and $t \to \infty$

$$\frac{d\sin\phi}{dt} = \frac{-4K(1+\sin\theta_i)(1-\sin\theta_i)e^{-2Kt}}{D^2}$$

where D is the denominator of eqn. (3).

- this indicates that the sign of $\frac{d \sin \phi}{dt}$ is constant and opposite to the sign of K.

Case a $K > 0$

- the trig circle shown describes the variation of ϕ with time

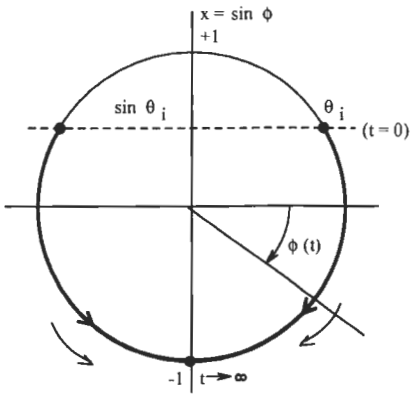

- Here according to the initial value of θ_i, $\phi(t)$ describes the left or the right arc to the point -1 which it reaches at $t \rightarrow \infty$.

- Note: $\theta_i = 90° \Rightarrow \sin\phi = 1 \Rightarrow$ this is an unstable equilibrium point. As soon as θ_i diverges by a small value ϵ, the sign of $\frac{d \sin \phi}{dt}$ enhances the deviation towards the stable point at -90°

Case b $K < 0$

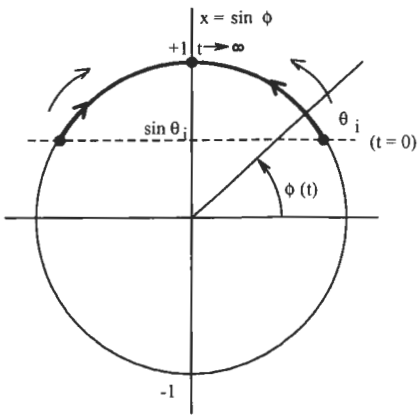

- here the stable point is at +90°

- Note: the only difference between $K < 0$ and $K > 0$ is a lead or lag of the VCO by 90° wrt the incoming signal. This is also valid for the triangle wave phase detector but not for the sawtooth phase detector.

Frequency Acquisition

- now suppose that we have an initial phase difference θ_i and a frequency difference Ω_o.

From eqn. (2) we have

$$t - t_o = \int \frac{d\phi}{\Omega_o - K\cos\phi}$$

three cases can be identified; one for $|\Omega_o| > |K|$ and two for $|\Omega_o| < |K|$:

$$t - t_o = \frac{2}{\sqrt{\Omega_o^2 - K^2}} \tan^{-1}\left[\frac{(\Omega_o + K)\tan\left(\frac{\phi}{2}\right)}{\sqrt{\Omega_o^2 - K^2}}\right] \quad ; \quad |\Omega_o| > |K| \qquad -(4)$$

$$= \frac{1}{\sqrt{K^2 - \Omega_o^2}} \ln\left[\frac{(\Omega_o + K)\tan\left(\frac{\phi}{2}\right) - \sqrt{K^2 - \Omega_o^2}}{(\Omega_o + K)\tan\left(\frac{\phi}{2}\right) + \sqrt{K^2 - \Omega_o^2}}\right] \; ; \; \left|(\Omega_o + K)\tan\frac{\phi}{2}\right| > \sqrt{K^2 - \Omega_o^2} \quad |\Omega_o| < |K| \qquad -(6)$$

$$= \frac{1}{\sqrt{K^2 - \Omega_o^2}} \ln\left[\frac{\sqrt{K^2 - \Omega_o^2} - (\Omega_o + K)\tan\left(\frac{\phi}{2}\right)}{\sqrt{K^2 - \Omega_o^2} + (\Omega_o + K)\tan\left(\frac{\phi}{2}\right)}\right] \; ; \; \left|(\Omega_o + K)\tan\frac{\phi}{2}\right| < \sqrt{K^2 - \Omega_o^2} \quad |\Omega_o| < |K| \qquad -(7)$$

- for the first case above where $|\Omega_o| > |K|$, we can rewrite (4) to give:

$$\phi(t) = 2\tan^{-1}\left\{\frac{\sqrt{\Omega_o^2 - K^2}}{\Omega_o + K}\tan\left[\frac{\sqrt{\Omega_o^2 - K^2}}{2}(t - t_o)\right]\right\} \qquad -(5)$$

note: as t increases, each time the quantity in square brackets increases by π, $\phi(t)$ repeats itself

- Hence, $\phi(t)$ is periodic with a period of

$$T = \frac{2\pi}{\sqrt{\Omega_o^2 - K^2}}$$

- Hence there is no steady state solution for $|\Omega_o| > |K|$. $\phi(t)$ travels within the phase detector characteristic according to a periodic law.

- for the second and third cases given by eqns (6) and (7), where $|\Omega_o| < |K|$, we will restrict our discussion to where Ω_o and K are both positive.

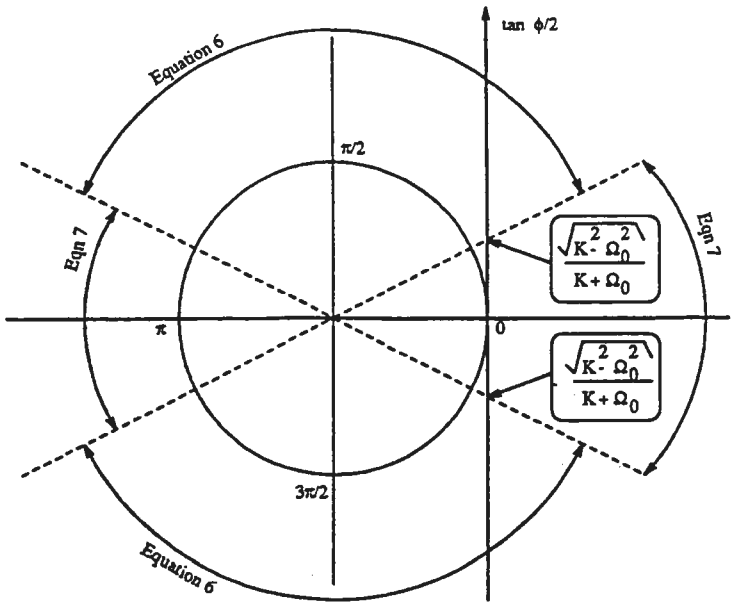

- the limit conditions then become:

$$\left|\tan\frac{\phi}{2}\right| >< \frac{\sqrt{K^2-\Omega_o^2}}{\Omega_o+K}$$

- it is possible to determine the above trigonometric circle:

Note: eqn (6) is used for $\phi/2$ near $\pi/2$ and $3\pi/2$

eqn (7) is used for $\phi/2$ near 0 and π

We can rewrite eqn (6) and (7) to give:

$$\tan\frac{\phi}{2} = \frac{\sqrt{K^2-\Omega_o^2}}{\Omega_o+K}\ \frac{1+\exp\left[\sqrt{K^2-\Omega_o^2}\,(t-t_o)\right]}{1-\exp\left[\sqrt{K^2-\Omega_o^2}\,(t-t_o)\right]}\quad ;\quad \left|\tan\frac{\phi}{2}\right| > \frac{\sqrt{K^2-\Omega_o^2}}{\Omega_o+K}$$

$$\tan\frac{\phi}{2} = \frac{\sqrt{K^2-\Omega_o^2}}{\Omega_o+K}\ \frac{1-\exp\left[\sqrt{K^2-\Omega_o^2}\,(t-t_o)\right]}{1+\exp\left[\sqrt{K^2-\Omega_o^2}\,(t-t_o)\right]}\quad ;\quad \left|\tan\frac{\phi}{2}\right| < \frac{\sqrt{K^2-\Omega_o^2}}{\Omega_o+K}$$

assuming that $\phi = \theta_i$ at $t = 0$ allows us to eliminate t_o.

$$\tan\frac{\phi}{2} = \frac{\sqrt{K^2-\Omega_o^2}}{K+\Omega_o}\ \left[\frac{\tan\frac{\theta_i}{2}+\frac{\sqrt{K^2-\Omega_o^2}}{K+\Omega_o}+\left[\tan\frac{\theta_i}{2}-\frac{\sqrt{K^2-\Omega_o^2}}{K+\Omega_o}\right]\exp\sqrt{K^2-\Omega_o^2}\,t}{\tan\frac{\theta_i}{2}+\frac{\sqrt{K^2-\Omega_o^2}}{K+\Omega_o}-\left[\tan\frac{\theta_i}{2}-\frac{\sqrt{K^2-\Omega_o^2}}{K+\Omega_o}\right]\exp\sqrt{K^2-\Omega_o^2}\,t}\right]$$

$$;\quad \left|\tan\frac{\phi}{2}\right| <> \frac{\sqrt{K^2-\Omega_o^2}}{\Omega_o+K} \qquad -(8)$$

Note: we have the same equation for both conditions on $\left|\tan\frac{\phi}{2}\right|$.

In order to find the change in ϕ with time, let:

$$x = \tan\left(\frac{\phi}{2}\right)\left[\frac{K+\Omega_o}{\sqrt{K^2-\Omega_o^2}}\right]$$

- now if we take $\frac{dx}{dt}$ we will find that $\frac{dx}{dt}$ has the same sign as its own numerator since its denominator is always positive.

- hence $\frac{dx}{dt}$ has the same sign as:

$$2\sqrt{K^2-\Omega_o^2}\left[\tan\frac{\theta_i}{2}+\frac{\sqrt{K^2-\Omega_o^2}}{K+\Omega_o}\right]\left[\tan\frac{\theta_i}{2}-\frac{\sqrt{K^2-\Omega_o^2}}{K+\Omega_o}\right]e^{\sqrt{K^2-\Omega_o^2}t}$$

- hence $\frac{dx}{dt}$ has the same sign as:

$$\tan^2\frac{\theta_i}{2}-\left[\frac{\sqrt{K^2-\Omega_o^2}}{K+\Omega_o}\right]^2 \qquad -(9)$$

- Consequently if:

$$\left|\tan\frac{\theta_i}{2}\right| > \frac{\sqrt{K^2-\Omega_o^2}}{K+\Omega_o}$$

then $\frac{dx}{dt}$ is positive and x is an increasing function of time.

- when $t\to\infty$, $x\to -1$ and $\tan\frac{\phi}{2}\to -\frac{\sqrt{K^2-\Omega_o^2}}{K+\Omega_o}$.

- the variation of $\frac{\phi}{2}$ is shown in Fig. 10-4a.

- now if:

$$\left|\tan\frac{\theta_i}{2}\right| < \frac{\sqrt{K^2-\Omega_o^2}}{K+\Omega_o}$$

- then from (9) we have that $\frac{dx}{dt}$ is neg, and x is a decreasing function of time.

- when $t\to\infty$, $x\to -1$ and $\tan\frac{\phi}{2}\to -\frac{\sqrt{K^2-\Omega_o^2}}{K+\Omega_o}$ as before.

- the variations of $\frac{\phi}{2}$ is shown in Fig. 10-4b.

- we can now derive the variation of $\frac{\phi}{2}$ with time since $\tan\phi/2$ is a monotonic function either increasing or decreasing with time according to the initial value of θ_i.

- note that the final value of ϕ is given by

$$\tan\frac{\phi_\infty}{2} = \frac{\sqrt{K^2-\Omega_o^2}}{K+\Omega_o}$$

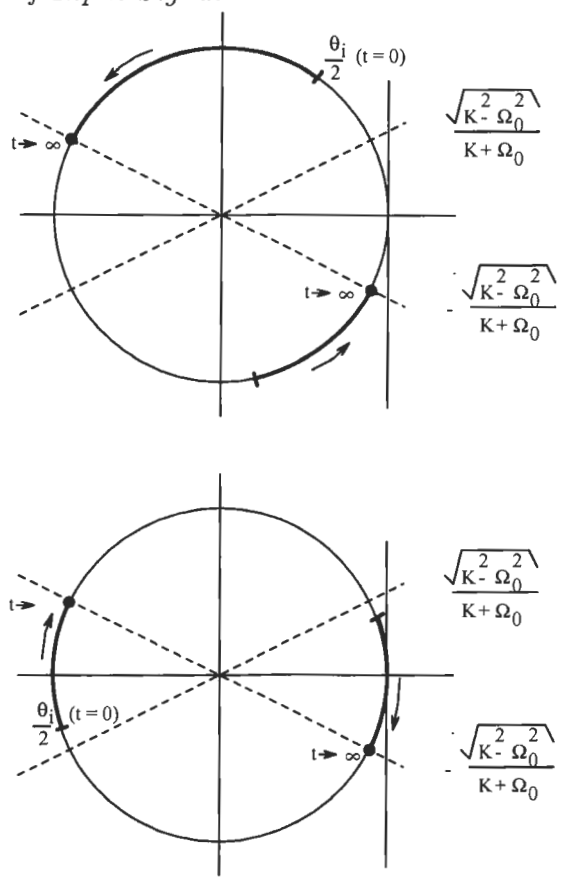

Figure 10.4 Trigonometrical representation of the phase error of a first-order loop during frequency acquisition.

(a) $\left|\tan\frac{\theta_i}{2}\right| > \frac{\sqrt{K_2 - \Omega_0^2}}{K + \Omega}$ (b) $\left|\tan\frac{\theta_i}{2}\right| < \frac{\sqrt{K_2 - \Omega_0^2}}{K + \Omega}$

- this gives

$$\cos\phi_\infty = \frac{\Omega_o}{K}$$

- taking into account the sign of $\tan\phi/2$, we have

$$\phi_\infty = -\cos^{-1}\frac{\Omega_o}{K}$$

And the stable VCO phase becomes:

$$\phi_{0\infty} = \Omega_o t + \theta_i - \phi_\infty = \Omega_o t + \theta_i + \cos^{-1}\frac{\Omega_o}{K}$$

The VCO output becomes:

$$y_o(t) = B\cos\left(\omega_o t + \Omega_o t + \theta_i + \cos^{-1}\frac{\Omega_o}{K}\right) = B\cos\left(\omega_i t + \theta_i + \cos^{-1}\frac{\Omega_o}{K}\right)$$

Hence the VCO leads the input $y_i(t)$ by an angle of $\cos^{-1}\frac{\Omega_o}{K}$.

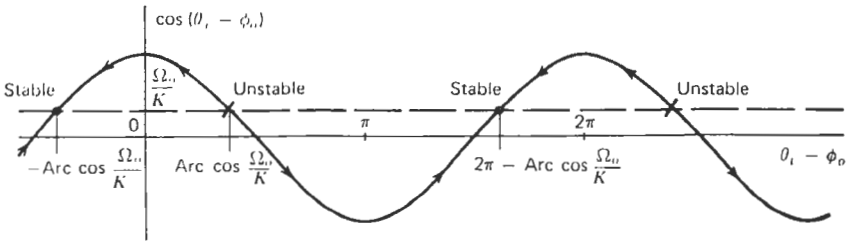

FIGURE 10.5. Path along the phase detector characteristic during the frequency acquisition of a first-order loop.

- Figure 10.5 shows the path followed along the phase detector by the phase difference between the input signal and the VCO signal, according to the initial value of $\theta_i - \theta_o$.

- From the above diagram we can obtain the four types of curves for the signal u_1 at the phase detector output as shown below:

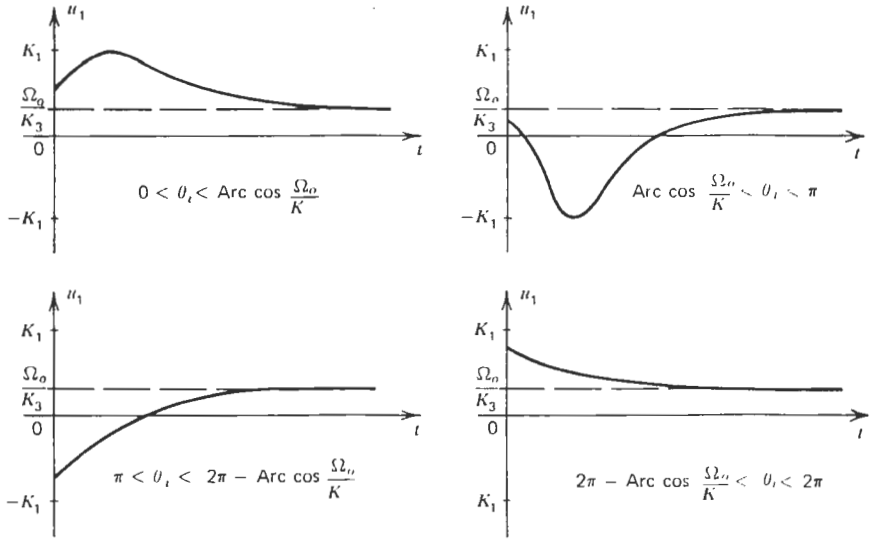

FIGURE 10.6. Phase detector output signal during the frequency acquisition of a first-order loop. (If $K_2 \neq 1$, replace K_3 by K_2K_3).

- Note: the above were derived for $\Omega_o > 0$ and $K > 0$. The case where:

$$\Omega_o < 0,\ K > 0$$

$$\Omega_o > 0,\ K < 0$$

$$\Omega_o < 0,\ K < 0$$

can be determined in a similar manner.

Conclusions for First Order PLL

- if difference between ω_i and ω_o is less than K, then after the transients shown above

in Fig. 10, the VCO reaches synchronism with the input y_i.

- the loop is then locked.
- the acquisition range corresponds to the interval $\omega_o - K$ to $\omega_o + K$ (this is the synchronization range!!)
- for every frequency in this interval, the steady state phase error is $-\cos^{-1}\left(\frac{\omega_i - \omega_o}{K}\right)$ for $\omega_i > \omega_o$, $K > 0$.
- if $|\omega_i - \omega_o|$ exceeds $|K|$, the VCO does not lock to the input signal and a frequency of $\sqrt{\Omega_o^2 - K^2}$ (rad/sec) appears at the phase detector output.

Signal Acquisition by a Second-Order Loop

- the signals applied to the phase detector are:

$$y_i(t) = A\cos(\omega_i t + \theta_i)$$

$$y_o(t) = B\cos(\omega_o t + \phi_o)$$

- as before we can express $y_i(t)$ as:

$$y_i(t) = A\sin(\omega_o t + \phi_i)$$

where

$$\begin{aligned}\phi_i(t) &= (\omega_i - \omega_o)t + \theta_i + \frac{\pi}{2} \\ &= \Omega_o t + \theta_i + \frac{\pi}{2}\end{aligned}$$

- The equations describing ϕ as a function of time are second order nonlinear differential equations for the PLL with Integrator with phase lead and also for the LPF with phase lead.

- We will first investigate the behaviour using the Phase Plane method.

Phase Plane Method

We have the general time domain equations as the following where we have introduced the above expression for $\phi_i(t)$

$$\tau_1\frac{d^2\phi}{dt^2} + K\tau_2\cos\phi\frac{d\phi}{dt} + K\sin\phi = 0 \qquad \text{; Integrator with phase lead}$$

$$\tau_1\frac{d^2\phi}{dt^2} + (1 + K\tau_2\cos\phi)\frac{d\phi}{dt} + K\sin\phi = \Omega_0 \qquad \text{; LPF with phase lead}$$

let $\dot{\phi} = \frac{d\phi}{dt}$ and $\ddot{\phi} = \frac{d^2\phi}{dt^2}$ divide the equations by $\tau_1\dot{\phi}$

$$\frac{\ddot{\phi}}{\dot{\phi}} + \frac{K\tau_2\cos\phi}{\tau_1} + \frac{K\sin\phi}{\tau_1\dot{\phi}} = 0 \qquad \text{; Integrator with phase lead}$$

$$\frac{\ddot{\phi}}{\dot{\phi}} + \frac{1 + K\tau_2\cos\phi}{\tau_1} + \frac{K\sin\phi}{\tau_1\dot{\phi}} = \frac{\Omega_o}{\tau_1\dot{\phi}} \qquad \text{; LPF with phase lead}$$

now

$$\ddot{\phi} = \frac{d^2\phi}{dt^2} = \frac{d}{dt}\left(\dot{\phi}\right) = \frac{d}{d\phi}\left(\dot{\phi}\right)\frac{d\phi}{dt} = \left(\frac{d\dot{\phi}}{d\phi}\right)\left(\dot{\phi}\right)$$

Hence we obtain:

$$\frac{d\dot{\phi}}{d\phi} = -\frac{K\sin\phi}{\tau_1\dot{\phi}} - \frac{K\tau_2\cos\phi}{\tau_1} \qquad -(12) \quad \text{; Integrator with phase lead}$$

$$\frac{d\dot{\phi}}{d\phi} = \frac{\Omega_o - K\sin\phi}{\tau_1\dot{\phi}} - \frac{1 + K\tau_2\cos\phi}{\tau_1} \qquad -(13) \quad \text{; LPF with phase lead}$$

- we can construct a plot with ϕ on the x axis and $\dot{\phi}$ on the y axis using the above equations.

- for each value of ϕ and $\dot{\phi}$ we can calculate the slope of the trajectory $\left(i.e., \frac{d\dot{\phi}}{d\phi}\right)$ and obtain an overall trajectory graph.

- this is shown in Fig 10.8, 10.9, 10.10 and 10.11 for an integrator with phase lead with various ζ.

Loop with Integrator and phase lead correction

- from equation (12), when ϕ increases by 2π, the slope of $\frac{d\dot{\phi}}{d\phi}$ returns to the same value.

- hence trajectories are needed only to be plotted in an interval of 2π for ϕ.

- When $\dot{\phi}$ is large:

$$\frac{d\dot{\phi}}{d\phi} \approx -K\frac{\tau_2}{\tau_1}\cos\phi = -2\zeta\omega_n\cos\phi$$

- the above equation shows that the trajectories are nearly sinusoidal

- however as ϕ increases from $-\pi$ to $+\pi$, $\left|\dot{\phi}\right|$ decreases a little bit.

- hence, a trajectory which leaves the plot on the right reenters on the left with $\left|\dot{\phi}\right|$ decreased a little bit.

- hence, successive trajectories from left to right approach the $\dot{\phi} = 0$ line

- eventually the separatrix AA is crossed and ϕ no longer varies by more than 2π.

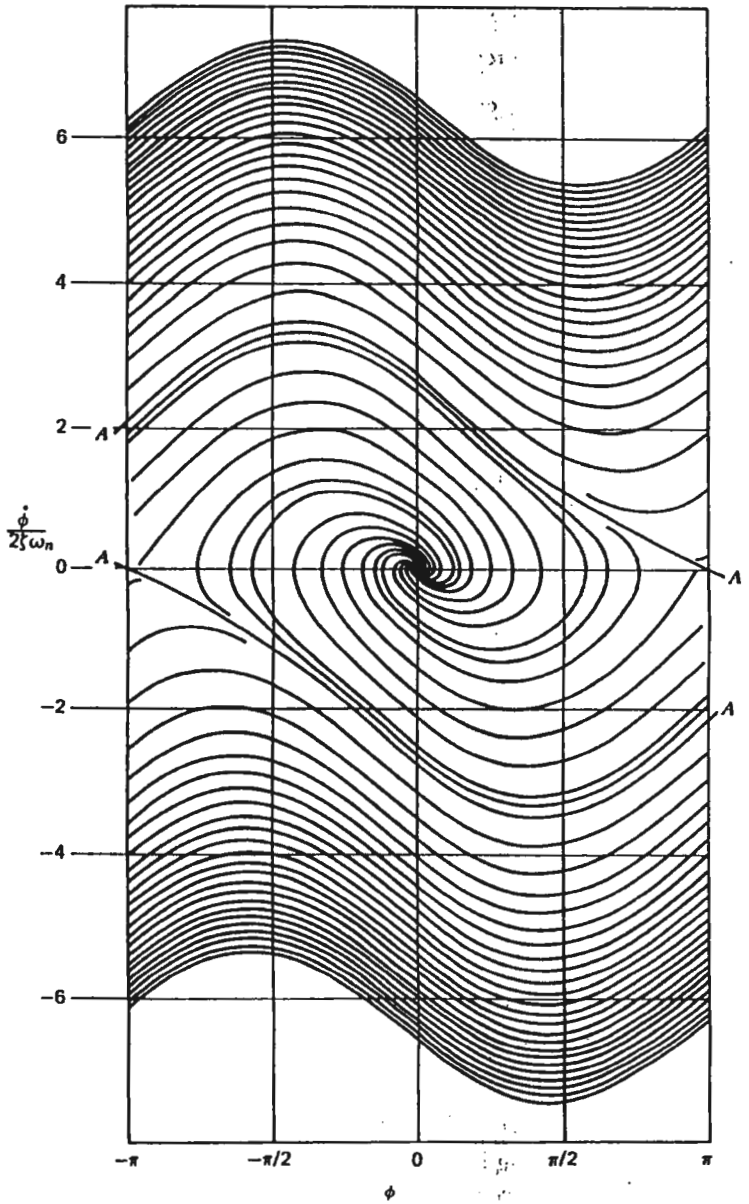

FIGURE 10.8. Phase-plane trajectories for a loop with $F(s)=(1+\tau_2 s)/(\tau_1 s)$ when $\zeta=0.5$ (from A. J. Viterbi; furnished through the courtesy of the Jet Propulsion Laboratory, California Institute of Technology).

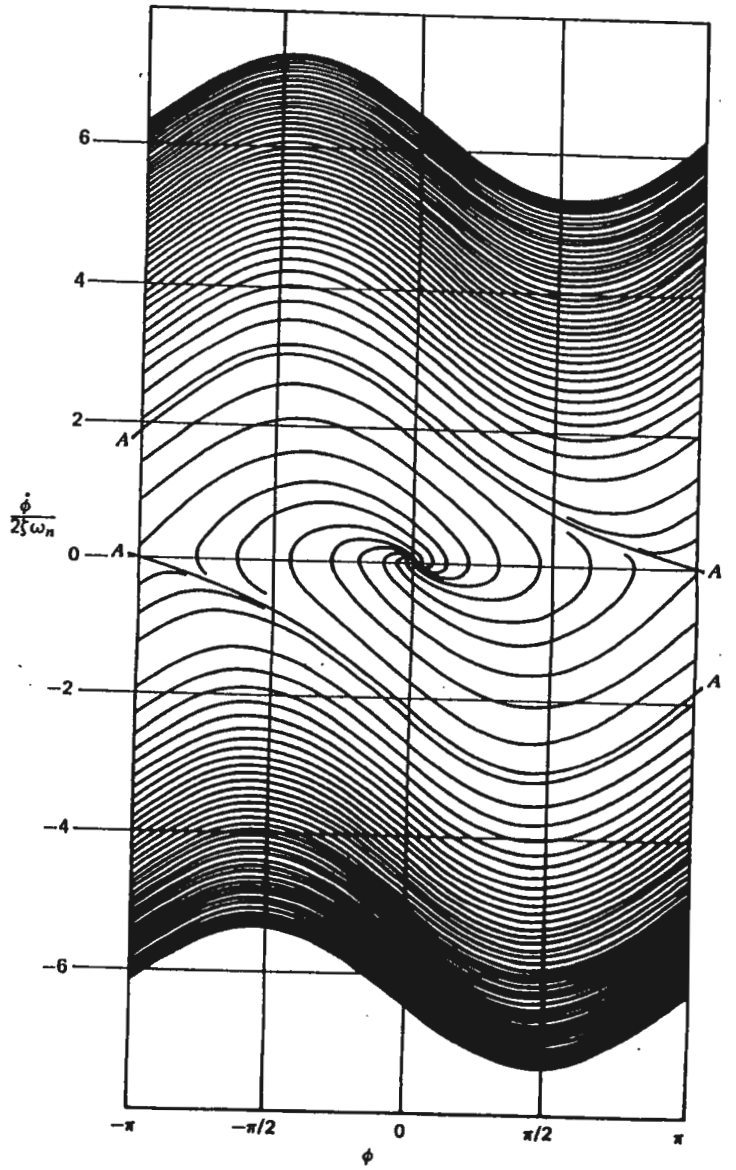

FIGURE 10.9. Phase-plane trajectories for a loop with $F(s)=(1+\tau_2 s)/(\tau_1 s)$ when $\zeta=\sqrt{2}/2$ (from A. J. Viterbi; furnished through the courtesy of the Jet Propulsion Laboratory, California Institute of Technology).

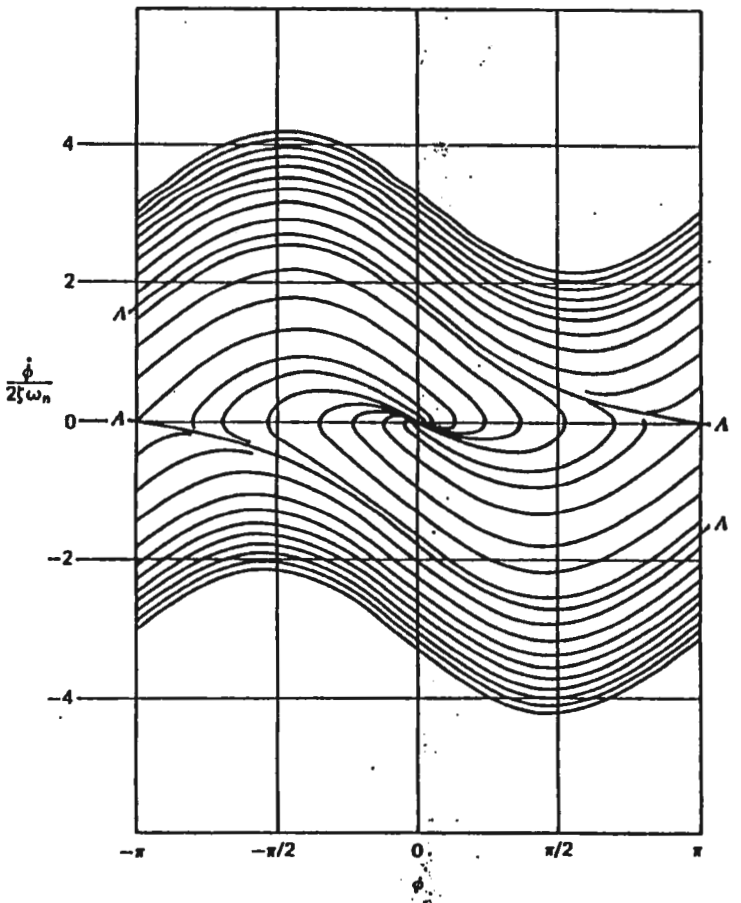

FIGURE 10.10. Phase-plane trajectories for a loop with $F(s)=(1+\tau_2 s)/(\tau_1 s)$ when $\zeta=1$ (from A. J. Viterbi; furnished through the courtesy of the Jet Propulsion Laboratory, California Institute of Technology).

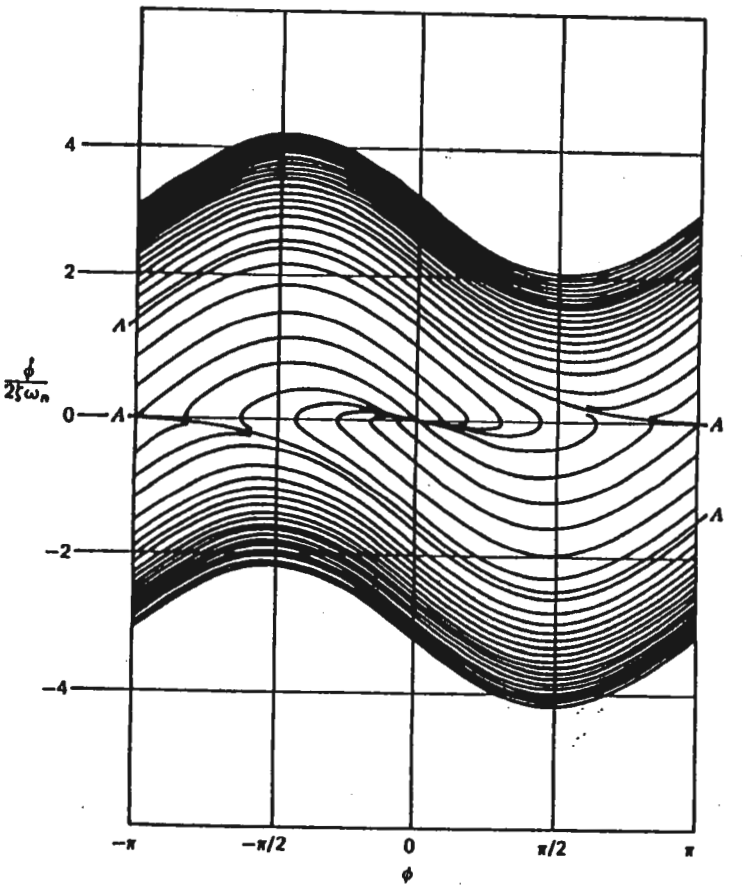

FIGURE 10.11. Phase-plane trajectories for a second-order loop with $F(s)=(1+\tau_2 s)/(\tau_1 s)$ when $\zeta=\sqrt{2}$ (from A. J. Viterbi; furnished through the courtesy of the Jet Propulsion Laboratory, California Institute of Technology).

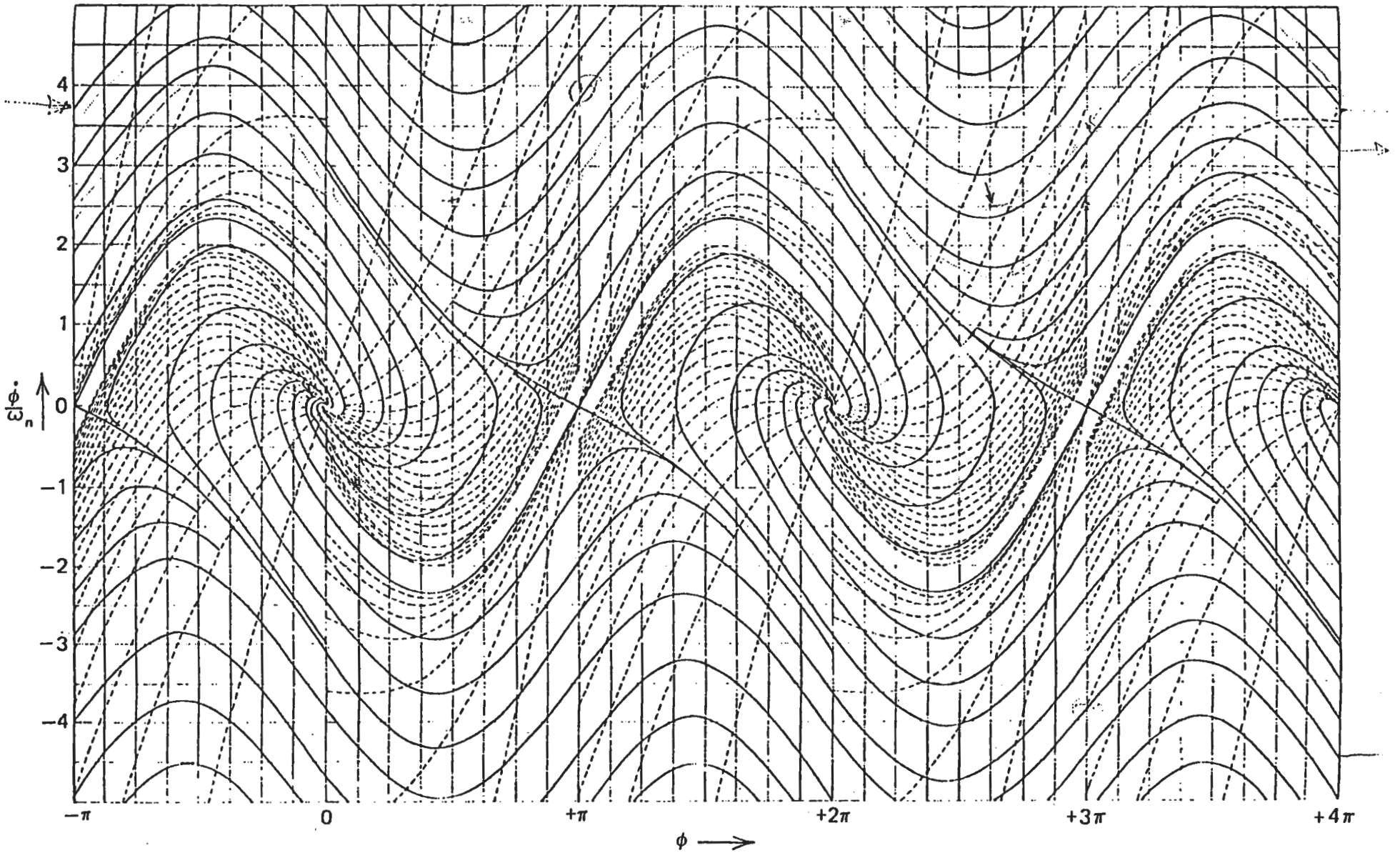

FIGURE 10.12. Phase-plane trajectories for a second-order loop with $F(s)=(1+\tau_2 s)/(\tau_1 s)$ when $\zeta=\sqrt{2}/2$, showing isochronous lines (from R. W. Sanneman and J. R. Rowbotham, *IEEE Trans. on Aerospace and Navigational Electronics*, March 1964 ANE-11, p. 19).

- all trajectories end at $\phi = 0$, $\dot{\phi} = 0$.

- the separatrix itself ends at $\phi = \pi$, $\dot{\phi} = 0$ corresponding to an unstable operating point.

- the stable operating point ($\phi = 0$, $\dot{\phi} = 0$) is reached

  - without being encircled if $\zeta > 1$

  - after being encircled several times if $\zeta < 1$

- equation (12) indicates trajectories are dependent only on ω_n and ζ, and not K. This is due to the assumed perfect integrator.

- Note: acquisition range is infinite whatever the initial frequency and phase difference. This is due to the assumption of a perfect integrator.

- once separatrix is crossed there can be no further cycle slipping.

- by calculating the decrease in $\dot{\phi}$ for each variation of ϕ from $-\pi$ to $+\pi$, the time required to reach the separatrix can be found approximately.

- defining this as the time required for acquisition gives:

$$T_{acq} \approx \frac{\Omega_o^2}{2\zeta\omega_n^3} \qquad -(14)$$

- Note: the initial phase difference $\phi(0)$ is not used in the above equation.

- acquisition is really the total time required for $\phi = \dot{\phi} = 0$. However for large Ω_o the time required to complete acquisition after crossing the separatrix is small compared to time required to reach the separatrix.

- when the initial Ω_o is small, it is more accurate to use the phase plane diagram directly to find T_{acq}.

- here we superimpose on the phase plane, isochronous curves.

- In Fig 10.12, the isochronous curves have a time between each of $\frac{1}{4\omega_n}$.

- Starting from any given point, we follow the corresponding trajectory and count the number of isochronous curves crossed before reaching acquisition (acquisition defined as a phase error condition or an angular frequency error condition or both).

- when the initial value Ω_o takes on an intermediate value, use the curves in Fig 10.13.

- These curves are for

$$\phi(0) = 0, \qquad \zeta = \frac{\sqrt{2}}{2}, \qquad \phi_\infty = 0.2\text{rad}$$

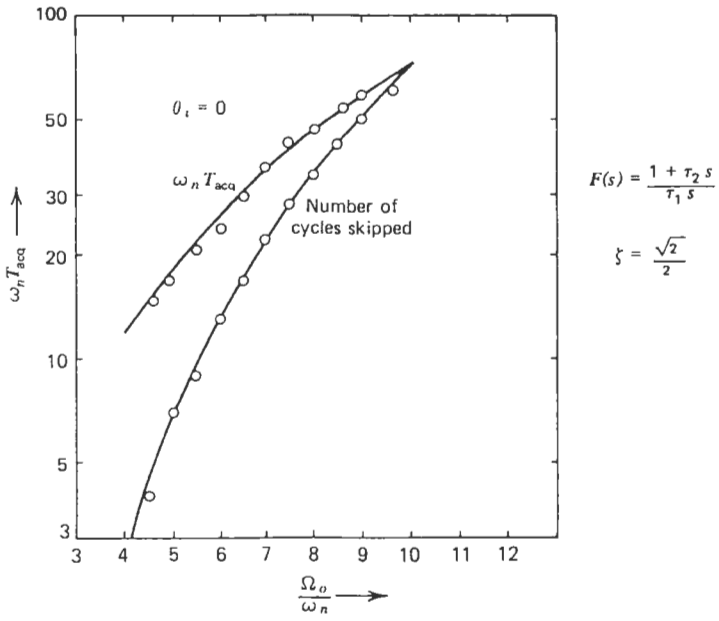

FIGURE 10.13. Acquisition time versus initial frequency error (from R. W. Sanneman and J. R. Rowbotham, *IEEE Trans. on Aerospace and Navigational Electronics*, March 1964 ANE-11, p. 20).

- Note: the acquisition time is really only sensitive to the initial phase difference, when Ω_o is small.

Linear Frequency Drift

- for the loop with an integrator with phase lead correction, phase plane study can also be used for an input signal having a linear frequency drift.

$$\phi_i(t) = \frac{1}{2}\mathcal{R}t^2 + \Omega_o t + \theta_i + \frac{\pi}{2}$$

- the differential equation 3.34 becomes:

$$\tau_1 \ddot{\phi} + K\tau_2 \cos\phi \ \dot{\phi} + K \sin\phi = \tau_1 \mathcal{R}$$

- the phase plane diagrams here are periodic in ϕ from $-\pi$ to $+\pi$, but the curves are not symmetrical

- the stable operating point, if it exists is at

$$\phi_\infty = \sin^{-1} \frac{\mathcal{R}}{\omega_n^2}$$

$$\dot{\phi}_\infty = 0$$

a) - when $\frac{\mathcal{R}}{\omega_n^2}$ is small, and the sign of $\mathcal{R}$ tends to decrease $\Omega(t)$, then acquisition always takes place.

- when $\frac{\mathcal{R}}{\omega_n^2}$ is small, and the sign of $\mathcal{R}$ tends to increase $\Omega(t)$, then acquisition may take place if Ω_o is not too large.

b) - when $\frac{\mathcal{R}}{\omega_n^2} = \frac{1}{2}$, and the sign of $\mathcal{R}$ tends to decrease $\Omega(t)$, then acquisition takes place.

- when $\frac{\mathcal{R}}{\omega_n^2} = \frac{1}{2}$, and the sign of $\mathcal{R}$ tends to increase $\Omega(t)$, then acquisition cannot take place.

c) - when $\frac{1}{2} < \frac{\mathcal{R}}{\omega_n^2} < 1$, and the sign of $\mathcal{R}$ tends to decrease $\Omega(t)$, then acquisition does not necessarily take place. The phase plane diagram has a corridor where acquisition cannot take place. This corridor increases in width as $\mathcal{R}$ increases.

d) - when $\frac{\mathcal{R}}{\omega_n^2} \geq 1$, then acquisition cannot take place. Here the steady state phase error $\phi_\infty = \sin^{-1} \frac{\mathcal{R}}{\omega_n^2}$ has no significance. If the loop was initially in lock, when $\frac{\mathcal{R}}{\omega_n^2} \geq 1$, the loop will definitely fall out of lock.

Low Pass Filter with Phase Lead Correction

- Here the phase plane trajectories are obtained from Equation 10.13

- coordinates of the stable operating point, when it exists is

$$\phi_\infty = \sin^{-1} \frac{\Omega_o}{K} \qquad \dot{\phi}_\infty = 0$$

- hence, a loop which initially is in lock will definitely fall out of lock if $\Omega_o > K$. Note that this is just the synchronization range which we started the course with.

$$\Omega_{syn} = K$$

- when $\Omega_o < K$, acquisition does not necessarily take place.- Acquisition occurs only if Ω_o is below Ω_{acq} where:

$$\Omega_{acq} \approx 2\sqrt{K\left(\zeta\omega_n + \frac{1}{2\tau_1}\right)} \qquad -(16)$$

- for most loops $\zeta\omega_n \gg \frac{1}{2\tau_1}$ and:

$$\Omega_{acq} \approx 2\sqrt{K\zeta\omega_n} \qquad -(17)$$

- rewriting synchronization range as:

$$\Omega_{syn} = K$$

- If the phase detector is triangular (linear between -90° and +90°) then:

$$\Omega_{acq} \approx \pi \sqrt{K\zeta\omega_n}$$

$$\Omega_{syn} = \frac{K\pi}{2}$$

- comparing the acquisition range and synchronization range for the two types of phase detectors, we see that the triangular detector increases both ranges by $\frac{\pi}{2}$!!

Analytical Approximation Method

- we can duplicate the results of the phase plane procedure for second order loops having sinusoidal phase detector analytically.

- at time $t = 0$ when the input signal is applied to the phase detector, the phase detector output signal is sinusoidal of frequency Ω_o. Here Ω_o is the frequency difference between the input, ω_i and the VCO, ω_o.

- after passing through the filter, this signal at Ω_o modulates the VCO.

- the VCO signal spectrum is then composed of discrete frequency lines and one of them is at the same frequency as the input signal.

- the result is that the phase detector output, in addition to Ω_o has a dc component that tends to move the average VCO frequency toward the input signal frequency.

- initially we have:

$$y_i(t) = A\cos\omega_i t$$

$$y_o(t) = B\cos(\omega_o t + \phi_o)$$

- the signal applied to the tuning port of the VCO is:

$$u_2 = u + \Delta u\cos(\Omega t - \psi) \qquad -(18)$$

if K_3 is the VCO modulation sensitivity

$$y_o(t) = B\cos\left[(\omega_o + K_3 u)t + \theta_o + K_3\frac{\Delta u}{\Omega}\sin(\Omega t - \psi)\right]$$

- now assuming $K_3\Delta u \ll \Omega$ - then:

$$\cos\left[\frac{K_3\Delta u}{\Omega}\sin(\Omega t - \psi)\right] \approx J_0\left(\frac{K_3\Delta u}{\Omega}\right)$$

$$\sin\left[\frac{K_3\Delta u}{\Omega}\sin(\Omega t-\psi)\right]\approx 2J_1\left(\frac{K_3\Delta u}{\Omega}\right)\sin(\Omega t-\psi)$$

Disregarding the freq. terms around $\omega_i+\omega_o$, the phase detector output signal is:

$$\begin{aligned}u_1(t)&=K_1J_0\left(\frac{K_3\Delta u}{\Omega}\right)\cos\left[(\omega_i-\omega_o-K_3u)t-\theta_o\right]\\&+K_1J_1\left(\frac{K_3\Delta u}{\Omega}\right)\Big\{\cos\left[(\omega_i-\omega_o-K_3u-\Omega)t-\theta_o+\psi\right]\\&\qquad-\cos\left[(\omega_i-\omega_o-K_3u+\Omega)t-\theta_o-\psi\right]\Big\}+\ldots\end{aligned}$$

But we also have:

$$\Omega=\omega_i-\omega_o-K_3u \qquad -(19)$$

Hence:

$$\begin{aligned}u_1(t)&=K_1J_0\left(\frac{K_3\Delta u}{\Omega}\right)\cos(\Omega t-\theta_o)\\&+K_1J_1\left(\frac{K_3\Delta u}{\Omega}\right)\left[\cos(\psi-\theta_o)-\cos(2\Omega t-\theta_o-\psi)\right]\end{aligned}$$

Hence $u_1(t)$ has these terms:

a) DC component

$$u_{10}=K_1J_1\left(\frac{K_3\Delta u}{\Omega}\right)\cos((\psi-\theta_o)$$

b) AC component at Ω

$$u_{11}=K_1J_0\left(\frac{K_3\Delta u}{\Omega}\right)\cos(\Omega t-\theta_i)$$

c) AC component at 2Ω

$$u_{12}=-K_1J_1\left(\frac{K_3\Delta u}{\Omega}\right)\cos(2\Omega t-\theta_o-\psi)$$

- Now since we assumed $K_3\Delta u\ll\Omega$, the amplitude of the 2Ω component is less than that of the Ω component, and will be disregarded.

$$u_1(t)\approx K_1J_1\left(\frac{K_3\Delta u}{\Omega}\right)\cos(\psi-\theta_o)+K_1J_0\left(\frac{K_3\Delta u}{\Omega}\right)\cos(\Omega t-\theta_o) \qquad -(20)$$

- Now the signal $u_2(t)$ at the loop filter output is related to $u_1(t)$

$$\tau_1\frac{du_2}{dt}=K_2\left[\tau_2\frac{du_1}{dt}+u_1(t)\right] \qquad \text{for integrator with phase lead}$$

$$\tau_1\frac{du_2}{dt}+u_2(t)=K_2\left[\tau_2\frac{du_1}{dt}+u_1(t)\right] \qquad \text{for LPF with phase lead}$$

- since the diff eqn are linear, we can calculate separately the response u_{20} to the dc component u_{10}, and the response u_{21} to the sinusoidal component u_{11}.

For both filters we get:

$$u_{21} = K_1 K_2 J_0\left(\frac{K_3 \Delta u}{\Omega}\right)\frac{\tau_2}{\tau_1}\cos(\Omega t - \theta_o) \quad , \qquad \text{for } \Omega > \tfrac{\omega_n}{2\zeta}$$

since u_2 is the VCO command signal, u_{21} is just the AC component of the signal applied to the tuning port of the VCO in eq (18)

$$\Delta u \cos(\Omega t - \psi) = K_1 K_2 J_0\left(\frac{K_3 \Delta u}{\Omega}\right)\frac{\tau_2}{\tau_1}\cos(\Omega t - \theta_o)$$

Note: the analysis has been based on the assumption that

$$K_3 \Delta u \ll \Omega$$

- we now concentrate on the slowly varying component u_{20} at the VCO modulation input. This is just the DC component in eqn (18). Hence eqn (19) becomes:

$$\Omega = \omega_i - \omega_o - K_3 u_{20} \qquad -(21)$$

- Now from before:

$$\begin{aligned} u_{10} &= K_1 J_1\left(\frac{K_3 \Delta u}{\Omega}\right)\cos(\psi - \theta_o) \\ &\approx K_1 J_1\left(\frac{K_3 \Delta u}{\Omega}\right) \end{aligned}$$

but

$$\begin{aligned} \Delta u &= K_1 K_2 J_0\left(\frac{K_3 \Delta u}{\Omega}\right)\frac{\tau_2}{\tau_1} \\ &\approx K_1 K_2 \frac{\tau_2}{\tau_1} \end{aligned}$$

Hence

$$\begin{aligned} u_{10} &\approx K_1 J_1\left(\frac{K \tau_2}{\Omega \tau_1}\right) \\ &\approx \frac{K_1}{2}\frac{K\tau_2}{\Omega\tau_1}; \qquad \text{if} \quad \frac{K\tau_2}{\tau_1} \ll \Omega \end{aligned} \qquad -(22)$$

- Now the loop filter response to u_{10} depends on the loop filter used.

Integrator with Phase Lead

- here we have:

$$\tau_1 \frac{du_{20}}{dt} = K_2\left[\tau_2 \frac{du_{10}}{dt} + u_{10}\right] \qquad -(23)$$

- eqn. (21), (22), and (23) yield:

$$\left(\frac{\tau_2}{\Omega} - \frac{\tau_1 \Omega}{\alpha^2}\right) d\Omega = dt \qquad -(25)$$

where

$$\boxed{\alpha^2 = \frac{K^2}{2}\frac{\tau_2}{\tau_1}}$$

- soln. of eqn (25) is:

$$\tau_2 \ln \Omega - \frac{\tau_1}{\alpha^2}\frac{\Omega^2}{2} = t - t_o$$

- now the initial condition is $\Omega = \Omega_o$ at $t = 0$.

- Consequently

$$t = \frac{\tau_1}{2\alpha^2}\left(\Omega_o^2 - \Omega^2\right) - \tau_2 \ln\left(\frac{\Omega_o}{\Omega}\right)$$

- now since

$$\alpha^2 = \frac{K^2}{2}\frac{\tau_2}{\tau_1}$$

and

$$\frac{K\tau_2}{\tau_1} = 2\zeta\omega_n$$

we have

$$\frac{t}{\tau_2} = \frac{\Omega_o^2 - \Omega^2}{(2\zeta\omega_n)^2} - \ln\left(\frac{\Omega_o}{\Omega}\right) \qquad -(26)$$

- letting

$$x = \frac{\Omega}{2\zeta\omega_n}$$

the variation of x with time are given below. The curves must be restricted to the region where the hypotheses are valid: *i.e.*, $x > 0$.

- note: for $x \geq 10$, the second term in eqn (26) is negligible as long as $x > 1$.

- hence

$$\frac{t}{\tau_2} \approx \frac{\Omega_o^2 - \Omega^2}{(2\zeta\omega_n)^2} \qquad -(27)$$

- in the zone where $x > 1$, Ω is a monotonic decreasing function of time, for all Ω_o. Hence the loop acquisition range is infinite.

- The acquisition time, defined as the time required for the frequency difference to pass from the initial value of Ω_o to $2\zeta\omega_n$ (*i.e.*, $x = 1$) is then:

$$T_{acq} = \tau_2\left[\left(\frac{\Omega_o}{2\zeta\omega_n}\right)^2 - 1 - \ln\left(\frac{\Omega_o}{2\zeta\omega_n}\right)\right] \qquad -(28)$$

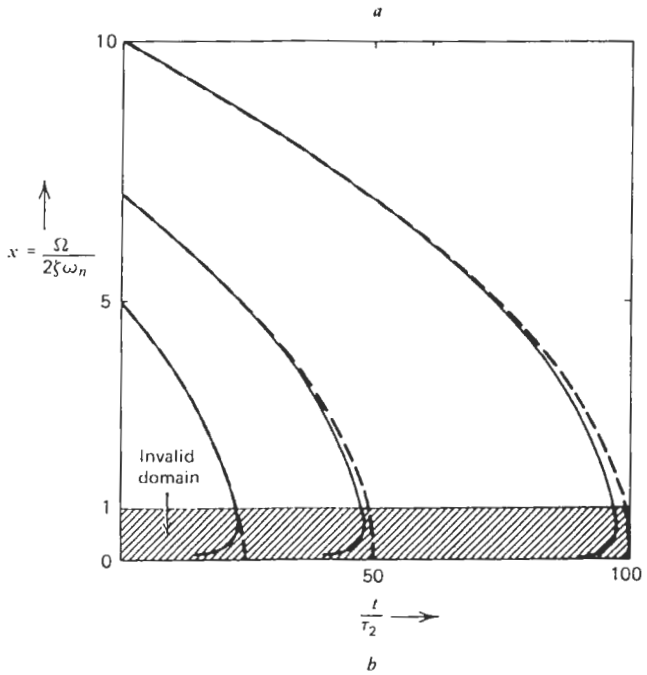

FIGURE 10.14. Representation of the frequency difference between input and VCO signals during acquisition for a loop with $F(s)=(1+\tau_2 s)/(\tau_1 s)$: (a) time versus angular frequency difference; (b) angular frequency difference versus time.

$$\approx \tau_2 \frac{\Omega_o^2}{(2\zeta\omega_n)^2} \quad ; \quad \text{for} \quad \frac{\Omega_o}{2\zeta\omega_n} > 10$$

$$\approx \frac{\Omega_o^2}{2\zeta\omega_n^3}$$

- this is just eqn (14) obtained earlier using the phase plane method.

b) Loop with Low Pass Filter having Phase Lead Correction

- here eqn (21) (22), and (24) yield the diff eqn:

$$(\alpha^2\tau_2 - \Omega^2\tau_1)\frac{d\Omega}{dt} = \Omega^3 - \Omega_o\Omega^2 + \alpha^2\Omega \qquad -(30)$$

- soln. of this eqn is:

$$t - t_o = \alpha^2\tau_2 \int \frac{d\Omega}{\Omega(\Omega^2 - \Omega_o\Omega + \alpha^2)} - \tau_1 \int \Omega \frac{d\Omega}{\Omega^2 - \Omega_o\Omega + \alpha^2}$$

- there are two possibilities depending on whether $\Omega^2 - \Omega_o\Omega + \alpha^2 = 0$ has real roots or not.

Case 1:

$$\Omega_o^2 > 4\alpha^2$$

$$> K^2 \frac{2\tau_2}{\tau_1}$$

- Here the roots are real and equal to:

$$\Omega_1 = \frac{\Omega_o + \sqrt{\Omega_o^2 - 4\alpha^2}}{2}$$

$$\Omega_2 = \frac{\Omega_o - \sqrt{\Omega_o^2 - 4\alpha^2}}{2}$$

- soln. to eqn (30) is then:

$$t = \tau_2 \ln \frac{\Omega}{\Omega_o} + \frac{\tau_1 + \tau_2}{2} \ln \frac{\alpha^2}{(\Omega - \Omega_1)(\Omega - \Omega_2)} + \frac{\Omega_o(\tau_2 - \tau_1)}{2\sqrt{\Omega_o^2 - 4\alpha^2}} \left[\ln \frac{\Omega - \Omega_1}{\Omega - \Omega_2} - \ln \frac{\Omega_2}{\Omega_1} \right] \quad -(31)$$

- the curves representing the variation of Ω versus time is shown in Fig 10.15b. Since at $t = 0$, $\Omega = \Omega_o$, the path of Ω follows the upper branch.

$$- \text{ as } t \to \infty, \quad \Omega \to \Omega_1 = \frac{\Omega_o + \sqrt{\Omega_o^2 - 4\alpha^2}}{2}$$

- since Ω is not zero as $t \to \infty$, acquisition does not take place. The VCO is attracted to the input signal frequency but does not reach it.

- Note: $\Omega_1 \approx \Omega_o/2$ and the VCO covers half the distance only to ω_i.

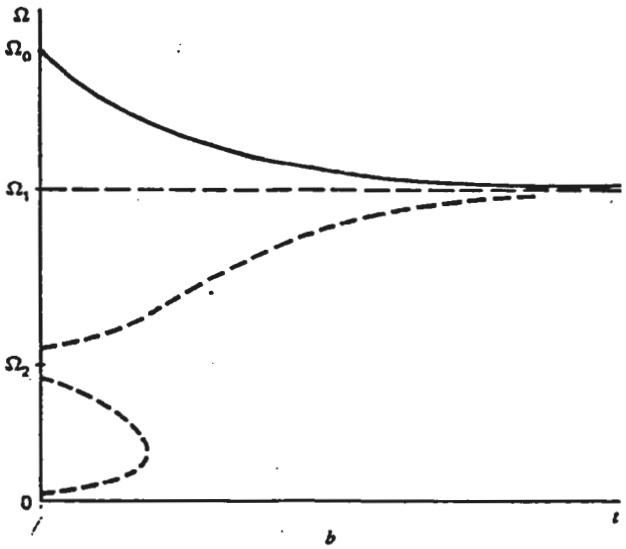

FIGURE 10.15. Representation of the frequency difference between input and VCO signals when acquisition cannot occur for a loop with $F(s) = (1 + \tau_2 s)/(1 + \tau_1 s)$:
(b) angular frequency difference versus time.

- Case II:

$$\Omega_o^2 < 4\alpha^2 = K^2 \frac{2\tau_2}{\tau_1}$$

- Here the soln to eqn (30) is:

$$t = \tau_2 \ln \frac{\Omega}{\Omega_o} + \frac{\tau_1 + \tau_2}{2} \ln \frac{\alpha^2}{\Omega^2 - \Omega_o \Omega + \alpha^2} + \frac{\Omega_o(\tau_2 - \tau_1)}{\sqrt{4\alpha^2 - \Omega_o^2}} \left[\tan^{-1} \frac{2\Omega - \Omega_o}{\sqrt{4\alpha^2 - \Omega_o^2}} - \tan^{-1} \frac{\Omega_o}{\sqrt{4\alpha^2 - \Omega_o^2}} \right] \quad -(32)$$

- the variation of Ω with time is shown in Fig. 10.16b.

- this curve is only valid in the zone covered by the hypothesis

$$\Omega > K \frac{\tau_2}{\tau_1}$$

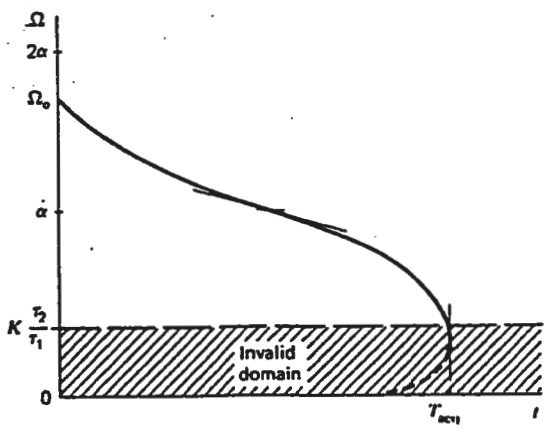

b

FIGURE 10.16. Representation of the frequency difference between input and VCO signals during acquisition for a loop with $F(s) = (1 + \tau_2 s)/(1 + \tau_1 s)$:
(b) angular frequency difference versus time.

- since acquisition is practically complete when the angular frequency difference is below $K\frac{\tau_2}{\tau_1}$, we can take the acquisition time T_{acq} as being the time required to move from Ω_o to $K\frac{\tau_2}{\tau_1}$.

- if $\Omega_o \gg K\frac{\tau_2}{\tau_1}$,

$$T_{acq} \approx \frac{2(\tau_1 - \tau_2)\Omega_o}{\sqrt{4\alpha^2 - \Omega_o^2}} \tan^{-1} \frac{\Omega_o}{\sqrt{4\alpha^2 - \Omega_o^2}} + \frac{\tau_1}{2} \ln \frac{K}{K - 2\Omega_o} \quad -(33)$$

- if in addition, $\Omega_o \ll 2\alpha = \sqrt{2}K\sqrt{\frac{\tau_2}{\tau_1}}$, (frequently encountered in practice),

$$T_{acq} \approx \frac{2(\tau_1 - \tau_2)\Omega_o}{2\alpha} \tan^{-1} \frac{\Omega_o}{2\alpha}$$
$$\approx \frac{2(\tau_1 - \tau_2)\Omega_o^2}{4\alpha^2}$$

- now the two conditions

$$\Omega_o \gg K\frac{\tau_2}{\tau_1} \qquad \Omega_o \ll \sqrt{2}K\sqrt{\frac{\tau_2}{\tau_1}}$$

requires that $\tau_2 \ll \tau_1$.

- hence

$$T_{acq} \approx \frac{2\tau_1\Omega_o^2}{4\alpha^2} = \frac{\Omega_o^2}{K^2\left(\frac{\tau_2}{\tau_1^2}\right)} = \frac{\Omega_o^2}{2\zeta\omega_n^3}$$

which is again just eqn (14) obtained earlier using the phase plane method.

- the limit condition between possible and impossible acquisition cases is:

$$\Omega_o^2 < 4\alpha^2 = 2K^2\left(\frac{\tau_2}{\tau_1}\right) = 2K\left(K\frac{\tau_2}{\tau_1}\right) = 2K\left(2\zeta\omega_n - \frac{1}{\tau_1}\right)$$

hence

$$|\Omega_o| < 2\sqrt{K\left(\zeta\omega_n - \frac{1}{2\tau_1}\right)} \qquad -(35)$$

Note: the limit condition given by Viterbi in eqn (16) from the phase plane method is

$$|\Omega_o| < 2\sqrt{K\left(\zeta\omega_n + \frac{1}{2\tau_1}\right)}$$

- since $\frac{1}{\tau_1}$ is generally negligible the two methods give comparable results.

- Recall: this method is not valid if Ω_o is below $K\left(\frac{\tau_2}{\tau_1}\right)$. Here the only valid method consists of using the phase plane trajectories, accounting for the initial phase offset.

LPF with Phase Lead

$$K\frac{\tau_2}{\tau_1} \ll \Omega_o < K\sqrt{\frac{\tau_2}{\tau_1}}$$

$$T_{acq} = \frac{2(\tau_1 - \tau_2)\Omega_o}{\sqrt{4\alpha^2 - \Omega_o^2}} \tan^{-1} \frac{\Omega_o}{\sqrt{4\alpha^2 - \Omega_o^2}} + \frac{\tau_1}{2} \ln \frac{K}{K - 2\Omega_o} \qquad -(1)$$

where

$$\alpha^2 = \frac{K^2}{2}\frac{\tau_2}{\tau_1} = K\omega_n\zeta \qquad -(2)$$

7. Additive Noise Response

- We will assume that the signal $y_i(t) = A\sin(\omega t + \theta_i)$ is accompanied by a noise n(t) which is stationary, Gaussian, has null mean value, and one-sided power spectral density of $N_0(\frac{W}{Hz})$ over the band $f - \frac{W}{2}$ to $f + \frac{W}{2}$

- the noise arises from the transmitter sets, antenna noise (galactic noise), circuits preceding the PLL.

7.1 Phase Detector Operating Principle

$$y(t) = A\sin(\omega t + \theta) + n(t)$$

- if the frequency band W is narrow and symmetrical wrt f, we have

$$n(t) = n_1(t)\sin\omega t + n_2(t)\cos\omega t$$

- where $n_1(t)$ and $n_2(t)$ are two low frequency random processes which are Gaussian, stationary, statistically independent, have null mean value, and a two-sided power spectral density N_0 over frequency range $-\frac{W}{2}$ to $+\frac{W}{2}$

- this means that

$$\overline{n_1^2(t)} = \overline{n_2^2(t)} = \overline{n^2(t)} = N_0 W$$

- Note W can actually range up to 2f, and the above approximation is still valid.

Analog Multiplier

- a real multiplier (although not commonly used) provides a convenient model for a sinusoidal phase detector

- we will consider the case of an input signal multiplied by ref signal and then filtered to get rid of sum frequency

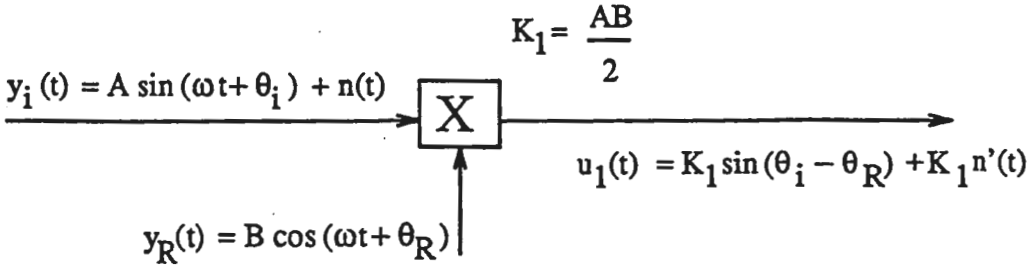

Here:

$$u_1(t) = AB\sin(\omega t + \theta_i)\cos(\omega t + \theta_R)$$
$$+ n_1(t)B\sin\omega t\cos(\omega t + \theta_R)$$
$$+ n_2(t)B\cos\omega t\cos(\omega t + \theta_R)$$

- expanding terms and removing all terms at 2ω (LPF), we have

$$\begin{aligned} u_1(t) &= \frac{AB}{2}\sin(\theta_i - \theta_R) + \frac{Bn_2(t)}{2}\cos\theta_R - \frac{Bn_1(t)}{2}\sin\theta_R \\ &= K_1\sin(\theta_i - \theta_R) + \frac{K_1}{A}n_2(t)\cos\theta_R - \frac{K_1}{A}n_1(t)\sin\theta_R \end{aligned} \qquad -(7.1)$$

Here we have the useful signal $K_1\sin(\theta_i - \theta_R)$ accompanied by a term $K_1 n'(t)$ where

$$n'(t) = \frac{n_2(t)}{A}\cos\theta_R - \frac{n_1(t)}{A}\sin\theta_R \qquad -(7.2)$$

- now since $n_1(t)$ and $n_2(t)$ are independent

$$\overline{n'(t)} = \frac{\cos\theta_R}{A}\overline{n_2(t)} - \frac{\sin\theta_R}{A}\overline{n_1(t)} = 0$$

also

$$\overline{n'(t)^2} = \frac{\cos^2\theta_R}{A^2}\overline{n_2(t)^2} + \frac{\sin^2\theta_R}{A^2}\overline{n_1(t)^2} = \frac{\overline{n^2(t)}}{A^2} = \frac{N_0 W}{A^2}$$

since $n_2(t)$ and $n_1(t)$ extend from $-\frac{W}{2}$ to $+\frac{W}{2}$, $n'(t)$ extends from $-\frac{W}{2}$ to $+\frac{W}{2}$ The above result can be interpreted as a phase modulation of the input signal by a random process $n'(t)$.

- That is

$$y_i(t) = A\sin(\omega t + \theta_i) + n(t)$$
$$\approx A\sin(\omega t + \theta_i + \phi_i(t)) \quad ; \quad \phi_i(t) = n'(t)$$

will give the same result at output of phase detector in equation (7.1).

- Note: This modulation is not a real modulation, but an equivalent mod. If it were real, we would have from equation (7.1)

$$u_1(t) = K_1\sin\{\theta_i - \theta_R + n'(t)\}$$

- The linear restriction would then be on $\theta_i - \theta_R + n'(t)$ but this restriction is nonexistent!

- Note: The above analysis is valid only for multiplication by signal $y_R(t) = B\cos(\omega t + \theta_R)$ where θ_R is independent of n(t). We will discuss this later.

Multiplier by sign $[\cos(\omega t + \theta_R)]$

- this type of multiplier is the 4 diode multiplier with reference amplitude higher than the input signal.

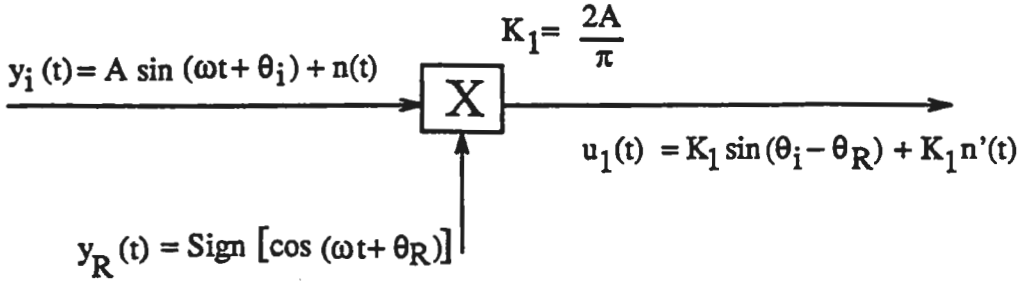

here

$$y_R(t) = \frac{4}{\pi}\left[\cos(\omega t + \theta_R) + \cdots + \frac{(-1)^p}{2p+1}\cos\{(2p+1)(\omega t + \theta_R)\} + \cdots\right]$$

multiplying by $A\sin(\omega t + \theta_i)$ and filtering yields

$$u_{1_S} = \frac{2A}{\pi}\sin(\theta_i - \theta_R)$$

- similarly, the product of $y_R(t)$ and the breakdown of $n(t)$ gives after filtering

$$u_{1_N}(t) = \frac{2}{\pi}n_2(t)\cos\theta_R - \frac{2}{\pi}n_1(t)\sin\theta_R$$

- Consequently, the phase detector output is

$$\begin{aligned} u_1(t) &= u_{1_S}(t) + u_{1_N}(t) \\ &= K_1\sin(\theta_i - \theta_R) + K_1 n'(t) \end{aligned} \qquad -(7.3)$$

where $\boxed{K_1 = \frac{2A}{\pi}}$

$$n'(t) = \frac{n_2(t)}{A}\cos\theta_R - \frac{n_1(t)}{A}\sin\theta_R$$

- again, $n'(t)$ is a low frequency, Gaussian process with 2 sided power spectral density N_0' uniform over $-\frac{W}{2}$ to $+\frac{W}{2}$ where

$$N_0' = \frac{N_0}{A^2}$$

- Consequently,

$$\overline{n'(t)} = 0$$

$$\overline{n'(t)^2} = \frac{\overline{n(t)^2}}{A^2} = \frac{N_0 W}{A^2}$$

- Note: if n(t) is true white noise (infinite Bandwidth), then

$$N_0' = \frac{N_0}{A^2}\frac{\pi^2}{8}$$

Phase Detector Linear over $-\pi/2$ to $+\pi/2$

- This characteristic arises from multiplication of square input signal by square reference signal.

- In the presence of noise, we must distinguish two cases:

a) a natural square wave to which $n(t)$ is added

b) sinusoidal input accompanied by $n(t)$ which is then hard limited

We shall examine case a)

- Here

$$y_i(t) = A\text{sign}\,[\sin(\omega t + \theta_i)] + n(t)$$

- Reference is

$$y_R(t) = \text{sign}\,[\cos(\omega t + \theta_R)]$$

- Multiplication of $y_i(t)$ and $y_R(t)$ and passing through an LPF leaves for the useful signal

$$u_{1_S} = \begin{cases} \frac{2A}{\pi}(\theta_i - \theta_R) & ; -\frac{\pi}{2} < \theta_i - \theta_R < \frac{\pi}{2} \\ \frac{2A}{\pi}(\pi - \theta_i + \theta_R) & ; \frac{\pi}{2} < \theta_i - \theta_R < \frac{3\pi}{2} \end{cases}$$

- We must now calculate the noise term $u_{1_N}(t)$

- Note: Since the useful signal is a square wave, the noise $n(t)$ bandwidth cannot be restricted. Therefore, assume $n(t)$ is stationary Gaussian, null mean and has one sided density N_0 from $f = 0$ to $f \to \infty$.

- We assume this noise is composed of components $v^{(i)}(t)$ as shown

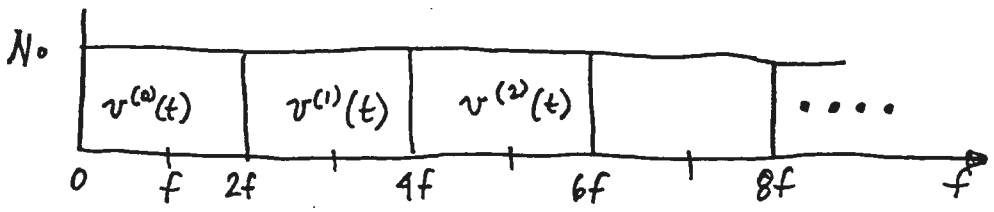

- Since $n(t)$ is Gaussian and $v^{(i)}(t)$ are nonoverlapping, then $v^{(i)}(t)$ are statistically independent.

- Now each $v^{(i)}(t)$ can be broken down as

$$v^{(p)}(t) = v_1^{(p)}(t)\sin[(2p+1)\omega t] + v_2^{(p)}(t)\cos[(2p+1)\omega t]$$

where $v_1^{(p)}(t)$ and $v_2^{(p)}$ (t) are independent and have 2 sided spectral density N_0 from $-f$ to $+f$.

$n(t)$ is now expressed

$$\begin{aligned} n(t) &= v_1^{(0)}(t)\sin\omega t + v_2^{(0)}(t)\cos\omega t \\ &\quad + v_1^{(1)}(t)\sin 3\omega t + v_2^{(1)}(t)\cos 3\omega t \\ &\quad + \cdots \end{aligned}$$

- Now $n(t)$ is multiplied by $y_R(t)$ and only the components below f pass through the LPF.

$$\begin{aligned} u_{1_N}(t) &= \frac{2}{\pi}\left[v_2^{(0)}\cos\theta_R - v_1^{(0)}\sin\theta_R + \cdots \right. \\ &\qquad \left. + (-1)^p \frac{v_2^{(p)}(t)\cos(2p+1)\theta_R - v_1^{(p)}(t)\sin(2p+1)\theta_R}{2p+1} + \cdots\right] \\ &= K_1 n'(t) \quad \text{where } \boxed{K_1 = \frac{2A}{\pi}} \end{aligned}$$

- This equation leads to

$$\overline{n'(t)} = 0$$

and

$$\overline{n'(t)^2} = \frac{2fN_0}{A^2}\,\frac{\pi^2}{8}$$

- Note: Since each process $v_1^{(p)}(t)$ and $v_2^{(p)}(t)$ has a uniform density in band $-f$ to $+f$, then $n'(t)$ also has uniform density from $-f$ to $+f$

$$N_o' = \begin{cases} \frac{\overline{n'(t)^2}}{2f} = \frac{N_0}{A^2}\,\frac{\pi^2}{8} & , -f \text{ to } +f \\ 0 & , \text{elsewhere} \end{cases}$$

Note: For same signal and spectral density N_0 of $n(t)$, the spectral density N_0' is 4 dB higher than in the case for sinusoidal phase detector.

- This results since a square signal has more power than a sinusoidal signal, and also since here we consider input noise bandwidth as being infinite.

Case b) Sinusoidal signal + $n(t)$ being hardlimited

- since input signal is sinusoidal, we shall assume that $n(t)$ has a narrow bandwidth around f.

- We must calculate the product

$$u(t) = A' \text{sign}[A\sin(\omega t + \theta_i) + n(t)] \times \text{sign}[\cos(\omega t + \theta_R)]$$

- now in the absence of noise

$$\text{sign}[A\sin(\omega t + \theta_i)] \equiv \text{sign}[\sin(\omega t + \theta_i)]$$

and the result is the same as in case a) above

$$u_{1_S} = \begin{cases} \frac{2A'}{\pi}(\theta_i - \theta_R) & ; -\frac{\pi}{2} < \theta_i - \theta_R < \frac{\pi}{2} \\ \frac{2A'}{\pi}(\pi - \theta_i + \theta_R) & ; \frac{\pi}{2} < \theta_i - \theta_R < \frac{3\pi}{2} \end{cases}$$

- again $n(t)$ can be broken down into

$$n(t) = n_1'(t)\sin(\omega t + \theta_i) + n_2'(t)\cos(\omega t + \theta_i)$$

- Consequently

$$\begin{aligned} A\sin(\omega t + \theta_i) + n(t) &= A\sin(\omega t + \theta_i) + n_1'(t)\sin(\omega t + \theta_i) + n_2'(t)\cos(\omega t + \theta_i) \\ &= \sqrt{[A + n_1'(t)]^2 + n_2'(t)^2}\ \sin[\omega t + \theta_i + \phi_i(t)] \end{aligned}$$

$$\text{where} \quad \tan\phi_i(t) = \frac{n_2'(t)}{A + n_1'(t)} \qquad -(7.5)$$

- When there is a high SNR preceding the limiter, eqn 7.5 is approximately

$$\phi_i(t) = \frac{n_2'(t)}{A} \qquad -(7.6)$$

- Note: $\phi(t)$ remains small and the limit conditions remain approximately the same

$$u_1(t) = \begin{cases} K_1[\theta_i - \theta_R + \phi_i(t)] & ; -\frac{\pi}{2} \lesssim \theta_i - \theta_R \lesssim \frac{\pi}{2} \\ K_1[\pi - \theta_i + \theta_R - \phi_i(t)] & ; \frac{\pi}{2} \lesssim \theta_i - \theta_R \lesssim \frac{3\pi}{2} \end{cases}$$

- since $\theta_i - \theta_R$ generally remains around zero, the phase detector output can be separated into a:

useful term $K_1(\theta_i - \theta_R)$ and a

noise term $K_1\phi_i(t) = K_1\frac{n_2'(t)}{A}$

- Again, as for sinusoidal detector, the system behaves as if input signal were modulated by low frequency random process $\frac{n_2'(t)}{A}$

- However, we have an added restriction here. The quantity $\theta_i - \theta_R + \phi_i(t)$ must remain small $\Rightarrow$ SNR must remain high

- When SNR is not high enough, eqn (7.5) must be used instead of (7.6), and $\phi_i(t)$ cannot be disregarded in the limit conditions

- It now becomes difficult to separate the phase detector output signal into a useful signal term and a noise term

- It can be worked out (pp. 150 Blanchard) to give

$$u_1(t) = \begin{cases} \frac{2A'}{\pi}[\theta_i - \theta_R + \phi_i(t)] & ; -\frac{\pi}{2} < \theta_i - \theta_R + \phi_i < \frac{\pi}{2} \\ \frac{2A'}{\pi}[\pi - \theta_i + \theta_R - \phi_i(t)] & ; \frac{\pi}{2} < \theta_i - \theta_R + \phi_i < \frac{3\pi}{2} \end{cases}$$

Note: This is exactly the same as the above low noise case with $\phi_i(t)$ in the limit conditions

Note: Here A' is peak amplitude of limiter output square wave

- Using the expressions for $u_1(t)$ and the probability density function $P(\phi_i)$ for $\phi_i(t)$, it is possible to get the expression for $\overline{u_1(t)} = f(\theta_i - \theta_R)$ representing the component proportional to the useful signal. This is shown in Figure 7.5 Blanchard.

- Note: For $SNR \to \infty$, the characteristic is the triangle function

  for $SNR \leq 1$, the characteristic appears sinusoidal due to signal-noise interaction.

  This is inferior performance compared to sinusoidal detector which remains linear with respect to additive noise whatever the input SNR.

Phase Detector Linear from $-\pi$ to $+\pi$

- For $SNR \to \infty$, the power spectral density of the equivalent modulation of the input signal is identical with that for a sinusoidal detector. Since the characteristic is linear from $-\pi$ to $+\pi$, there are advantages of the linear phase detector:

  -reduce intermod when loop is used as phase demodulator or frequency discriminator

  -better transient performance

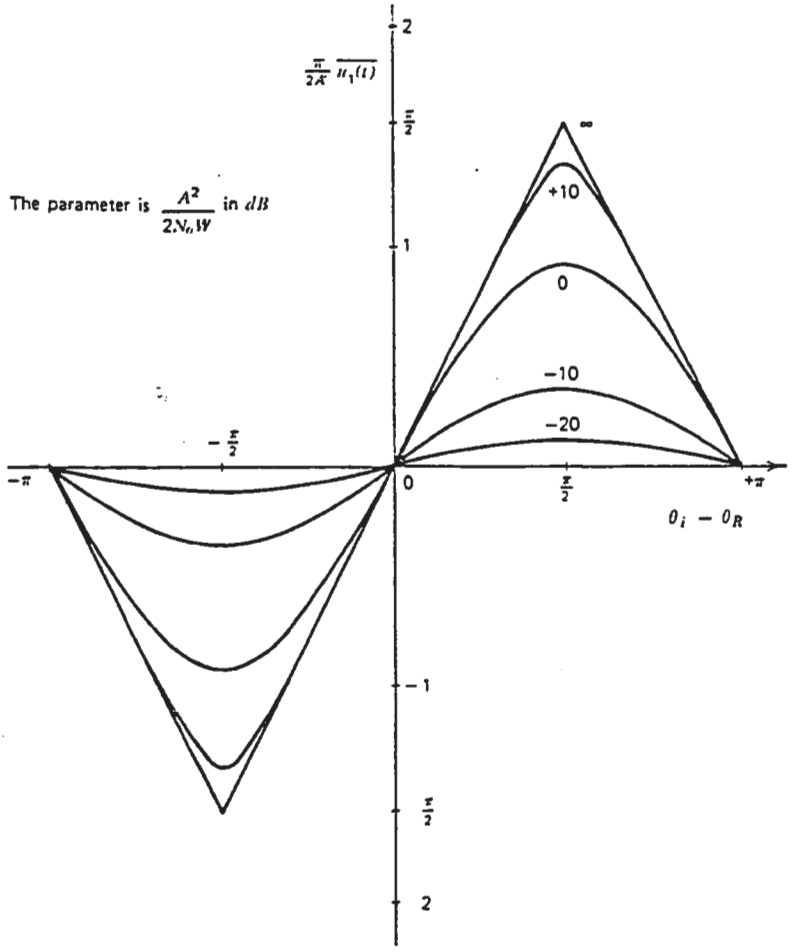

FIGURE 7.5. Characteristic of a triangular phase detector in presence of noise, A' being the peak amplitude of the limiter output square wave signal (by permission of A. Pouzet; from an unpublished CNES Internal Document).

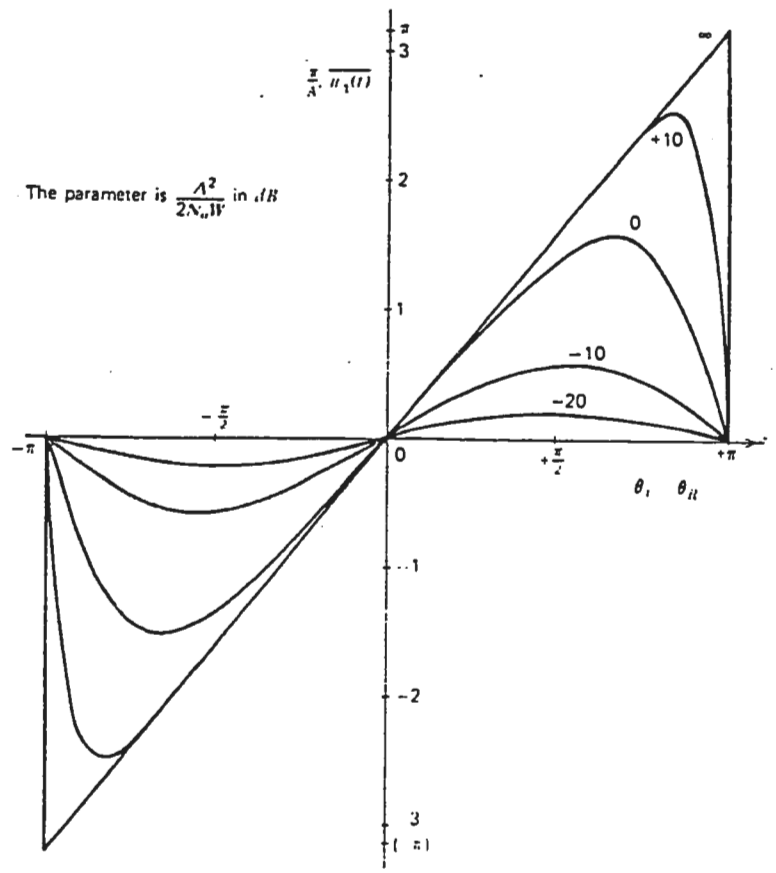

FIGURE 7.6. Characteristic of a sawtooth phase detector in presence of noise, A' being the peak amplitude of the flip-flop output signal (by permission of A. Pouzet; from an unpublished CNES Internal Document).

- For $SNR \leq 1$, interaction of signal and noise causes
  - useful signal term is reduced
  - spectral density N_o' of equivalent mod increases
- Characteristic is shown in Figure 7.6, Blanchard
- Note: Characteristic becomes sinusoidal when $SNR < 1$.

Additive Noise Response of the Loop

- We saw that when a signal at the input of a phase detector is accompanied by additive noise $n(t)$, we can define an equivalent phase modulation of the input by a low frequency noise $n'(t)$.
- When the input signal is sinusoidal, the properties of $n'(t)$ are the same for "analog" multiplication ($A = B$) or "sign" multiplication ($B \gg A$).
- For both linear phase detectors ($-\frac{\pi}{2}$ to $\frac{\pi}{2}$) and ($-\pi$ to π) the sinusoidal signal plus noise $n(t)$ is passed through a hard limiter.
- If SNR is large, we can again define an equivalent modulation $n'(t)$ which has the same properties as $n'(t)$ for the sinusoidal phase detectors.
- If SNR is small, the useful signal decreases and there is an increase in spectral density of $n'(t)$.

Note: (An unlinear relationship between $n(t)$ and $n'(t)$).

- We will analyze only "sinusoidal" phase detectors in PLLs. However, this analysis is applicable to "linear" phase detectors with large SNR.

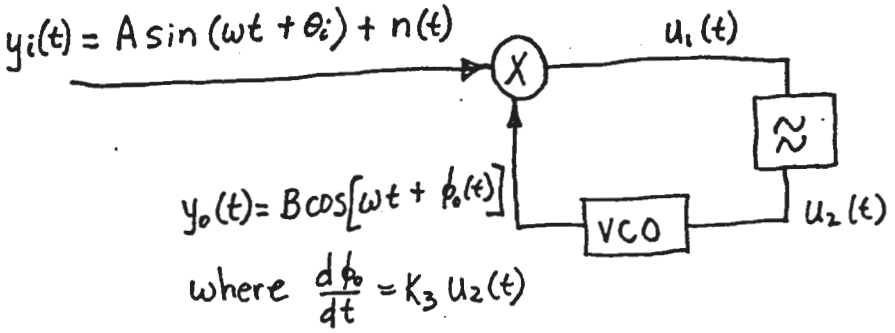

- In the absence of noise, the loop is locked with a null phase error (VCO is in Quadrature with input).
- However with input noise, u_1 becomes a noise signal $u_1(t)$.

- this causes u_2 to become a noise signal $u_2(t)$ which causes the VCO to have random phase $\phi_o(t)$.

- This $\phi_o(t)$ refers to variations with respect to a noiseless phase value.

- This means $\phi_o(t)$ can be defined with respect to an incoming signal:

$$y_u(t) = A\sin(\omega t + \theta_i)$$

and not with respect to the actual incoming signal

$$y_i(t) = A\sin(\omega t + \theta_i) + n(t) \approx A\sin(\omega t + \theta_i + n'(t))$$

- Note: Phase error is really $-\phi_o(t)$ and not $n'(t) - \phi_o(t)$. Consequently, $\phi_o(t)$ must remain small for linearity approximation to hold.

- Note: Representation of noise as an "equivalent" modulation $n'(t)$ is valid only if the reference phase θ_R is constant $\Rightarrow$ independent of noise processes $n_1(t)$ and $n_2(t)$.

  - This is approximated when BW preceding loop is much greater than the loop equivalent noise BW.

- Note: PLL does not just act as a narrow band filter with respect to the noisy input since this implies that the output is a sinusoid accompanied by additive noise. In reality, the sinusoid is phase modulated by a random process.

- Let us find the properties of $\phi_o(t)$ in terms of properties of $n'(t)$.

- We have

$$\frac{\Phi_o(j\omega)}{\Phi_i(j\omega)} = H(j\omega) = \frac{KF(j\omega)}{j\omega + KF(j\omega)}$$

- Consequently, $\phi_o(t)$ is an output from a filter with input $n'(t)$.

- Now $n'(t)$ is stationary, Gaussian, has a null mean, and spectral density $\frac{N_o}{A^2}$ (in rad^2/Hz) in band ($-\frac{W}{2}$ to $\frac{W}{2}$).

- Therefore, $\phi_o(t)$ is stationary, Gaussian, has a null mean and spectral density

$$S_{\phi_o}(f) = \frac{N_o}{A^2}|H(j2\pi f)|^2$$

Standard Deviations of $\phi_o(t)$

$$\sigma^2_{\phi_o} = \frac{N_o}{A^2}\int_{-\infty}^{\infty}|H(j2\pi f)|^2 df$$

a) For first order loop

$$H(j\omega) = \frac{K}{j\omega + K}$$

and

$$\sigma_{\phi_o}^2 = \frac{N_o}{A^2}\frac{K}{2}$$

b) Loop with Integrator and Correction

$$H(j\omega) = \frac{\omega_n^2 + j2\zeta\omega_n\omega}{\omega_n^2 - \omega^2 + j2\zeta\omega_n\omega}$$

and

$$\sigma_{\phi_o}^2 = \frac{N_o}{A^2}\frac{\omega_n}{4\zeta}(1 + 4\zeta^2)$$

c) Low Pass Filter and Correction

$$\sigma_{\phi_o}^2 = \frac{N_o}{A^2}\frac{\omega_n}{4\zeta}[1 + (2\zeta - \frac{\omega_n}{K})^2]$$

Equivalent Noise Bandwidths of Loops, $2B_n$

$$B_n = \int_0^\infty |H(j2\pi f)|^2 df$$

Note:

$$\sigma_{\phi_o}^2 = \frac{N_o}{A^2}(2B_n)$$

Signal to Noise Ratio of Loop

$$\left(\frac{S}{N}\right)_L = \rho_L = \frac{A^2/2}{N_o B_n} = \frac{1}{\sigma_{\phi_o}^2}$$

Note: N_o is the one sided density

a) First order loop

$$(2B_n) = \frac{K}{2}$$

Note: $2B_n$ is in Hz

K is in rad/sec.

Note: Loop performance improves with K (reduced phase error etc.). However, here we see that as K increases, there is reduced protection against incoming noise.

b) Integrator and Correction

$$(2B_n) = \frac{\omega_n}{4\zeta}(1 + 4\zeta^2)$$

Note: $2B_n$ is in Hz

ω_n is in rad/sec.

Note: $2B_n$ is independent of K.

Low Pass Filter and Correction

$$(2B_n) = \frac{\omega_n}{4\zeta}\left[1 + (2\zeta - \frac{\omega_n}{k})^2\right]$$

Note: $2B_n$ is in Hz

ω_n is in rad/sec.

Normally $K >> \omega_n$ then

$$(2B_n) \approx \frac{\omega_n}{4\zeta}(1 + 4\zeta^2)$$

Note: This is same as for Integrator with correction.

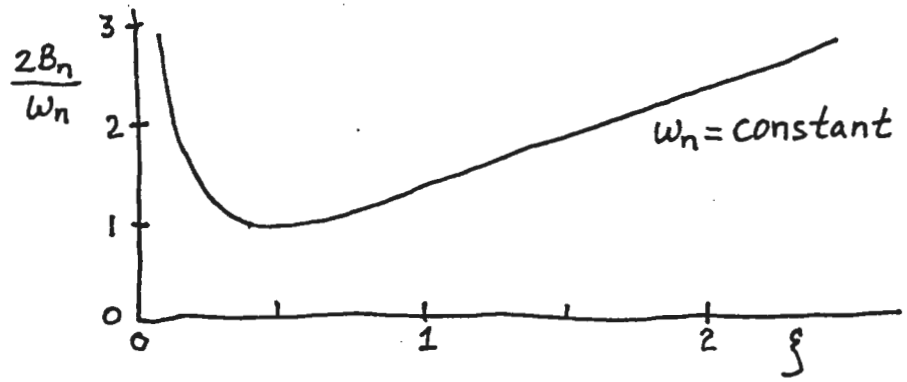

Note: There is an optimum value for ζ when the sole disturbance is additive white noise.

Note: Variations in $2B_n$ around $\frac{2B_n}{\omega_n} = 1$ are small for $0.25 \leq \zeta \leq 1$. Max deterioration which results in value of $\sigma^2_{\phi_o}$ is 1 dB.

Example: Page 161 Blanchard.

Parameter Choice Optimization

- When input to PLL is phase modulated, then the PLL behaves like a filter with transfer function $H(j\omega)$ for the modulation and the equivalent modulation by the noise.

- The optimum value for ζ as defined by Wiener is no longer 1/2.

- Optimum filtering of a signal $y(t) = \phi_i(t) + n'(t)$ will minimize $E[\phi_o^2(t) - \phi_i^2(t)]$ where ϕ_o is the VCO signal phase. Here $n'(t)$ is Gaussian with two sided spectral density $\frac{N_o}{A^2}$ over a bandwidth of $(-\frac{W}{2}\text{to}\frac{W}{2})$ where W is greater than the cutoff of $H(j\omega)$.

- If we consider only causal (physically realizable) filters, then $H(j\omega)$ must be chosen to be optimum

$$H(j\omega) = 1 - \frac{\sqrt{N_o/A^2}}{\Psi(j\omega)}$$

where Ψ is defined as follows. Provided that the power spectrum $S_y(f)$ of the composite signal $y(t)$ can be expressed in the form of a rational function of f, then it can be written

$$S_y(f) = \Psi(j2\pi f)\ \Psi(-j2\pi f)$$

Example

Take input signal as a phase step and find the optimum $H(j\omega)$

$$\phi_i(t) = \theta\Upsilon(t) \quad \Rightarrow \quad \Phi_i(s) = \frac{\theta}{s}$$

where θ is the value of the phase step

Here

$$y(t) = \theta\Upsilon(t) + n'(t)$$

$$S_y(\omega) = \frac{\theta^2}{\omega^2} + \frac{N_o}{A^2}$$

Let:

$$B_o^2 = \frac{\theta^2 A^2}{N_o}$$

$$S_y(\omega) = \frac{N_o}{A^2}\ \frac{B_o^2 + \omega^2}{\omega^2} = \left[\sqrt{\frac{N_o}{A^2}}\ \frac{B_o + j\omega}{j\omega}\right]\left[\sqrt{\frac{N_o}{A^2}}\ \frac{B_o - j\omega}{-j\omega}\right]$$

or

$$\Psi(j2\pi f) = \sqrt{\frac{N_o}{A^2}}\ \frac{B_o + j\omega}{j\omega}$$

Therefore

$$H_{opt}(j\omega) = 1 - \frac{\sqrt{N_o/A^2}}{\sqrt{\frac{N_o}{A^2}}\ \frac{B_o+j\omega}{j\omega}} = \frac{B_o}{j\omega + B_o}$$

Note: This is the transfer function of a first order loop with $K = B_o$.

Therefore, a first order loop is optimum if $K = \theta\sqrt{A^2/N_o}$.

Note: If SNR is large K is large, H_{opt} has large BW and loop tracks phase step with small error.

Note: If SNR is small, K is small, H_{opt} has small BW in order to minimize the noise error.

Example For a case where input signal is frequency step of value $\Delta\omega$, following the same procedure gives

$$H_{opt}(j\omega) = \frac{B_1^2 + j\omega\sqrt{2}B_1}{B_1^2 - \omega^2 + j\omega\sqrt{2}B_1}$$

where

$$B_1^4 = \frac{\Delta\omega^2 A^2}{N_o}$$

Note: This is the transfer function of a second order loop with integrator and correction. The parameters are

$$\zeta = \frac{1}{\sqrt{2}} \quad ; \quad \omega_n^2 = B_1^2 = \Delta\omega\sqrt{\frac{A^2}{N_o}}$$

Note: Damping factor is no longer 0.5 as it was for the case of only additive noise and no signal.

Example Case where input signal is linear frequency ramp

$$y(t) = \frac{1}{2}\mathcal{R}t^2\Upsilon(t) + n'(t)$$

- this gives

$$H_{opt}(j\omega) = \frac{B_2^3 + j\omega 2B_2^2 - 2B_2\omega^2}{B_2^3 + j\omega 2B_2^2 - 2B_2\omega^2 - j\omega^3}$$

- this requires a complicated loop filter for optimization.

Two Important Points

1) Type of loop filter required depends only on the nature of the signal disturbance

2) The values of the loop parameters depends on the SNR. When this is variable, the filter is usually optimized for the lowest anticipated value of SNR. The loop parameters can be adjusted automatically if desired as the SNR increases.

Output Signal Power Spectrum

- spectrum of $y_o(t)$ is that of a signal phase modulated by the process $\phi_o(t)$ which is a filtered version (by the loop transfer function $H(j\omega)$) of $n'(t)$.

- must calculate power spectrum of a signal which is phase modulated by a Gaussian random process.

- let $v(t) = e^{j\phi_o(t)}$

- now the spectrum of $y_o(t)$ is related to that of $v(t)$ by

$$S_{y_o}(f) = \frac{B^2}{4}\left[S_v(f - f_o) + S_v(-f - f_o)\right]$$

Here, B is the peak amplitude of $y_o(t)$.

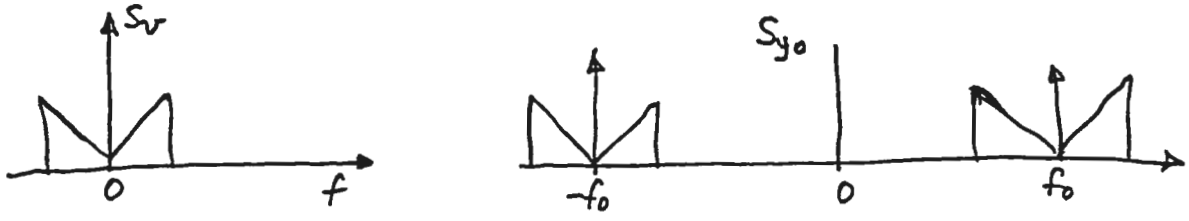

- the power spectrum of $v(t)$ is found from the autocorrelation function $R_v(\tau)$ and Fourier Transforming.

- Now, since $\phi_o(t)$ is Gaussian.

$$R_v(\tau) = \exp\left[-\{R_{\phi_o}(0) - R_{\phi_o}(\tau)\}\right]$$

Therefore,

$$\begin{aligned} S_v(f) &= \int_{-\infty}^{\infty} R_v(\tau) e^{-j2\pi f\tau} d\tau \\ &= e^{-R_{\phi_o}(0)} \int_{-\infty}^{\infty} e^{R_{\phi_o}(\tau)} e^{-j2\pi f\tau} d\tau \end{aligned}$$

Now we assume $R_{\phi_o}(0) = \sigma^2_{\phi_o}$ to stay below 1 rad^2. Also since $\phi_o(t)$ is a real process, and hence $\left|R_{\phi_o}(\tau)\right| \leq R_{\phi_o}(0)$ then

$$e^{R_{\phi_o}(\tau)} \approx 1 + R_{\phi_o}(\tau)$$

and

$$\begin{aligned} S_v(f) &= e^{-\sigma^2_{\phi_o}} \int_{-\infty}^{\infty} \left[1 + R_{\phi_o}(\tau)\right] e^{-j2\pi f\tau} d\tau \\ &= e^{-\sigma^2_{\phi_o}} \left[\delta(f) + S_{\phi_o}(f)\right] \end{aligned}$$

where $\delta(f)$ is Dirac delta function

$S_{\phi_o}(f)$ is power spectral density of VCO phase $\phi_o(t)$

therefore

$$S_{y_o}(f) = \frac{B^2}{4} e^{-\sigma_{\phi_o}^2} \left[\delta(f - f_o) + \delta(-f - f_o) + S_{\phi_o}(f - f_o) + S_{\phi_o}(-f - f_o)\right]$$

- one-sided power spectral density is

$$S_{y_o}(f+) = \frac{B^2}{2} e^{-\sigma_{\phi_o}^2} \left\{\delta(f - f_o) + \frac{N_o}{A^2} |H[j2\pi(f - f_o)]|^2\right\}$$

- recall that the nonmodulated signal power is

$$P = B^2/2$$

- We can conclude the following

1) We have a reduction in the f_o frequency spike since $e^{-\sigma_{\phi_o}^2} \approx 1 - \sigma_{\phi_o}^2 < 1$

2) Appearance of a continuous spectrum which is the scaled and frequency translated power spectrum of $\phi_o(t)$

3) The power of the spectrum is

$$P_{cont} = \left[P e^{-\sigma_{\phi_o}^2}\right] \left[\sigma_{\phi_o}^2\right] \approx P\sigma_{\phi_o}^2$$

Note: The power spectrum obtained for $S_{y_o}(f)$ does not represent a nonmodulated sinusoid and additive noise since we have no amplitude modulation of the sinusoid but only phase modulation.

Signal to Noise Ratio at the Phase Demodulation Output

- We first calculate the noise power obtained at the output of a phase demodulator.

- This is at the mixer output (error signal) when the modulating signal frequency is high enough, and we have a low modulation index.

- We have

$$\frac{u_1(j\Omega)}{\Phi_i(j\Omega)} = K_1 \frac{\Phi(j\Omega)}{\Phi_i(j\Omega)} = K_1[1 - H(j\Omega)]$$

$y_i(t)$ is accompanied by stationary, Gaussian noise with null mean and Power Spectral Density N_o.

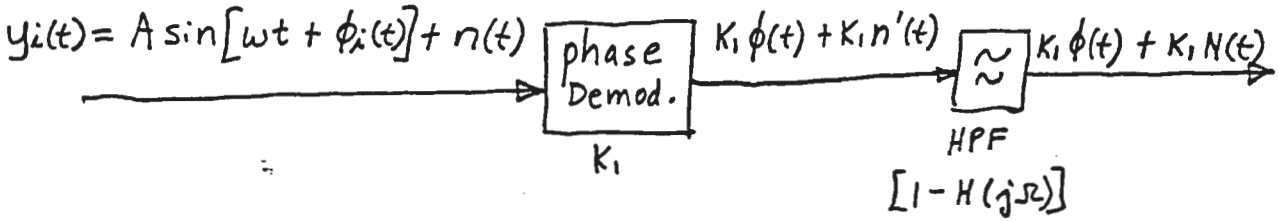

Now

$$y_i(t) \approx A\sin[\omega t + \phi_i(t) + n'(t)]$$

where $n'(t)$ has Power Spectral Density $\frac{N_o}{A^2}$

- Now $N(t)$ is the process $n'(t)$ filtered by $[1 - H(j\Omega)]$
- Also $N(t) = n'(t) - \phi_o(t)$
- We have

$$\overline{N^2(t)} = \int_{-W/2}^{W/2} \frac{N_o}{A^2} |1 - H(j2\pi F)|^2 \, dF$$

- We also have for the phase demodulated signal

$$\overline{\phi^2(t)} = \int_{-W/2}^{W/2} S_{\phi_i}(F) |1 - H(j2\pi F)|^2 \, dF$$

where S_{ϕ_i} is the Power Spectral Density of $\phi_i(t)$

- Select a second order loop so that only a small part of S_{ϕ_i} is suppressed by $|1 - H(j\Omega)|$
- then

$$\overline{\phi^2(t)} \approx \int_{-W/2}^{W/2} S_{\phi_i}(F) dF \approx \overline{\phi_i^2(t)}$$

- also

$$\overline{N^2(t)} \approx \int_{-W/2}^{W/2} \frac{N_o}{A^2} dF = \frac{N_o W}{A^2}$$

and

$$\left(\frac{S}{N}\right)_{output} = \frac{A^2}{N_o W} \overline{\phi_i^2(t)}$$

- Now coherent (synchronous) phase demodulation refers to "multiplication of a low-index phase-modulated sinusoid by a reference having the same phase to within $\frac{\pi}{2}$ as the pure carrier."

- This type of demodulation is theoretically unaffected by threshold phenomena (ie., the output signal is always $K_1\phi_i(t) + K_1 n'(t)$ for all $n'(t)$).

- A PLL with $H(j\Omega)$ narrow compared to $S_{\phi_i}(F)$ provides the requirements of coherent phase demodulation.

- Two restrictions for this "coherent" demodulation to hold are

  - $\phi_i(t)$ remains small so that $\sin[\phi_i(t)] \approx \phi_i(t)$

  - random modulation of VCO, $\phi_o(t)$ caused by the input noise also remains small. this is easily obtained since loop BW is small.

- The SNR at the coherent demodulator output is identical to that obtained when input signal is noncoherently demodulated.

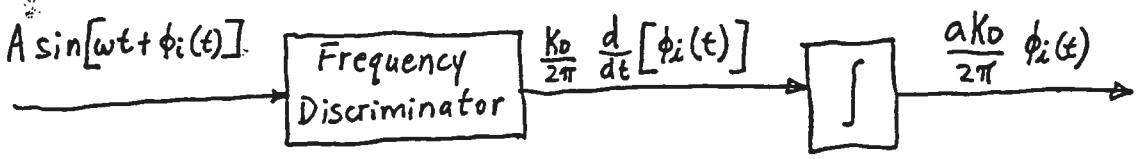

- However, the equation for the noncoherent demodulator is valid only for SNR ≥ 10 (ie., for $\frac{A^2}{2N_oW} \geq 10$).

- For coherent demodulator, the equation is valid for any SNR as long as $\sigma^2_{\phi_o} \leq \frac{1}{10}$ rad^2 (i.e., for $\frac{A^2}{N_o(2B_n)} \geq 10$) .

- Now $2B_n \ll W$ and therefore coherent demodulation can operate at lower SNR.

- Note: Both demodulators suppress the low frequency components of the modulation signal. The coherent demodulator suppresses the low frequency components because they go through the loop (i.e., no error, or phase signal). For conventional demodulators, the discriminator is like a differentiator, but the compensating integrator is nonideal, often realized as a LPF. As we reduce the cutoff frequency of the integrator, we also decrease the phase demodulation sensitivity.

  - This does not happen for the coherent demodulator.

- Note: Coherent demodulator is restricted to modulation index less than 1/2 rad or 1 rad.

  This does not apply to conventional demodulators. The modulator index depends

on the BPF (bandwidth W) which precedes the demodulators. This advantage disappears in the presence of noise.

See example in Blanchard.

Signal to Noise Ratio at the Frequency Demodulator Output

- We saw that when a frequency modulated signal is applied to a PLL, the VCO modulation signal $u_2(t)$ represents a low pass filtered version of the modulator signal.

- Also we saw that the peak frequency deviation is restricted by the modulator phase error value.

- When the frequency deviation is fixed as far as the highest frequency F_m of the modulating spectrum, we have to have ω_n much larger than F_m.

- It is advisable then to follow the loop with a second LPF with cutoff at F_m in order to reduce noise power at the output.

- It turns out that the PLL behaves as a noncoherent discriminator as far as SNR is concerned.

- However, the PLL behaves far better below SNR threshold (about 10 dBs).

- Note: When the high frequency modulation signals are limited, the LPF function of the loop can help reduce output noise ⇒ output SNR depends on type of loop filter.

Standard (Noncoherent) Discriminator

- When signal to the discriminator is accompanied by stationary, Gaussian noise $n(t)$, with null mean and P.S.D. of N_o, we can define an equivalent frequency modulation by a stationary, Gaussian, low frequency noise $n''(t)$ with null mean and P.S.D. of $\frac{N_o}{A^2}F^2$ (in Hz^2/Hz).

- the noise power at the discriminator output is

$$\overline{u_N^2(t)} = K_D^2 \int_{-W/2}^{W/2} \frac{N_o}{A^2} F^2 \, dF = K_D^2 \frac{N_o}{A^2} \frac{W^3}{12}$$

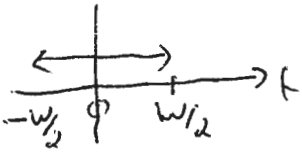

- We can filter the noise at the discriminator output (cutoff of F_m)

$$= \frac{2K_D^2}{3} \frac{N_o}{A^2} F_m{}^3$$

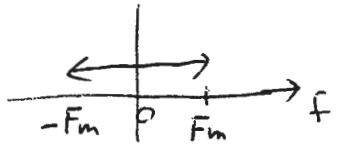

- the useful signal power at discriminator output is

$$\overline{u_s{}^2(t)} = K_D{}^2 \overline{f_{inst}^2(t)}$$

- if the modulating signal is sinusoid

$$\overline{f_{inst}^2(t)} = \frac{1}{2}\Delta f_i^2$$

where Δf_i is the peak frequency deviation.

- Hence,

$$\left(\frac{S}{N}\right)_D = \frac{3}{4}\frac{A^2}{N_o}\frac{\Delta f_i^2}{F_m^3}$$

- Now SNR for AM modulation with 100% modulation percentage is

$$\left(\frac{S}{N}\right)_{AM} = \frac{A^2}{2N_oF_m}$$

- Consequently, $\frac{3}{2}\frac{\Delta f_i^2}{F_m^2}$ is the FM improvement factor.

- This factor intervenes where input signal power exceeds the discriminator threshold.

- The threshold depends on preceding BW given by Carsons Rule

$$W = 2F_m + 2\Delta f_i$$

Note: The minimum BW required for AM is

$$W = 2F_m$$

Consequently, the SNR improvement is obtained at the expense of increased BW

First Order Loop

- Recall, this loop behaves like a discriminator with $K_D = \frac{2\pi}{K_3}$ followed by an LPF with $RC = \frac{1}{K}$.

- Output noise power is

$$\overline{u_N^2(t)} = K_D^2 \int_{-W/2}^{W/2} \frac{N_o}{A^2} \frac{F^2}{1 + \frac{(2\pi F)^2}{K^2}}\, dF$$

$$= K_D^2 \left(\frac{K}{2\pi}\right)^2 \frac{N_o}{A^2}\left[W - \frac{K}{\pi}\tan^{-1}\left(\frac{\pi W}{K}\right)\right]$$

- there are 2 cases

1) $K \gg \pi W$

here $\tan^{-1}\frac{\pi W}{K} \approx \frac{\pi W}{K} - \frac{\pi^3 W^3}{3K^3}$

and $\overline{u_N^2(t)} = K_D^2 \frac{N_o}{A^2}\frac{W^3}{12}$

Note: This is the same as for the standard (noncoherent) discriminator without filtering.

Note: The maximum modulation frequency F_m is only limited by preceding bandwidth (Carsons formula)

Note: The maximum frequency deviation is limited by the phase detector linearity

$$\Delta\phi = \frac{\Delta\omega_i}{K} < \frac{1}{2} \text{ rad}$$

2) $K \ll \pi W$ (this is not a practical case since W is far too large compared with the frequency deviation)

here

$$\tan^{-1}\frac{\pi W}{K} \approx \frac{\pi}{2}$$

and

$$\overline{u_N^2(t)} = \left(\frac{K}{2\pi}\right)^2 K_D^2 \frac{N_o}{A^2}\left(W - \frac{K}{2}\right)$$

$$\approx K_D^2 \left(\frac{K}{2\pi}\right)^2 \frac{N_o W}{A^2}$$

- Assuming that the maximum frequency of the signal to be transmitted is the 3 dB cutoff (which equals $\frac{K}{2\pi}$), we have

$$\overline{u_N^2(t)} \approx {K_D}^2 \frac{N_o}{A^2} {F_m}^2 W$$

Note: The noise power here far exceeds that for a standard discriminator followed by an LPF with a sharp cutoff at F_m. This is due to the LPF rolloff of -6 dB/octave being insufficient to suppress the noise. A standard discriminator followed by an LPF with the same characteristics will produce the same result.

Second Order Loop with Integrator and Correction or with LPF and Correction

- the discriminator slope is still $K_D = \frac{2\pi}{K_3}$.

- Also

$$|H(j\Omega)|^2 = \frac{1 + 4\zeta^2 \frac{\Omega^2}{\omega_n^2}}{\left(1 - \frac{\Omega^2}{\omega_n^2}\right)^2 + 4\zeta^2 \frac{\Omega^2}{\omega_n^2}}$$

- this transfer function has an overshoot and consequently a supplementary filtering is used.

- the complete transfer function becomes

$$|G(j\Omega)|^2 = \left[\left(1 - \frac{\Omega^2}{{\omega_n}^2}\right)^2 + 4\zeta^2\frac{\Omega^2}{{\omega_n}^2}\right]^{-1}$$

- the noise power is

$$\overline{u_N{}^2(t)} = {K_D}^2 \int_{-W/2}^{W/2} \frac{N_o}{A^2} F^2 |G(j2\pi F)|^2 \, dF$$

- for $\pi W \gg \omega_n$

$$\overline{u_N{}^2(t)} = {K_D}^2 \frac{N_o}{A^2}\left(\frac{\omega_n}{2\pi}\right)^3 \frac{\pi}{2\zeta}$$

- now $\zeta = \frac{1}{\sqrt{2}}$ corresponds to a maximally flat response with cutoff at $\frac{\omega_n}{2\pi}$.

- letting $2\pi F_m$ equal ω_n, and $\zeta = \frac{1}{\sqrt{2}}$

$$\overline{u_N{}^2(t)} = {K_D}^2 \frac{N_o}{A^2}\frac{\pi}{\sqrt{2}} {F_m}^3$$

- Comparing this with the expression for noise power from the standard discriminator, we find that the only change is the coefficient $\frac{2}{3}$ is replaced by $\frac{\pi}{\sqrt{2}} \Rightarrow$ noise power increases by 5.2 dB.

- However, this is pessimistic since a sharp cutoff at F_m was assumed for the standard discriminator.

- Note: It can be shown that if the input frequency modulation spectrum is

$$S_{f_i}(\Omega) = \frac{C}{\Omega^2 + a^2}$$

then a PLL with loop filter $\frac{1+\tau s}{1+\tau' s}$ corresponds to an optimum Wiener filter

- as regards the input signal phase if we consider the VCO phase as the output
- and as regards the input signal frequency if we consider the VCO command signal as the output provided it is followed by a supplementary LPF of $\frac{1}{1+\tau'' s}$

Recall - the choice of τ, τ', τ'' depends on the modulation constants C and a, and on the $\frac{A^2}{N_o}$ ratio.

12. Nonlinear Operation in the Presence of Noise

- Chapter 7 was based on the assumption that phase detector was operating in the linear zone.

- this implies that the VCO is already synchronized

- we will see what happens when the input signal phase variations or the level of additive noise are such as to invalidate the low phase error assumption.

- this situation in fact diminishes the VCO sensitivity to input signal phase variations; or heightens the noise to a point where synchronism is lost.

- this situation is called the operating threshold

- We will use $\varphi_n(t)$ to represent the VCO random modulation due to additive noise; and $\phi_o(t)$ to represent the VCO response to an input phase modulation $\phi_i(t)$; and $\varphi_o(t)$ for loop response to additive noise within the linear hypothesis.

Influence of Additive Noise

- PLL operation in presence of noise beyond the linear zone has no precise math soln for loops of second order.

- Results are obtained using simplifying hypotheses which are close to experimental results.

Analysis of Problem

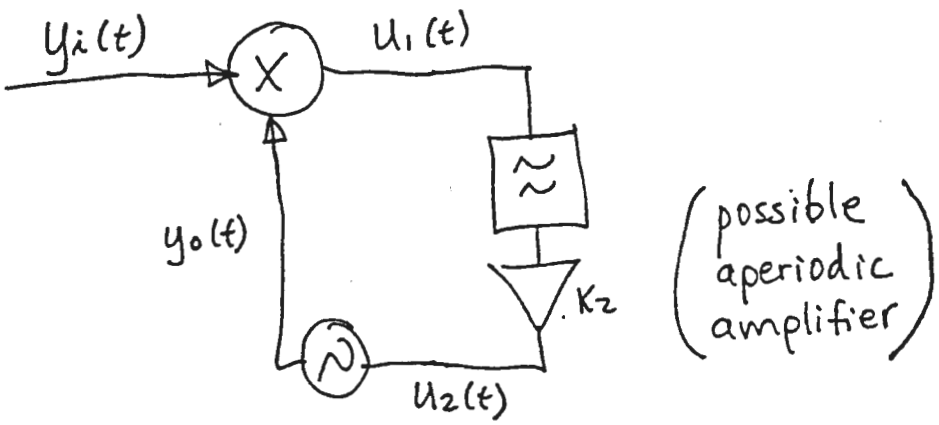

- here we use sinusoidal phase detector to keep analysis simple in presence of high additive noise.

- In absence of noise, we have:

$$y_i(t) = A\sin(\omega_o t + \phi_i(t))$$

$$y_o(t) = B\cos(\omega_o t + \phi_o(t))$$

also

$$u_1(t) = K_1\sin(\phi_i(t) - \phi_o(t))$$

and

$$u_2(t) = K_2 u_1(t) * f(t)$$

and

$$\frac{d\phi_o}{dt} = K_3 u_2(t)$$

- Combining yields eqn. (3.4) (obtained much earlier in the course)

$$\frac{d\phi_o}{dt} = K\sin[\phi_i(t) - \phi_o(t)] * f(t)$$

- when input signal is accompanied by additive noise $n(t)$, a noise term is added to $u_1(t)$ and after filtering induces a supplementary VCO phase modulation $\varphi_n(t)$

- split the noise into inphase and quadrature components:

$$y_i(t) = A\sin(\omega_o t + \phi_i(t)) + n_1(t)\sin(\omega_o t) + n_2(t)\cos(\omega_o t)$$

- after multiplication by:

$$y_o(t) = B\cos\Big(\omega_o t + \phi_o(t) + \varphi_n(t)\Big)$$

and lowpass filtering, we get:

$$u_1(t) = K_1\Big\{\sin[\phi_i(t) - \phi_o(t) - \varphi_n(t)] - \frac{n_1(t)}{A}\sin[\phi_o(t) + \varphi_n(t)] + \frac{n_2}{A}\cos[\phi_o(t) + \varphi_n(t)]\Big\} \qquad -(12.1)$$

- Hence, the signal applied to the VCO is:

$$\frac{d(\phi_o + \varphi_n)}{dt} = K\Big\{\sin[\phi_i(t) - \phi_o(t) - \varphi_n(t)] - \frac{n_1(t)}{A}\sin[\phi_o(t) + \varphi_n(t)] + \frac{n_2(t)}{A}\cos[\phi_o(t) + \varphi_n(t)]\Big\} * f(t) \qquad -(12.2)$$

- if we assume that the total phase error remains low, i.e.,

$$\phi_i(t) - \phi_o(t) - \varphi_n(t) \ll \pi/2$$

then:

$$\sin\left[\phi_i(t) - \phi_o(t) - \varphi_n(t)\right] \approx \phi_i(t) - \phi_o(t) - \varphi_n(t)$$

Note: for this to be verified, both $\phi_i(t) - \phi_o(t)$ from the modulation and $\varphi_n(t)$ from the additive noise must be small.

- now if $\phi_o(t)$ and $\varphi_n(t)$ vary slowly compared to $n_1(t)$ and $n_2(t)$, then the quantity:

$$-\frac{n_1(t)}{A}\sin[\phi_o(t) + \varphi_n(t)] + \frac{n_2}{A}\cos[\phi_o(t) + \varphi_n(t)]$$

can be replaced by a noise term $n'(t)$ as described in chapter 7.

- the phase detector output signal is then:

$$u_1(t) = K_1[\phi_i(t) - \phi_o(t) - \varphi_o(t) + n'(t)]$$

where we have already assumed we are in the linear domain

-the additive noise $n(t)$ is interpreted as a supplementary phase modulation $n'(t)$ of the input signal phase.

- Hence VCO phase becomes the sum of response $\phi_o(t)$ and response $\varphi_o(t)$ (to the input signal equivalent modulation $n'(t)$).

- $\varphi_o(t)$ is Gaussian with null mean and spectral density $S_{\varphi_o}(f)$ (given by eqn. (7.8).

$$S_{\varphi_o}(f) = \frac{N_o}{A^2}\left|H(j2\pi f)\right|^2$$

- this process has a variance (eqn (7.9) and (7.15))

$$\sigma^2_{\varphi_o} = \int_{-\infty}^{\infty} \frac{N_o}{A^2}\left|H(j2\pi f)\right|^2 df = \frac{N_o}{A^2}(2B_n)$$

- Since we know $\varphi_o(t)$ is Gaussian, and since we know its variance, we know its probability density function.

$$p(\varphi_o) = \frac{1}{\sqrt{2\pi}\sigma_{\varphi_o}}\exp\left[\frac{-\varphi_o^2}{2\sigma^2_{\varphi_o}}\right]$$

- we can also find the autocorrelation function from $S_{\varphi_o}(f)$

$$R_{\varphi_o}(\tau) = \int_{-\infty}^{\infty} S_{\varphi_o}(f)\, e^{j2\pi f\tau} df$$

- for integrator with phase lead correction with $\zeta < 1$ this gives (eqn (7.22))

$$R_{\varphi_o}(\tau) = \frac{N_o}{A^2}\frac{\omega_n}{4}\exp[-\zeta\omega_n\tau]\left[\frac{1+4\zeta^2}{\zeta}\cos(\omega_n\sqrt{1-\zeta^2}\,\tau) + \frac{1-4\zeta^2}{\sqrt{1-\zeta^2}}\sin(\omega_n\sqrt{1-\zeta^2}\,\tau)\right]$$

- Hence, adopting the linear hypothesis, the process $\varphi_n(t) = \varphi_o(t)$ is Gaussian, has null mean, and known autocorrelation function.

- The process is completely defined

- However, if linear hypothesis is abandoned, the output process $\varphi_n(t)$ must be derived from eqn (12.2).

12.1.2 Fokker-Planck Method

- consider eqn (12.2) and suppose input signal is not modulated.

- also suppose

$$\phi_i(t) = \theta_i$$

$$\phi_o(t) = \theta_i$$

- this implies the loop is in lock with null static phase error (frequency difference between input and VCO is zero)

- Here eqn (12.2) becomes:

$$\frac{d\varphi_n}{dt} = K\Big\{-\sin\varphi_n(t) - \frac{n_1(t)}{A}\sin\Big[\theta_i + \varphi_n(t)\Big] + \frac{n_2(t)}{A}\cos[\theta_i + \varphi_n(t)]\Big\} * f(t) \qquad -(12.3)$$

if bandwidth W of additive noise $n(t)$ is large compared with loop bandwidth, then the term $n'(t)$ given by:

$$n'(t) = \frac{n_1(t)}{A}\sin[\theta_i + \varphi_n(t)] + \frac{n_2(t)}{A}\cos[\theta_i + \varphi_n(t)]$$

is Gaussian, has null mean, and uniform spectral density equal to $\frac{N_o^2}{A^2}$ from $-\frac{W}{2}$ to $\frac{W}{2}$

- Hence $n'(t)$ obtained at phase detector output still has the same properties as in Ch. 7.1, independently of the properties of the process $\varphi_n(t)$ modulating the VCO.

- this is true providing the variation of $\varphi_n(t)$ are slow compared with processes $n_1(t)$ and $n_2(t)$.

- Differential eqn. governing loop operation is:

$$\frac{d\varphi_n}{dt} = K\Big\{-\sin[\varphi_n(t)] + n'(t)\Big\} * f(t) \qquad -(12.4)$$

First-Order Loop

Here eqn (12.4) becomes:

$$\frac{d\varphi_n}{dt} = -K \sin \varphi_n(t) + Kn'(t) \qquad -(12.5)$$

- The derivative of the process $\varphi_n(t)$ at any instant does not depend on past history of the process $\varphi_n(t)$, but only on the value of the process at the instant considered.

- This is a property of a Markov process

- The probability density function at each instant $p(\varphi_n, t)$ is given by the Fokker-Planck eqn:

$$\frac{\partial p(\varphi_n, t)}{\partial t} = \frac{\partial}{\partial \varphi_n}[A_1(\varphi_n)p(\varphi_n, t)] + \frac{1}{2}\frac{\partial^2}{\partial \varphi_n^2}[A_2(\varphi_n)p(\varphi_n, t)] \qquad -(12.6)$$

where

$$A_1(\varphi_n) = \lim_{\Delta t \to 0} \frac{E[\Delta\varphi_n|\varphi_n]}{\Delta t}$$

$$A_2(\varphi_n) = \lim_{\Delta t \to 0} \frac{E[\Delta\varphi_n^2|\varphi_n]}{\Delta t}$$

- where the expected values are conditional expected values on φ_n.

- now from eqn (12.5)

$$\Delta\varphi_n = -K \sin \varphi_n \Delta t + K \int_t^{t+\Delta t} n'(u)\, du$$

- and since $n'(t)$ has null mean value:

$$E[\Delta\varphi_n|\varphi_n] = -K \sin \varphi_n \Delta t$$

- Hence

$$A_1(\varphi_n) = -K \sin \varphi_n$$

- also

$$\Delta\varphi_n^2 = K^2 \sin^2 \varphi_n \Delta t^2 - 2K^2 \sin \varphi_n \Delta t \int_t^{t+\Delta t} n'(u)\, du + K^2 \int_t^{t+\Delta t} \int_t^{t+\Delta t} n'(u)n'(v)\, du\, dv$$

- Hence

$$E[\Delta\varphi_n^2|\varphi_n] = K^2 \sin^2 \varphi_n \Delta t^2 - 2K^2 \sin \varphi_n \Delta t \int_t^{t+\Delta t} E[n'(u)]\, du + K^2 \int_t^{t+\Delta t} \int_t^{t+\Delta t} E[n'(u)n'(v)]\, du\, dv$$

now

$$E[n'(u)] = 0$$

Hence

$$A_2(\varphi_n) = \lim_{\Delta t \to 0} \frac{K^2}{\Delta t} \int_t^{t+\Delta t} \int_t^{t+\Delta t} E[n'(u)n'(v)]\, du\, dv$$

Since $n'(t)$ is Gaussian, white process with $\frac{N_o}{A^2}$ spectral density, then:

$$E[n'(u)n'(v)] = \frac{N_o}{A^2}\delta(u-v)$$

Then

$$A_2(\varphi_n) = K^2 \frac{N_o}{A^2}$$

Finally, the Fokker-Planck eqn (eqn 12.6) becomes:

$$\frac{\partial p(\varphi_n, t)}{\partial t} = -\frac{\partial}{\partial \varphi_n}[-K \sin(\varphi_n) p(\varphi_n, t)] + \frac{K^2}{2} \frac{N_o}{A^2} \frac{\partial^2 p(\varphi_n, t)}{\partial \varphi_n^2}$$

- if we assume a stationary solution exists for $\varphi_n(t)$ then the probability density function is also stationary

$$\frac{\partial p(\varphi_n, t)}{\partial t} = 0$$

- the steady state Fokker-Planck eqn reduces to

$$0 = -\frac{d}{d\varphi_n}[-K \sin \varphi_n p(\varphi_n)] + \frac{K^2}{2} \frac{N_o}{A^2} \frac{d^2 p(\varphi_n)}{d\varphi_n^2}$$

- Solution of this eqn is

$$p(\varphi_n) = \frac{\exp[\rho_L \cos \varphi_n]}{2\pi I_o(\rho_L)} \quad , -\pi < \varphi_n < \pi \qquad -(12.8)$$

where ρ_L is the signal to noise ratio in the loop

$$\rho_L = \frac{A^2}{N_o(K/2)} = \frac{A^2}{N_o(2B_n)} = \frac{1}{\sigma_{\varphi_o}^2}$$

and I_o is the modified Bessel function of the first kind of order 0.

- Result : The process $\varphi_n(t)$ outside the linear hypothesis is no longer Gaussian.

: The process does have a null mean value

: its variance is (from eqn (12.8))

$$\sigma_{\varphi_n}^2 = \frac{\pi^2}{3} + \sum_{k=1}^{\infty} (-1)^k \frac{I_k(\rho_L)}{I_o(\rho_L)}$$

: when ρ_L is large, $p(\varphi_n)$ decreases sharply.

- For low values of φ_n,

$$\cos\varphi_n \approx 1 - \frac{1}{2}\varphi_n^2$$

Also

$$I_o(\rho_L) = \frac{\exp(\rho_L)}{\sqrt{2\pi\rho_L}}$$

Hence, eqn. (12.8) reduces to:

$$p(\varphi_n) = \frac{\exp[\rho_L]\exp[-1/2\rho_L\varphi_n^2]}{\frac{2\pi[\exp\rho_L]}{\sqrt{2\pi\rho_L}}}$$

$$= \frac{1}{\sqrt{2\pi}\sqrt{1/\rho_L}}\exp\left[\frac{-\varphi_n^2}{2(1/\rho_L)}\right]$$

- This is Gaussian!! Hence, when the signal to noise ratio in the loop is large, distribution of φ_n tends to be Gaussian with variance $1/\rho_L$ which agrees with the linear analysis.

- Alternatively when $\rho_L \to 0$, eqn (12.8) becomes:

$$p(\varphi_n) = \frac{1}{2\pi} \qquad -\pi < \varphi_n < \pi$$

- Here the variance tends towards $\frac{\pi^2}{3}$.

14. Data (Carrier) Synchronizers

- optimum detection of data requires a local clock generator that is in close phase agreement with the received data stream.

- this is called synchronous detection.

- a data stream often must be modulated onto a carrier frequency before it can be transmitted over a communications channel.

- optimum demodulation requires a local carrier source at the receiver whose phase is in close agreement with the received signal.

- this is called coherent demodulation.

- the receiver circuits that generate the carrier and clock waveforms are called carrier and clock synchronizers. PLLs are widely used in synchronizers.

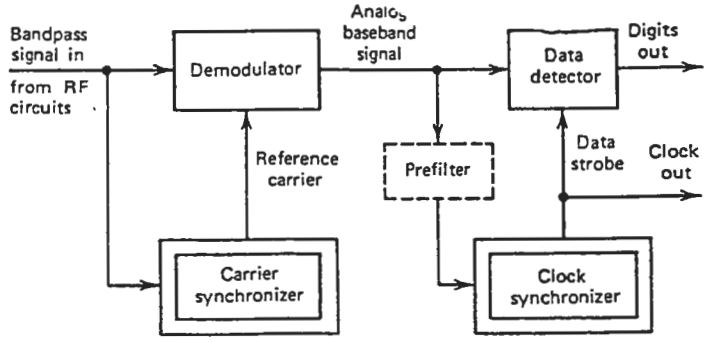

Figure 11.1 Digital receiver illustrating locations of synchronizers.

1. General Principles

- efficient modulation techniques suppress the carrier completely, all transmitted energy being in the data sidebands.

- if a reliable carrier component is present then carrier tracking loops are all that is required.

- also efficient data streams contain no discrete component at the clock frequency. For example, NRZ (non-return to zero) signaling actually has a spectral null at the clock frequency.

- since a conventional PLL requires a discrete spectral component at the frequency to be

tracked, it cannot be used as a data synchronizer.

- suitable nonlinear circuits can regenerate a clock or carrier from an input signal that contains neither.

- Two different configurations are shown below:

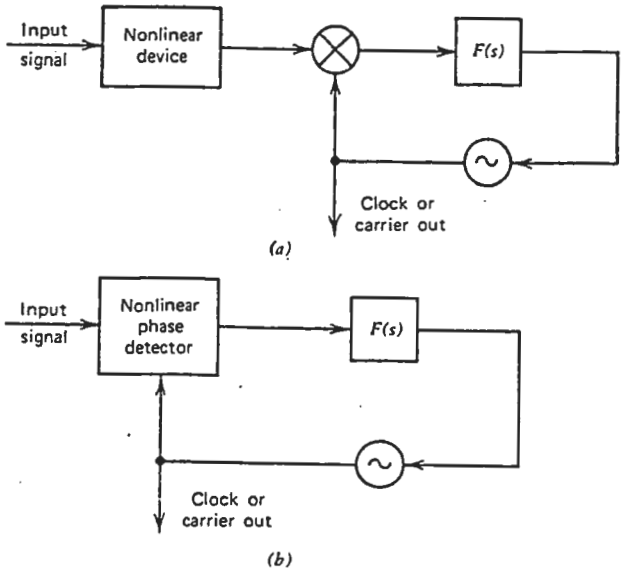

Figure 11.2 Nonlinear regenerator configurations: (*a*) separate nonlinearity; (*b*) nonlinear phase detector.

- in the case (a) employing a separate nonlinearity, a narrow band BPF could be used in place of a PLL to avoid problems related to fast acquisition.

- However, the PLL can provide automatic compensation for frequency drift of either the signal or circuit components.

- the design of synchronizers requires three steps:

1) devise a suitable nonlinearity

2) identify disturbances and analyze performance. This analysis is usually very difficult due to the nonlinearity.

3) select PLL parameters

2. Carrier Synchronizers

- initially we will consider binary signaling, with rectangular NRZ bit waveforms, binary

phase shift keying (BPSK) the carrier.

- if the data bit is +1, the bandpass signal is transmitted with a phase of +90°
- if the bit is 0, the signal is transmitted with a phase of -90°
- each pulse is T seconds in duration and the pulses are T seconds apart.
- if equal numbers of 1's and 0's are transmitted, the carrier is completely suppressed.
- the transmitted signal is:

$$s(t) = \sqrt{2}\, Am(t)\sin(\omega_i t + \theta_i)$$

where A is the amplitude of the baseband signal

$m(t)$ is the baseband data waveform

ω_i is the carrier frequency

θ_i is the signal phase.

Circuit Configurations

- there are three main types of carrier synchronizers:

a) the squaring loop

b) the Costas loop

c) the remodulator (also called inverse modulator, reverse modulator, or unmodulator)

a) The squaring loop is shown below:

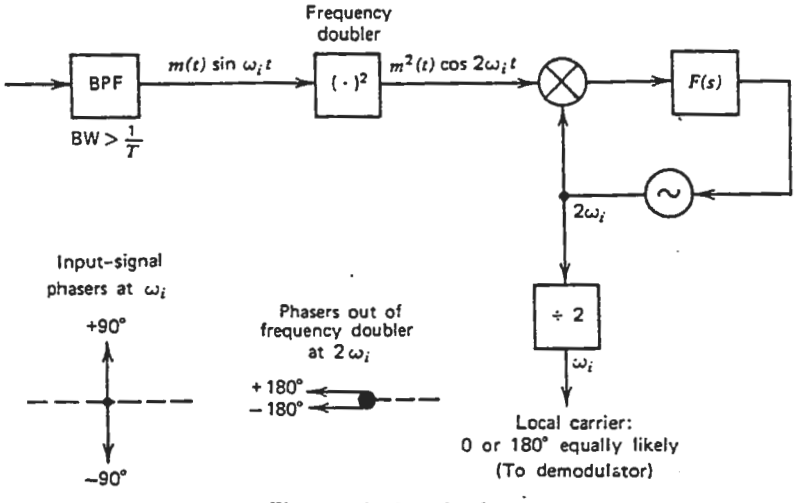

Figure 11.3 Squaring loop.

- here the nonlinear element is modeled as a square law device. The output from the nonlinearity is:

$$v_{sq}(t) = 2A^2m^2(t)\sin^2(\omega_i t + \theta_i) = A^2m^2(t)[1 - \cos(2\omega_i t + 2\theta_i)]$$

- a conventional PLL operating at $2\omega_i$ locks to the second harmonic component, and the VCO output is divided by two to give the desired reference carrier.

- a second harmonic component exists for any message waveform where avg $[m^2] \neq 0$.

- intuitively we can consider the nonlinearity as a frequency doubler.

- the input consists of two phasers at $\pm 90°$

- frequency doubling also doubles the phases of the phasers to $\pm 180°$.

- the input phasers at $\pm 90°$ cancel one another on the average $\Rightarrow$ no carrier component.

- output phasers however reinforce each other to produce a strong second harmonic.

- Note: the divide by 2 circuit can operate in either of two phases determined by the random starting state of the divider. Hence, it is impossible to decide whether the current bit is a 1 or a 0 without further information.

- this ambiguity is not a defect of the squaring loop but is inherent to all suppressed carrier, phase shift keying modulation.

- In general, if the information is transmitted in N different phases, there is an N fold ambiguity in the data recovery.

- the above ambiguity can only be resolved with encoding or other information carried in the message.

b) The remodulator is shown in two versions below

- the two versions have identical performance

- in the first circuit, the incoming signal is demodulated and the message $m(t)$ is recovered.

- this baseband signal $m(t)$ is used to remodulate the incoming signal.

- if the waveforms are rectangular and time aligned, then the remodulation removes the modulation completely

- output from the balanced modulator has a pure carrier component at the input frequency.

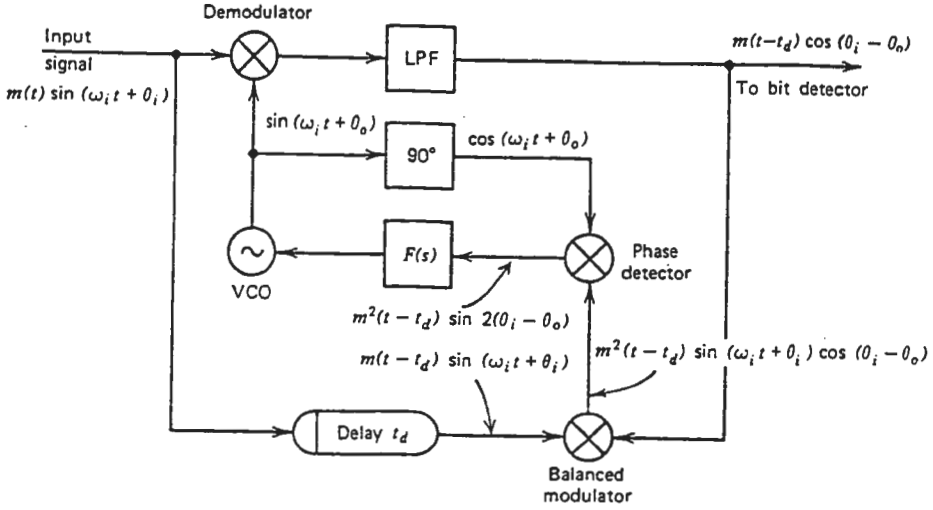

Figure 11.4 Remodulator.

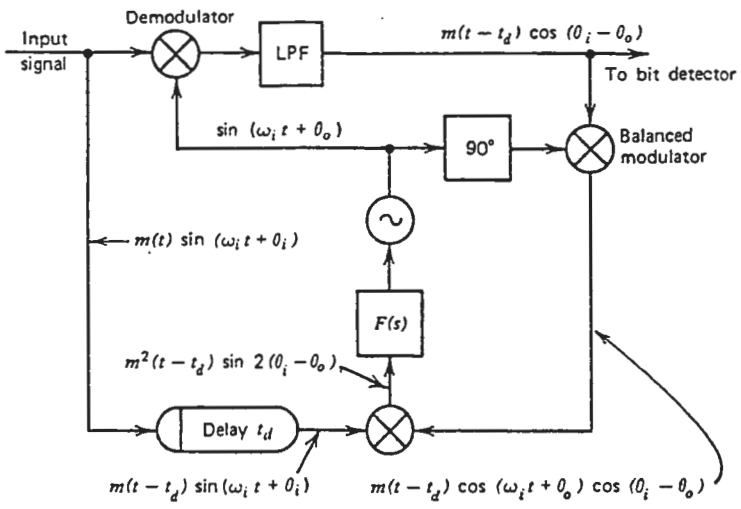

Figure 11.5 Inverse modulator. (Terms "remodulator" and "inverse modulator" are used interchangeably and indiscriminantly.)

- The PLL tracks this component.

- The second version (Fig 11.5) imposes the recovered message modulation on the VCO output so that both inputs to the phase detector are identically modulated.

- the low frequency product of two such waveforms yields a DC component of the same amplitude as if the inputs had no modulation.

- Note : the balanced modulator, demodulator and phase detectors above are all modeled as ideal multipliers.

:some factors of 2 have been neglected in the equations given in the figures

: often the same type of circuit such as a diode ring modulator is used for the balanced modulator and the phase detectors.

- Note : the DC output from the phase detector in both versions is proportional to $\sin 2(\theta_i - \theta_o)$

Consequently, there are two stable tracking points for each cycle of input.

- following the demodulator is a LPF that rejects the double frequency mixer products and noise. This filter is essential when no BPF filtering is used at the input to the remodulators.

- any physical filter has delay, denoted t_d.

- the waveforms multiplied at the balanced modulator in Fig 11.4, and at the phase detector in Fig 11.5 must be time aligned.

- otherwise the modulations are not well correlated at the modulator and the available DC output of the phase detector is reduced.

- if time misalignment is as great as one pulse interval, correlation falls to zero at the modulator, and DC falls to zero at the phase detector.

- to compensate for the filter delay, a fixed delay t_d is inserted into the signal path before the multiplier.

- it is also necessary that

$$(\omega_i)(t_d) = k\pi \qquad , \quad k = 1, 2, 3, \ldots$$

for circuit phasing to be correct.

c) The Costas loop is shown below:

- operation can be visualized as follows:

- in the absence of modulation, the Q arm acts as a conventional PLL with the usual error voltage being developed at the output of the Q arm multiplier.

- When modulation is present, the polarity of the Q arm output reverses each time the modulation changes sign. Average output is zero for random data irrespective of the phase error.

- The I arm multiplier produces a signal in quadrature to that from the Q arm.

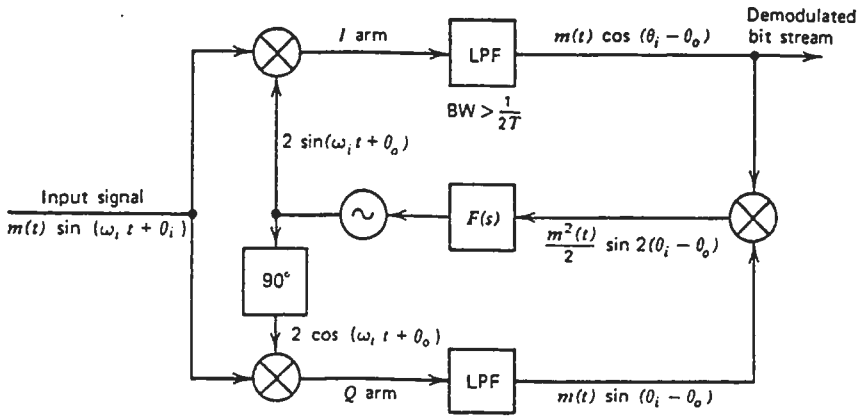

Figure 11.6 Costas loop.

- If phase is nearly correct for tracking, then the I arm output is the data message.

- this is also used for reversing the Q arm voltage in the third multiplier.

- this cancels the polarity reversals that invalidated the Q arm output as an error voltage.

- Note: the third multiplier output is proportional to $\sin 2(\theta_i - \theta_o)$ the same as for the squaring loop and the remodulator.

Multiphase Synchronization

-modified versions of the above three circuits are used for multiphase modulation.

- four phase examples are now discussed.

a) N times multiplier

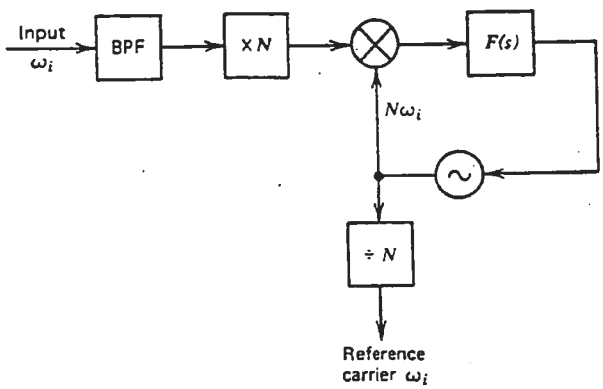

Figure 11.7 $\times N$ multiplier.

- operation is a simple extension of the squaring loop when rectangular pulses are used.

- for rounded pulses, the desired N^{th} harmonic is regenerated by intermodulation among data sidebands.

- at least N^{th} order intermod is required to produce the carrier

- if the message waveform bandwidth is sufficiently narrow, then the circuit may fail to regenerate a carrier on some data patterns

- For example, a data pattern which causes the phase to advance by 1/N cycle for each symbol is interpreted by the circuit as an unmodulated signal displaced by 1/NT Hz from the actual carrier. Here T is the symbol interval.

b,c) Four Phase Remodulator and Costas Loops are shown below.

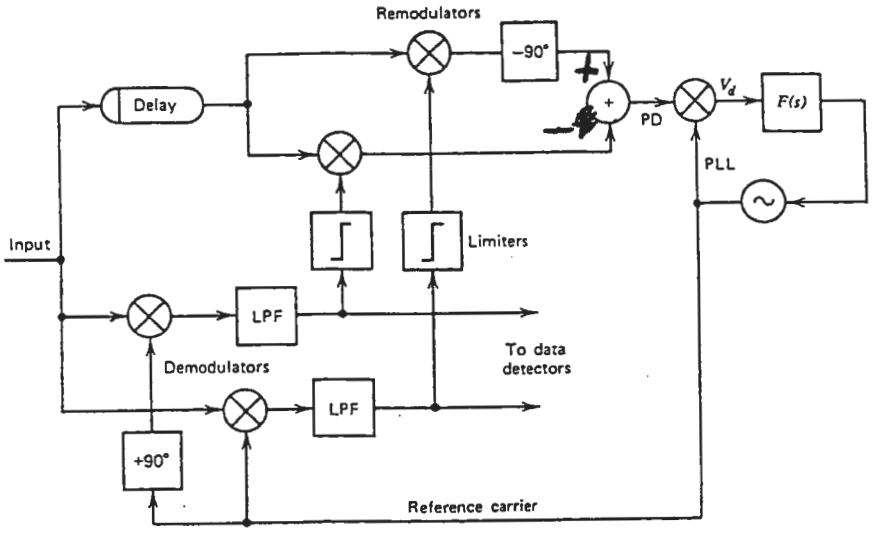

Figure 11.8 Four-phase remodulator.

- independent messages $x(t)$ and $y(t)$ modulate two quadrature components of the carrier, in the transmitter.

- the transmitted signal is then:

$$s(t) = x(t)\cos(\omega_i t + \theta_i) - y(t)\sin(\omega_i t + \theta_i)$$

- after manipulations, the low frequency output of the phase detector for either the remodulator or the Costas loop is found to be:

$$\begin{aligned} v_d(t) = &[x\sin\theta_e + y\cos\theta_e]\ \text{sgn}\ [x\cos\theta_e - y\sin\theta_e] \\ &- [x\cos\theta_e - y\sin\theta_e]\ \text{sgn}\ [x\sin\theta_e + y\cos\theta_e] \end{aligned}$$

where $\theta_e = \theta_i - \theta_o$ and sgn is the hard limiting operation.

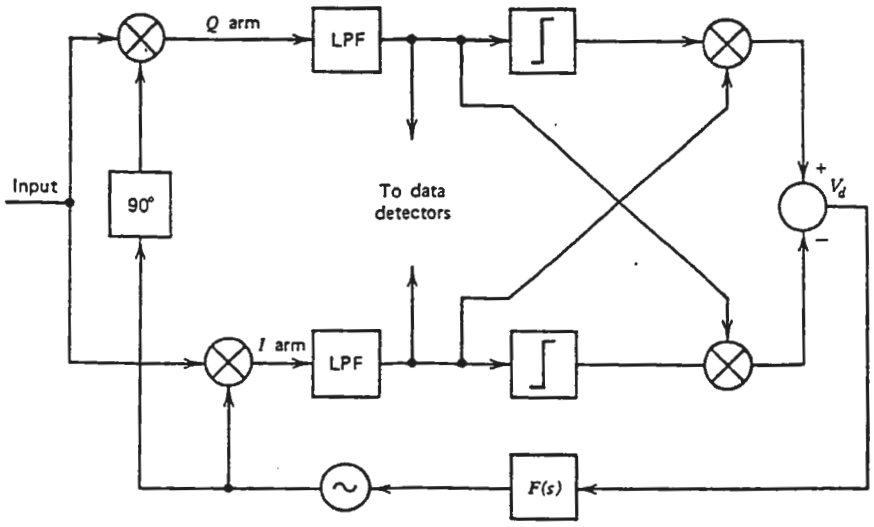

Figure 11.9 Four-phase Costas loop.

- if the message waveform is rectangular then the average DC output is:

$$V_d = \begin{cases} 2\sin\theta_e & , -45° < \theta_e < 45° \\ -2\cos\theta_e & , 45° < \theta_e < 135° \\ -2\sin\theta_e & , 135° < \theta_e < 225° \\ 2\cos\theta_e & , 225° < \theta_e < 315° \end{cases}$$

- this is a "near-sawtooth" characteristic shown below:

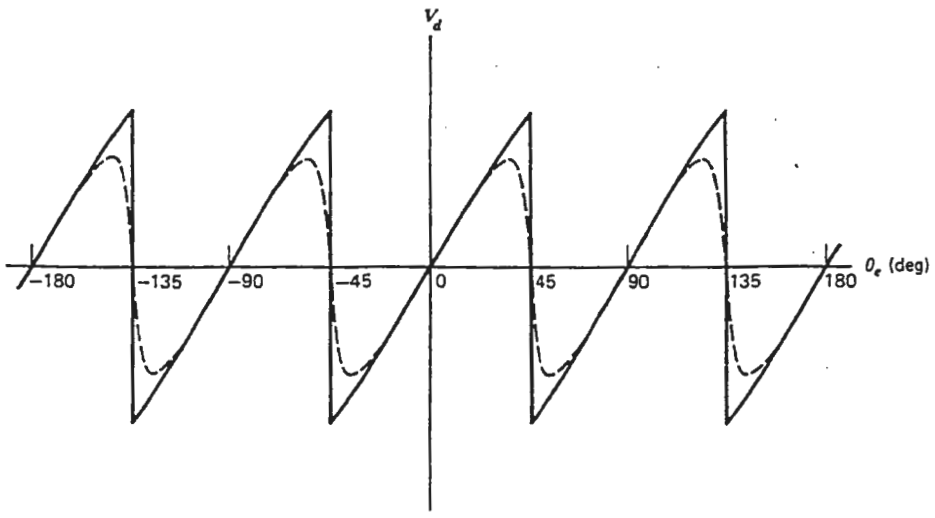

Figure 11.10 Phase-detector characteristic of four-phase remodulator or Costas loop.

- if the bandwidth is limited, the pulses cannot be rectangular and the "near-sawtooth" characteristic is modified.

- calculations are difficult for rounded pulses, especially if the pulses overlap due to narrow band transmission.

- the tendency is for the discontinuities and sharp peaks of the sawtooth to be rounded off (as shown in Fig 11.10)

- Noise also causes rounding of the sawtooth

- A stable lock can be achieved at 0, 90°, 180°, 270° ⇒ hence there is a fourfold ambiguity that must be resolved by other means.

- The limiters shown in the circuits are essential for correct operation since without them the circuit has only second order nonlinearities in the multipliers.

- Recall that a four phase signal requires at least a fourth order nonlinearity ⇒ hence the limiters.

- Note: the Costas loop and Remodulator include the data demodulator as part of the circuit. A demodulator is entirely separate if a N times multiplier is used.

- both the Costas loop and the remodulator remove a modulation by multiplying the demodulated message waveform in analog form.

- better noise rejection is possible if the message value is optimally detected and the digital message value is used for the modulation-removal multiplication.

- this type of synchronizer is called a decision directed (also called data aided or decision feedback).

- it has less noise-caused jitter of the reference carrier

- however, additional delays are needed to compensate for the delay of the data detection circuit. These delays and the demodulator LPF delay must be accounted for when considering stability.

- also note the remodulator has two feedback loops ⇒ difficult to analyze dynamic performance.

- a decision-directed circuit cannot acquire the carrier until the clock is acquired, and may not be able to acquire the clock until the carrier has been acquired. Hence they

may not be usable when fast acquisition is required.

Carrier Synchronizer Performance

- in general, these analyses are very difficult due to the nonlinear element.

- we will analyze the simplest case, that of a squaring loop with an ideal square-law nonlinearity.

- the results of this analysis will be used to identify features common to all carrier synchronizers.

Analysis of Squaring Loop

- referring to Fig 11.2 shown earlier, we have the input signal (after BPF filtering) as:

$$s(t) = \sqrt{2}\, Am(t)\cos(\omega_i t + \theta_i) + n(t)$$

- here n(t) is the bandpass Gaussian noise
m(t) is the data modulation after filtering.

- due to filtering m(t) cannot be a rectangular waveshape.

- the discontinuities are rounded into continuous transitions and the individual pulses overlap somewhat.

- the filtered signal has amplitude variations even if the original signal had a constant envelope.

- also the filtered signal has an envelope null at each phase reversal.

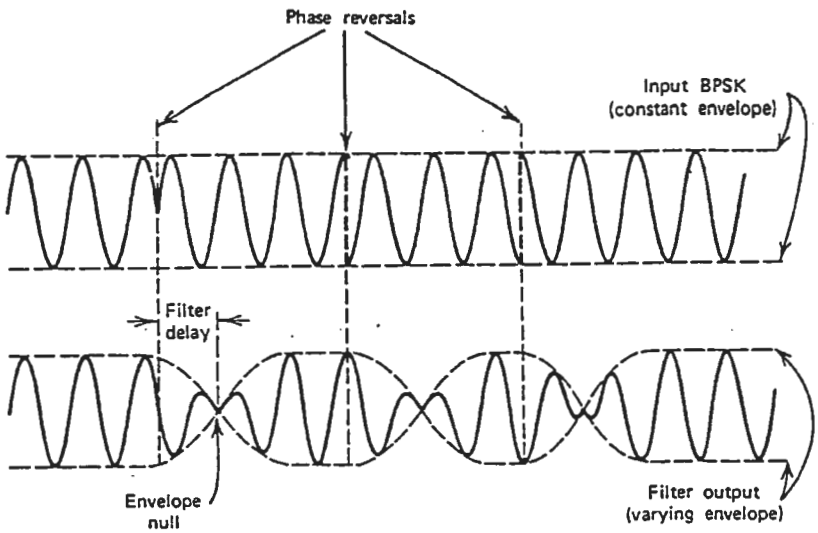

Figure B.1 Effect of filter on data-modulated signal.

- the filtered input is applied to a squaring device described by:

$$v_{sq}(t) = K_{sq} s^2(t)$$

- this characteristic is not optimum in any sense, but is easiest to handle mathematically. For example, a full wave, linear rectifier will yield about 2 dB less phase jitter on the recovered carrier at large SNR than the square law device.

- we expand the bandpass noise into two quadrature components about the carrier:

$$s(t) = \sqrt{2}\,[Am(t)\cos(\omega_i t + \theta_i) + n_c \cos(\omega_i t) + n_s \sin(\omega_i t)] \qquad -(1)$$

- we then calculate $s^2(t)$, discard the low frequency terms near DC and consider only the high frequency terms near $2\omega_i$.

$$\begin{aligned} v_{sq}(t) = K_{sq}\Big[& A^2 m^2(t)\cos 2(\omega_i t + \theta_i) + n_c^2 \cos 2\omega_i t \\ & - n_s^2 \cos 2\omega_i t + 2n_s Am(t)\sin(2\omega_i t + \theta_i) \\ & + 2n_c Am(t)\cos(2\omega_i t + \theta_i) - 2n_c n_s \sin(2\omega_i t)\Big] \end{aligned} \qquad -(2)$$

- Output from the VCO is:

$$v_o(t) = V_o \sin 2(\omega_i t + \theta_o) \qquad -(3)$$

- Here we temporarily assume θ_o to be fixed even though it is random. Note that $2\theta_o$ is the phase of the VCO signal at $2\omega_i$.

- Now useful phase detector output, discarding double frequency products is:

$$\begin{aligned} v_d &= K_m v_{sq}(t) v_o(t) \\ &= K_m K_{sq} V_o \Big[\frac{1}{2} A^2 m^2(t)\sin 2(\theta_i - \theta_o) + \frac{1}{2}(n_c^2 - n_s^2)\sin 2\theta_o \\ &\quad - n_c n_s \cos 2\theta_o + n_s Am(t)\cos(\theta_i - 2\theta_o) \\ &\quad - n_c Am(t)\sin(\theta_i - 2\theta_o)\Big] \end{aligned} \qquad -(4)$$

- Define

$$\begin{aligned} \sigma_m^2 &= \text{avg}\,[m^2(t)] \\ K_d &= \frac{1}{2} K_m K_{sq} V_o A^2 \sigma_m^2 \\ n_c' &= \frac{n_c}{A\sigma_m} \\ n_s' &= \frac{n_s}{A\sigma_m} \end{aligned} \qquad -(5)$$

- We can represent the squared modulation as:

$$m^2(t) = m_o^2(t) + \sigma_m^2$$

where:

$$\text{avg } [m_o^2(t)] = 0$$

- the difference frequency output of the phase detector becomes:

$$\begin{aligned} v_d = K_d \Big[& \sin 2(\theta_i - \theta_o) && \Leftarrow \text{ DC error term} \\ & + \left(\frac{m_o^2}{\sigma_m^2}\right) \sin 2(\theta_i - \theta_o) && \Leftarrow \text{ self noise} \\ & + (n_c'^2 - n_s'^2) \sin 2\theta_o - 2n_c' n_s' \cos 2\theta_o && \Leftarrow \text{ noise} \times \text{ noise} \\ & + 2\left(\frac{n_c' m}{\sigma_m}\right) \cos(\theta_i - 2\theta_o) && \Leftarrow \text{ signal} \times \text{ noise} \\ & - 2\left(\frac{n_s' m}{\sigma_m}\right) \sin(\theta_i - 2\theta_o) \Big] && \Leftarrow \text{ signal} \times \text{ noise} \end{aligned}$$

- self noise is usually neglected. If $\theta_i - \theta_o = 0$, or if $m_o^2 = 0$ (true if the filtered pulses were rectangular) then the self noise will vanish.

- the sum of the noise×noise and signal×noise terms is denoted by $n'(t)$.

- Hence the phase detector output is:

$$\begin{aligned} v_d(t) &= K_d[\sin 2(\theta_i - \theta_o) + n'(t)] \\ &\approx K_d[2(\theta_i - \theta_o) + n'(t)] \end{aligned} \qquad -(7)$$

Note: equations identical to (6) are obtained for both the Costas loop and the remodulator provided the LPFs are equivalent to the BPF of the squaring loop and that the multipliers are ideal multipliers.

: However, Costas loops and remodulator loops often have hard limiters since high-frequency multipliers which are linear on both ports are hard to construct ⇒ analysis for Squaring loop is not directly applicable.

- we want to determine the VCO phase jitter ϵ due to $n'(t)$

- to do this we find the one-sided spectral density $\Phi_{n'}(\omega)$ and determine the phase variance as:

$$\sigma_\epsilon^2 = \overline{(2\theta_{no})^2} = \frac{1}{2\pi} \int_0^\infty \Phi_{n'}(\omega) \, |H(j\omega)|^2 \, d\omega \qquad -(8)$$

- to find $\Phi_{n'}$, we first determine the autocorrelation of $n'(t)$ starting with the expected value E of $n'(t_1)n'(t_2)$

$$E[n'(t_1)n'(t_2)] \qquad \text{where} \quad t_2 = t_1 + \tau$$

- replacing the time dependence with simple subscripts the expected value becomes:

$$E[n'_1 n'_2]$$

- using the independence of signal and noise, and also of n_c and n_s, and assuming θ_i and θ_o are fixed, yields:

$$\begin{aligned} E[n'_1 n'_2] = \sin^2 2\theta_o \Big\{ & E[n^2_{c'1} n^2_{c'2}] + E[n^2_{s'1} n^2_{s'2}] \\ & - E[n^2_{s'1}]E[n^2_{c'2}] - E[n^2_{c'1}]E[n^2_{s'2}] \Big\} \\ & + 4\cos^2 2\theta_o \Big\{ E[n_{c'1} n_{c'2}]E[n_{s'1} n_{s'2}] \Big\} \\ & + 4\left(\frac{E[m_1 m_2]}{\sigma_m^2}\right) \Big\{ \cos^2(\theta_i - 2\theta_o) E[n_{s'1} n_{s'2}] \\ & + \sin^2(\theta_i - 2\theta_o) E[n_{c'1} n_{c'2}] \Big\} \end{aligned} \qquad -(9)$$

- The noises $n_{c'}$ and $n_{s'}$ are stationary, Gaussian, and have the same statistics (mean value, standard deviation, etc.)

- Hence:

$$E[n^2_{s'1}] = E[n^2_{c'1}] = E[n^2_{s'2}] = E[n^2_{c'2}] = \sigma_N^2 \qquad -(10a)$$

and

$$E[n_{c'1} n_{c'2}] = E[n_{s'1} n_{s'2}] = R_N(\tau) \qquad -(10b)$$

where σ_N^2 is the variance

$R_N(\tau)$ is the autocorrelation

- now for Gaussian processes we also have:

$$E[n^2_{c'1} n^2_{c'2}] = E[n^2_{s'1} n^2_{s'2}] = \sigma_N^4 + 2R_N^2(\tau) \qquad -(11)$$

- Substitute (10) and (11) into (9) and using $\sin^2 + \cos^2 = 1$ yields:

$$E[n'_1 n'_2] = 4R_N^2(\tau) + 4R_N(\tau)\,\frac{E[m_1 m_2]}{\sigma_m^2} \qquad -(12)$$

- Note: this is independent of the phase angle.

Note: $E[m_1 m_2]$ is not stationary and therefore does not have a corresponding spectral density. Hence a further step is required before transforming into the frequency domain.

- each data symbol is represented by a pulse with waveform $p(t)$

- for a filtered binary modulation, the data message can be written as:

$$m(t) = \sum a_k p(t - kT) \qquad -(13)$$

where: $a_k = \pm 1$.

- now since the data is random, separate bits are independent

$$\begin{aligned} E[a_k] &= 0 \\ E[a_k a_j] &= 0 \quad \text{for} \quad j \neq k \end{aligned} \qquad -(14)$$

- using (13) and (14) and recalling that $t_2 = t_1 + \tau$ yields:

$$\begin{aligned} E[m_1 m_2] &= E\left[\sum_n a_n p(t_1 - nT) \sum_k a_k p(t_1 + \tau - kT)\right] \\ &= \sum_n \sum_k p(t_1 - nT) p(t_1 + \tau - kT) E[a_n a_k] \\ &= \sum_k p(t_1 - kT) p(t_1 + \tau - kT) \end{aligned} \qquad -(15)$$

Note: by changing the dummy index, this can be seen to be periodic function of t_1 with period T. This property is called cyclostationary.

- to remove the time dependence, we obtain the time average of the statistical expectation.

- because of the periodicity, the time average is computed over a T second interval

$$\begin{aligned} \overline{E[m_1 m_2]} &= \frac{1}{T} \int_0^T E[m_1 m_2] dt \\ &= \frac{1}{T} \sum \int_0^T p(t - kT) p(t + \tau - kT) dt \\ &= \frac{1}{T} \int_{-\infty}^{\infty} p(t) p(t + \tau) dt \end{aligned} \qquad -(16)$$

- here the summation is from $-\infty$ to ∞

- the second line is just an infinite sum of adjacent integrals which simplifies to a single infinite integral.

- eqn (16) is the conventional definition of autocorrelation of a random pulse train, $R_m(\tau)$.

- using (16) in (12) we finally obtain:

$$R_{n'}(\tau) = 4R_N^2(\tau) + \frac{4R_N(\tau)R_m(\tau)}{\sigma_m^2} \qquad -(17)$$

- now the two-sided spectral density of the noise is the Fourier transform of (17)

$$\Psi_{n'}(\omega) = \frac{4}{2\pi}\int_{-\infty}^{\infty} \Psi_N(\omega - \psi)\Psi_N(\psi)d\psi + \frac{4}{2\pi\sigma_m^2}\int_{-\infty}^{\infty} \Psi_N(\omega - \psi)\Psi_m(\psi)d\psi \qquad -(18)$$

- here Ψ_N and Ψ_m are the Fourier transforms of R_N and R_m

- the one sided density is:

$$\Phi_{n'} = \begin{cases} 2\Psi_{n'} & , \omega \geq 0 \\ 0 & , \omega < 0 \end{cases}$$

- to find the tracking jitter of the PLL, we now substitute $\Phi_{n'}$ from (18) into (8)

- the above analysis is based on the following restrictions:

1) the PLL operates in the linear region
2) the data stream is binary, with zero mean, and independent data values
3) signaling pulses all have the same wave shape which is a real function of time (implies a symmetrical bandpass input filter)
4) noise is Gaussian.

Note: Noise need not be white,

pulses need not be rectangular and can even overlap.

Simplifications

- assume the bandwidth of the PLL is much smaller than that of the input filter. Here eqn (8) reduces to:

$$\sigma_\epsilon^2 = \Phi_{n'}(0)B_L \qquad -(19)$$

since only the lowest frequency components of the noise contribute to the jitter

- also assume white noise is applied to the BPF which has a rectangular passband with one sided bandwidth B_i.

- let the one sided noise density in the passband be N_o (two sided noise density of $N_o/2$ as shown in Figure B2).

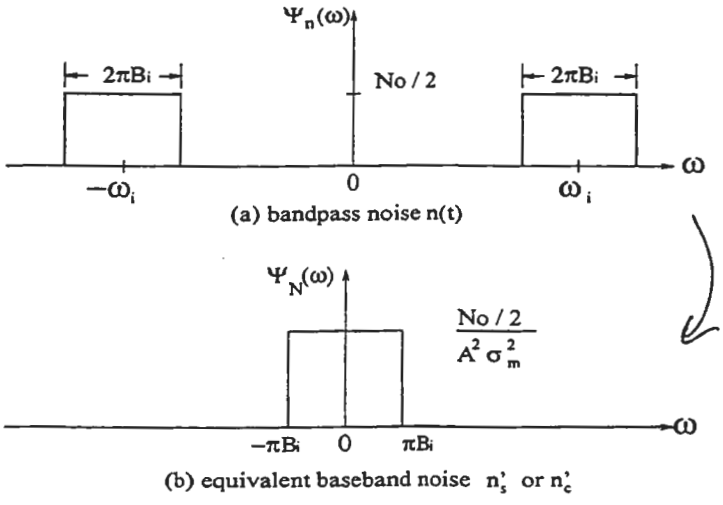

half of noise power goes to BB, half to 2nd harmonic

Figure B2 Spectral densities of input noise

- from Eqn (1), it can be shown that the ~~one~~ two sided density of n_s or n_c is $N_o/2$.

- recalling eqn (5), the two sided spectral density of the equivalent baseband noise n_s' or n_c' is:

$$\Psi_N(\omega) = \begin{cases} \frac{N_o}{2A^2\sigma_m^2} & , |\omega| \leq \pi B_i \\ 0 & , |\omega| > \pi B_i \end{cases} \qquad -(20)$$

as shown in Fig. B2(b)

- using (20), the first integral in eqn(18) becomes:

$$I_1 = \frac{N_o^2 B_i}{A^4 \sigma_m^4}$$

- the third simplification is to assume $m(t)$ has a rectangular waveshape (this is actually impossible at the output of a BPF)

- with this assumption:

$$R_m(\tau) = \begin{cases} 1 - \frac{|\tau|}{T} & , |\tau| \leq T \\ 0 & , |\tau| > T \end{cases} \qquad -(21a)$$

and hence

$$\Psi_m(\omega) = T \left(\frac{\sin \frac{\omega T}{2}}{\frac{\omega T}{2}} \right)^2 \qquad -(21b)$$

- Hence the second integral in eqn (18) becomes

$$I_2 = \frac{2N_o}{\sigma_m^4 A^2}$$

- now since the binary data values are ± 1, we have:

$$\sigma_m^4 = 1 \qquad \text{and} \qquad I_2 = \frac{2N_o}{A^2}$$

- using these expressions for I_1 and I_2 we finally obtain the zero frequency spectral density of the noise as:

two sided spectrum - multiply by $2B_L$

$$\Psi_{n'}(0) = \frac{N_o^2 B_i}{A^4} + \frac{2N_o}{A^2} \qquad -(22)$$

And the phase jitter in eqn (19) becomes:

$$\begin{aligned} \sigma_\epsilon^2 &= 4\left(\frac{B_L N_o}{A^2}\right)\left(1 + \frac{N_o B_i}{A^2}\right) \\ &= 4\left(\frac{B_L N_o}{A^2}\right)\left(1 + \frac{1}{2\rho_i}\right) \end{aligned} \qquad -(23)$$

where $\rho_i = \frac{A^2/2}{N_o B_i} = SNR$ in the input filter bandwidth. $2B_L$ is the double sideband noise bandwidth of the PLL.

Discussion of Carrier Synchronizer Performance in General

- the quantity in the first set of parenthesis is the jitter variance of an ordinary PLL. Hence, jitter variance of a squaring loop is $4\left(1 + \frac{1}{2\rho_i}\right)$ times larger.

- the factor 4 arises because of phase magnification effect of the frequency doubler (the factor becomes 2 for RMS jitter).

- this phase magnification appears only in the PLL at $2\omega_i$.

- When the VCO frequency is divided by 2 to obtain ω_i, the magnification is removed from the recovered ω_i.

- However, the PLL must track the magnified phase.

- Whereas a simple PLL might hold lock down to 0 dB loop SNR, a squaring loop will lose lock around +6 dB.

- lock will probably fail if σ_ϵ^2 exceeds approximately 0.5 rad^2.

- for values above this, appreciable cycle slipping occurs

- the second set of parentheses in eqn (23) increases jitter due to squaring loss.

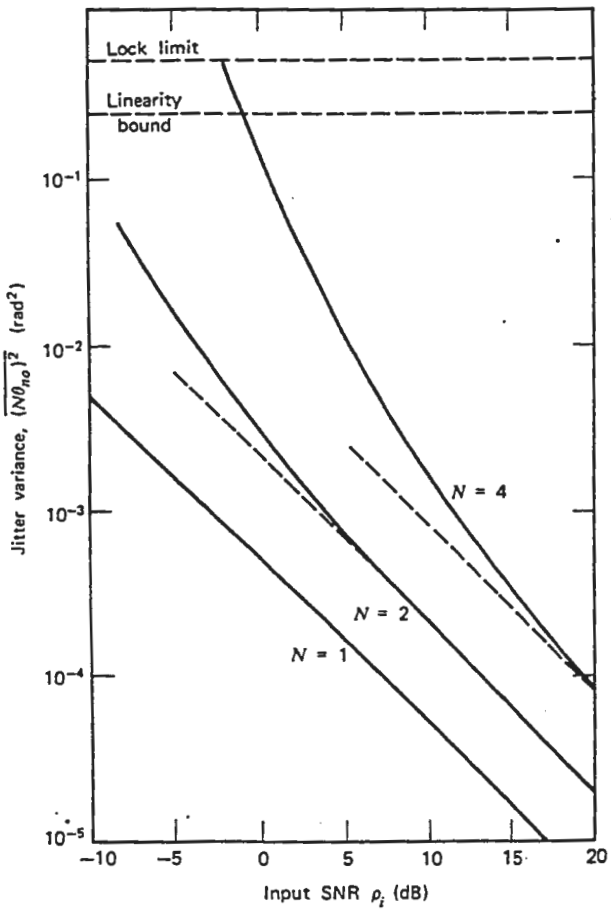

Figure 11.11 Synchronizer jitter example. ($B_i/2B_L = 1000$, N=order of nonlinearity in regenerator.)

- if filter bandwidth is too small ⇒ filter cuts off too much of the useful spectrum ⇒ ρ_i is small.

- the optimum filter for detection approaches the signal-matched filter asymptotically for small ρ_i

- more precisely if the signal has a spectrum $\Phi_s(\omega)$, the SNR at the output of a squarer is maximized with a BPF where:

$$|Y(j\omega)|^2 = \frac{\Phi_s(\omega)}{\Phi_s(\omega) + N_o/2}$$

- it turns out that this same filter is often optimum for synchronization

- Note: Adjacent channel interference (due to multiple, identical channels close in frequency in a communications system) must be strongly excluded from the nonlinear regenerator. Otherwise, significant performance degradation will occur.

- The Costas loop and remodulator are protected against ACI by baseband filters. The N times multiplier uses a BPF for protection.

- since baseband filters are easier to build, prefer Costas loop or regenerator to a N times multiplier.

- The Fokker-Planck method will give probability density of jitter and cycle slipping statistics. It is more advanced than the preceding analysis.

- Note: Carrier synchronizers can lock to data-related sidebands at frequencies spaced $\frac{k}{NT}$ from the carrier. Should know the carrier frequency to within one side frequency to avoid this problem.

  this occurs since $m(t)$ does not have a rectangular wave shape due to filtering and transmission $\Rightarrow$ $m^2(t)$ has spectral lines at $\frac{k}{T}$ $\Rightarrow$ produces sidebands about carrier at $\cos(N\omega_i t)$ of separations $\frac{k}{T}$

  after division by N, sidebands about $\cos(\omega_i t)$ of separations $\frac{k}{NT}$ Hz.

- protection against sideband lock obtained by placing a hard limiter between BPF and squarer.

- The limiter eliminates data related envelope variations.

- this is limited in effectiveness due to physical circuit not bing perfect, and due to complete nulls in the envelope at each phase reversal

- this is also limited due to possibility of signal not being centered in the filter passband $\Rightarrow$ this causes AM-to-PM conversion $\Rightarrow$ the PM sidebands are not affected by a limiter.

- a second anti-sideband approach is to use a frequency discriminator to aid correct acquisition, for example a quadricorrelator as shown could be used:

- here the LPFs establish the frequency difference over which the quadricorrelator will operate.

- the output contains a DC component proportional to the frequency difference including the proper sign.

- there is also a ripple component of equal amplitude

- this ripple can be a problem if the quadricorrelator were to be used as an FM demodulator

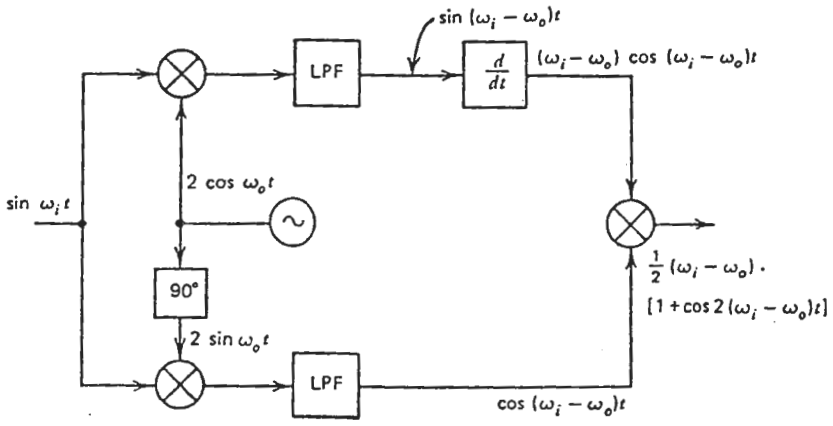

Figure 5.14 Quadricorrelator (frequency-difference detector).

- however, when the quadricorrelator is used for acquisition aid, this ripple vanishes when the loop locks.

- in general, the components in the quadricorrelator are already present in the PLL to which the quadricorrelator helps acquire lock. The only additional components are the filters, differentiator and two of the mixers.

BPSK Receiver Bit Error Rate

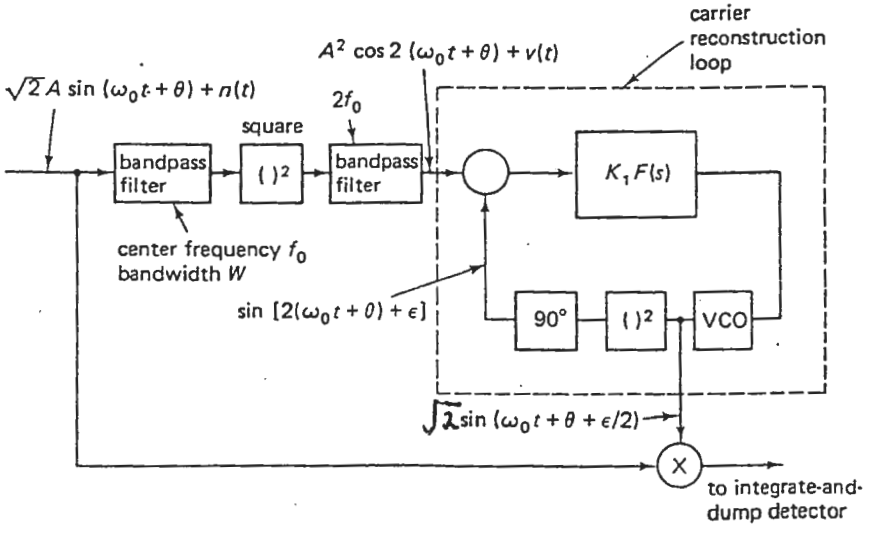

Fig. 12-23 Square-law carrier recovery for coherent phase detection of BPSK signals

- here we will apply the effect of the phase error in the loop, ϵ to determine its impact on bit error probability.

- we consider the received BPSK signal in additive white Gaussian noise:

$$s(t) + n(t) = \sqrt{2} A m(t) \sin(\omega_o t + \theta) + n(t) \qquad -(31)$$

here $m(t) = \pm 1$

$n(t)$ has zero mean and one sided power spectral density N_o.

- the signal is detected with the reference carrier shown above, having a phase error $\epsilon/2$

- dividing $n(t)$ into inphase and quadrature components with respect to the reference:

$$n(t) = \sqrt{2} n_s(t) \sin\left(\omega_o t + \theta + \frac{\epsilon}{2}\right) + \sqrt{2} n_c(t) \cos\left(\omega_o t + \theta + \frac{\epsilon}{2}\right) \qquad -(32)$$

where $n_s(t)$ and $n_c(t)$ each have one sided power spectral density N_o. (2 sided is $\frac{N_o}{2}$)

- the detected signal and noise $n'(t)$ are integrated and dumped every T seconds, to produce an output, z_i

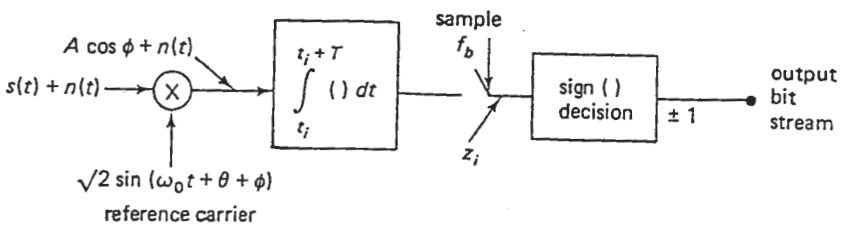

Fig. 12-21 PSK signal detection with a noisy phase reference with error ϕ_ϵ; the bit rate $f_b = 1/T$

$$\begin{aligned} z_i &= \int_{t_i}^{t_i+T} \left[A \cos\left(\frac{\epsilon}{2}\right) + n_s(t)\right] dt \\ &= AT \cos\left(\frac{\epsilon}{2}\right) + \int_{t_i}^{t_i+T} n_s(t) dt \end{aligned} \qquad -(33)$$

where the reference carrier phase error $\epsilon/2$ is constant over the interval $(t_i,\ t_i + T)$.

- Now $z_i(t)$ is Gaussian (since n_s is Gaussian) and has a variance of:

$$\begin{aligned} \sigma_{z_i}^2 &= \int_{t_i}^{t_i+T} \int_{t_i}^{t_i+T} \overline{n_s(t)\ n_s(u)}\ du\ dt \\ &= \int_0^T \int_0^T R_{n_s}(t-u)\ du\ dt \\ &= \int_0^T \int_0^T \frac{N_o}{2} \delta(t-u)\ du\ dt \\ &= \frac{N_o T}{2} \end{aligned} \qquad -(34)$$

- the error probability has been computed and is plotted below (Fig 12.25) for various values of δ where:

$$\delta = \frac{4\rho}{E_b/N_o} = \frac{1}{B_L T} \frac{1}{\left(1 + \frac{B_i T}{2E_b/N_o}\right)} \qquad -(42)$$

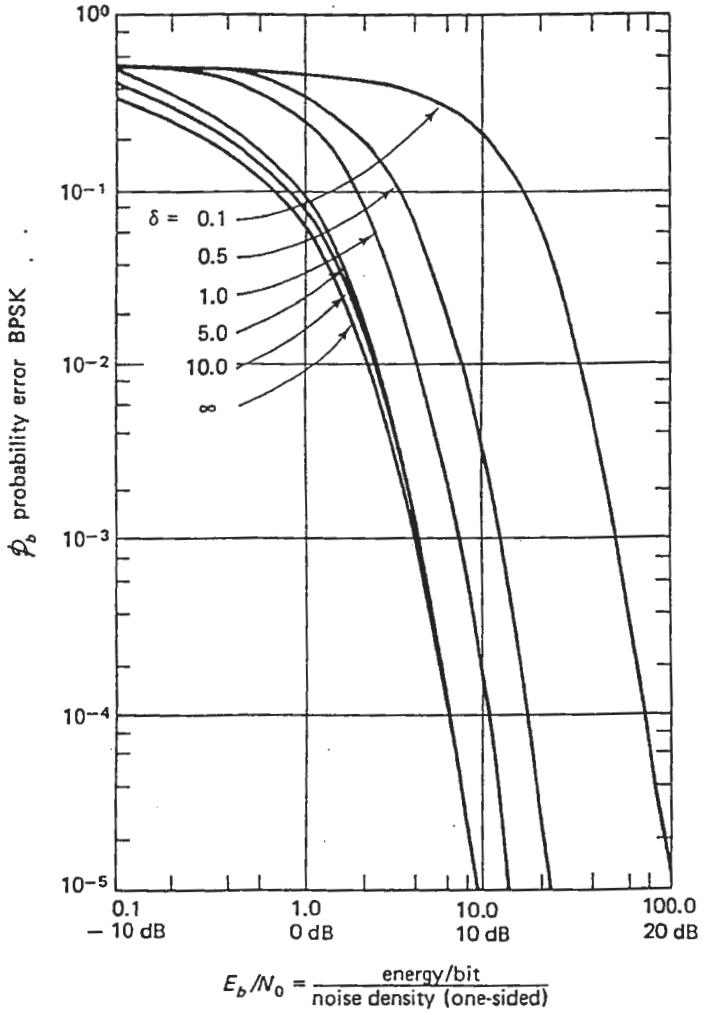

Fig. 12-25 BPSK error probability $\mathcal{P}_b$ versus E_b/N_0 for various values of δ, the normalized bandwidth factor [Lindsey, 1966]

Note: as $B_L \to 0$, $\delta \to \infty$

: for large δ, the error probability approaches the value for no phase noise.

Note: practically no degradation for $\mathcal{P}_b < 10^{-2}$ occurs for δ as small as 5.

: hence we can use it as a design goal:

$$5 < \frac{1}{B_L T} \frac{1}{\left[1 + \frac{B_i T}{2E_b/N_o}\right]} \qquad -(43)$$

QPSK Receiver Bit Error Rate

- a similar type of analysis can be performed for QPSK

- first the output signal and noise statistics at the output of the $(\ )^4$ device are determined

- then the output phase variance of the PLL is computed

- finally the bit error rate obtained using the noisy reference is calculated.

- the result is given in Fig 12.28 for various values of β, where

$$\beta = \frac{SNR_{PLL}}{E_b/N_o}$$

- For a receiver where $B_iT = 2$ where T is the symbol duration, B_i is the bandwidth of the filter preceding the $(\ )^4$ device:

$$\beta = \frac{B_i/B_L}{14.4 + 55.5(N_o/E_b) + 20.5(N_o/E_b)^2 + 2.34(N_o/E_b)^3} \qquad -(44)$$

- For a receiver where $B_iT = 3$

$$\beta = \frac{B_i/B_L}{22.4 + 135(N_o/E_b) + 73.2(N_o/E_b)^2 + 11.8(N_o/E_b)^3} \qquad -(45)$$

- Note for low distortion, the bandpass filter bandwidth is usually chosen so that $B_iT \geq 2$.

-Note: practically no degradation for P_b occurs for β as small as 5.

- Table 12.8 gives values of B_i/B_L versus E_b/N_o for $\beta = 5$ and can be used as a design goal.

Table 12-8 B_i/B_L Required to Maintain a Normalized SNR Factor $\beta = 5$ where $a = B_iT$. The Values of B_i/B_L for $\beta = 1$ are 1/5 of this Value.

E_b/N_o	Bandwidth Ratio B_i/B_L	
(dB)	$a = 2$	$a = 3$
1	362.963	908.7
2	290.8	698.4
3	238.3	549.7
4	199.5	442.5
5	170.4	363.9
6	148.4	305.6
7	131.5	261.7
8	118.6	228.4
9	108.6	202.9
10	100.8	183.2

-Note: Spilker gave different coeff. in eqn(44) and eqn(45) as follows:

- For $B_iT = 2$

$$\beta = \frac{B_i/B_L}{14.4 + 55.5(N_o/E_b) + 61.5(N_o/E_b)^2 + 14.02(N_o/E_b)^3}$$

- For $B_iT = 3$

$$\beta = \frac{B_i/B_L}{22.4 + 135(N_o/E_b) + 219.3(N_o/E_b)^2 + 70.8(N_o/E_b)^3}$$

-hence different values in Table 12.8. but an error was also found in that calculation.

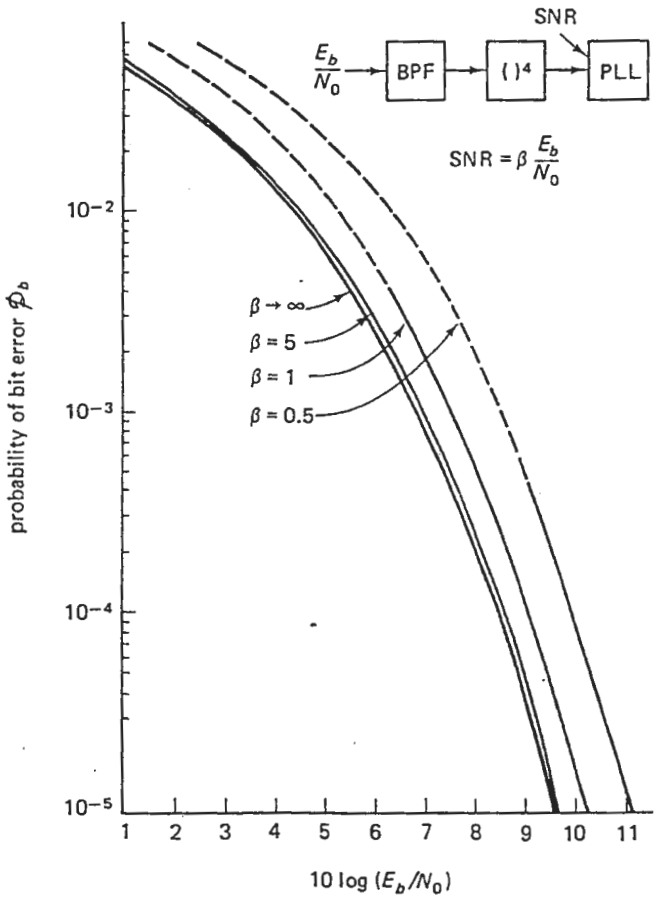

Fig. 12-28 Probability of bit error $\mathcal{P}_b$ versus E_b/N_0 for QPSK [Sherman, 1969]

15. Clock Synchronizers

- there are many types of clock synchronizers, as in the table below:

Table 15-1 Types of Clock Synchronizers

1. *Nonlinear-filter synchronizer*

   This open loop type of synchronizer functions by linearly filtering the received bit stream to and to magnify the observability of the bit transitions. The filter output is then passed through a memoryless even-law nonlinearity to produce a spectral line at the bit rate. This synchronizer is commonly used in high-bit rate links and links which normally operate at high SNR.

2. *Inphase/Midphase (IP/MP) synchronizer*

   (Also termed the data transition tracking synchronizer) This synchronizer operates in a closed loop and combines the operations of bit detection and bit synchronization. The bit detector determines which bits represent a change from the previous bit and whether a (10) or a (01) transition has occurred. This transition information is then utilized to provide the correct sign to a tracking error channel. The IP/MP synchronizer can be employed even at low SNR and medium data rates. It also operates well even in the presence of relatively long times between transitions.

3. *Early-late bit synchronizer*

   This type of bit synchronizer is similar to the inphase/midphase technique. It too involves a closed loop system but has a somewhat different method of obtaining the bit-timing error estimate.

4. *Optimum (maximun-likelihood) synchronizer*

   This type of synchronizer an optimal means for searching for the correct is an open-loop system rather than a tracking technique. This approach is generally not practical; nevertheless it does represent a bound on obtainable performance.

- clock synchronizers can be distinguished as wideband or narrowband and the designs are significantly different

- we assume the digital information is transmitted by weighted pulses, each with identical shape. The weights are ± 1 for binary transmission.

- the baseband data pulse stream is given by:

$$m(t) = \sum_n a_n p(t - nT)$$

where a_n is the data weight p(t) is the pulse shape

note: a_n takes on more than two values if the data is nonbinary.

- the characteristics of wideband and narrowband regimes is given in the following table:

Table 15-2 Signaling-Bandwidth Regimes

1. *Wideband Regime*	
	Bandwidth occupancy greatly exceeds the signaling rate $1/T$
	Signaling pulses are essentially confined to single symbol interval T. Pulses may be, but need not be, rectangular
	Dominant disturbance is usually white, additive, gaussian noise. In some applications, jamming or other cochannel interference may be dominant
	Coding may be used on the digital message, implying that input SNRs might be quite low
	Examples of wideband links may be found in military and deep space communications
2. *Narrow band Regime*	
	Bandwidth occupancy is very small, approaching the Nyquist limit of $1/2T$ Hz in base band or $1/T$ Hz in double-side band modulated signals
	Pulse shapes spread over many symbol intervals T; pulses overlap. Rectangular shape is not even a good approximation
	Dominant disturbance is often from overlapping pulses, known variously as *intersymbol interference* (ISI) (in communications systems) and *pulse crowding* (in playback of digital magnetic recordings). Signal-to-noise ratios are often large (e.g., 30 dB minimum is typical in some telephone-line applications), although small SNRs are also encountered

Maximum Likelihood Trackers

- if the pulse waveform is strictly confined to the interval, T, then there is an optimum clock timing known as the maximum likelihood (ML) estimate, or the maximum a posteriori (MAP) estimate.

- usual derivation of the optimum estimate assumes an open loop search and measure implementation. Also it assumes impractically that the phase holds stable with time.

- However, it is necessary in practice to use a closed-loop tracking synchronizer to accommodate relative phase drift between the incoming signal and the local clock.

- Tracking synchronizers have been devised which converge to the ML estimate and have much the same phase error statistics. One form is shown below:

- note the resemblance to a Costas loop. This is because the Costas loop is an approximation to a tracking ML estimator of carrier phase.

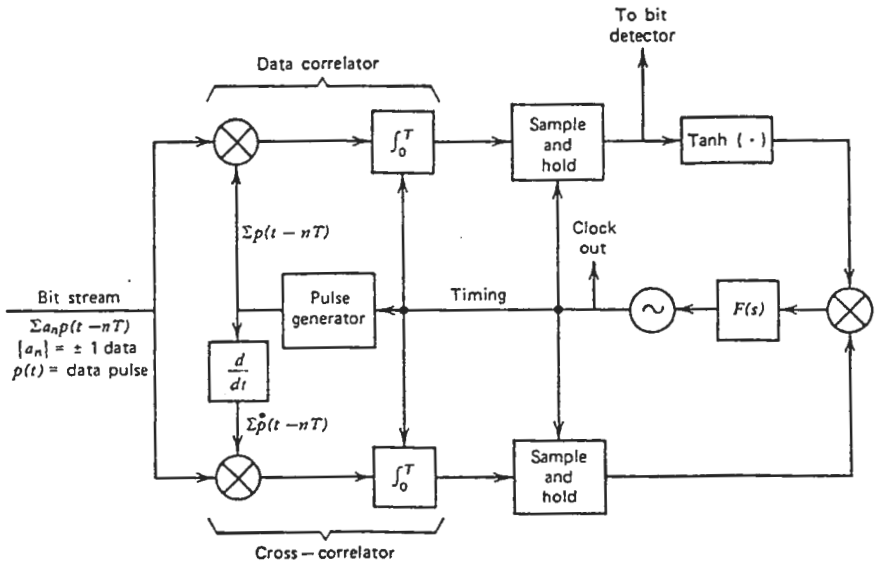

Figure 11.12 Clock synchronizer based on maximum-likelihood estimate.

- In the upper arm, the incoming signal is correlated symbol by symbol with a stored replica of the signal pulse shape.

- the correlator is sampled at T second intervals and the integrator is dumped after each sample.

- Once the timing is properly aligned, the upper correlator gives optimum filtering for detection of the data value.

- The correlator samples can be used for data decisions.

- In the lower arm, the incoming signal is correlated against the derivative of the signal pulse shape.

- This correlator output is sampled at T second intervals and then the integrator is dumped.

- When the local time agrees with that of an incoming signal, average output of lower correlator is zero.

- If the incoming pulses were all of the same polarity, then the lower correlator polarity would show the direction of the timing error.

- However, with random data, the lower correlator has random polarity of samples.

- the samples from the upper arm contain the data sign information. Hence multiplying the two arm outputs removes the randomness and gives a signal having error sense

information.

- loop is closed through the usual loop filter and VCO and here also with a pulse generator

- The tanh nonlinearity arises out of the ML derivation and is approximated with a soft limiter.

- The variation of the timing error has been derived for the case having:

  - white noise
  - large SNR
  - $B_L T \ll 1$
  - $p(0) = p(T) = 0$

- This analysis, due to Mengali, yields:

$$\sigma_{\epsilon_t}^2 = \frac{TB_L}{\gamma b} \qquad -(9)$$

here ϵ_t = normalized timing error wrt T.

$\gamma = \frac{E_p}{N_o}$ $\qquad b = T^2 \frac{E_{\dot{p}}}{E_p}$

N_o = one sided noise density

$E_p = \int_0^T p^2(t)dt$ = energy per bit pulse $p(t)$

$E_{\dot{p}} = \int_0^T \dot{p}^2(t)dt$ = energy of $\left(\dot{p}(t) = \frac{dp(t)}{dt}\right)$

- Eqn (9) should be regarded as a lower bound on the achievable jitter from a tracking clock synchronizer.

- Eqn (9) does not hold for a rectangular pulse since $p(0) \neq 0$ and $p(T) \neq 0$. Also for this case, the circuit in Fig. 11.12 cannot find the ML timing estimate for a rectangular pulse.

- This is unfortunate because of the practical importance of rectangular signal pulses.

Early-Late Gate

- is employed frequently for rectangular pulses

- the circuit has two integrators, each integrating over a time interval of T/2 seconds.

- integration by the early gate occurs in the T/2 sec preceding its data transitions.

- integration by the late gate occurs in the T/2 sec following its data transitions.

- gate intervals adjoin one another but do not overlap.

- if timing error is zero, data transition falls exactly on boundary between early and late

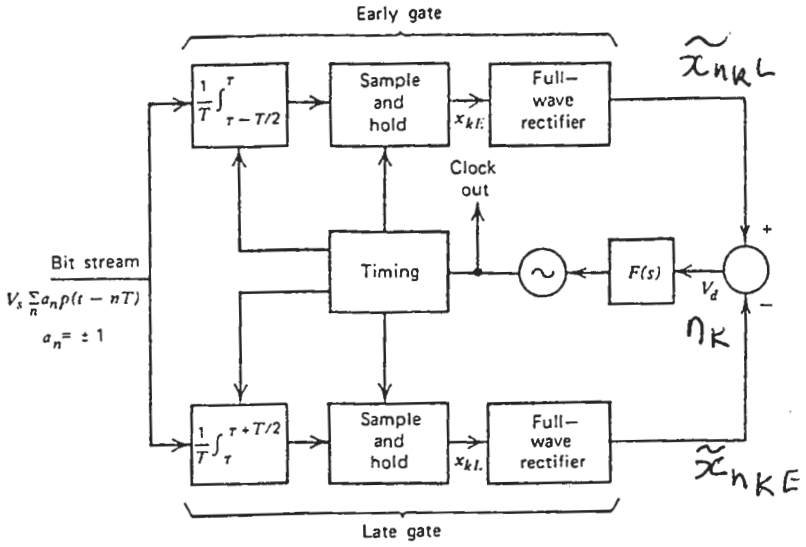

Figure 11.13 Early gate–late gate synchronizer. Suitable for rectangular pulses.

gates

- if timing error is not zero, transition falls within one or the other gate.

- since signal polarity changes within the gate containing a transition, the integration reaches a lesser magnitude than when the transition is external to the gate.

- comparison of magnitudes of the two integrations gives indications of the timing error.

- waveforms are shown in Fig. 11.14

- timing error is denoted by τ where $|\tau| \leq T/2$

- the loop only sees the integrated value after T/2 sec through the sample and hold circuit

-designate the samples as x_{kE} and x_{kL} where k denotes the k^{th} pulse:

$$\left.\begin{aligned} x_{kE} &= \frac{1}{T_I}\int_{\tau+(k-1/2)T}^{\tau+kT} S(t)dt \\ x_{kL} &= \frac{1}{T_I}\int_{\tau+kT}^{\tau+(k+1/2)T} S(t)dt \end{aligned}\right\} -(10)$$

- here T_I is the time constant of the integrators

- the incoming binary signal (after demodulation) is:

$$S(t) = A\sum_n a_n p(t-nT) \qquad -(11)$$

- here the pulse $p(t)$ is taken as rectangular, of duration T

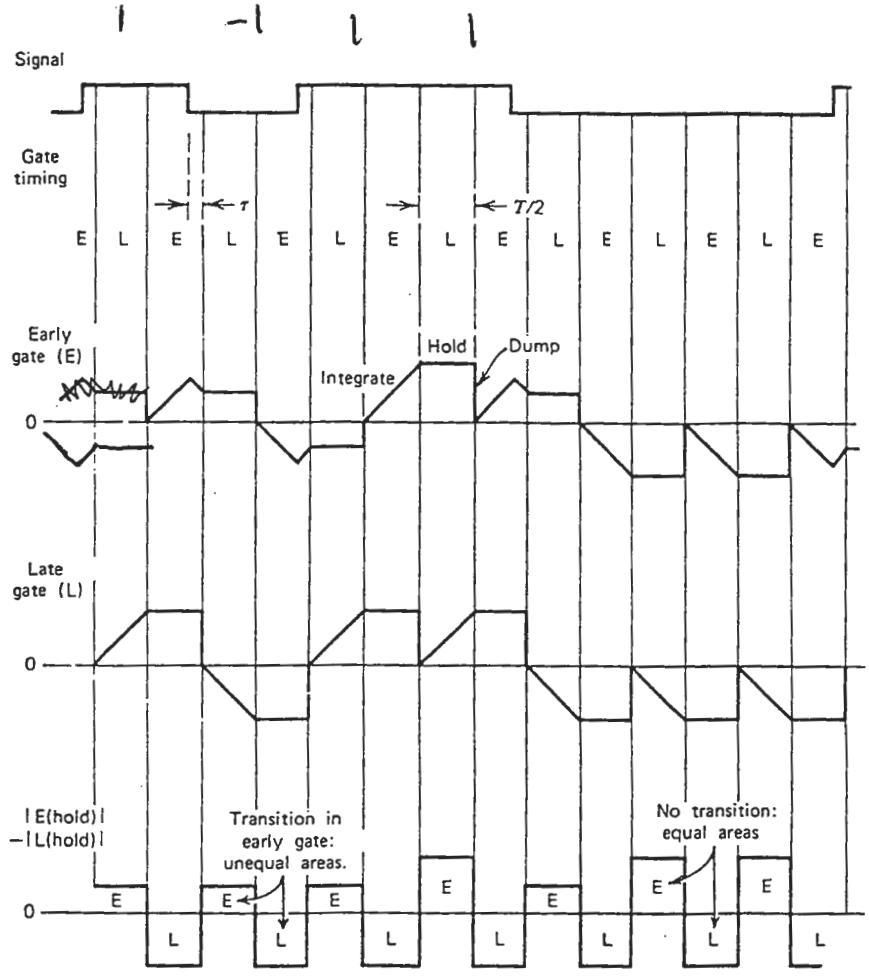

Figure 11.14 Waveforms of early–late gate (rectangular input).

- For $\tau \geq 0$

$$\left.\begin{aligned} x_{kE} &= \frac{A}{T_I}\left[\left(\frac{1}{2}T - \tau\right)a_{k-1} + \tau a_k\right] \\ x_{kL} &= \frac{A}{T_I}\frac{a_k T}{2} \end{aligned}\right\} \quad -(12)$$

- their magnitudes are compared

- the integrators are then dumped and the cycle repeats

- as shown in Fig 11.14, the samples are compared sequentially not simultaneously.

- this causes a strong ripple at the bit rate (undesirable) but leads to simple circuitry.

- the error from a pair of samples is:

$$\begin{aligned} y_k &= |x_{kE}| - |x_{kL}| && \text{, all } \tau \\ &= \frac{A}{T_I}\left[\left|\left(\frac{1}{2}T - \tau\right)a_{k-1} + a_k\tau\right| - \frac{1}{2}T\,|a_k|\right] && \text{, } \tau > 0 \end{aligned} \quad -(13)$$

- the average error voltage applied to the loop is:

$$V_d = E[y_k]$$

where $E[\ ]$ is the expected value (mean value).

Table 11.3 Error Sample Values ($\tau > 0$)

Data Sequence	$y_k T_I/A$	
$a_{k-1} = a_k$	0	
$a_{k-1} \neq a_k$	-2τ;	$(0 \leq \tau \leq T/4)$
	$2\tau - T$;	$(T/4 \leq \tau \leq T/2)$
and similarly for $\tau < 0$		

- a nonzero error signal is generated only when a transition occurs between bits.

- if there should be a long run of data without transitions, no error information is supplied to the loop.

- the phase of the VCO will drift off due to noise and circuit offsets.

- if the run is long enough the loop eventually slips one or more clock cycles

- a clock slip is serious since it destroys frame synchronization. The frame sync must be reacquired in addition to bit timing.

- probability of a transition between bit is 0.5 for random binary data.
- The average error voltage is (using table 11.3 but including negative τ)

$$V_d = \begin{cases} \frac{-A}{T_I}\tau, & |\tau| \leq \frac{T}{4} \\ \frac{A}{T_I}(\tau - \frac{1}{2}T), & \frac{T}{4} \geq \tau \geq \frac{T}{2} \\ \frac{A}{T_I}(\tau + \frac{1}{2}T), & -\frac{T}{4} \geq \tau \geq -\frac{T}{2} \end{cases} \qquad -(15)$$

- This characteristic is periodic and triangular and is shown below:

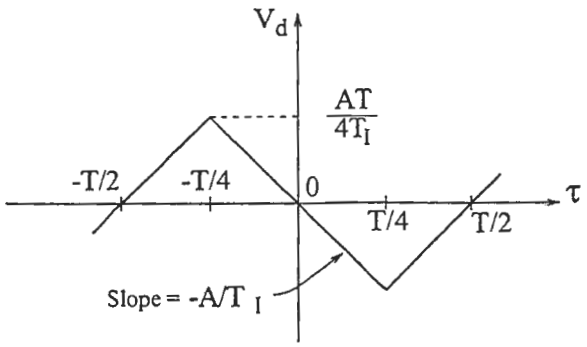

Figure 11.15 Average error output of early-late gate

- Variations on the basic idea may include shorter gate times. This might improve noise performance but also introduces dead regions where the timing error will fall into neither gate.

- with gate shorter than T/2, they should still adjoin one another to prevent a dead zone in the region of expected tracking crossover.

- Noise analysis of a nonlinear synchronizer is formidable.

- The Fokker-Planck method has been used to obtain slip probability.

- An approximate linear analysis can be performed

- At the individual gated integrators, superposition of signal and noise still applies.

- The input to the integrator is:

$$S(t) + n(t)$$

where $n(t)$ is white, Gaussian, zero mean noise with one sided spectral density $N_o \left(\frac{V^2}{\text{Hz}}\right)$.

- The noise variance of the integrated samples can be shown to be:

$$E\left(x_{nkE}^2\right) = E\left(x_{nkL}^2\right) = \frac{N_o T}{4T_I^2} \qquad -(16)$$

- Here x_{nk} is the noise contribution to the k^{th} sample, either early or late.

- Assume the timing error is zero so that the signal integration is:

$$\frac{ATa_k}{2T_I}$$

- each sample is applied to a full wave rectifier, yielding:

$$\left|\frac{ATa_k}{2T_I} + x_{nk}\right|$$

- for large SNR, the first term dominates the second, and the rectifier output can be written as:

$$\frac{AT}{2T_I} + x_{nk}\ \text{sign}(a_k)$$

here a_k is the data value within the gate interval.

- Note: we are neglecting the squaring loss inherent to all rectifiers.

- Define:

$$\tilde{x}_{nk} = x_{nk}\text{sign}(a_k)$$

- this is just the noise samples with random, data related polarity reversals.

- since the signal and noise are independent, the statistics (mean, variance, etc.) of $\tilde{x}_{nk}$ are identical to those of x_{nk}.

- Hence

$$E(\tilde{x}_{nk}^2) = E(x_{nk}^2) = \frac{N_o T}{4T_I^2}$$

- Now signal components of the summer output tend to cancel, while noise components add on a power basis (since they are completely independent).

- hence, the phase detector output becomes:

$$V_{dk} \approx -\frac{A}{T_I}\tau + n_k + \text{ ripple} \qquad -(17)$$

where

$$n_k = (\tilde{x}_{nkE} - \tilde{x}_{nkL})$$

- the ripple term can be troublesome in reality, but since we are not dealing with reality here, we ignore it.

- Define

$$n_k' = \frac{n_k T_I}{A}$$

Hence

$$V_{dk} = \frac{A}{T_I}(-\tau + n_k') \qquad -(17a)$$

- Note: n_k' has units of time and is considered as an additive source of timing error.

- From its definition, we know n_k' has zero mean and its variance is:

$$\begin{aligned} E(n_k'^2) &= \left(\frac{T_I}{A}\right)^2 E\left[(\tilde{x}_{nkE} - \tilde{x}_{nkL})^2\right] \\ &= \left(\frac{T_I}{A}\right)^2 \left[E(\tilde{x}_{nkE}^2) + E(\tilde{x}_{nkL}^2)\right] \qquad -(18) \\ &= \frac{N_o T}{2A^2} \quad (\text{sec}^2) \end{aligned}$$

- we used the following noise property to obtain the last result:

$$E[\tilde{x}_{nkE}\tilde{x}_{nkL}] = 0$$

$$E[\tilde{x}_{nk}\tilde{x}_{nJ}] = 0, \qquad k \neq J$$

$$\tilde{x}_{nk}^2 = [x_{nk}\text{sign}x_k]^2 = x_{nk}^2$$

- Noise samples occur at regular intervals of T/2. They are independent, so their spectrum is flat over the Nyquist band of 0 to 1/T Hz.

- The Spectral Density of the noise samples is:

$$\Phi_{n_k'} = \frac{E[n_k'^2]}{1/T} = \frac{N_o T^2}{2A^2} \quad \left(\frac{\text{sec}^2}{\text{Hz}}\right) \qquad -(19)$$

- This noise propagates through the loop, is filtered by the closed loop transfer function, and causes a time jitter ϵ at the VCO output.

- The time jitter can be approximated, for $B_L T \ll 1$, as:

$$\sigma_\epsilon^2 = E[\epsilon^2] = \Phi_{n_k'} B_L \qquad (\text{sec})^2 \qquad -(20)$$

- Normalizing with respect to the bit interval yields:

$$\sigma_{\epsilon_t}^2 = E\left[\left(\frac{\epsilon}{T}\right)^2\right] = \frac{N_o B_L}{2A^2} \qquad -(21)$$

- This is (finally) the variance of fractional timing error introduced by additive noise.

Transition Tracking Loop (In-Phase/mid-phase) Synchronizer

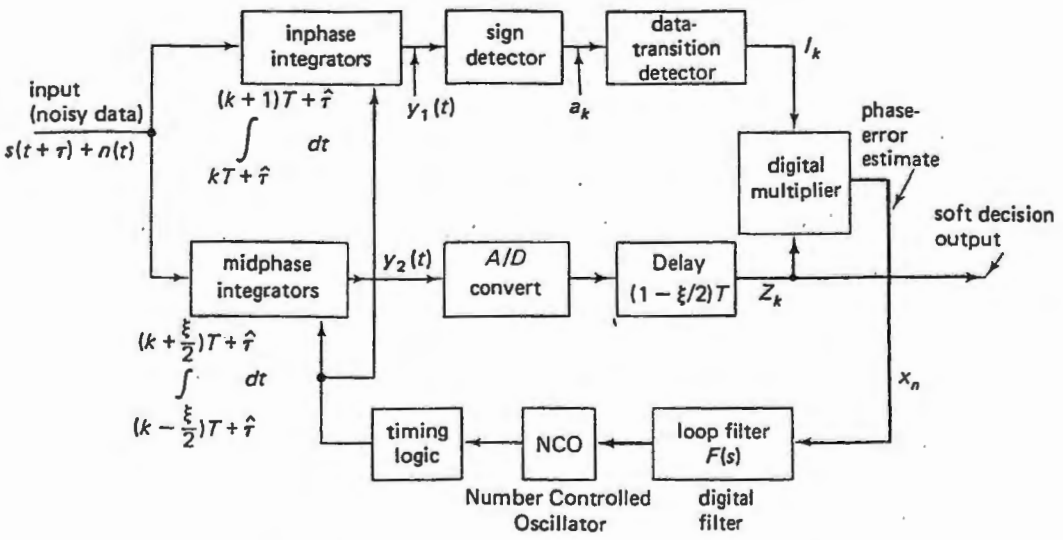

Fig. 14-5 In-phase/Mid-phase bit synchronizer with inphase and midphase channels. The input clock offset is τ, and the clock phase estimate is $\hat{\tau}$. The midphase integrator window width is ξT sec. The timing error is $\epsilon \triangleq \tau - \hat{\tau}$.

- an analogy can be made of the inphase × midphase bit stream product to the inphase × quadrature carrier product of the Costas loop for carrier recovery.

- here the inphase branch determines the polarity of the bit transitions when and if they occur.

- the midphase channel determines the magnitude of the bit-timing error.

- the midphase error Z_k is multiplied by I_k where:

$$I_k = \begin{cases} \pm 1 & \text{if a transition has been sensed} \\ 0 & \text{if no transition has been sensed} \end{cases}$$

- filtered output of multiplier is used to drive the VCO, and to control the integrate-and-dump operations

- note that a NCO (number controlled oscillator) is a digital control voltage version of a VCO.

- the midphase integration window ξT can be narrowed to T/4 to improve SNR.

- advantage of this inphase/midphase synchronizer is that during long periods between transitions, the discriminator does not allow any noise to perturb the loop. It holds the last valid estimate since $I_k = 0$.

- assume the input signal $S(t)$ is a random pulse train of rectangular pulses $p(t)$ with a clock offset τ.

$$S(t) = \sum_n A a_n p[t - nT + \tau(t)] + n(t)$$

where

$$p(t) = \begin{cases} 1, & 0 < t < T \\ 0, & \text{elsewhere} \end{cases}$$

and

$$a_n = \pm 1$$

$n(t)$ is white Gaussian noise with one-sided spectral density N_o.

- the inphase-channel sign-detector is a hard limiter, hence:

$$\alpha_k = \pm 1$$

- adjacent decisions are used to detect transitions according to:

$$I_k = \frac{\alpha_{k-1} - \alpha_k}{2} = -1,\ 0,\ 1$$

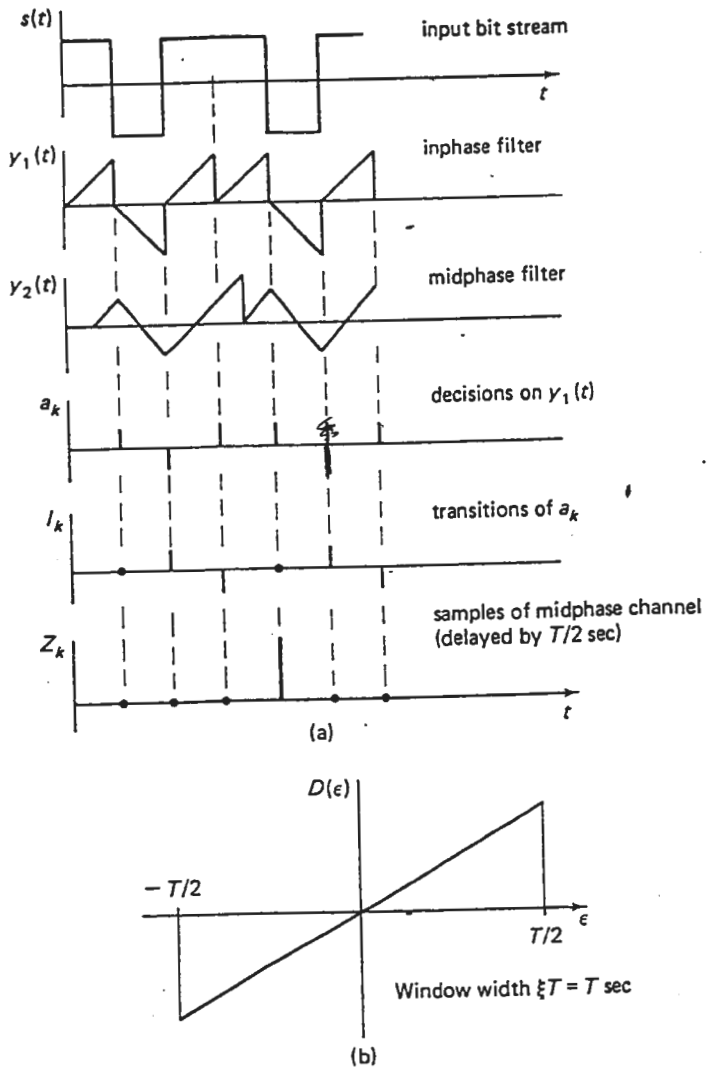

Fig. 14-6 Waveforms of the in-phase/midphase loop showing outputs of the inphase and midphase integrate-and-dump filter. The phase detector output is $\overline{a_k I_k} = 0$ for this example where the bit timing error is zero. (a) Waveforms for $\xi = 1$. (b) The synchronizer phase discriminator characteristic increases linearly until $\epsilon = T/2$.

- The output from the midphase filter, Z_k is sampled at T second intervals offset from the inphase intervals by a delay of T/2 seconds. This places the two channels in coincidence.

- note: the midphase integrator output is more easily multiplied by $I_k = \pm 1,\ 0$ if it is first digitized with a quantizer of 3 or more bits/sample.

- hence the sign of the midphase integrator gives a "hard" bit decision, and a 3 bit quantizer gives a "soft" decision.

- in the example of Fig. 14.6, the "phase detector" output $I_k Z_k = 0$ where the bit timing

error is zero.

- the phase detector characteristic increases linearly until $\epsilon = T/2$.

- Let

$$\epsilon = \tau - \hat{\tau} \quad \text{be the timing error}$$

$$\gamma = \frac{E_b}{N_o} = \frac{A^2 T}{N_o}$$

- When a symbol transition occurs, the output of the midphase channel is:

$$\begin{aligned} Z_k &= \pm \left[2\epsilon A + \int_{(k-1/2)T}^{(k+1/2)T} n(t)dt \right] \\ &= \pm 2\epsilon A + N_k \end{aligned} \qquad -(22)$$

- the sign of the correction above depends on whether the bit transition is positive or negative.

- the timing error output is:

$$\begin{aligned} x(t,\epsilon) &= Z_k I_k \\ &= \begin{cases} \pm Z_k & ; I_k = \pm 1 \\ 0 & ; I_k = 0 \end{cases} \\ &= \begin{cases} 2\epsilon A + N_k & ; I_k = \pm 1 \\ 0 & ; I_k = 0 \end{cases} \end{aligned}$$

and the phase discriminator characteristic can be written as:

$$\begin{aligned} D(\epsilon) &= E[x(t,\epsilon)] \\ &= E[Z_k I_k] \qquad ; \ |\epsilon| < T/2 \\ &= \frac{1}{2}[2\epsilon A] \\ &= \epsilon A \qquad ; \ |\epsilon| < T/2 \end{aligned} \qquad -(23)$$

here the 1/2 indicates that the transitions occur half the time. Now the ~~data transition detector~~ sign detector output produces errors at a rate:

$$\mathcal{P}_b = \frac{1}{2} \operatorname{erfc} \sqrt{\frac{E_b}{N_o}}$$

An error in the data transition detector causes the estimate of the timing error ϵ to reverse sign.

- For a 1→0 (actally $+1 \rightarrow -1$) transition and a bit error probability $\mathcal{P}_b$, the phase detector sign can be shown to have the probabilities shown below:

Table 14.1 Probability of Various Output Bit Patterns For an Input Bit Pattern 10

True Bit Pattern	*10*	*Probability*	*Phase-Detector Multiplier I_k*
Detected Output Bits	10	$(1-P_b)^2$	+1
	01	P_b^2	-1
	00	$P_b(1-P_b)$	0
	11	$P_b(1-P_b)$	0

- Neglect the interdependence between inphase transition errors and midphase noise;
- Assume P_b is constant with respect to ε $(for\,|\varepsilon| < T)$.

Now including the effects of P_b, for a data transition density of 50%:

$$\begin{aligned} D(\varepsilon) &\approx \left[(1-P_b)^2 - P_b^2\right] A\varepsilon \\ &\approx \left[1-2P_b\right] A\varepsilon \\ &\approx \left[1 - erfc\left(\frac{E_b}{N_o}\right)^{1/2}\right] A\varepsilon \\ &\approx \left(A\, erf\sqrt{\gamma}\right)\varepsilon \end{aligned}$$

- Hence, transition errors lower the effective loop gain of the synchronizer. However, a high error rate of $P_b = 10^{-2}$ produces only a 2% decrease in loop gain

- adding in the noise

$$D(\varepsilon) = A erf\sqrt{\frac{E_b}{N_0}}\left(\varepsilon + \frac{N_K}{Aerf\sqrt{\frac{E_b}{N_0}}}\right) \quad for\ I_K = \pm 1$$

- Now only the noise density in the vicinity of $\omega = 0$ is of interest due to the use of narrow band loop filters.

- Also successive values of N_k are independent since the integration intervals are nonoverlapping.

- Hence:

$$\Psi_N(0,0) = \frac{1}{1/T} E\left[N_k^2\right] = \frac{1}{2}\left(\frac{N_0}{2}\right) T^2$$

where the ½ factor occurs since the transitions occur half the time, and N_0 is the one sided noise power spectral density.

- Normalize with respect to constant ~~$1/T$~~

$$\Psi_\varepsilon = \frac{1}{A^2\left(erf\sqrt{\frac{E_b}{N_0}}\right)^2}\Psi_N$$

$$= \frac{1}{A^2\left(erf\sqrt{\frac{E_b}{N_0}}\right)^2}\frac{N_0}{4}T^2$$

$$= \frac{T^3}{4\frac{E_b}{N_0}\left(erf\sqrt{\frac{E_b}{N_0}}\right)^2}$$

- Now for a closed loop noise bandwidth B_L:

$$\frac{\sigma_\varepsilon^2}{T^2} = \frac{\Psi_\varepsilon B_L}{T^2}$$

$$= \frac{TB_L}{4\frac{E_b}{N_0}\left(erf\sqrt{\frac{E_b}{N_0}}\right)^2}$$

- Simon has also demonstrated that use of a midphase window of $\xi = ¼$ gives a 3 dB improvement. However, the acquisition window is only half as wide as for a window of $\xi = ½$.

- finally for small values of $\frac{\gamma}{B_L T}$:

$$\frac{\sigma_\epsilon^2}{T^2} = 1/12 \qquad \text{for} \quad |\epsilon| < T/2$$

- hence, the mean square timing error is uniformly distributed over $|\epsilon| < T/2$.

Other Wide Band Synchronizers: Transition Detectors

- Transition detectors generate a unipolar pulse at each signal crossing. Hence, the resulting sequence of pulses contains a clock rate component.

- The Delay Line Multiplier is shown below:

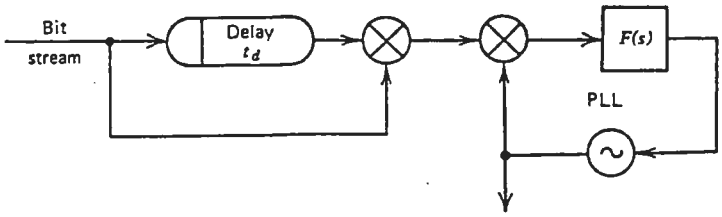

Figure 11.16 Delay-line multiplier. This system also works with PSK IF input.

- this circuit is attractive due to its simplicity for high SNR.

- the output of the multiplier contains a discrete spectral component at the clock frequency.

- the amplitude of the regenerated clock depends on the pulse waveform and delay time t_d(denote Δ in the Figure 14.4).

- for rectangular pulses, $t_d = T/2$ gives the max. clock amplitude.

- the delay line multiplier can also regenerate a clock spectral component from a passband PSK signal.

- here the amplitude is proportional to $\cos\omega_i\, t_d$, where ω_i is the carrier frequency.

- hence, delay is chosen so that $\omega_i\, t_d = n\pi$, $n = 0, 1, 2, 3 \ldots$.

- if the signaling pulses are rectangular, and $t_d = T/2$ then the output consists of unipolar pulses of duration $T/2$ with the leading edge at the location of each data transition.

- generally, the output $m(t, t_d)$ contains a periodic component at the bit rate, $p(t, t_d)$ and a random (or pseudonoise) component $r(t, t_d)$.

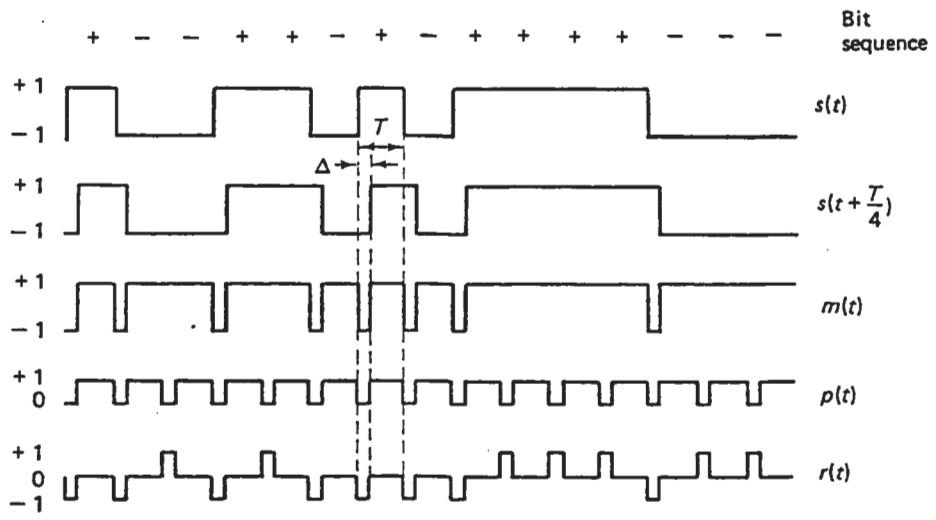

Fig. 14-4 Product of maximal-length sequence and its decomposition; $m(t) = p(t) + r(t)$, displacement $\Delta = T/4$ where $p(t)$ is periodic and $r(t)$ is pseudo-random.

- also the output expected value of $m(t, t_d)$ is the value at t_d of the autocorrelation function of $S(t)$

$$E[m(t, t_d)] = R_s(t_d) = E[S(t)S(t - t_d)]$$

- note the periodic pulse train $p(t, t_d)$ has amplitudes 0,1 and has a value of +1 when the unshifted and shifted waveforms match.

- the random component is ternary with amplitudes of -1,0,+1, and has a value of ± 1 only during interval for which adjacent digits overlap.

- the sequence of ± 1 digits represent a cyclically shifted and inverted version of $S(t)$

- Since the possible transition times for $p(t)$ and $r(t)$ are identical, the two waveforms are not necessarily uncorrelated.

- Hence, the autocorrelation function for $m(t, t_d)$ with $t_d < T$ is:

$$\begin{aligned} R_m(\tau, t_d) &= E[m(t, t_d)m(t + \tau, t_d)] \\ &= E[\{p(t, t_d) + r(t, t_d)\}\{p(t + \tau, t_d) + r(t + \tau, t_d)\}] \\ &= R_p(\tau, t_d) + R_r(\tau, t_d) + R_{pxr}(\tau, t_d) + R_{pxr}(-\tau, t_d) \end{aligned}$$

- the term $R_{pxr}(\tau, t_d) = 0$. This apparently is to be expected from something called the spectral decomposition theorem.

- hence:

$$R_m(\tau, t_d) = R_p(\tau, t_d) + R_r(\tau, t_d)$$

- it is straightforward to see that R_P is a periodic triangular function with a constant dc shift, and R_r is triangular.

- hence, the power spectral density is the Fourier transform of triangular functions

$$\Psi_m(f,t_d) = \left(1-\frac{t_d}{T}\right)^2\delta(f) + \left(\frac{t_d}{T}\right)^2 \sum_{\substack{n=-\infty \\ n\neq 0}}^{\infty} \text{sinc}^2\frac{nt_d}{T}\delta\left(f+\frac{n}{T}\right)$$
$$+\left(\frac{t_d}{T}\right)^2 \text{sinc}^2 ft_d \quad , \quad t_d < T$$

- if $t_d = T/2$ the spectral components at the clock rate are:

$$\Psi_m\left(\frac{1}{T},\frac{T}{2}\right) = \left(\frac{1}{2}\right)^2 \text{sinc}^2\frac{1}{2}\left[\delta\left(f+\frac{1}{T}\right)+\delta\left(f-\frac{1}{T}\right)\right] \qquad -(31)$$

- Note: even if the input waveform $S(t)$ has finite rise and fall times, the product $m(t,T/2)$ contains a line component at $f_c = 1/T$.

The Differentiator Synchronizer and the Zero Crossing Synchronizer are shown below:

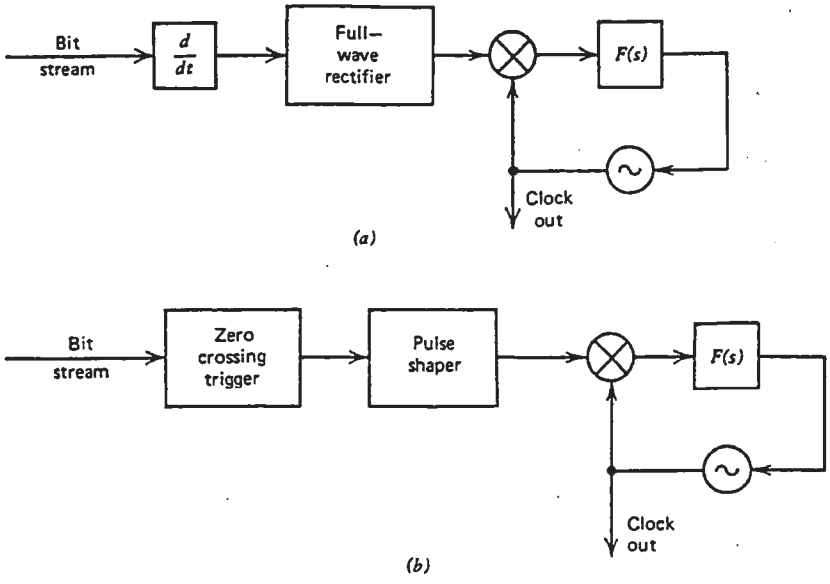

Figure 11.17 Transition detectors: (*a*) differentiator; (*b*) crossing trigger.

- in the differentiator synchronizer, replacing the full wave rectifier with a square law operation yields:

$$\left\{\frac{d\,S(t)}{dt}\right\}^2 \approx \left\{\frac{S(t)-S(t-\Delta)}{\Delta}\right\}^2 = \frac{2}{\Delta^2} - \frac{2S(t)S(t-\Delta)}{\Delta^2} \quad ; \quad \Delta \text{ small}$$
$$\approx \frac{2}{\Delta^2}[1-m(t)] \quad , \quad \Delta \ll T \qquad -(32)$$

- here we have used $S(t)^2 = 1$ in the absence of noise since this expression contains the product $S(t)S(t-\Delta)$ as in the delay line multiplier synchronizer, then it also contains a periodic line component similar to eqn (31) above.

Bit Error Rate due to Clock Timing Error

- we will now calculate the effects of the clock timing error on the error rate performance

- we will first present the BER probability for NRZ data in a Gaussian channel conditioned on a given clock timing error, ϵ.

- then we compute the expected bit error by averaging over the clock timing statistics.

- for a given clock timing error ϵ

$$\mathcal{P}_b(\epsilon) = \frac{1}{4}\text{erfc}\left\{\sqrt{\frac{E_b}{N_o}}\,\frac{R_s(\epsilon)+R_s(T-\epsilon)}{R_s(0)}\right\} + \frac{1}{4}\text{erfc}\left\{\sqrt{\frac{E_b}{N_o}}\,\frac{R_s(\epsilon)-R_s(T-\epsilon)}{R_s(0)}\right\} \quad -(33)$$

two adjacent bits of same polarity

two adjacent bits of opposite polarity

where R_s is the autocorrelation function of the input waveform.

- for NRZ data:

$$Rs(\epsilon) = \begin{cases} 1-\frac{|\epsilon|}{T} & ;\ |\epsilon| < T \\ 0 & ;\ |\epsilon| \geq T \end{cases} \quad -(34)$$

substitute (34) into (33) yields:

$$\mathcal{P}_b(\epsilon) = \frac{1}{4}\text{erfc}\left(\sqrt{\frac{E_b}{N_o}}\right) + \frac{1}{4}\text{erfc}\left\{\sqrt{\frac{E_b}{N_o}}\left(1-2\frac{|\epsilon|}{T}\right)\right\} \quad -(35)$$

- and the expected bit error probability is obtained by averaging $\mathcal{P}_b(\epsilon)$ over ϵ to obtain:

$$\mathcal{P}_b = \int \mathcal{P}_b(\epsilon)p(\epsilon)d\epsilon$$

- now $p(\epsilon)$ is well approximated by the Tikhonov density function:

$$p(\epsilon) = \frac{\exp\left[\frac{\cos 2\pi\epsilon}{(2\pi\sigma_\epsilon)^2}\right]}{I_o\left[\frac{1}{(2\pi\sigma_\epsilon)^2}\right]}$$

- note: this density function is the same as we used on page 14-25 for BER calculations for the carrier synchronizers.

- the result is plotted in Fig 14.10.

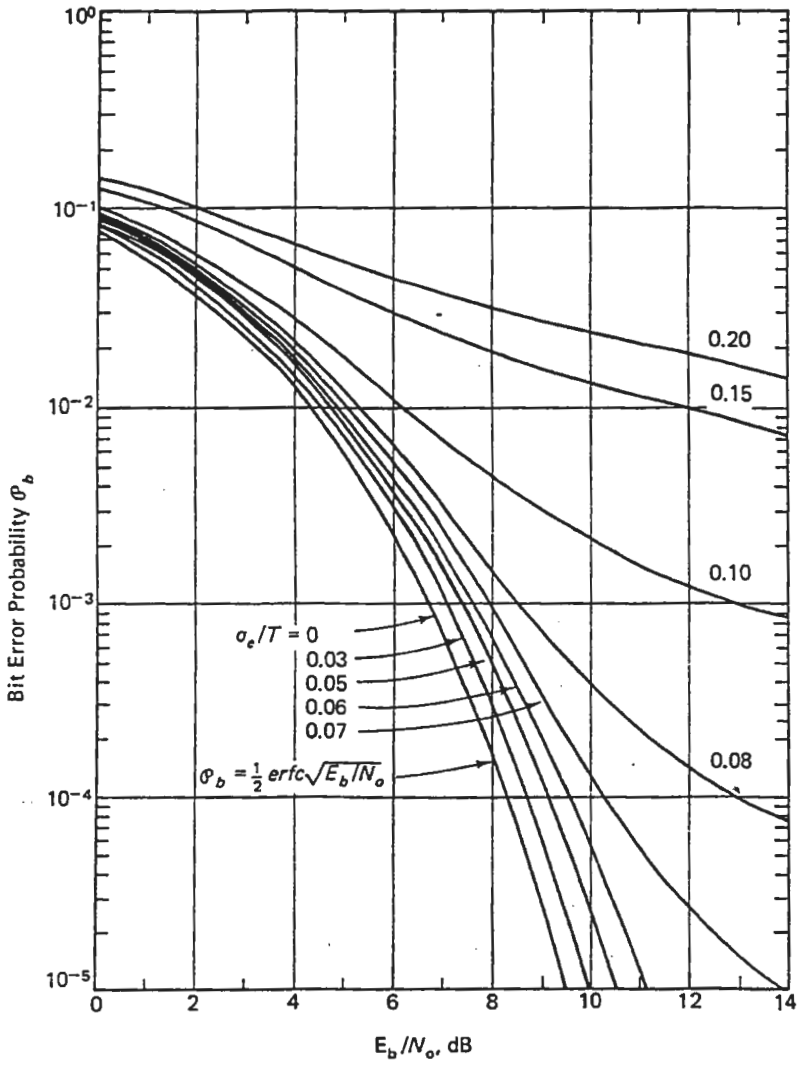

Fig. 14-10 Average probability of bit error versus E_b/N_0 with standard deviation of the symbol sync error σ_ϵ as a parameter (NRZ) [From Lindsey and Simon, 1973, 469, Fig. 9-37]

- Note that if $\frac{\sigma_\epsilon}{T} \leq 0.05$, a degradation of only about half a dB is realized for any specified $\mathcal{P}_b$

- However if $\frac{\sigma_\epsilon}{T}$ gets as large as 0.07, large degradation can result

Narrow Band Synchronizers

- band limited pulse trains have individual pulses which overlap one another

- due to this overlap, gated integrators (correlators) are unsatisfactory for data decision filtering

- if the gate time is one symbol in duration, the tails of the current pulse are lost and

there is interference from tails of neighboring pulses

- If gate time spans more than one pulse interval, there are even worse problems

- narrow band receivers almost always use filters rather than correlators. Detection of data is accomplished by sampling the filter output.

- to avoid intersymbol interference (ISI), the pulses are given a Nyquist shaping. This causes the tails of one pulse to go through zero at the sampling times of all other pulses.

- Nyquist shaping works well to eliminate ISI at sample times in data detection circuits

- However, Nyquist shaping does not eliminate effects of ISI on the clock synchronizer.

- The recovered clock will have a jitter caused by ISI.

- This jitter is called pattern noise or pattern jitter and may predominate over additive noise.

- Consider the following general type of narrowband synchronizer, and neglect additive noise

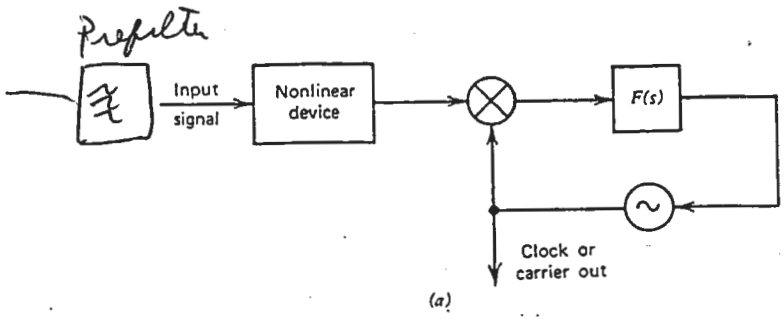

Figure 11.2 Nonlinear regenerator configurations: (*a*) separate nonlinearity;

- the output of the ~~regenerator~~ nonlinear device is:

$$v_o(t) = A_c \sin \omega_s t + a(t) \sin \omega_s t + b(t) \cos \omega_s t$$

where $\omega_s = 2\pi/T$ is the clock frequency, A_c is the amplitude of the regenerated clock, $a(t)$ and $b(t)$ are zero mean, random disturbances caused by the data and ISI.

- the PLL locks to the first term

- if tracking is accomplished with a phase error θ_e, then the phase detector output contains the terms:

$$a(t) \sin \theta_e.$$

$$b(t)\cos\theta_e$$

- to avoid interference from $a(t)$, design the loop so that θ_e is small. Hence we assume $a(t)$ is not significant.

- statistics for $a(t)$ and $b(t)$ are very difficult to determine, however, special cases, simulations, and experiments all point to the following observation:

- the nonlinearity spreads the spectra, If the data spectrum extends from 0 to $\frac{1}{2T}$, then $a(t)$ and $b(t)$ extend from 0 to $\frac{1}{T}$ approximately.

- the inphase $a(t)$ term is an ordinary low pass spectrum

- however, the quadrature $b(t)$ term is a bandpass spectrum!!

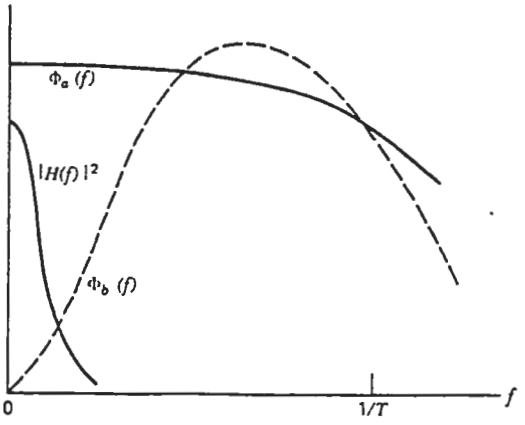

Figure 11.18 Quadrature spectra from clock regenerator. ($|H(f)|^2$ shows transmission through PLL.)

- this is shown in Fig 11.18. Also, the PLL transfer function $|H(f)|^2$ is plotted.

- since the quadrature density is not flat within the loop passband, simple formulas assuming white noise are not applicable.

- a consequence of $\Phi_b(f)$ is that the phase variance it causes rises as a steep function of the loop bandwidth, such as B_L^2 or B_L^3. Hence, B_L should be kept small.

- a second consequence is that the resulting jitter has a high-frequency content. This can be suppressed by including an extra pole in the PLL at a frequency well above the open loop gain crossover.

- a third consequence, due to $\Phi_a(f)$ being large, is that the loop phase error must be kept small. If θ_o is not zero, some of $\Phi_a(f)$ is cross coupled into a quadrature disturbance that

generates phase jitter.

- the existence of quadrature disturbances means that phase modulation is included in the regenerated clock wave ⇒ zero crossings of the regenerated clock are not equi-spaced.

- note : if the bandwidth were wide enough to avoid pulse overlap (wide band synchronization) then it should be possible to avoid quadrature disturbances ⟹ pattern jitter is not a problem.

: it is possible to modify the pulse shape to suppress all pattern jitter, but the modified pulse is not the same one used for data detection.

- examples of full wave rectifiers used as narrow band nonlinear regenerators are shown:

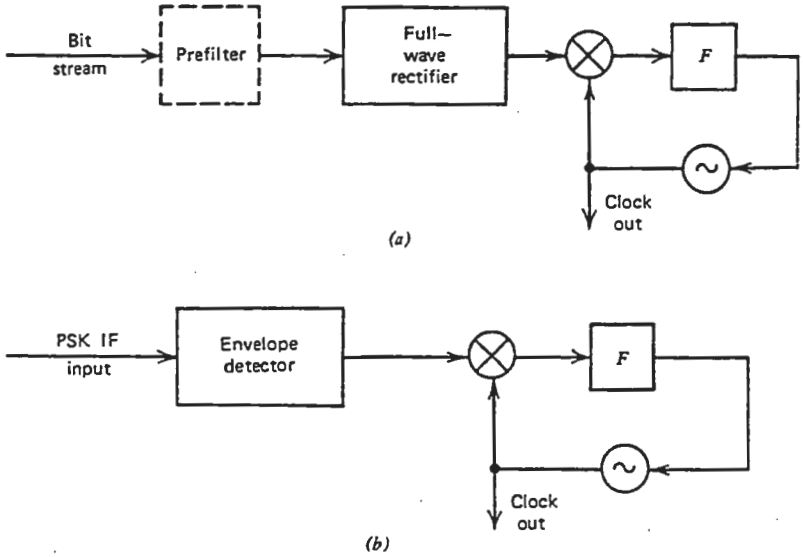

Figure 11.19 Clock rectifiers: (*a*) baseband input; (*b*) passband input.

- Input in 11.19 is a baseband pulse stream

- Input in 11.19b is the envelope variations of a passband signal. The envelope variations are created by the band limiting of the signal, and for many modulation formats contain a spectral line at the clock frequency or a related harmonic. This is easily ~~removed~~ isolated by rectification (envelope detection).

- many types of rectifier characteristics are possible. The square law is mathematically the most tractable, the absolute value (linear) provides 2 dB less jitter in practice.

- in the baseband full wave rectifier the noisy input bit stream is fed to a filter matched to the input waveshape.

- the filter output for a 00100 sequence is the autocorrelation function of a single input pulse (i.e., triangle function).

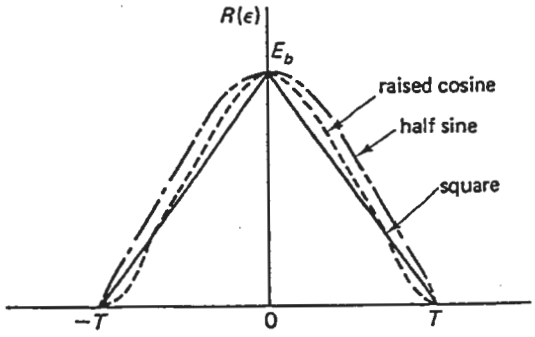

Fig. 14-2 Autocorrelation function of the square, half-sine, and raised-cosine input waveforms, each of which has the same energy E_b for a single bit.

- an RC lowpass filter can be used as an approximation to the matched filter if $f_c = 1/T$.

- the output waveform $x(t)$ is the summation of delayed autocorrelation of the input pulse waveform.

- three types of even law nonlinearities are used:

$$y(t) = \begin{cases} x^2(t) \\ \log\{\cosh[x(t)]\} \\ |x(t)| \end{cases}$$

- all three nonlinearities produce a spectral line at the clock frequency.

- the $\log\{\cosh[x(t)]\}$ acts as a square law device for small inputs and a magnitude device for large inputs.

- the output of a magnitude nonlinearity is shown below:

- the spectral line at the bit rate is recovered with a PLL having an equivalent bandpass memory time, KT, where:

$$KT \triangleq \frac{(\sum C_i)^2 T}{\sum C_i^2}$$

and C_i is the relative weighting assigned to the i^{th} preceding time interval.

- if equal weighting is applied for kT second memory, then $K = k$

- if exponential weighting is applied (i.e., $C_i = DC_{i-1}$; $D < 1$) then:

$$K = \frac{1+D}{1-D}$$

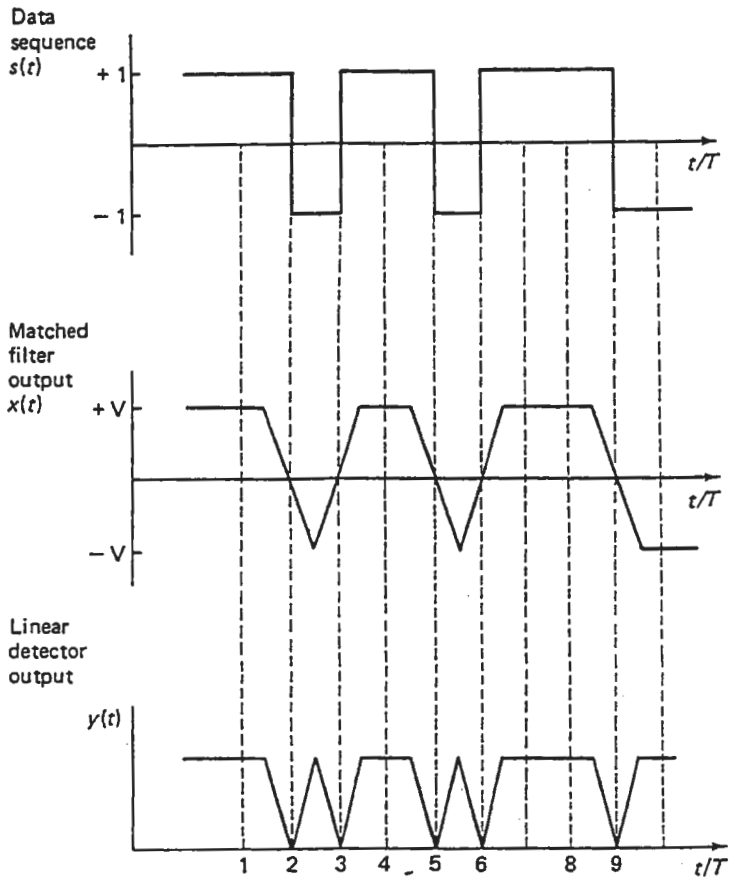

Fig. 14-3 Bit synchronizer waveform: the matched filter synchronizer of Fig. 14-1*a*. A magnitude non-linearity is employed, and the input is noise-free. The inputs are rectangular pulses.

- for a rectifier synchronizer using an RC- LPF with $B = 1/T$ followed by a square law detector, the expected magnitude of timing error, ϵ for a raised-cosine input waveform is:

$$\overline{|\epsilon|} \approx \frac{0.33T}{\sqrt{K\frac{E_b}{N_o}}} \quad ; \quad \begin{matrix} \frac{E_b}{N_o} > 5 \\ K > 18 \end{matrix}$$

where N_o is the one-sided noise density. - at high SNR, the timing error ϵ becomes Gaussian with standard deviation of:

$$\sigma_\epsilon = \frac{0.411T}{\sqrt{K\frac{E_b}{N_o}}} \quad ; \quad \frac{E_b}{N_o} \gg 1$$

- further examples are the sampled derivative detectors and the derivative-product regenerator shown below:

- in the sampled derivative detectors, the strobe pulse is aligned with the peak of the

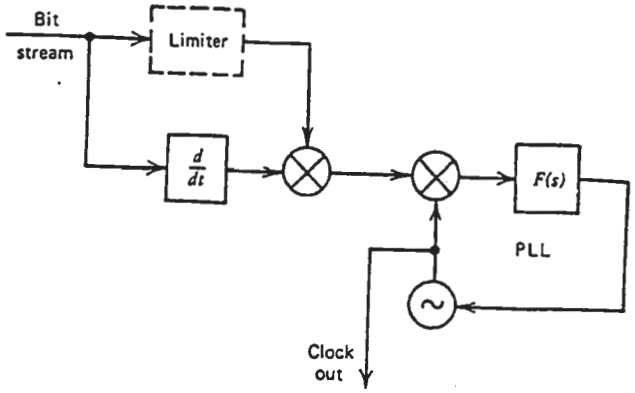

Figure 11.21 Derivative-product regenerator.

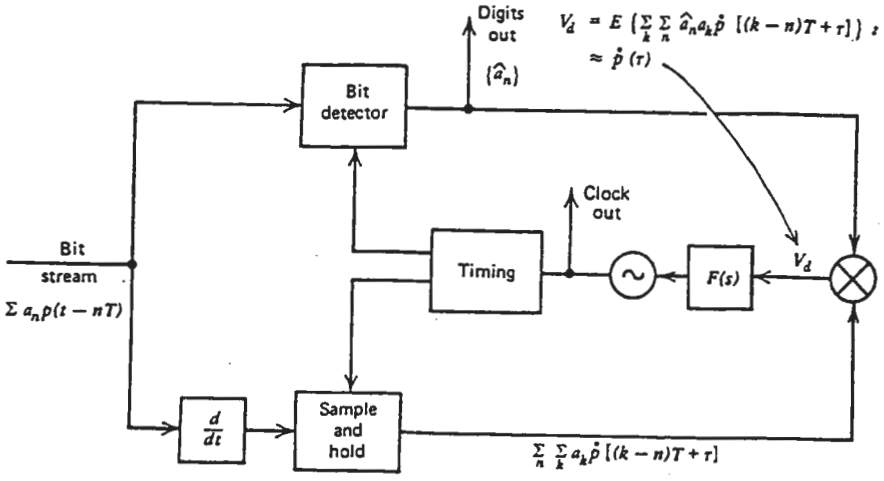

Figure 11.20 Sampled-derivative phase detector. Sets timing to coincide with peak of data pulse.

signaling pulse. This alignment is optimum for data detection if the signal pulse is symmetric about its peak.

- the derivative-product regenerator avoids sampling

- the zero crossing detector of Fig 11.17b can also be used as a narrow band regenerator.

- All the forgoing narrow band synchronizers have at least a quadratic nonlinearity. The requirement for the order of the nonlinearity is tied to the pulse bandwidths as follows

- the Nyquist baseband pulses occupy a bandwidth given by:

$$BW = \frac{1+k}{2T}$$

where k is the roll-off-factor (or excess bandwidth factor).

- now the amplitude of the regenerated clock is proportional to k for a quadratic nonlinearity regenerator.

- Hence a quadratic regenerator cannot produce a clock for k=0 (i.e., for a minimum band, Nyquist pulses).
- The above mentioned synchronizers can be tabulated as follows:

Table 15-3 Summary of Clock Synchronizers

quadratic nonlinearities	fourth law nonlinearities	hard nonlinearities
- square law rectifier	- absolute value rectifier	- derivative cct with limiter in one arm
- derivative-product regenerator without limiter		- derivative cct with bit detector in one arm
		- zero crossing detector

Note: all narrowband synchronizers suffer from pattern jitter for excess bandwidth less than 100%.

- Nyquist pulses are well suited for optimum data detection, but not for clock recovery. Modification of the pulse shape by means of linear filtering can suppress the jitter (prefiltering).

- to suppress pattern jitter for a square law rectifier as the regenerator, requires the spectrum of the filtered baseband pulse train to be symmetrical ~~about~~ about $\frac{1}{2T}$ and band limited to the interval $(\frac{1}{4T}, \frac{3}{4T})$.

- since Nyquist shaping provides the high frequency band limitation needed, the prefilter required is a highpass to shape the low frequency portion of the spectrum.

Note: this prefilter suppresses the low frequency additive noise in addition to the pattern jitter.

Note: prefilters can be applied to sampled-derivative and derivative-product circuits (Fig 11.20 and 11.21) with similar benefits.

Note: if the channel is nonlinear $\Rightarrow$ pulse shapes are distorted depending on data pattern, $\Rightarrow$ prefilters do not work well.

16.I. Introduction to Spread Spectrum

The One Concept

Excessive Time/Bandwidth Occupancy

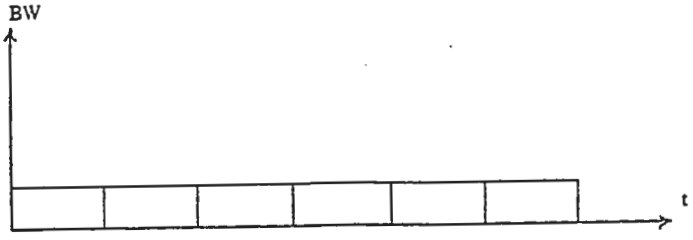

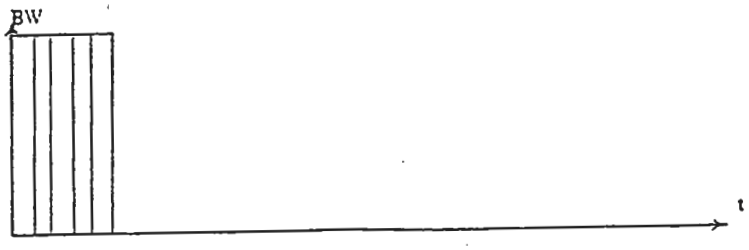

Symbol

1	-1

X

PN sequence

1	-1	-1	1	1	-1	1	-1	1	-1	1	1	-1	-1

=

T_X/R_X

1	-1	-1	1	1	-1	1	1	-1	1	-1	-1	1	1

X

Stored reference

1	-1	-1	1	1	-1	1	-1	1	-1	1	1	-1	-1

=

Despread

1	-1

The Two Principal Techniques

1. Direct Sequence Spread, Phase Shift Keying
2. Frequency Hopped Spread, Frequency Shift Keying

Direct Sequence Spread, Phase Shift Keying

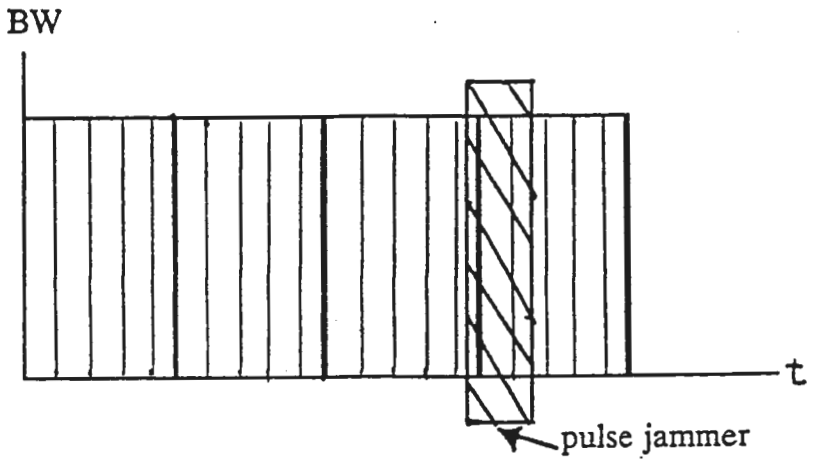

Frequency Hopped, Frequency Shift Keying

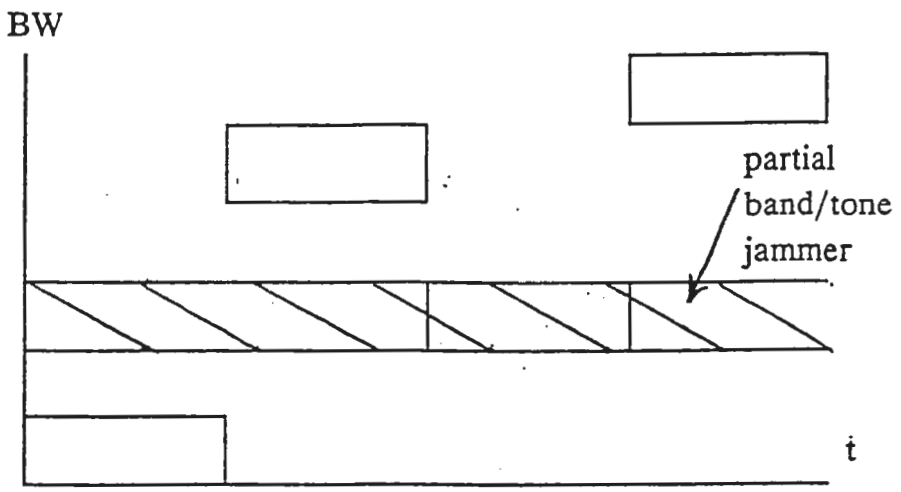

The Three Unique Subsystems

1. Pseudo-Noise Generators:
   * Fibonacci Generators; Galois Generators.
   * Galos Fields
   * M Sequences; Balance Property.
   * Gold Sequences; Cross Correlation Property

2. Sequence Synchronizers
   * Acquisition; Probabilities of Detection/ False Alarm, Markov Chain
   * Tracking; Delay Locked Loops, Tau Dither Loop

3. Coded Symbol Detectors
   * Block Code/Interleaver, Reed Solomon Code
   * Soft Decision Decoding, Hard Decision Decoding

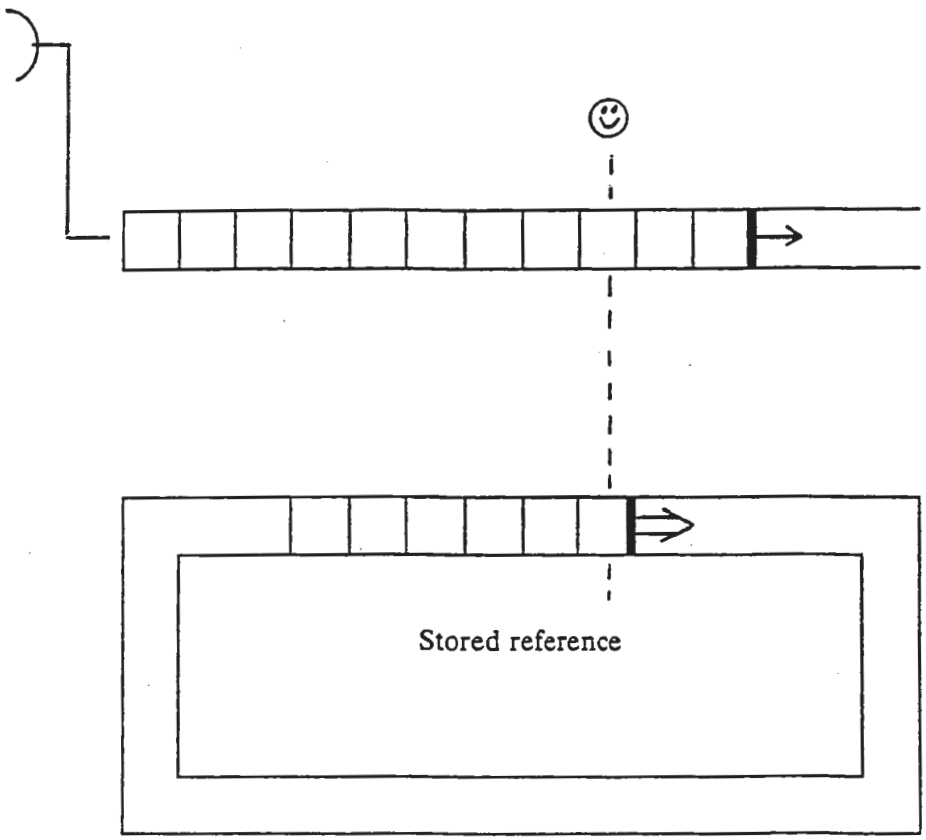

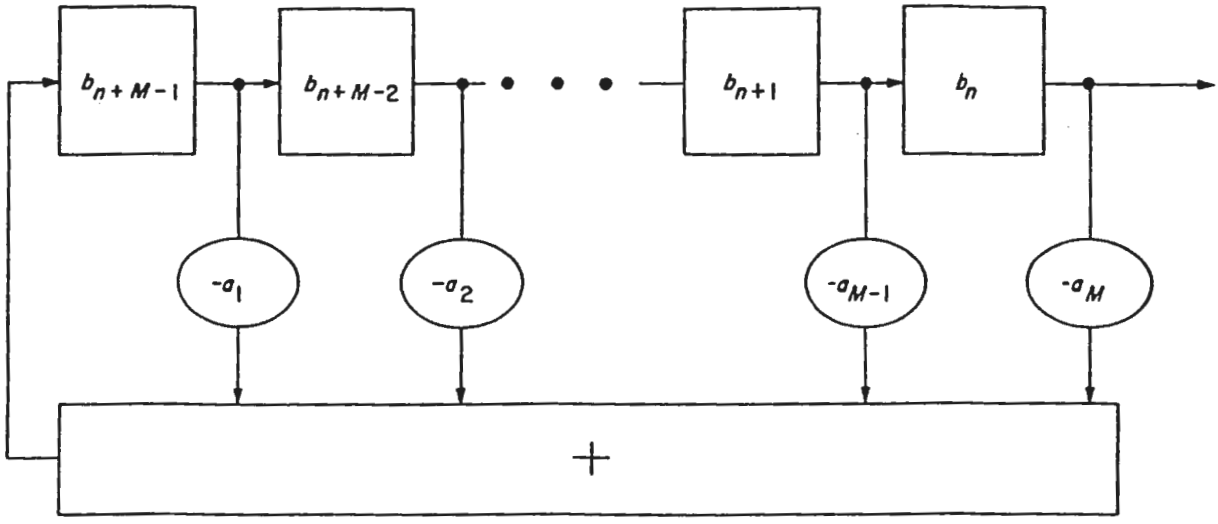

Figure 5.5. An M-stage linear-feedback shift register in Fibonacci form.

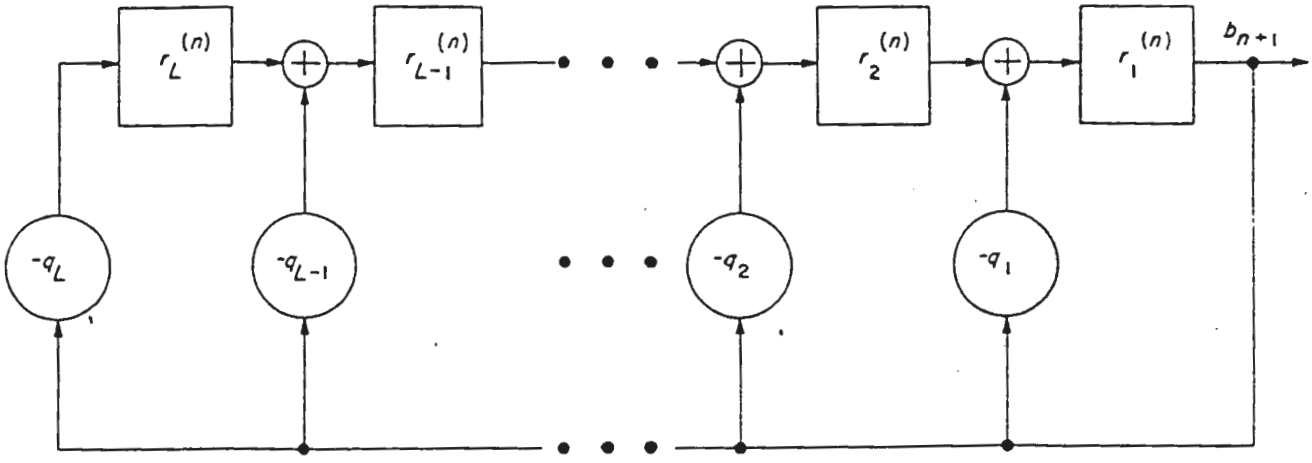

Figure 5.6. A minimum-memory LFSR in the Galois configuration for generating $\{b_n\}$.

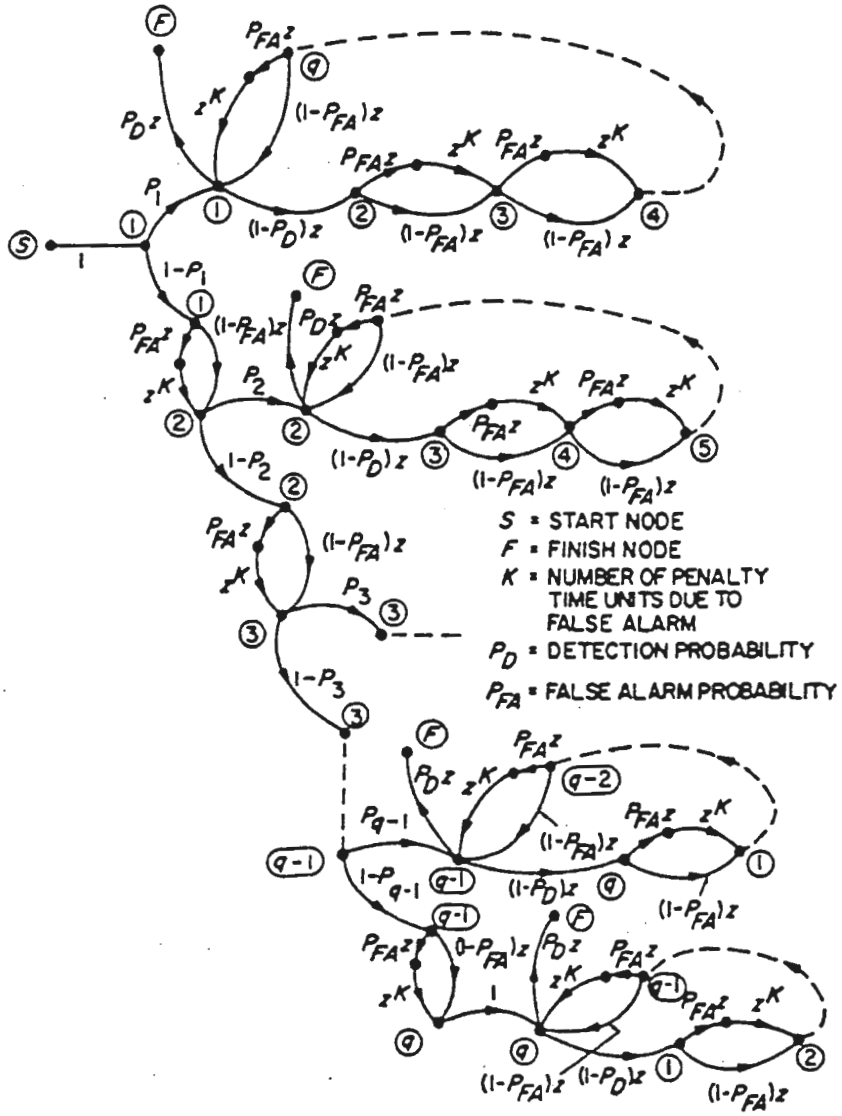

Figure 1.8. Generating function flow graph for acquisition time.

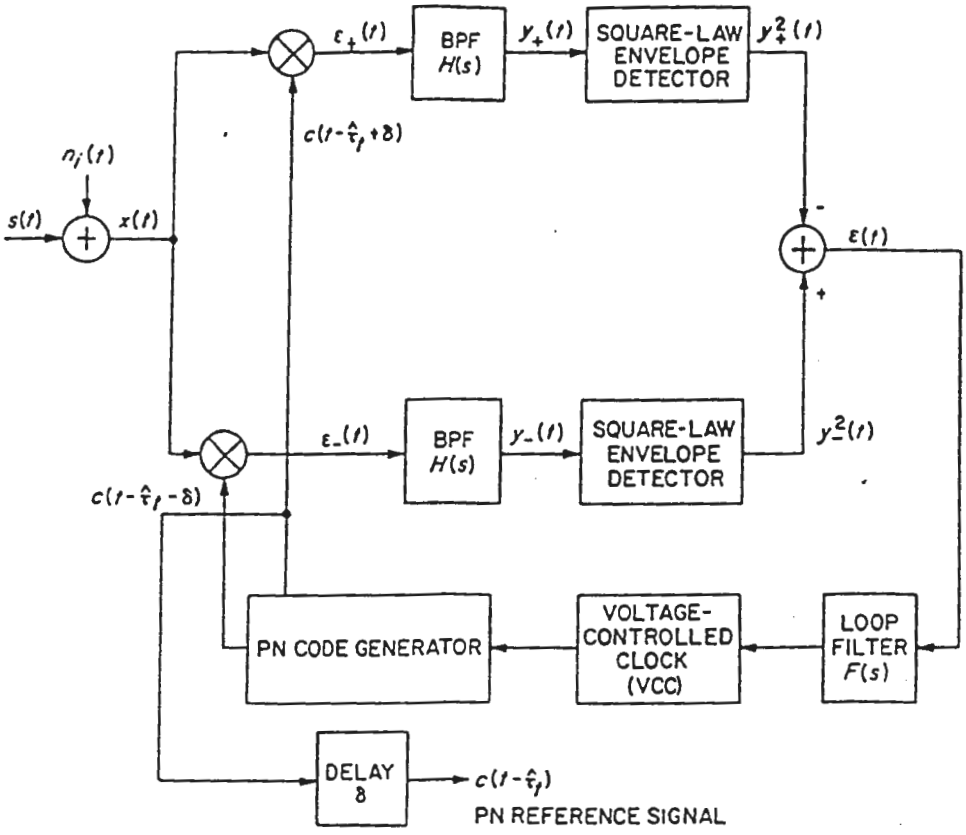

Figure 2.1. A non-coherent delay-locked loop.

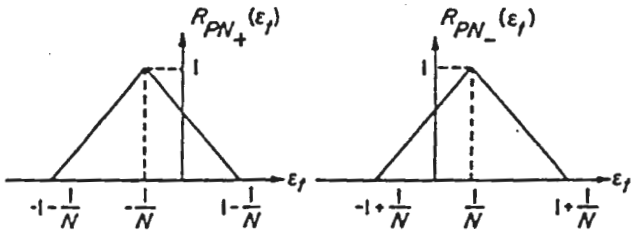

Figure 2.2. Autocorrelation functions of the advanced and retarded PN code.

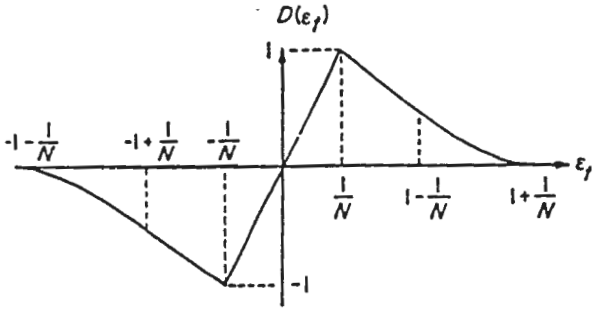

Figure 2.3. Discriminator characteristic.

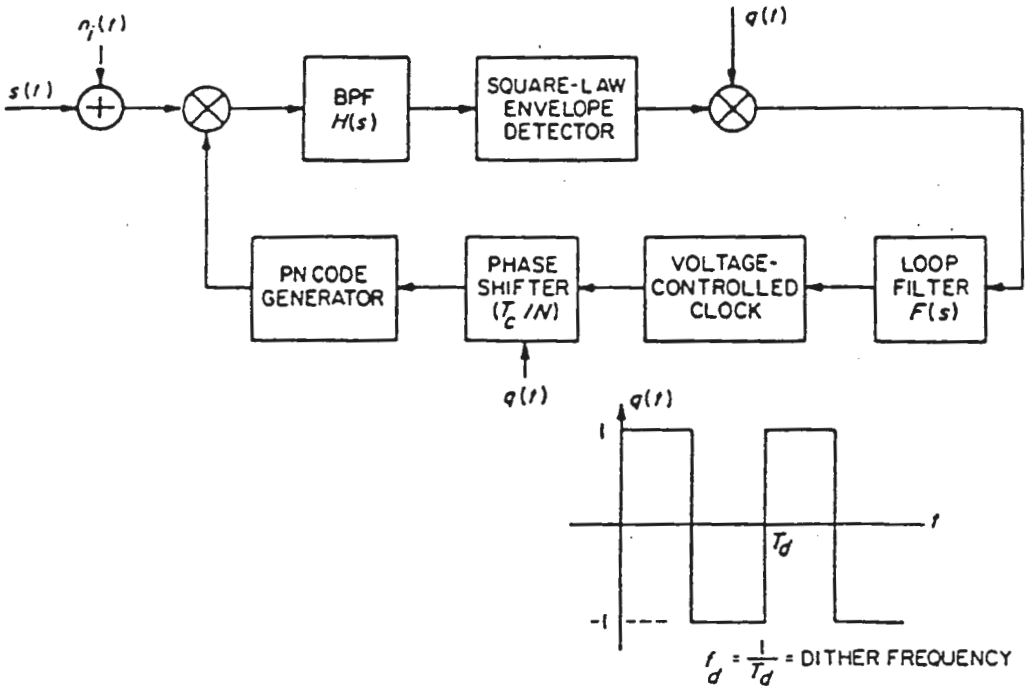

Figure 2.9. A non-coherent tau-dither loop.

The Four Classical Uses

1. Anti Jam, AJ
   * Broad Band Jammers
   * Partial Band, Multitone Jammers
   * Pulse Jammers

2. Low Probability of Intercept, LPI
   * Search Based on Sequence Properties
   * Search Based on Chip Properties

3. Time of Arrival, TOA
   * Short Chip Duration/Low Data Rate Combination

4. Multiple Accessing, SSMA
   * Sequence Cross Correlation
   * Singnal to (Noise + Interference) Ratio

The Fifth Application

Regulatory Interference Specification Compromise, RISC

16. Code Synchronizers

Pseudonoise (PN) Code Tracking in Direct Sequence (DS) Receivers

- Before code tracking can take place, PN code acquisition must first be accomplished.

- Here, the code in the receiver (the stored reference) must be time aligned to within one chip in as short a time as possible.

- Following the acquisition, code tracking accurately aligns the stored reference with the incoming sequence to fractions of a chip.

- there are predominantly two PN tracking loop configurations, the delay locked loop (DLL) and the tau-dither loop (TDL).

- These can each be operated in coherent or noncoherent mode.

- Both types fall within the class of early late gate type loops, in that the received PN code is correlated either simultaneously or alternately with delayed and advanced versions of the receiver stored reference code.

- This produces the timing error correcting characteristic.

- Modifications of the TDL and DLL are the double dither loop (DDL), the product of sum and difference DLL ($\Sigma\Delta$ DLL) and the modified code tracking loop (MCTL).

- These loops attempt to mitigate disadvantages of each configuration.

- The complex sums DLL, another variation, is used in environments where severe dynamic range variation can result in fast fading and scintillation.

- Here we will concentrate on non-coherent PN tracking loops where PN acquisition and tracking is performed prior to carrier sync. This is the most common situation for spread spectrum (SS) communications.

- Note: for SS ranging, the code is acquired and coherently tracked as a baseband modulation.

- We will also concentrate on steady state tracking performance based on linear theory. This is justified since in most situations the equivalent loop SNR is high enough.

- We will also present the acquisition (transient) behaviour and slip time (mean time to lose lock) for DLL and TDL based on nonlinear theory.

1. The Delay Locked Loop

- Figure 2.1 shows the noncoherent DLL.

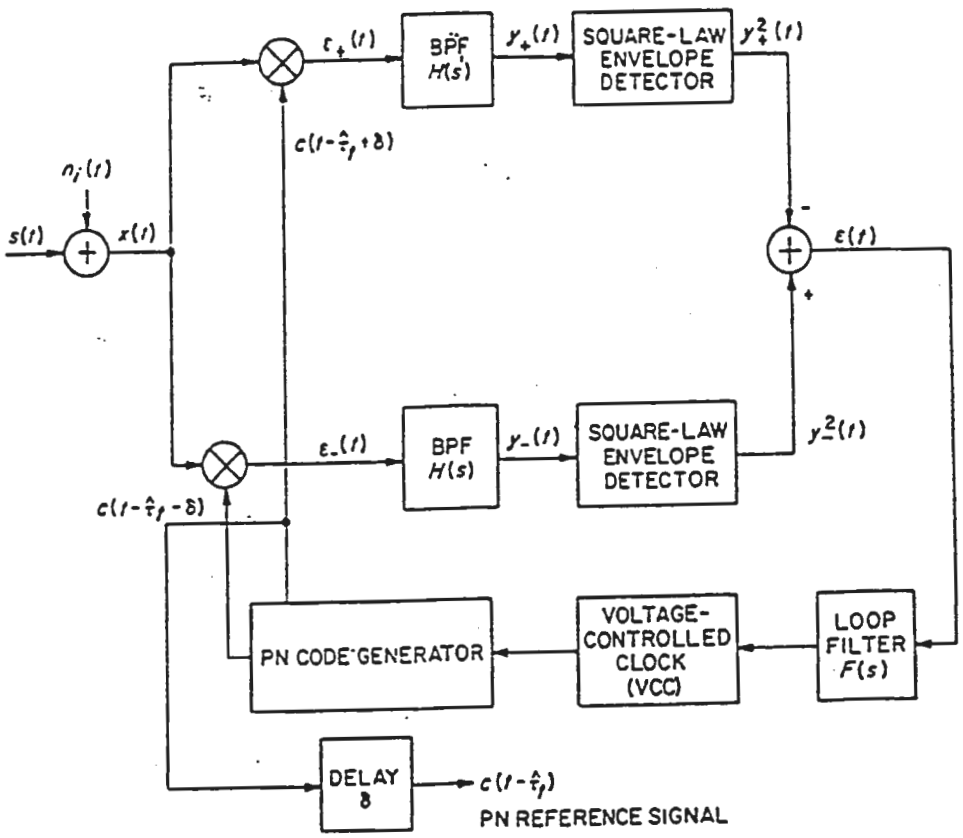

Figure 2.1. A non-coherent delay-locked loop.

- Here, the input $x(t)$ is cross-correlated with advanced and retarded versions of the local PN code generator sequence.

- Results of cross correlation operations are bandpass filtered, square-law envelope detected, and differenced to produce an error (discriminator) characteristic.

- The loop is closed by applying this to a loop filter and VCO that drives the PN code generator.

- The advance (and retard) interval δ (equivalently, the correlator spacing) is restricted to a range $\delta \leq T_c$, where T_c is the PN chip duration.

- We shall define

$$\delta \triangleq T_c/N$$

where N is any integer larger than unity.

- This restriction in δ is for convenience purposes.

- Hence the advanced and retarded PN signals are $2T_c/N$ apart.

- Also, the loop has "T_c/N of correlator spacing".

- When the advance (and retarded) interval is half a code chip; $N = 2$; and the loop is called a one delta loop.

Mathematical loop model and equation of operation

- We have the received signal $x(t)$ as sum of signal $s(t)$ and additive noise $n_i(t)$

$$x(t) = s(t) + n_i(t)$$

where

$$s(t) = \sqrt{2S}\; c(t-\tau_t)\; m(t-\tau_t)\; \cos[\omega_o t + \theta(t)] \tag{2.1}$$

and the bandpass representation of $n_i(t)$ is

$$n_i(t) = \sqrt{2}\{N_c(t)\cos[\omega_o t + \theta(t)] - N_s(t)\sin[\omega_o t + \theta(t)]\} \tag{2.2}$$

Here S = average signal power

$c(t-\tau_t)$ = received PN code with transmission delay τ_t

$m(t-\tau_t)$ = data modulation with same delay τ_t

$\theta(t) = \theta_o + \Omega_o t$ = unknown carrier phase consisting of a constant plus a Doppler term

$N_c(t)$ and $N_s(t)$ are (approximately) statistically independent, stationary, low pass white Gaussian noise processes, with single sided noise spectral density N_o and one sided bandwidth $B_N \ll \omega_o/2\pi$

- If the advanced and retarded PN reference signals are $c(t-\hat{\tau}_t+\delta)$ and $c(t-\hat{\tau}_t-\delta)$, where $\hat{\tau}_t$ is the DLL's estimate of τ_t, then the cross correlator (phase detector) outputs become

$$\begin{aligned}\epsilon_{\pm}(t) = {} & \sqrt{2S}\; K_m\; m(t-\tau_t)\; \overline{c(t-\tau_t)c(t-\hat{\tau}_t \pm \delta)}\; \cos[\omega_o t + \theta(t)] \\ & + \sqrt{2S}\; K_m\; m(t-\tau_t)\Big[c(t-\tau_t)\; c(t-\hat{\tau}_t \pm \delta) \\ & \quad - \overline{c(t-\tau_t)\; c(t-\hat{\tau}_t \pm \delta)}\Big]\; \cos[\omega_o t + \theta(t)] \\ & + K_m\; c(t-\hat{\tau}_t \pm \delta)\; n_i(t)\end{aligned} \tag{2.3}$$

Here : K_m is the phase detector gain (identical for both). Note that this implies that DLL is sensitive to gain imbalance.

: The overbar refers to statistical expectation.

For large PN code period p we have

$$R_{PN_+}(\epsilon_t) \triangleq \overline{c(t-\tau_t)c(t-\hat{\tau}_t+\delta)} = \begin{cases} 0 & ; \epsilon_t \le -\frac{1}{N} - 1 \\ 1 + \frac{1}{N} + \epsilon_t & ; -1 - \frac{1}{N} \le \epsilon_t \le -\frac{1}{N} \\ 1 - \frac{1}{N} - \epsilon_t & ; -\frac{1}{N} < \epsilon_t \le 1 - \frac{1}{N} \\ 0 & ; \epsilon_t > 1 - \frac{1}{N} \end{cases}$$

$$R_{PN_-}(\epsilon_t) \triangleq \overline{c(t-\tau_t)c(t-\hat{\tau}_t-\delta)} = R_{PN_+}(\epsilon_t - \frac{2}{N})$$

$$R_{PN_\pm}(\epsilon_t) = R_{PN_\pm}(\epsilon_t + np) \; ; \; n = \pm 1, \; \pm 2, \; \pm 3... \tag{2.4}$$

- Here ϵ_t denotes the normalized transmission delay error

$$\epsilon_t \triangleq (\tau_t - \hat{\tau}_t)/T_c$$

Figure 2.2 gives the two autocorrelation functions.

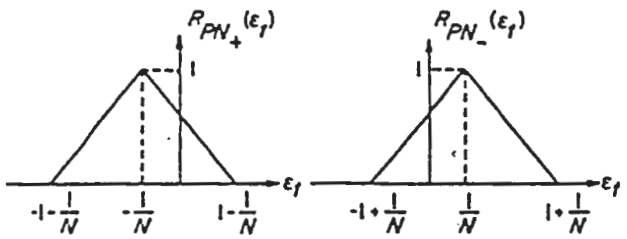

Figure 2.2. Autocorrelation functions of the advanced and retarded PN code.

- Let $H_l(s)$ denote LP equivalent of the BPF transfer function $H(s)$, and let $S_{c\pm}(t-\tau_t, \epsilon_t)$ denote the PN code self-noise process:

$$S_{c\pm}(t-\tau_t, \epsilon_t) \triangleq c(t-\tau_t)c(t-\hat{\tau}_t \pm \delta) - \overline{c(t-\tau_t)c(t-\hat{\tau}_t \pm \delta)}$$

Then combining (2.2) and (2.3) we get (see Figure 2.1)

$$\begin{aligned} y_\pm(t) &= \sqrt{2S}\, K_m \hat{m}(t-\tau_t) R_{PN_\pm}(\epsilon_t) \cos[\omega_o t + \theta(t)] \\ &+ \sqrt{2S}\, K_m \hat{S}_{c\pm}(t-\tau_t, \; \epsilon_t) \cos[\omega_o t + \theta(t)] \\ &+ \sqrt{2}\, K_m \hat{N}_{c\pm}(t) \cos[\omega_o t + \theta(t)] \\ &- \sqrt{2}\, K_m \hat{N}_{s\pm}(t) \sin[\omega_o t + \theta(t)] \end{aligned} \tag{2.5}$$

where

$$\begin{aligned}\hat{m}(t) &= H_l(t) * m(t)\\ \hat{S}_{c\pm}(t,\epsilon_t) &= H_l(t) * [m(t)S_{c\pm}(t,\epsilon_t)]\\ \hat{N}_{c\pm}(t) &= H_l(t) * [c(t-\hat{\tau}_t \pm \delta)N_c(t)]\\ \hat{N}_{s\pm}(t) &= H_l(t) * [c(t-\hat{\tau}_t \pm \delta)N_s(t)]\end{aligned} \tag{2.6}$$

Note: In the above, we have written differential equations in compact form by use of the impulse response function of the LP equivalent of the BPF.

- When the single sided loop Bandwidth B_L is much less than the PN chip rate $1/T_c$, then effect of the PN code self noise on loop performance can be neglected.

- Hence, ignoring self noise term in (2.5) and second harmonic terms produced by square law detectors, the input to the loop filter is

$$e(t) \triangleq y_-^2(t) - y_+^2(t) = SK_m^2\hat{m}^2(t-\tau_t)D(\epsilon_t) + K_m^2 n_e(t,\epsilon_t) \tag{2.7}$$

where the loop (S curve) discriminator characteristic is

$$D(\epsilon_t) \triangleq R_{PN\_}^2(\epsilon_t) - R_{PN_+}^2(\epsilon_t) = \begin{cases} 0 & ;\ \epsilon_t \le -1-\frac{1}{N}\\ -(1+\frac{1}{N}+\epsilon_t)^2 & ;\ -1-\frac{1}{N} < \epsilon_t \le -1+\frac{1}{N}\\ -\frac{4}{N}(1+\epsilon_t) & ;\ -1+\frac{1}{N} < \epsilon_t < -\frac{1}{N}\\ 4\epsilon_t(1-\frac{1}{N}) & ;\ |\epsilon_t| \le \frac{1}{N}\\ \frac{4}{N}(1-\epsilon_t) & ;\ \frac{1}{N} < \epsilon_t < 1-\frac{1}{N}\\ (1+\frac{1}{N}-\epsilon_t)^2 & ;\ 1-\frac{1}{N} < \epsilon_t \le 1+\frac{1}{N}\\ 0 & ;\ \epsilon_t > 1+\frac{1}{N}\end{cases} \tag{2.8}$$

and

$$D(\epsilon_t) = D(\epsilon_t + np) \quad ; \quad n = \pm 1,\ \pm 2,\ \pm 3,\ \cdots$$

$D(\epsilon_t)$ is shown in Figure 2.3

Also in equation (2.7), $n_e(t,\epsilon_t)$ is the equivalent additive noise given by

$$\begin{aligned}n_e(t,\epsilon_t) &= \hat{N}_{c\_}^2(t) - \hat{N}_{c_+}^2(t) + \hat{N}_{s\_}^2(t) - \hat{N}_{s_+}^2(t)\\ &\quad + 2\sqrt{S}\hat{m}(t-\tau_t)\{R_{PN\_}(\epsilon_t)\hat{N}_{c\_}(t) - R_{PN_+}(\epsilon_t)\hat{N}_{c_+}(t)\}\end{aligned} \tag{2.9}$$

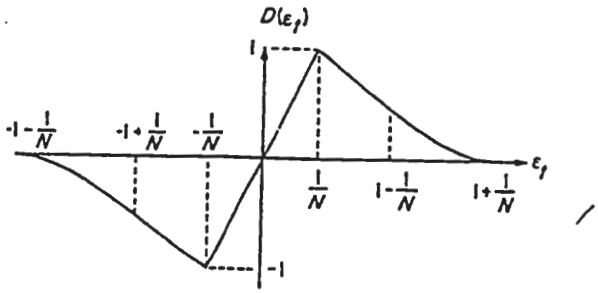

Figure 2.3. Discriminator characteristic.

The instantaneous (normalized) delay estimate $\hat{\tau}_t/T_c$ of the PN code generator is related to $e(t)$, (in operation form) by

$$\frac{d}{dt}\left(\frac{\hat{\tau}_t}{T_c}\right) = K_{vcc}F(t) * e(t) \tag{2.10}$$

Here $F(t)$ is the loop filter impulse response;

K_{vcc} is the constant of the voltage-controlled clock (vcc) which drives the PN code generator.

- Combining (2.7) and (2.10) and letting $K \triangleq K_m{}^2K_{vcc}$ denote the loop gain, the stochastic integro-differential equation for the operation of the DLL (Fig. 2.1) becomes:

$$\frac{d}{dt}\left(\frac{\hat{\tau}_t}{T_c}\right) = KF(t) * \left[S\hat{m}^2(t-\tau_t)D(\epsilon_t) + n_e(t,\epsilon_t)\right] \tag{2.11}$$

or

$$\frac{d}{dt}(\epsilon_t) = \frac{d}{dt}\left(\frac{\tau_t}{T_c}\right) - KF(t) * \left[S\hat{m}^2(t-\tau_t)D(\epsilon_t) + n_e(t,\epsilon_t)\right] \tag{2.12}$$

Now decompose $\hat{m}^2(t-\tau_t)D(\epsilon_t)$ into its mean value plus a modulation self noise term. Note: since $\hat{m}^2(t)$ is a cyclostationary process, both statistical and time averages are needed to find its mean value.

$$\hat{m}^2(t-\tau_t)D(\epsilon_t) = <\overline{\hat{m}^2(t-\tau_t)}> D(\epsilon_t) + \left[\hat{m}^2(t-\tau_t) - <\overline{\hat{m}^2(t-\tau_t)}>\right] D(\epsilon_t) \tag{2.13}$$

- Here, $< >$ denotes time average, and

$$<\overline{\hat{m}^2(t-\tau_t)}> \triangleq M_2 = \int_{-\infty}^{\infty} S_m(f)|H_l(j2\pi f)|^2 df \tag{2.14}$$

with $S_m(f)$ being the power spectral density of the data modulation.

- It can be shown that if the loop bandwidth B_L is much less than the data symbol rate $R_s = 1/T_s$, then the modulation self noise term can be ignored.

- Hence, (2.12) simplifies to

$$\dot{\epsilon}_t = \frac{\dot{\tau}_t}{T_c} - KF(t) * \eta S M_2 \left[D_n(\epsilon_t) + \frac{n_e(t, \epsilon_t)}{\eta S M_2} \right] \tag{2.15}$$

where:

$$D_n(\epsilon_t) \underline{\underline{\Delta}} \frac{1}{\eta} D(\epsilon_t)$$

= normalized discriminator characteristic with unit slope at the origin.

: the dot denotes differentiation with time

$$\eta \underline{\underline{\Delta}} \frac{4(N-1)}{N} \tag{2.16}$$

Statistical Characterization of the Equivalent Additive Noise

It is necessary in what follows to determine the autocorrelation function $R_e(\tau)$ of the equivalent additive noise $n_e(t, \epsilon_t)$.

- Define

$$R_e(\tau, \epsilon_t) \underline{\underline{\Delta}} \overline{n_e(t, \epsilon_t) n_e(t+\tau, \epsilon_t)} \tag{2.17}$$

With $n_e(t, \epsilon_t)$ defined in (2.9), one obtains "after considerable algebraic manipulation"

$$R_e(\tau, \epsilon_t) = 8R^2_{\hat{N}}(\tau) + 4SR_{\hat{m}}(\tau) R_{\hat{N}}(\tau) f(\epsilon_t) \tag{2.18}$$

where

$$R_{\hat{N}}(\tau) = \frac{N_o}{2} \int_{-\infty}^{\infty} |H_l(j2\pi f)|^2 \, e^{j2\pi f \tau} df$$

$$R_{\hat{m}}(\tau) = \int_{-\infty}^{\infty} S_m(f) \, |H_l(j2\pi f)|^2 \, e^{j2\pi f \tau} df$$

(and)

$$f(\epsilon_t) \underline{\underline{\Delta}} R^2_{PN_+}(\epsilon_t) + R^2_{PN_-}(\epsilon_t) = \begin{cases} 0 & ; \epsilon_t \le -1 - \frac{1}{N} \\ (1 + \frac{1}{N} + \epsilon_t)^2 & ; -1 - \frac{1}{N} < \epsilon_t \le -1 + \frac{1}{N} \\ 2\left[\frac{1}{N^2} + (1+\epsilon_t)^2\right] & ; -1 + \frac{1}{N} < \epsilon_t < -\frac{1}{N} \\ 2\left[\left(1 - \frac{1}{N}\right)^2 + \epsilon_t^2\right] & ; |\epsilon_t| \le \frac{1}{N} \\ 2\left[\frac{1}{N^2} + (1-\epsilon_t)^2\right] & ; \frac{1}{N} < \epsilon_t < 1 - \frac{1}{N} \\ \left(1 + \frac{1}{N} - \epsilon_t\right)^2 & ; 1 - \frac{1}{N} < \epsilon_t \le 1 + \frac{1}{N} \\ 0 & ; \epsilon_t > 1 + \frac{1}{N} \end{cases} \tag{2.19}$$

- Since DLL bandwidth is narrow with respect to the equivalent noise bandwidth of $n_e(t, \epsilon_t)$, we can approximate $n_e(t, \epsilon_t)$ as a delta correlated process with equivalent single sided noise spectral density

$$N_e(\epsilon_t) = 2\int_{-\infty}^{\infty} R_e(\tau, \epsilon_t)d\tau \tag{2.20}$$

- Sub (2.18) and (2.19) into (2.20) and "simplifying" yields

$$N_e(\epsilon_t) = 4N_o^2\int_{-\infty}^{\infty} |H_l(j2\pi f)|^4\, df + 4SN_o f(\epsilon_t)\int_{-\infty}^{\infty} S_m(f)\,|H_l(j2\pi f)|^4\, df \tag{2.21}$$

- Alternately,

$$N_e(\epsilon_t) = 2SN_o\left[2M_4 f(\epsilon_t) + 2\frac{K_L}{\rho_H}\right] \tag{2.22}$$

where

$$K_L \triangleq \frac{\int_{-\infty}^{\infty} |H_l(j2\pi f)|^4\, df}{\int_{-\infty}^{\infty} |H_l(j2\pi f)|^2\, df}$$

$$M_4 \triangleq \int_{-\infty}^{\infty} S_m(f)\,|H_l(j2\pi f)|^4\, df \tag{2.23}$$

and B_H is the two sided noise bandwidth of the equivalent low pass filter $H_l(s)$. (Equivalently, the bandpass noise BW of H(s)).

$$B_H = \int_{-\infty}^{\infty} |H_l(j2\pi f)|^2 df \tag{2.24}$$

Also, the signal to noise ratio in this BW is

$$\rho_H = \frac{S}{N_o B_H} \tag{2.25}$$

Linear Analysis of DLL Tracking Performance

- When equivalent loop SNR is large, the DLL tracking performance can be determined from (2.15) with $D_n(\epsilon_t)$ replaced by ϵ_t.

- With this assumption, and also assuming $\dot{\tau}_t = 0$, one can find by inspection of (2.15) an expression for the mean squared tracking jitter

$$\sigma_\epsilon^2 = \overline{\epsilon_t^2} = \frac{\overline{N_e(\epsilon_t)}B_L}{(\eta S M_2)^2} \tag{2.26}$$

Sub (2.19) and (2.22) into (2.26)

$$\sigma_\epsilon^2 = \frac{N_o B_L}{2S}\left[\frac{M_4\left[1+\frac{16}{\eta^2}\sigma_\epsilon^2\right]+\frac{8K_L}{\rho_H\eta^2}}{M_2^2}\right] \tag{2.27}$$

solving for σ_ϵ^2

$$\sigma_\epsilon^2 = \frac{1}{2\rho}\left\{\frac{M_4+\frac{8K_L}{\rho_H\eta^2}}{M_2^2\left[1-\frac{8}{\eta^2\rho}\left(\frac{M_4}{M_2^2}\right)\right]}\right\} \tag{2.28}$$

where $\rho \triangleq \frac{S}{N_o B_L}$

-Since for the linear analysis, ρ is assumed to be large, then (2.28) can be simplified to

$$\sigma_\epsilon^2 = \frac{1}{2\rho}\left\{\frac{M_4+\frac{8K_L}{\rho_H\eta^2}}{M_2^2}\right\} \triangleq \frac{1}{2\rho\mathcal{S}_L} \tag{2.29}$$

where $\mathcal{S}_L$ is the squaring loss of the DLL (i.e., the ratio of the signal $\times$ signal to the signal $\times$ noise plus noise $\times$ noise).

- Alternatively, in terms of data symbol signal to noise ratio $E_s/N_o \triangleq ST_s/N_o$, and the ratio of bandpass filter bandwidth B_H to data rate R_s

$$\mathcal{S}_L = \frac{s\times s}{s\times N + N\times N} = \frac{M_2^2}{M_4 + K_L\frac{B_H/R_s}{2E_s/N_o}\left(\frac{N}{N-1}\right)^2} \tag{2.30}$$

Here we have also used definition of η in (2.16) .

Note : equation (2.30) is similar to expression for squaring loss in a Costas loop used for carrier sync of BPSK signal.

: also from (2.30), one can see that the squaring loss of a DLL with a correlator spacing $\delta = T_c/N$ is equal to squaring loss of a DLL with a correlator spacing of $T_c/2$ (a one delta loop) and a data rate of $4[(N-1)/N]^2 R_s$.

: hence, one need plot only curves for the squaring loss of the "one-delta" loop. All other cases can be derived from these curves by modifying appropriately the data rate R_s.

- Tables 2.1 and 2.2 give closed form results for M_2 and M_4 corresponding to one- and two-pole Butterworth filters and NRZ or Machester coded data.

Also for an n-pole Butterworth filter

$$K_L = \frac{n-1}{n} \tag{2.31}$$

Table 2.1
Evaluation of M_2 for one- and two-pole Butterworth filters.

	(Signal × Signal Distortion)$^{1/2}$, M_2: $\lvert H_I(j2\pi f)\rvert^2 = \dfrac{1}{1+\left(\dfrac{f}{f_c}\right)^{2n}}$ NRZ: $S_m(f) = T_s\dfrac{\sin^2\pi fT_s}{(\pi fT_s)^2}$
$n=1$	$1-\dfrac{1}{2B_{II}/R_s}[1-\exp(-2B_{II}/R_s)]$
$n=2$	$1-\dfrac{1}{4B_{II}/R_s}\{1-\exp(-2B_{II}/R_s)[\cos(2B_{II}/R_s)-\sin(2B_{II}/R_s)]\}$
	Manchester Code: $S_m(f) = T_s\dfrac{\sin^4\pi fT_s/2}{(\pi fT_s/2)^2}$
$n=1$	$1-\dfrac{1}{2B_{II}/R_s}[3-4\exp(-B_{II}/R_s)+\exp(-2B_{II}/R_s)]$
$n=2$	$1-\dfrac{1}{4B_{II}/R_s}\{3-4\exp(-B_{II}/R_s)[\cos(B_{II}/R_s)-\sin(B_{II}/R_s)]$ $+\exp(-2B_{II}/R_s)[\cos(2B_{II}/R_s)-\sin(2B_{II}/R_s)]\}$

Table 2.2
Evaluation of M_4 for one- and two-pole Butterworth filters.

	Signal × Noise Distortion, M_4: $\lvert H_I(j2\pi f)\rvert^2 = \dfrac{1}{1+\left(\dfrac{f}{f_c}\right)^{2n}}$ NRZ
$n=1$	$1-\dfrac{3-(3+2B_{II}/R_s)\exp(-2B_{II}/R_s)}{4B_{II}/R_s}$
$n=2$	$1-\dfrac{5-\{4B_{II}/R_s\cos(2B_{II}/R_s)+5[\cos(2B_{II}/R_s)-\sin(2B_{II}/R_s)]\}\exp(-2B_{II}/R_s)}{16B_{II}/R_s}$
	Manchester Code
$n=1$	$1-\dfrac{9-4(3+B_{II}/R_s)\exp(-B_{II}/R_s)+(3+2B_{II}/R_s)\exp(-2B_{II}/R_s)}{4B_{II}/R_s}$
$n=2$	$1-\dfrac{15-\{8B_{II}/R_s\cos(B_{II}/R_s)+20[\cos(B_{II}/R_s)-\sin(B_{II}/R_s)]\}\exp(-B_{II}/R_s)}{16B_{II}/R_s}$ $-\dfrac{\{4B_{II}/R_s\cos(2B_{II}/R_s)+5[\cos(2B_{II}/R_s)-\sin(2B_{II}/R_s)]\}\exp(-2B_{II}/R_s)}{16B_{II}/R_s}$

and

$$B_H = 2f_c\left[\frac{\frac{\pi}{2n}}{\sin\left(\frac{\pi}{2n}\right)}\right] \tag{2.32}$$

where f_c is the 3 dB cutoff frequency of the equivalent low pass filter $H_l(j2\pi f)$.

- Figures 2.4 to 2.6 plot S_L (of equation (2.30)) in dB versus B_H/R_S with E_s/N_o as a parameter for $N = 2$ and the case of Manchester coded data; for one-pole, two-pole, and infinite-pole (ideal) Butterworth filters for $H_l(s)$.

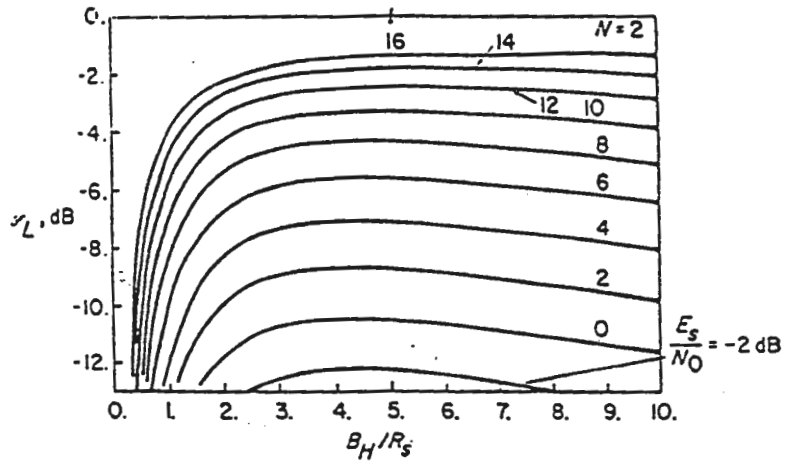

Figure 2.4. Squaring loss variations versus B_{II}/R_s for various values of E_s/N_0; one-pole Butterworth filter, Manchester coding.

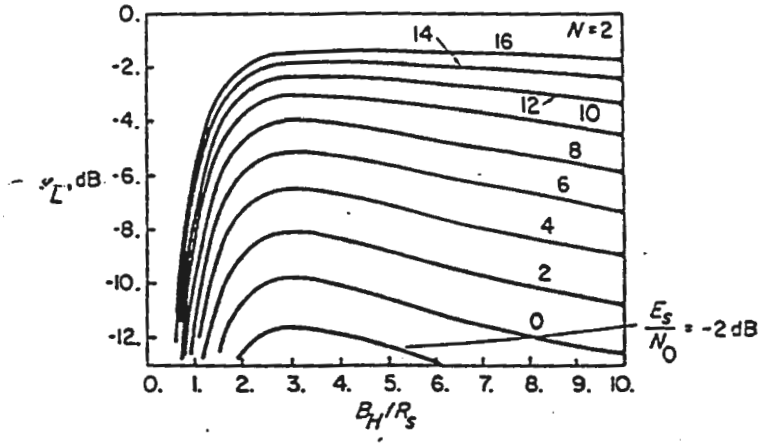

Figure 2.5. Squaring loss variations versus B_{II}/R_s for various values of E_s/N_0; two-pole Butterworth filter, Manchester coding.

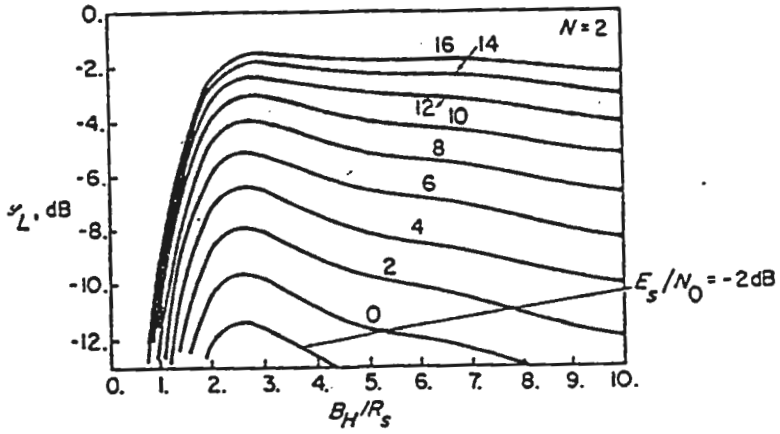

Figure 2.6. Squaring loss variations versus B_{II}/R_s for various values of E_s/N_0; ideal filter, Manchester coding.

- At each value of E_s/N_0, there is an optimum bandwidth for minimizing the loop squaring

loss.

- From (2.29) this optimization of $\mathcal{S}_L$ also minimizes the loops tracking jitter.

Note: similar optimizations of squaring loss as a function of B_H/R_s is also observed for NRZ data.

As examples, Figures 2.7 and 2.8 give $\sigma_{\epsilon_{min}}$ versus E_s/N_o with $\delta_s = \frac{1}{B_L T_s}$ (ratio of data rate to loop BW) as a parameter, for 2-pole Butterworth and ideal filters and Manchester coded data. Here we have made the substitution

$$\rho \triangleq \frac{S}{N_o B_L} = \frac{E_s}{N_o}\delta_s \tag{2.33}$$

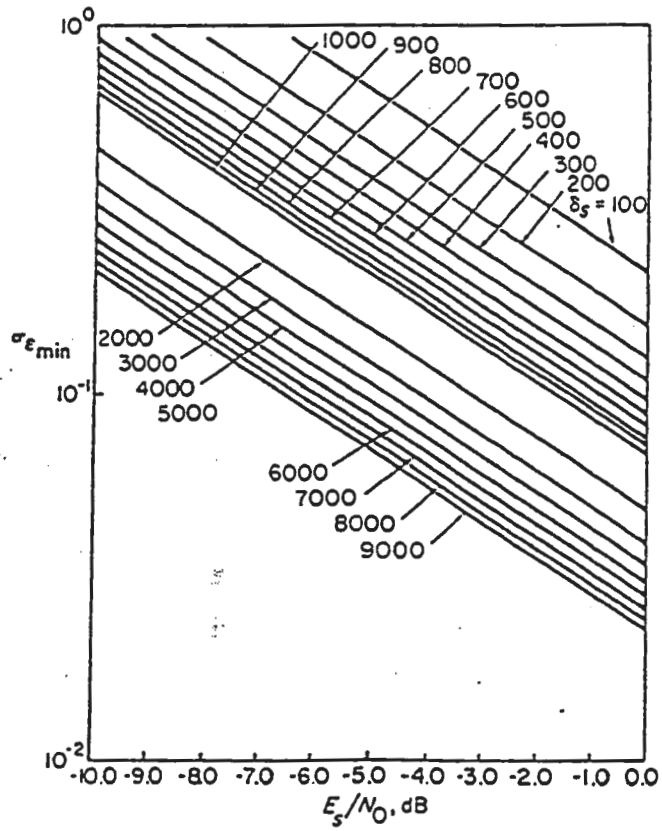

Li.. .' tracking jitter performance of non-coherent DLL; two-pole Butterworth filter.

Figure 2.7.

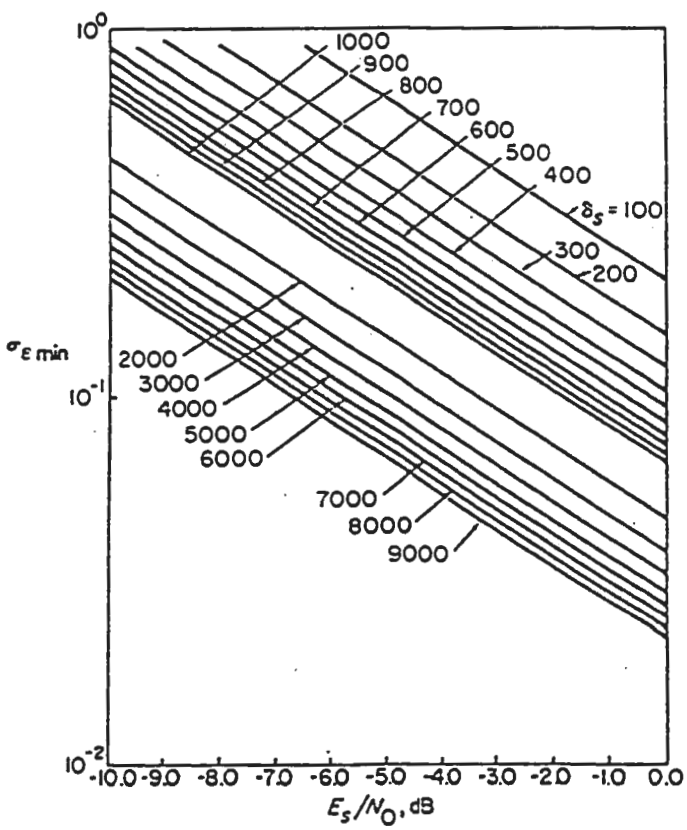

Linear tracking jitter performance of non-coherent DLL; ideal filter.

Figure 2.8.

2. The Tau-Dither Loop

- The non-coherent tau dither loop is shown in Figure 2.9.

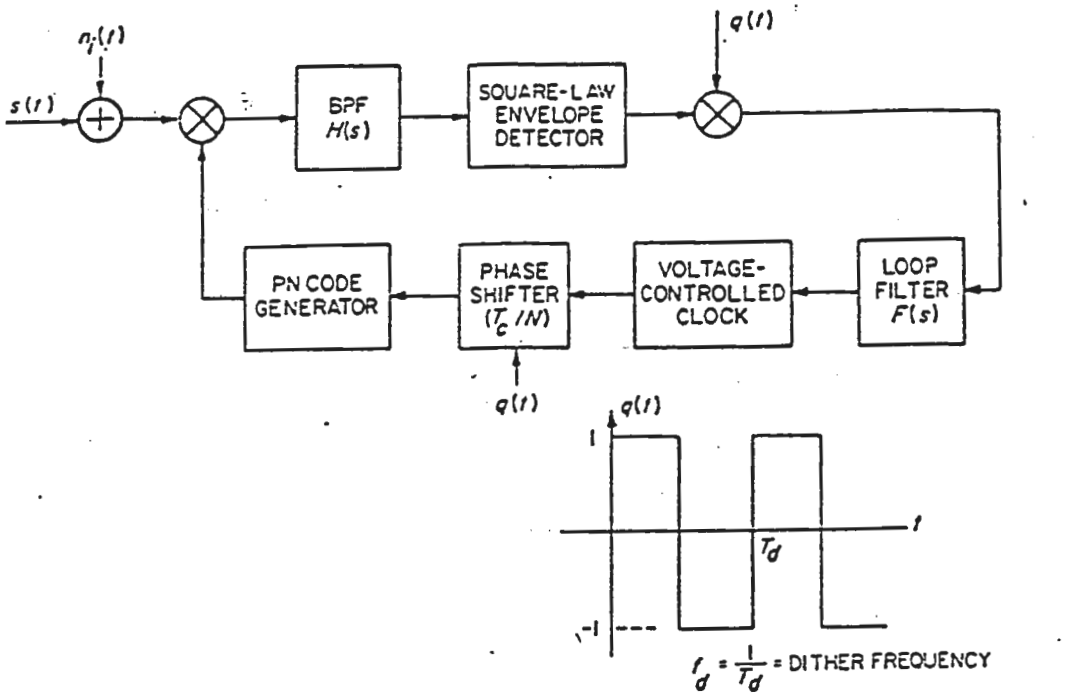

Figure 2.9. A non-coherent tau-dither loop.

- Here the received signal plus noise is alternately (as opposed to simultaneously) correlated with the advanced and retarded versions of the locally generated PN code to produce an error signal.

- This signal when bandpass filtered, envelope detected, and alternately inverted by the binary signal $q(t)$, drives the voltage controlled clock (vcc) through the loop filter $F(s)$.

- Advantage of TDL over the DLL is that only a single input correlator is required, eliminating problems of gain imbalance and other mismatches that are present in a two channel loop like the DLL.

Mathematical Loop Model and Equation of Operation

- We shall draw on the notation and results already obtained for the DLL.

- One can show that when the dither frequency f_d is low relative to the noise bandwidth B_H of the BPF, the TDL has the equivalent loop model shown in Figure 2.10.

- Starting then with $y_+(t)$ and $y_-(t)$ (as defined in Equation (2.5), the input to the loop

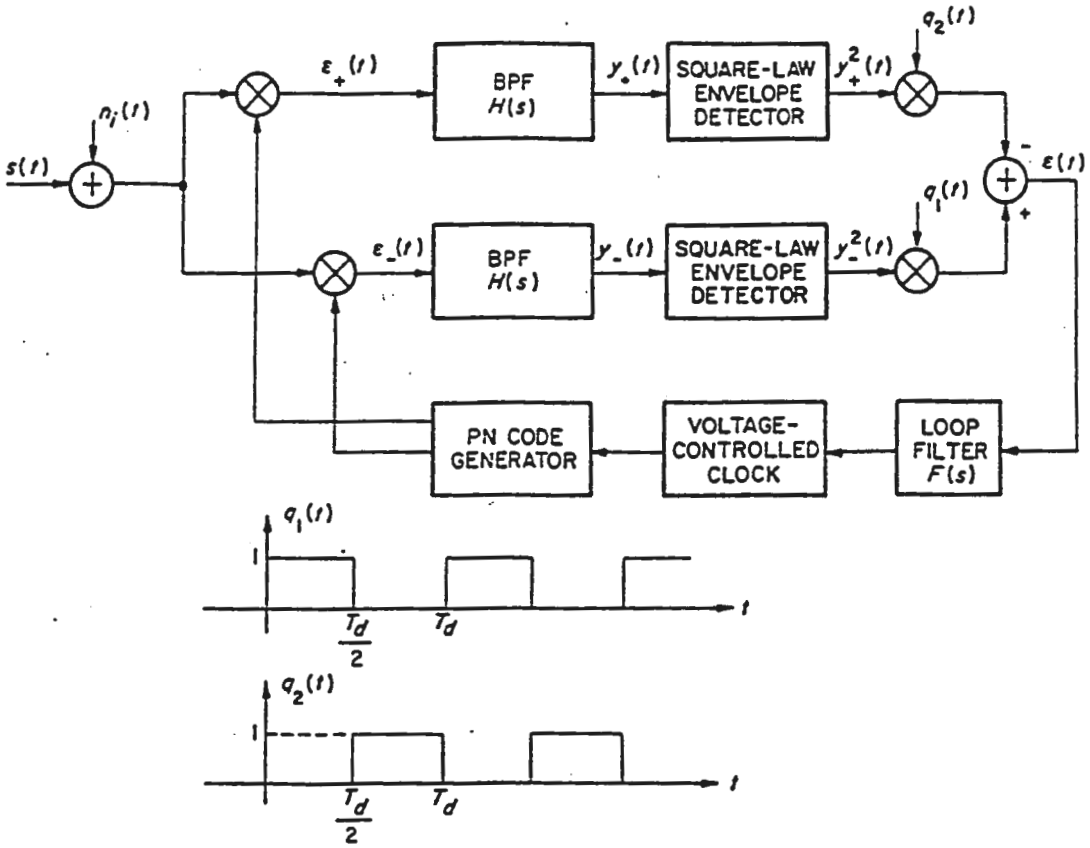

Figure 2.10. An equivalent loop model for the tau-dither loop.

filter is

$$\begin{aligned} e(t) &\triangleq y_-^2(t)q_1(t) - y_+^2(t)q_2(t) \\ &= SK_m^2\hat{m}^2(t-\tau_t)\left[q_1(t)R_{PN_-}^2(\epsilon_t) - q_2(t)R_{PN_+}^2(\epsilon_t)\right] \\ &\quad + K_m^2 n_e'(t,\epsilon_t) \end{aligned} \tag{2.34}$$

In the above expression

$$\begin{aligned} n_e'(t,\epsilon_t) &= q_1(t)\left[\hat{N}_{c_-}^2(t) + \hat{N}_{s_-}^2(t)\right] - q_2(t)\left[\hat{N}_{c_+}^2(t) + \hat{N}_{s_+}^2(t)\right] \\ &\quad + 2\sqrt{S}\hat{m}(t-\tau_t)\Big\{q_1(t)R_{PN_-}(\epsilon_t)\hat{N}_{c_-}(t) \\ &\quad - q_2(t)R_{PN_+}(\epsilon_t)\hat{N}_{c_+}(t)\Big\} \end{aligned} \tag{2.35}$$

Recognizing that

$$q_1(t) - q_2(t) = q(t)$$

and

$$q_1(t) + q_2(t) = 1$$

equation (2.34) simplifies to

$$e(t) = SK_m^2\hat{m}^2(t-\tau_t)D'(t,\epsilon_t) + K_m^2 n_e'(t,\epsilon_t) \tag{2.36}$$

where

$$D'(t,\epsilon_t) \triangleq q_1(t)R^2_{PN_-}(\epsilon_t) - q_2(t)R^2_{PN_+}(\epsilon_t)$$

$$= \begin{cases} 0 & ;\ \epsilon_t \le -1-\frac{1}{N} \\ -q_2(t)\left[1+\frac{1}{N}+\epsilon_t\right]^2 & ;\ -1-\frac{1}{N} < \epsilon_t \le -1+\frac{1}{N} \\ q(t)\left[(1+\epsilon_t)^2+\left(\frac{1}{N}\right)^2\right]-\frac{2}{N}(1+\epsilon_t) & ;\ -1+\frac{1}{N} < \epsilon_t < -\frac{1}{N} \\ q(t)\left[\left(1-\frac{1}{N}\right)^2+\epsilon_t^2\right]+2\left(1-\frac{1}{N}\right)\epsilon_t & ;\ |\epsilon_t| \le \frac{1}{N} \\ q(t)\left[(1-\epsilon_t)^2+\left(\frac{1}{N}\right)^2\right]+\frac{2}{N}(1-\epsilon_t) & ;\ \frac{1}{N} < \epsilon_t < 1-\frac{1}{N} \\ q_1(t)\left[1+\frac{1}{N}-\epsilon_t\right]^2 & ;\ 1-\frac{1}{N} < \epsilon_t \le 1+\frac{1}{N} \\ 0 & ;\ \epsilon_t > 1+\frac{1}{N} \end{cases} \tag{2.37}$$

$$D'(t,\epsilon_t) = D'(t,\epsilon_t+np) \quad ; \quad n = \pm 1,\ \pm 2,\ \pm 3\cdots \tag{2.38}$$

As in the DLL, since the loop BW is narrow with respect to data rate, and here also with respect to the dither frequency $f_d = \frac{1}{T_d}$, we can replace $\hat{m}^2(t-\tau_t)D'(t,\epsilon_t)$ with

$$< \overline{\hat{m}^2(t-\tau_t)}D'(t,\epsilon_t) > = < \overline{\hat{m}^2(t-\tau_t)} > < D'(t,\epsilon_t) > \tag{2.39}$$

Since $< q(t) >= 0$ and $< q_1(t) >=< q_2(t) >= 1/2$, we get

$$D'(\epsilon_t) \triangleq < D'(t,\epsilon_t) > = \begin{cases} 0 & ;\ \epsilon_t \le -1-\frac{1}{N} \\ -\frac{1}{2}(1+\frac{1}{N}+\epsilon_t)^2 & ;\ -1-\frac{1}{N} < \epsilon_t \le -1+\frac{1}{N} \\ -\frac{2}{N}(1+\epsilon_t) & ;\ -1+\frac{1}{N} < \epsilon_t < -\frac{1}{N} \\ 2\epsilon_t(1-\frac{1}{N}) & ;\ |\epsilon_t| \le \frac{1}{N} \\ \frac{2}{N}(1-\epsilon_t) & ;\ \frac{1}{N} < \epsilon_t < 1-\frac{1}{N} \\ \frac{1}{2}(1+\frac{1}{N}-\epsilon_t)^2 & ;\ 1-\frac{1}{N} < \epsilon_t \le 1+\frac{1}{N} \\ 0 & ;\ \epsilon_t > 1+\frac{1}{N} \end{cases} \tag{2.40}$$

Hence, (2.36) simplifies to

$$e(t) = SK_m^2 M_2 D'(\epsilon_t) + K_m^2 n_e'(t,\epsilon_t) \tag{2.41}$$

where M_2 is defined in (2.14).

Comparing $D'(\epsilon_t)$ of (2.40) with $D(\epsilon_t)$ of (2.8), we see that the TDL suffers an effective reduction in signal power of 3 dB relative to DLL.

Using (2.10) and the assumptions leading to (2.15), we get the stochastic differential equation which characterizes the TDL as

$$\dot{\epsilon}_t = \frac{\dot{\tau}_t}{T_c} - \frac{1}{2} KF(t) * M_2 \left[D_n(\epsilon_t) + \frac{n_e'(t,\ \epsilon_t)}{\frac{1}{2}\eta S M_2} \right] \tag{2.42}$$

where $D_n(\epsilon_t) \triangleq \frac{2}{\eta} D'(\epsilon_t)$ is identical to the normalized discriminator characteristic of the DLL.

Statistical Characterization of the Equivalent Additive Noise

We must find the power spectral density $N_e'(\epsilon_t)$ of the delta correlated process $n_e'(t, \epsilon_t)$, that is

$$N_e'(\epsilon_t) = 2 \int_{-\infty}^{\infty} R_e'(\tau, \epsilon_t) d\tau \tag{2.43}$$

where

$$R_e'(\tau, \epsilon_t) \triangleq \overline{n_e'(t, \epsilon_t)\ n_e'(t+\tau, \epsilon_t)} \tag{2.44}$$

Denoting the autocorrelation and cross-correlation functions of the switching waveforms by

$$\begin{aligned} R_{q_1}(\tau) &\triangleq < q_1(t) q_1(t+\tau) > \\ R_{q_2}(\tau) &\triangleq < q_2(t) q_2(t+\tau) > \\ R_{q_1 q_2}(\tau) &\triangleq < q_1(t) q_2(t+\tau) > \end{aligned} \tag{2.45}$$

we find that

$$R_{q_1}(\tau) = R_{q_2}(\tau) = \frac{1}{2} - R_{q_1 q_2}(\tau) \triangleq R_q(\tau) \tag{2.46}$$

Here $R_q(\tau)$ is shown in Figure 2.11.

- Sub (2.35) into (2.44) and using (2.46) we find "after considerable algebraic manipulations"

$$R_e'(\tau, \epsilon_t) = 8R_{\hat{N}}^2(\tau) R_q(\tau) + 8R_{\hat{N}}^2(0) \left[2R_q(\tau) - \frac{1}{2} \right] + 4SR_{\hat{m}} R_{\hat{N}}(\tau) R_q(\tau) f(\epsilon_t) \tag{2.47}$$

where $R_{\hat{N}}(\tau)$, $R_{\hat{m}}(\tau)$ and $f(\epsilon_t)$ are defined in (2.19).

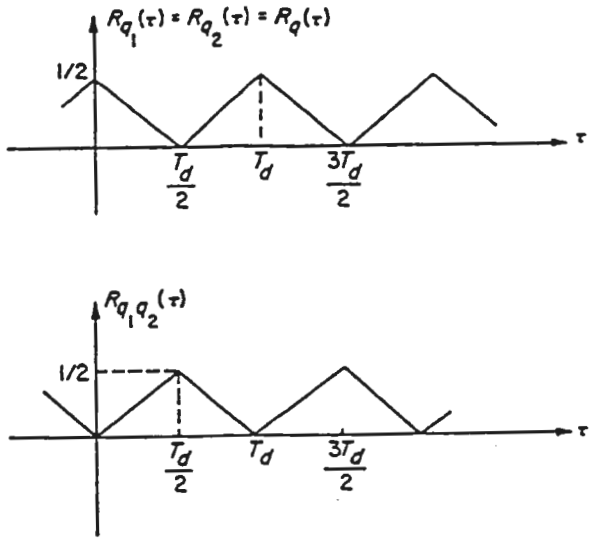

Figure 2.11. Autocorrelation functions of $q_1(t)$ and $q_2(t)$ and cross-correlation function of $q_1(t)$ and $q_2(t)$.

- Integration of (2.47), as required in (2.43), can alternatively be accomplished in the frequency domain

$$\begin{aligned} N_e'(\epsilon_t) = 16 \int_{-\infty}^{\infty} \left[S_{\hat{N}}(f) * S_{\hat{N}}(f)\right] S_q(-f) df \\ + 8Sf(\epsilon_t) \int_{-\infty}^{\infty} \left[S_{\hat{m}}(f) * S_{\hat{N}}(f)\right] S_q(-f) df \end{aligned} \tag{2.48}$$

- In the above we have

$$\begin{aligned} S_{\hat{N}}(f) &= \mathcal{FT}\left\{R_{\hat{N}}(\tau)\right\} = \frac{N_o}{2}\left|H_l(j2\pi f)\right|^2 \\ S_{\hat{m}}(f) &= \mathcal{FT}\left\{R_{\hat{m}}(\tau)\right\} = S_m\left|H_l(j2\pi f)\right|^2 \\ S_q(f) &= \mathcal{FT}\left\{R_q(\tau)\right\} = \frac{1}{4}\delta(f) + \frac{1}{4}\sum_{\substack{n=-\infty \\ n \text{ odd}}}^{\infty} \left(\frac{2}{n\pi}\right)^2 \delta\left(f - \frac{n}{T_d}\right) \end{aligned} \tag{2.49}$$

Sub (2.49) into (2.48) and "after much simplification" we obtain an expression analogous to (2.22) (for DLL):

$$N_e'(\epsilon_t) = \frac{SN_o}{2}\left[2M_4' f(\epsilon_t) + 2\frac{K_L'}{\rho_H}\right] \tag{2.50}$$

where

$$M_4' = M_4 + 2\sum_{n=1,3,5\cdots}^{\infty} \left(\frac{2}{n\pi}\right)^2 M_{4_n}$$

$$K_L' = K_L + 2\sum_{n=1,3,5\cdots}^{\infty} \left(\frac{2}{n\pi}\right)^2 K_{L_n}$$

with

$$M_{4_n} \triangleq \int_{-\infty}^{\infty} S_m(f)\,|H_l(j2\pi f)|^2 \left|H_l\left[j2\pi\left(\frac{n}{T_d}-f\right)\right]\right|^2 df$$

$$K_{L_n} \triangleq \frac{\int_{-\infty}^{\infty} |H_l(j2\pi f)|^2 \left|H_l\left[j2\pi\left(\frac{n}{T_d}-f\right)\right]\right|^2 df}{\int_{-\infty}^{\infty} |H_l(j2\pi f)|^2\, df} \tag{2.51}$$

and K_L and M_4 are defined in (2.23),

ρ_H is defined in (2.25).

Linear Analysis of TDL Tracking Performance

- As for the DLL, we can write down by inspection of (2.42) an expression for the mean squared tracking jitter for the case $\dot{\tau}_t = 0$

$$\sigma_\epsilon'^2 = \frac{\overline{N_e'(\epsilon_t)}B_L}{\left(\frac{1}{2}\eta S M_2\right)^2} \tag{2.52}$$

- Using (2.50) and (2.19), equation (2.52) gives

$$\sigma_\epsilon'^2 = \frac{1}{2\rho}\left\{\frac{M_4' + \frac{8K_L'}{\rho_H\eta^2}}{M_2^2\left[1-\frac{8}{\eta^2\rho}\left(\frac{M_4'}{M_2^2}\right)\right]}\right\} \tag{2.53}$$

- to a first approximation

$$\sigma_\epsilon'^2 = \frac{1}{2\rho}\left\{\frac{M_4' + \frac{8K_L'}{\rho_H\eta^2}}{M_2^2}\right\} = \frac{1}{2\rho\mathcal{S}_L'} \tag{2.54}$$

- Here, $\mathcal{S}_L'$ is the squaring loss of the TDL and is given by (2.30) with M_4 and K_L replaced with M_4' and K_L'.

- A comparison of the linear tracking jitter performances of the DLL and TDL depends only on the ratio of $\mathcal{S}_L'$ to $\mathcal{S}_L$.

$$\frac{\mathcal{S}_L'}{\mathcal{S}_L} = \frac{M_4 + \frac{8K_L}{\rho_H\eta^2}}{M_4' + \frac{8K_L'}{\rho_H\eta^2}} \tag{2.55}$$

- From the definitions of M_{4_n} and K_{L_n} (given by (2.51)), we see that $M_{4_n} < M_4$ and $K_{L_n} < K_L$ for any n (in particular n odd) and T_d finite.

- Hence, from (2.51)

$$M_4' < M_4 + \frac{8}{\pi^2}\sum_{n=1,3,5\cdots}^{\infty}\frac{1}{n^2}M_4 = 2M_4$$

$$K_L' < K_L + \frac{8}{\pi^2}\sum_{n=1,3,5\cdots}^{\infty}\frac{1}{n^2}K_L = 2K_L \tag{2.56}$$

- Substitute the bounds of (2.56) into (2.55) to get

$$\frac{S_L'}{S_L} > \frac{1}{2} \tag{2.57}$$

- Hence, the linear theory mean-squared timing error for the TDL is less than 3 dB worse than that of the DLL.

- The integrals in (2.51) are difficult to evaluate. However, where $H_l(s)$ is an ideal filter, some simplifications are possible.

- In particular

$$K_{L_n} = \frac{\int_{-B_H/2+n/T_d}^{B_H/2} df}{\int_{-B_H/2}^{B_H/2} df} = \begin{cases} 1 - \dfrac{n}{B_H T_d} & ; n \le \lfloor B_H T_d \rfloor \triangleq n_o \\ 0 & ; n > n_o \end{cases} \tag{2.58}$$

Here $\lfloor x \rfloor$ denotes the largest integer less than or equal to x.

- Thus from (2.51)

$$K_L' = 1 + \frac{8}{\pi^2} \sum_{n=1,3,5\ldots}^{n_o} \frac{1}{n^2} - \frac{8}{\pi^2 B_H T_d} \times \sum_{n=1,3,5\ldots}^{n_o} \frac{1}{n} \tag{2.59}$$

- Figure 2.12 plots K_L' vis $B_H T_d$

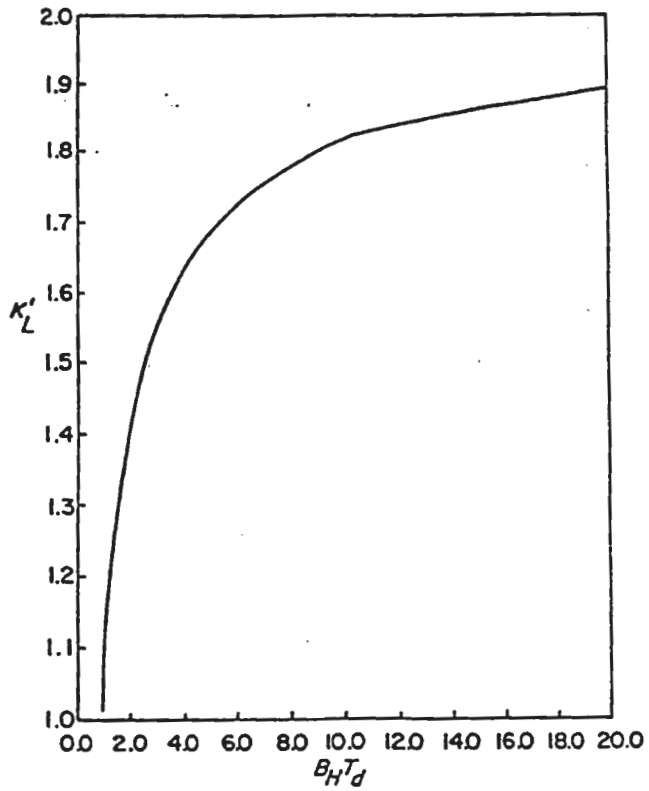

Figure 2.12. A plot of K_L' versus $B_H T_d$; ideal filter.

- Similarly, for case of Manchester coded data of rate $R_S = 1/T_s$

$$M_{4_n} = \int_{-\frac{B_H}{2}+\frac{n}{T_d}}^{\frac{B_H}{2}} \frac{\sin^4\left(\frac{\pi f T_s}{2}\right)}{\left(\frac{\pi f T_s}{2}\right)^2} df = \int_{-\frac{B_H T_s}{4}}^{\frac{B_H T_s}{4}} \frac{\sin^4 \pi x}{(\pi x)^2} dx - \int_{-\frac{B_H T_s}{4}}^{-\frac{B_H T_s}{4}+\frac{nT_s}{2T_d}} \frac{\sin^4 \pi x}{(\pi x)^2} dx \qquad (2.60)$$

and

$$M_4' = \left[1 + \frac{8}{\pi^2} \sum_{n=1,3,5\ldots}^{n_o} \frac{1}{n^2}\right] \int_{-\frac{B_H T_s}{4}}^{\frac{B_H T_s}{4}} \frac{\sin^4 \pi x}{(\pi x)^2} dx - \frac{8}{\pi^2} \sum_{n=1,3,5\ldots}^{n_o} \frac{1}{n^2} \int_{\frac{B_H T_s}{4}\left[1-\frac{2n}{B_H T_d}\right]}^{-\frac{B_H T_s}{4}} \frac{\sin^4 \pi x}{(\pi x)^2} dx \qquad (2.61)$$

- The first integral in (2.61) is really $M_2 = M_4$.

- Figure 2.13 plots M_4' (normalized by M_2) vs $B_H T_d$ for various ratios of filter bandwidth to data rate B_H/R_S.

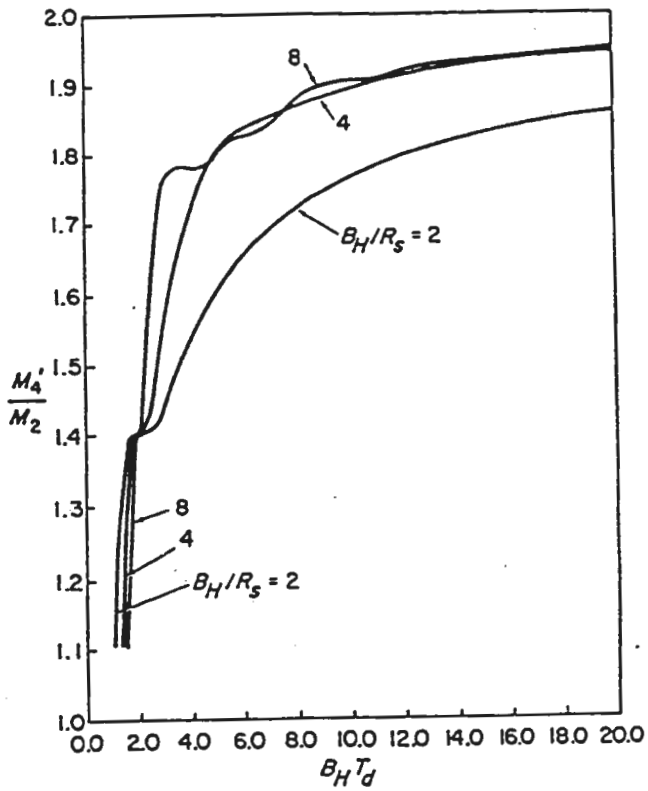

Figure 2.13. Plots of M_4'/M_2 versus $B_H T_d$ with B_H/R_s as a parameter; ideal filter, Manchester coding.

- It is reasonable to expect that a plot of S_L' versus B_H/R_s with E_s/N_o as a parameter, would give an optimum filter bandwidth (in the sense of minimizing the loop squaring loss) for each value of E_s/N_o.

- Figure 2.14 illustrates this for the case of an ideal filter with S_L' determined from (2.54) (together with (2.14), (2.59) and (2.61).

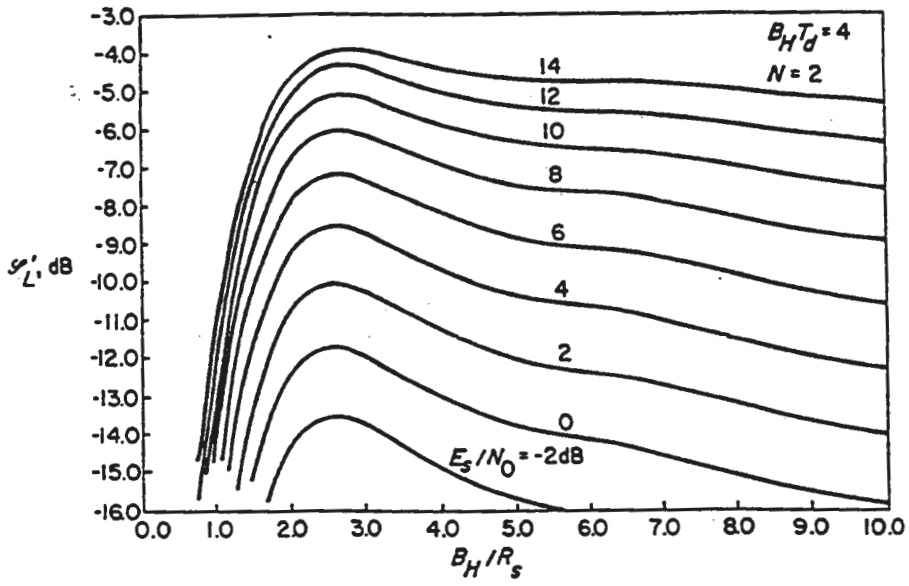

Figure 2.14. Squaring loss variations versus B_H/R_s for various values of E_s/N_0; ideal filter, Manchester coding.

- The corresponding minimum tracking jitter performance (described by (2.54)) is shown in Figure 2.15.

- In both figures, B_HT_d was chosen as 4.

- Comparing Figure 2.15 with Figure 2.8, we see that over the entire range of parameter variations chosen, the TDL is about 1.06 dB poorer than the DLL.

- As B_HT_d increases (normally by lowering the dither frequency relative to the arm filter BW), the performance penalty increases, approaching 1.5 dB as B_HT_d approaches infinity.

- It is interesting to see how the optimized performance results presented here compare with early results of Gill [3] and Hartmann [6].

- Both these authors neglected band limiting effects of the arm filters.

- Hence, if one sets $K_L = M_2 = M_4 = 1$ in (2.29), and substitutes $\frac{E_s/N_o}{B_H/R_s}$ for ρ_H, one arrives at Gills' result for normalized mean squared tracking error of DLL

$$\sigma_\epsilon^2 = \frac{1}{2\rho}\left[1 + \frac{2B_H/R_s}{E_s/N_o}\right] \tag{2.62}$$

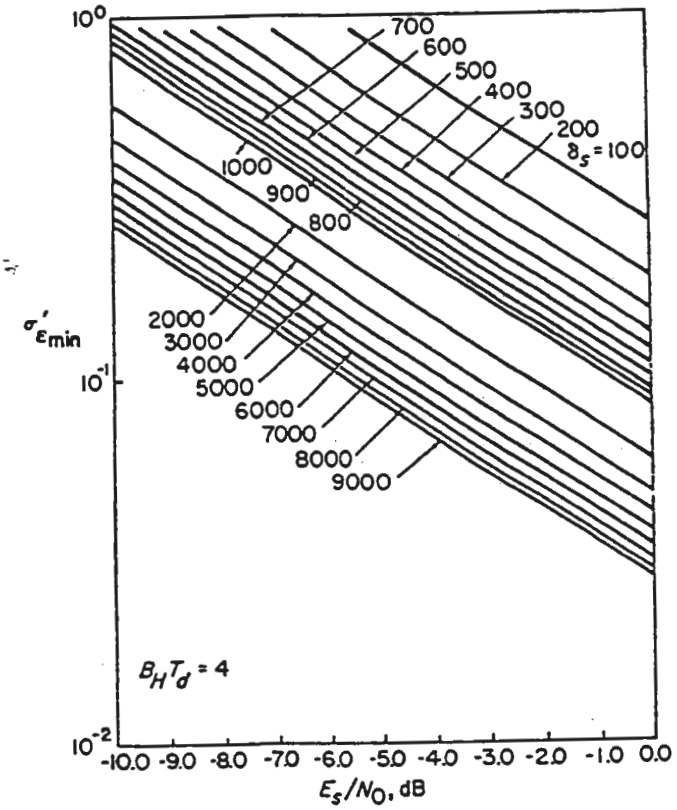

Figure 2.15. Linear tracking jitter performance of non-coherent TDL; ideal filter.

- Hartmann's analysis for the TDL gave the normalized mean squared tracking error as

$$\sigma'^2_\epsilon = \frac{1}{\rho}\left[0.905 + \frac{4B_H/R_s}{E_s/N_o}\left(0.453 - \frac{0.2}{B_H T_d}\right)\right] \tag{2.63}$$

which for $B_H T_d = 4$ becomes

$$\sigma'^2_\epsilon = \frac{1}{\rho}\left[0.905 + \frac{1.612 B_H/R_s}{E_s/N_o}\right] \tag{2.64}$$

- Comparisons of (2.62) and (2.64) with Figures 2.8 and 2.15 reveal that both Gill's and Hartmann's results are optimistic by about 0.9 dB.

- Note: if arm filter bandlimiting effects are totally ignored for the TDL, then again $K_L = M_2 = M_4 = 1$ and M'_4 and K'_L would achieve their upper bounds (as in (2.56)). Then (2.54) would simplify (for $N = 2$) to

$$\sigma'^2_\epsilon = \frac{1}{\rho}\left[1 + \frac{2B_H/R_s}{E_s/N_o}\right] \tag{2.65}$$

- Comparing (2.65) with (2.62), we observe the often stated (incorrect) result that the TDL suffers a 3 dB degradation in SNR performance relative to the DLL.

- Note: increasing the N (decreasing the advance/retard interval) decreases the mean squared tracking jitter for both DLL and TDL. This is observed from (2.29) and (2.54) together with (2.16).

- However, increasing N also decreases the linear tracking region of the discriminator characteristic (Figure 2.3) and thus increases the loop's tendency to lose lock.

- Thus, tradeoff between decreasing mean squared tracking jitter at the expense of increased sensitivity to loss of lock is characteristic of all early-late gate type of loops.

3. Acquisition (Transient) Behavior of the DLL and TDL

- Here we treat transient response of DLL and TDL with emphasis on acquisition behavior in presence of initial code rate offset of incoming PN code relative to that of clock that generates the stored reference PN code in Rx.

- There are two questions of interest:

1. What is max relative code rate offset (due to code Doppler, clock drift, etc.) between received and locally generated PN codes so that received signal can still be acquired? Also (equivalently), what is max search rate (velocity) to achieve acquisition?
2. How long do the transients last (how long to acquire)?

- The first question is answered by obtaining (in a noise free environment) the phase plane trajectories.

- Here we plot normalized code delay error rate $\dot{\epsilon}_t$ versus normalized code delay error ϵ_t, with normalized time as parameter along the curve.

- We first rewrite the system equation (2.15) in normalized form

$$\frac{d}{d\tau}(y-x) = GF(\tau) * D_n(x) \tag{2.66}$$

where

$$\begin{aligned} \tau &\triangleq \omega_n t \\ \frac{d}{d\tau} &= \frac{1}{\omega_n}\frac{d}{dt} \\ x &\triangleq \epsilon_t \\ y &\triangleq \tau_t/T_c \\ G &\triangleq \frac{\eta S K M_2}{\omega_n} \end{aligned} \tag{2.67}$$

Here, ω_n is the radian natural frequency of the loop.

- For a 2nd order loop with a linear closed loop transfer function $H(s)$,

$$H(s) = \frac{1 + 2\zeta s/\omega_n}{1 + \left(\frac{1}{G} + 2\zeta\right)\left(\frac{s}{\omega_n}\right) + \left(\frac{s}{\omega_n}\right)^2} = \frac{\omega_n GF(s)}{s + \omega_n GF(s)} \tag{2.68}$$

the product of the loop gain G and the filter transfer function $F(s)$ becomes

$$GF(s) = \frac{1 + 2\zeta s/\omega_n}{1/G + s/\omega_n} \tag{2.69}$$

- For a critically damped loop $\left(\zeta = \frac{1}{\sqrt{2}}\right)$, (2.69) simplifies

$$GF(s) = \frac{1 + \sqrt{2}s/\omega_n}{1/G + s/\omega_n} \tag{2.71}$$

- Sub (2.71) into (2.66) gives

$$\dot{y}/G + \ddot{y} = \dot{x}/G + \ddot{x} + D_n(x) + \sqrt{2}D_n'(x)\dot{x} \tag{2.72}$$

- Here the dot represents derivative with respect to normalized time τ. Also, the prime represents derivative with respect to normalized code delay error, x.

- The solution of the 2nd order partial differential equation in (2.66) for the phase plane trajectories is helped by defining

$$\gamma \triangleq \frac{\ddot{x}}{\dot{x}} = \frac{d\dot{x}}{dx}$$

- hence

$$\gamma = -\left\{\frac{D_n(x) + [\sqrt{2}D_n'(x) + 1/G]\dot{x} - \dot{y}/G - \ddot{y}}{\dot{x}}\right\} \tag{2.73}$$

for a constant search velocity, $\ddot{y} = 0$

$$\gamma = -\left\{\frac{D_n(x) + [\sqrt{2}D_n'(x) + 1/G]\dot{x} - \dot{y}/G}{\dot{x}}\right\} \tag{2.74}$$

- Statistical methods of solving differential equations can be applied to (2.74) to compute the trajectories in the $(\dot{x}, x)$ plane for given initial conditions (Newton's method).

- One then looks for the max $\dot{y}$ for which the phase plane trajectories will eventually reach the (0, 0) point (the phase and frequency lock condition for the DLL).

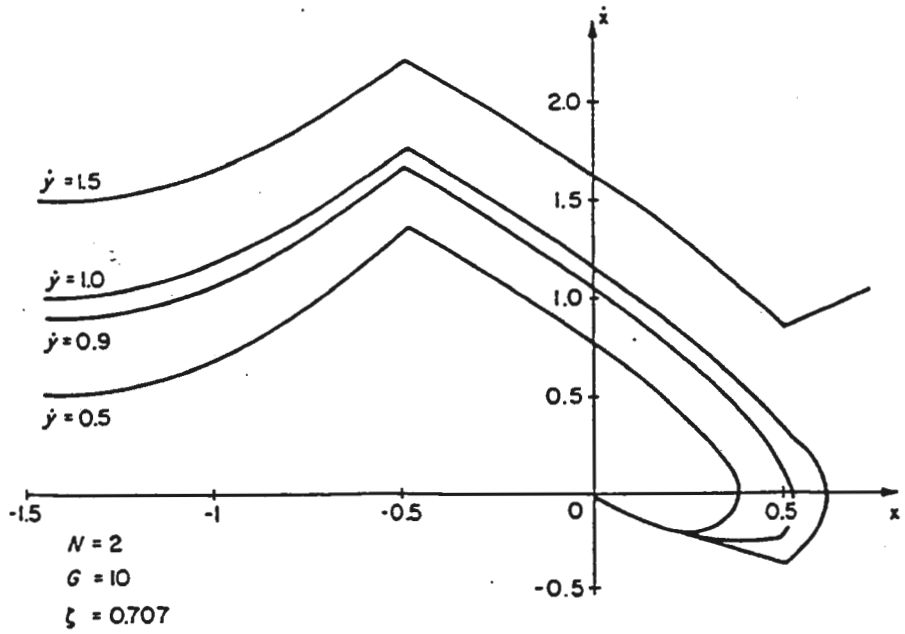

Figure 2.16. Acquisition trajectories for $N = 2$ (reprinted from [14]).

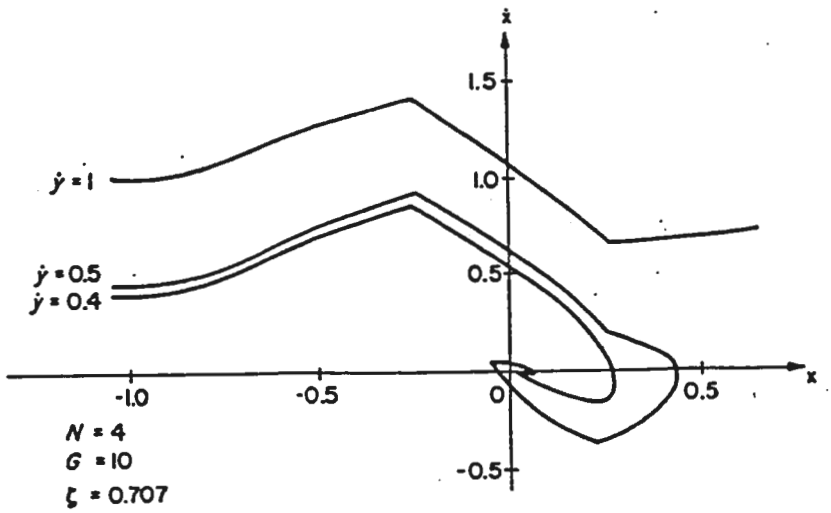

Figure 2.17. Acquisition trajectories for $N = 4$ (reprinted from [14]).

- Acquisition trajectories for $G = 10, \zeta = 1/\sqrt{2}, N = 2$ and $N = 4$ are given in Figures 2.16 and 2.17.

- It is found that max normalized search rate for $N = 2$ is $\dot{y} = 1.0$. Also for $N = 4$, max normalized search rate is $\dot{y} = 0.5$.

- Also, the open loop gain has little effect on trajectories for $G > 10$.

- Second question above is dealt with by using definition of γ as a starting point and computing acquisition transients as function of time, and then finding the acquisition

time.

- Figure 2.18 shows transient response of DLL for $G = 100$, $\zeta = 1/\sqrt{2}$, $N = 2$ and $N = 4$.

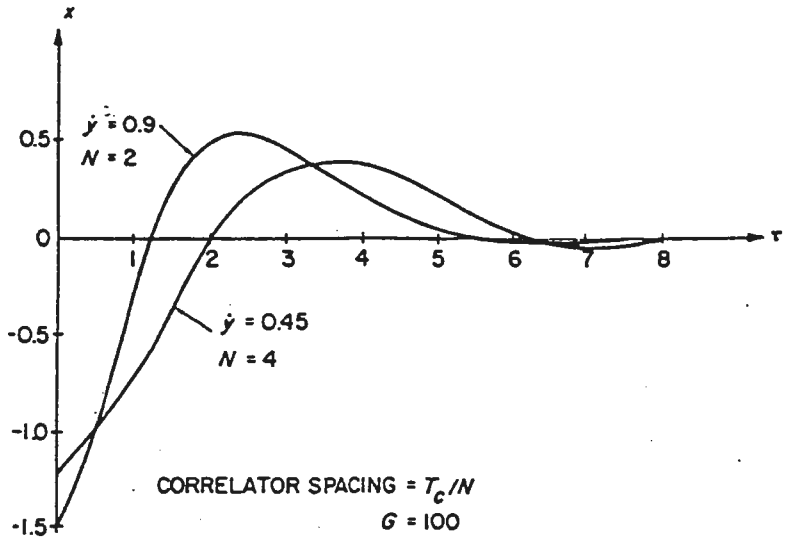

Figure 2.18. Transient response of delay lock loop (reprinted from [14]).

Table 2.3
Acquisition time (sec).

B_L (Hz)	100	200	300	400	
$N = 2$	0.0244	0.0122	0.0081	0.0061	$\dot{y} = 0.9$
$N = 4$	0.0292	0.0146	0.0097	0.0073	$\dot{y} = 0.45$

- The search rate is chosen to be $\dot{y} = 0.9$ for first case and $\dot{y} = 0.45$ for second case.

- The graphs show acquisition time (time for the transient to subside within $|x| = 0.1$) is shorter for $N = 2$ than for $N = 4$.

- The actual acquisition time is computed from the definition of normalized time (equation (2.67) and relation between single sided loop bandwidth B_L and the loop radian natural frequency ω_n.

- Now

$$\omega_n = \left(\frac{8\zeta}{4\zeta^2 + 1}\right) B_L \tag{2.75}$$

- then for critically damped loops

$$\omega_n = \frac{B_L}{.5303}$$

and

$$t_{ACQ} = \frac{.5303\ \tau_{ACQ}}{B_L} \tag{2.76}$$

- Table 2.3 gives results for different values of loop bandwidth.

- The actual max search velocity in chips/second (interpreted as the max allowable drift in the code) can be found from defn of normalized search velocity $\dot{y}$.

- As a function of B_L, the search velocity (v_s) is

$$v_s = \left(\frac{8\zeta}{4\zeta^2+1}\right)\dot{y}B_L \qquad \text{chips/sec} \tag{2.77}$$

- for critically damped loops

$$v_s = 1.8857\,\dot{y}B_L \qquad \text{chips/sec} \tag{2.78}$$

- Note: the above has focussed on DLL. However, a comparison of (2.15) and (2.42) shows that, except for a factor of two in the equivalent gain G, the TDL and DLL have identical acquisition performance.

Mean Time to Loss of Lock for DLL and TDL

- Ability of code tracking loop to maintain lock is important.

- The most informative measure of this is the probability of remaining in lock for a given interval of time.

- Unfortunately, evaluation of this is difficult.

- An alternative measure is the mean time to lose lock.

- For a carrier tracking loop, this measure is well defined. However, for a PN code tracking loop its definition loop requires clarification.

- We will define out of lock to occur when loop error signal goes beyond its uncorrelated value (a delay error exceeds range of the discriminator characteristic around the lock point, $\pm T_c(N+1)/N$.

- Mean time to loss of lock is a special case of general problem of finding nth moment of the first passage time of the error process in a synchronous control system (SCS).

- Solutions to problems of this type are obtained by assuming noise process driving the system is wideband compared to system BW.

- Then the error process can be assumed to be Markovian and its probability density function is a solution to the Fokker-Plank equation.

- By applying the appropriate boundary conditions to the time dependent solution of the one dimensional Fokker-Plank equation, the first moment of the first passage time (mean time to lose lock) of the error process $x(t)$ in a first order SCS with symmetrical boundaries $\pm b$ and symmetrical restoring force $h(x)$ [i.e., $h(x) = h(-x)$] is

$$\overline{T} = \frac{1}{K_2} \int_o^b \int_o^b \exp[u(y) - u(x)]\, dx\, dy \tag{2.79}$$

where $u(x)$ is the symmetrical potential function which is related to the restoring force by

$$u(x) \triangleq -\int^x h(y)\, dy \tag{2.80}$$

- Also, K_2 is 2nd order intensity coefficient in the Fokker-Planck equation.

- For DLL, error process x is the normalized delay error, ϵ_t, and $h(t)$ is linearly related to normalized discriminator characteristic

$$h(x) = -\rho_L D_n(x) \quad ; \quad \rho_L \triangleq 2\rho \mathcal{S}_L = \sigma_L^{-2} \tag{2.81}$$

Thus,

$$u(x) = \rho_L \int^x D_n(y) dy \triangleq \rho_L \mathcal{D}_n(x) \tag{2.82}$$

Also

$$b = \frac{N+1}{N}$$

and K_2 evaluates to

$$K_2 = \frac{2\eta^2 B_L}{\rho_L} \tag{2.83}$$

- Sub (2.82) and (2.83) into (2.79) to get mean time to loss of lock of DLL

$$B_L \overline{T} = \frac{\rho_L}{2\eta^2} \int_o^{\frac{N+1}{N}} \int_o^{\frac{N+1}{N}} \exp\{\rho_L [\mathcal{D}(y) - \mathcal{D}(x)]\}\, dy dx \tag{2.84}$$

- Comparing (2.15) with (2.42), we see that (2.84) also applies to a first order TDL if ρ_L is replaced by

$$\rho_L' \triangleq 2\rho \mathcal{S}_L' \tag{2.85}$$

- Figure 2.19 give $B_L \overline{T}$ versus $\sigma_L = 1/\sqrt{\rho_L}$ for $N = 2, 4, 8$.

- The mean time to lose lock decreases with increasing N.

5. The Double Dither Loop (DDL)

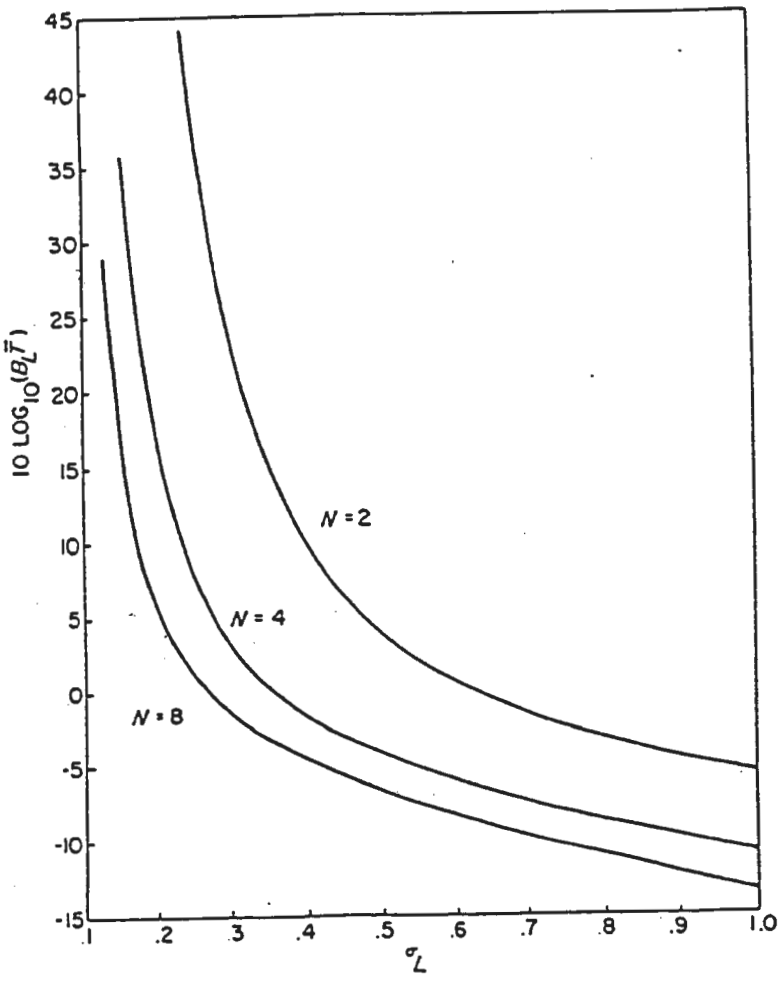

Figure 2.19. Mean time to loss-of-lock performance of delay-locked loop.

- The DDL combines the desirable features of DLL and TDL (i.e. the effect of detector imbalance is eliminated at no significant cost in noise performance).

- First redraw Figure 2.9 in its conceptually equivalent form shown in Figure 2.20.

- Here, a single pair of time synchronous dither switches is used to achieve the alternation between early and late codes at input phase detector, and the post detection multiplication by the square wave $q(t)$.

- Salient feature of DDL is that it uses two sets of time synchronous dither switches, that time share two square law envelope detectors alternately between the two correlators. See Figure 2.21.

- For implementation, the 2 switched post-multipliers and summer can be replaced by a single switched differencer. See Figure 2.22.

- An equivalent loop model for Figure 2.21 which is good for analysis (analogous to Figure

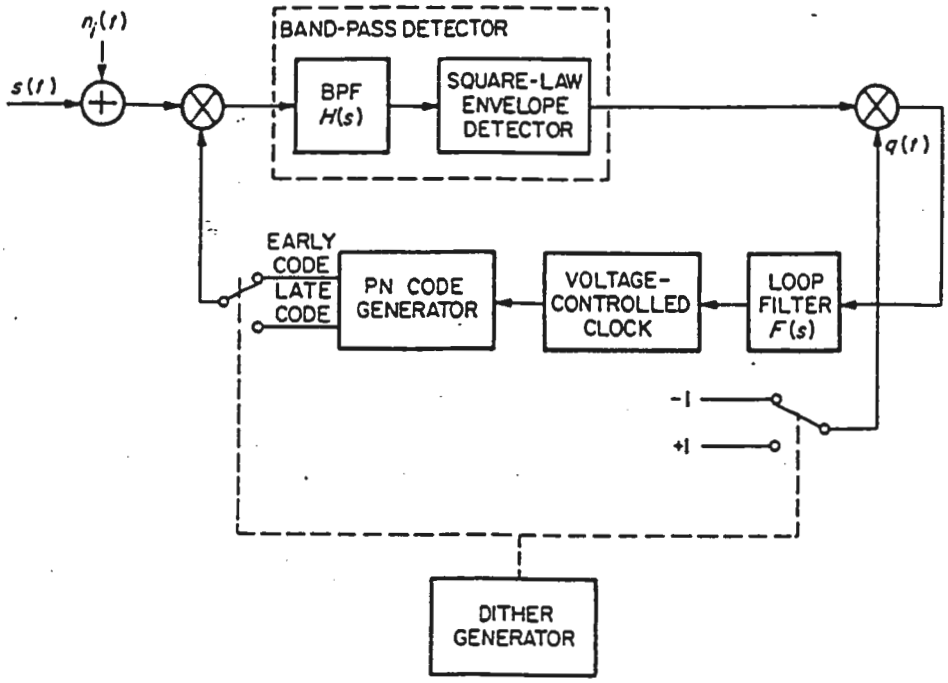

Figure 2.20. A conceptually equivalent version of Figure 2.9.

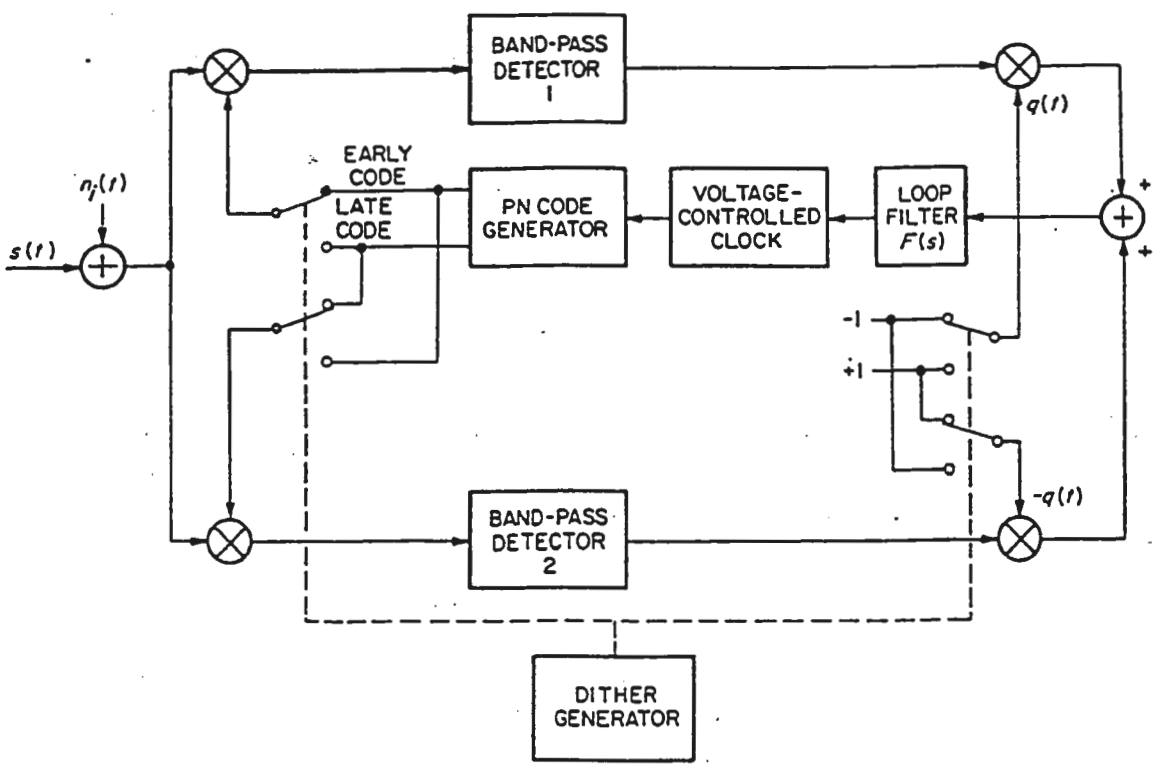

Figure 2.21. A non-coherent double dither loop.

2.10) is shown in Figure 2.23.

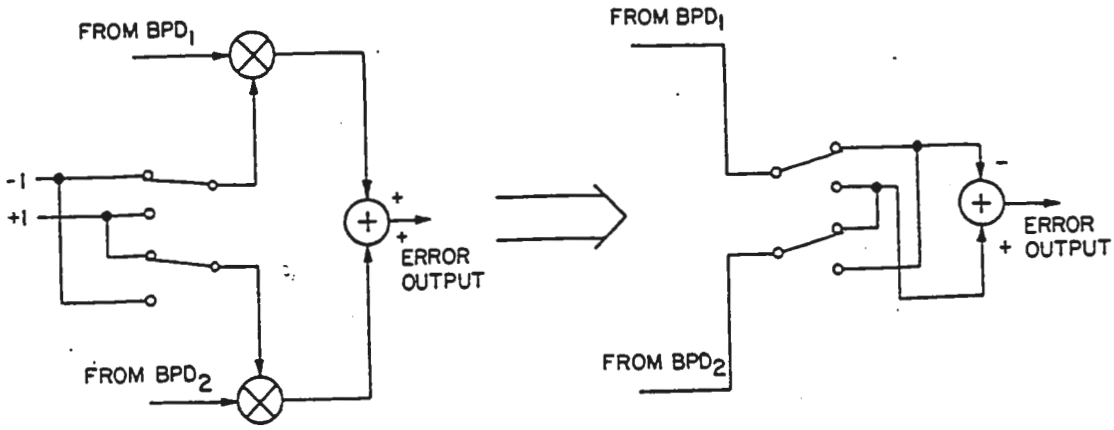

Figure 2.22. A simplification of the implementation in Figure 2.21.

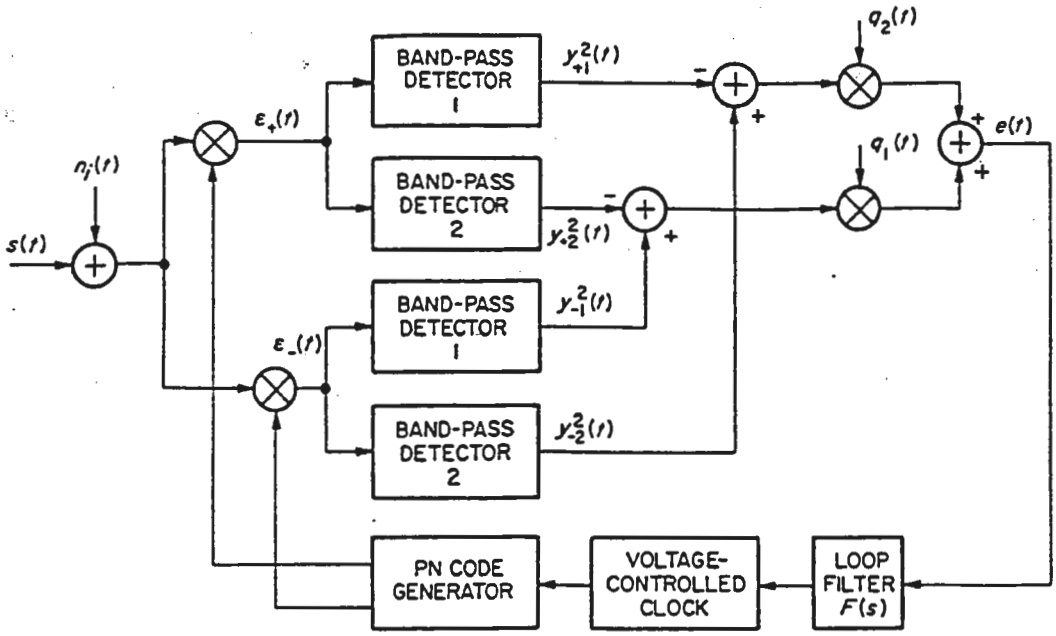

Figure 2.23. An equivalent loop model for the double dither loop.

- Input to loop filter is

$$\begin{aligned} e(t) &= \left[y^2_{-1}(t) - y^2_{+2}(t)\right] q_1(t) + \left[y^2_{-2}(t) - y^2_{+1}(t)\right] q_2(t) \\ &= y^2_{-1}(t)q_1(t) - y^2_{+1}(t)q_2(t) \\ &\quad - \left[y^2_{+2}(t)q_1(t) - y^2_{-2}(t)q_2(t)\right] \end{aligned} \tag{2.86}$$

- If both bandpass detectors of the DDL are identical, then in Figure 2.23

$$y_{+1}(t) = y_{+2}(t) = y_+(t)$$

$$y_{-1}(t) = y_{-2}(t) = y_-(t)$$

and (2.86) reduces to

$$e(t) = y^2_{-1}(t) - y^2_{+1}(t) \tag{2.87}$$

- (Again $q_1(t) + q_2(t) = 1$)

- Note: (2.87) is identical to (2.7) and hence under ideal balanced conditions DDL has the same performance as the DLL.

- This conclusion is also obtained from Figure 2.21. While the TDL of Figure 2.9 time shares the early and late PN codes over a single channel, the DDL allows both the early and late codes to be present for correlation in each half dither interval.

- The DDL error signal can be thought of as being generated by alternately switching between two DLL's (which differ only in that the bandpass detectors in the 2 channels of one loop are in the reverse position in the other loop.)

- If both channels of each loop contain identical bandpass detectors, then the reversal produces no change and the effective alternate switching between the two error signals has no effect.

- However, if the bandpass detectors of DDL are not identical, then the effective switching between the two hypothetical DLL's causes the DC offsets to cancel in the time averaged error signal.

- Also, the error signal will have a gain proportional to the average of the 2 channel gains of the DDL.

6. Product of Sum and Difference DLL

- This loop also purports to combat gain imbalance problem of DLL without sacrificing tracking performance.

- This is accomplished by replacement of the "difference of squares" operation of DLL with a "sum and difference product."

- The DLL computes as its error signal

$$\begin{aligned} e(t) &= \left[K_{m_-} H(t) * \epsilon'_-(t)\right]^2 - \left[K_{m_+} H(t) * \epsilon'_+(t)\right]^2 \\ &= K_{m_-}^2 y_-'^2(t) - K_{m_+}^2 y_+'^2(t) \end{aligned} \tag{2.88}$$

Here $\epsilon'_\pm(t)$ and $y'_\pm(t)$ are normalized versions of their counterpart definitions in (2.3) and (2.5).

- For example

$$\epsilon'_{\pm}(t) \triangleq x(t)\, c(t - \hat{\tau}_t \pm \delta) = \epsilon_{\pm}(t)/K_m \tag{2.89}$$

- On the other hand, the ΣΔ DLL shown in Figure 2.24 computes its error signal as

$$\begin{aligned} e(t) &= \left[K_{m_+} H(t) * \left\{\epsilon'_-(t) + \epsilon'_+(t)\right\}\right]\left[K_{m_-} H(t) * \left\{\epsilon'_-(t) - \epsilon'_+(t)\right\}\right] \\ &= K_{m_+} K_{m_-} \left(y'_-(t) + y'_+(t)\right)\left(y'_-(t) - y'_+(t)\right) \\ &= K_{m_+} K_{m_-} \left(y'^2_- - y'^2_+(t)\right) \end{aligned} \tag{2.90}$$

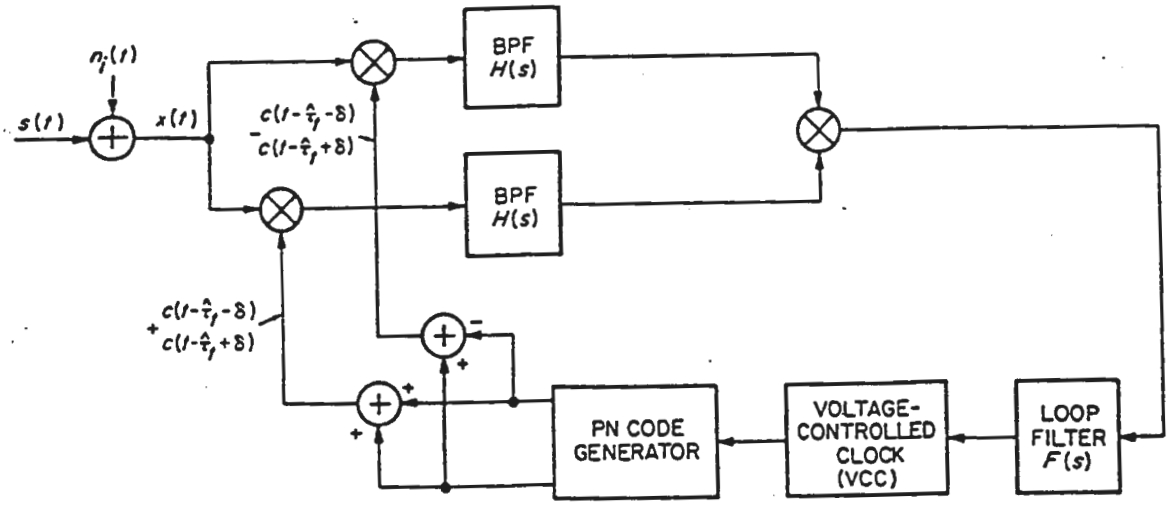

Figure 2.24. A non-coherent ΣΔ DLL.

- From (2.88), any unbalance in the arms gains ($K_{m_-} \neq K_{m_+}$) will produce undesirable loop DC offset, whereas (2.90) is insensitive to this effect.

- If $K_{m_-} = K_{m_+}$, the two loops will have identical performance.

7. The Modified Code Tracking Loop (MCTL)

- Another loop that attempts to combat gain imbalance problem of DLL without sacrificing tracking performance, but which has also hardware simplicity rivaling TDL, is the MCTL.

- MCTL is shown in Figure 2.25.

- Main idea is to replace sum channel signal of the ΣΔ DLL with a reference signal derived from the on-time PN code.

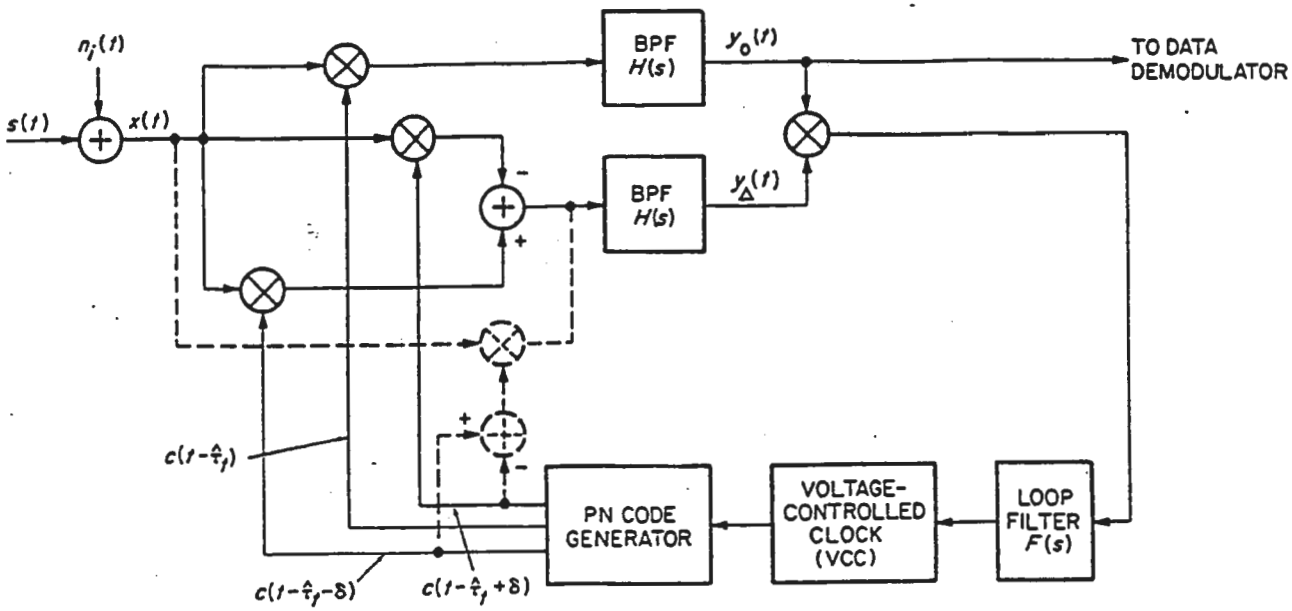

Figure 2.25. The modified code tracking loop (MCTL).

- Hence, an entire processing channel is eliminated.

- Second advantage is that the on-time channel experiences less noise power than the sum channel of Figure 2.24. Hence, it should serve as a better demodulation reference for the difference channel signal.

- As a result, the mean-squared tracking jitter of Figure 2.25 is smaller than that of DLL of Figure 2.1 or of the $\Sigma\Delta$ DLL of Figure 2.24.

- The implementation of Figure 2.25 can be reconfigured to closely resemble Figure 2.24 and thereby achieve a further reduction in hardware.

- The difference channel signal can be generated as per the dashed lines of Figure 2.25, eliminating one mixer.

- Note: in this alternate mechanization, the reference signal formed from the difference of the early and late PN codes is not a constant envelope waveform. This places linearity requirements on the single remaining mixer.

- This constraint also applies to $\Sigma\Delta$ DLL of Figure 2.24 which could also be implemented (analogous to Figure 2.25) by forming sum and difference signals after the input mixers.

- The loop model and performance is analogous to DLL. To highlight the similarities, we use the same equation numbers as for the DLL (with a prime superscript).

- Assuming an input as in (2.1) and (2.2) and making similar assumptions leading up to (2.7), the input to the loop filter of the MCTL is (for a one delta loop, N=2):

$$e(t) = y_o(t)y_\Delta(t) = SK_m^2\hat{m}^2(t-\tau_t)\tilde{D}(\epsilon_t) + K_m^2\tilde{n}_e(t,\epsilon_t) \tag{2.7'}$$

(where)

$$\tilde{D}(\epsilon_t) \triangleq R_{PN}(\epsilon_t)\left\{R_{PN\_}(\epsilon_t) - R_{PN_+}(\epsilon_t)\right\} = \begin{cases} 0 & ;\ \epsilon_t \le -1 \\ -\frac{3}{2} - \frac{5}{2}\epsilon_t - \epsilon_t^2 & ;\ -1 < \epsilon_t \le -\frac{1}{2} \\ 2\epsilon_t + 2\epsilon_t^2 & ;\ -\frac{1}{2} < \epsilon_t \le 0 \\ 2\epsilon_t - 2\epsilon_t^2 & ;\ 0 < \epsilon_t \le \frac{1}{2} \\ \frac{3}{2} - \frac{5}{2}\epsilon_t + \epsilon_t^2 & ;\ \frac{1}{2} < \epsilon_t \le 1 \\ 0 & ;\ \epsilon_t > 1 \end{cases} \tag{2.8'}$$

$$\tilde{D}(\epsilon_t) = \tilde{D}(\epsilon_t + np) \quad ; \quad n = \pm 1,\ \pm 2,\ \pm 3,\ \ldots \tag{2.8'}$$

- Here $\tilde{D}(\epsilon_t)$ is the loop discriminator characteristic and $\tilde{n}_e(t,\epsilon_t)$ is the equivalent additive noise.

$$\begin{aligned} \tilde{n}_e(t,\epsilon_t) = {} & \hat{N}_{c_o}(t)\hat{N}_{c_\Delta}(t) + \hat{N}_{s_o}(t)\hat{N}_{s_\Delta}(t) \\ & + \sqrt{S}\,\hat{m}(t-\tau_t)\Big\{R_{PN}(\epsilon_t)\hat{N}_{c_\Delta}(t) \\ & + \left[R_{PN\_}(\epsilon_t) - R_{PN_+}(\epsilon_t)\right]\hat{N}_{c_o}(t)\Big\} \end{aligned} \tag{2.9'}$$

with

$$\begin{aligned} \hat{N}_{c_o}(t) &= H_l(t) * [c(t-\hat{\tau}_t)N_c(t)] \\ \hat{N}_{s_o}(t) &= H_l(t) * [c(t-\hat{\tau}_t)N_s(t)] \\ \hat{N}_{c_\Delta}(t) &= H_l(t) * [\{c(t-\hat{\tau}_t+\delta) - c(t-\hat{\tau}_t-\delta)\}\,N_c(t)] \\ \hat{N}_{s_\Delta}(t) &= H_l(t) * [\{c(t-\hat{\tau}_t+\delta) - c(t-\hat{\tau}_t-\delta)\}\,N_s(t)] \end{aligned} \tag{2.6'}$$

- Figure 2.26 gives comparative illustration of the discriminator characteristics of the DLL and MCTL.

- Note: the non zero region of MCTL is only 2/3 that of the DLL. The modified loop has a 1/3 less pull in capability.

: although both discriminators have identical slopes at $\epsilon_t = 0$, the DLL always creates a larger error voltage for any value of timing error.

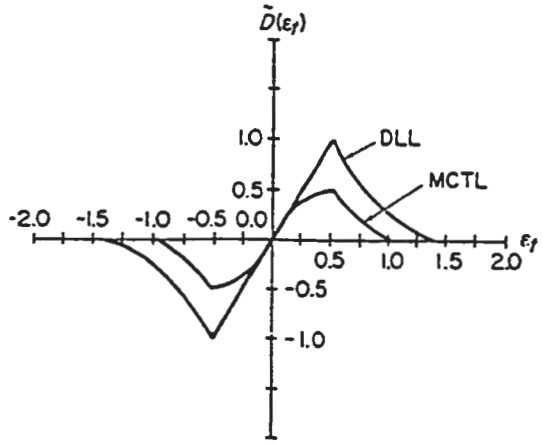

Figure 2.26. One-delta loop discriminator characteristics for the DLL and MCTL (reprinted from [11]).

despite these disadvantages, the MCTL does have improved noise performance. Specifically, the equivalent noise spectral density $\tilde{N}_e(\epsilon_t)$ of $\tilde{n}_e(t, \epsilon_t)$ is given by

$$\tilde{N}_e(\epsilon_t) = 2SN_o \left[M_4 \left\{ R_{PN}^2(\epsilon_t) + \tfrac{1}{2} \left[R_{PN_+}(\epsilon_t) - R_{PN_-}(\epsilon_t) \right]^2 \right\} + \frac{K_L}{\rho_H} \right] \quad (2.22')$$

with K_L and M_4 defined in (2.23), and ρ_H in (2.25).

- Following steps similar to those leading to (2.29), we find the normalized mean-squared timing error for MCTL is

$$\tilde{\sigma}_\epsilon^2 = \frac{1}{2\rho \tilde{S}_L} \quad (2.29')$$

where the squaring loss $\tilde{S}_L$ is:

$$\tilde{S}_L = \frac{M_2^2}{M_4 + K_L \frac{B_H/R_s}{E_s/N_o}} \quad (2.30')$$

- Comparing (2.30′) with (2.30) for $N = 2$, we find that the N × N power of the MCTL is one half that of the DLL.

- This produces an associated reduction in mean-squared tracking jitter.

- To see the magnitude of this reduction, we numerically compare the minimum squaring loss of (2.30) with that of (2.30′).

- This is shown in Figure 2.27 for NRZ data and a 2 pole Butterworth BPF; and in Figure 2.28 for Manchester data and a 2 pole Butterworth BPF. The appropriate expressions for K_L, M_2 and M_4 are obtained from Tables 2.1 and 2.2.

- The appropriate expressions for K_L, M_2 and M_4 are obtained from Tables 2.1 and 2.2.

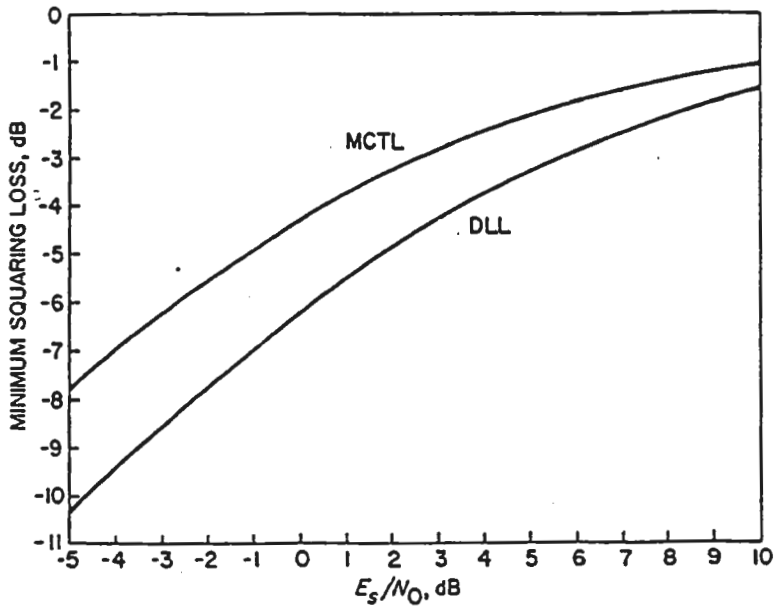

Figure 2.27. Minimum squaring loss comparison for NRZ data modulation (reprinted from [11]).

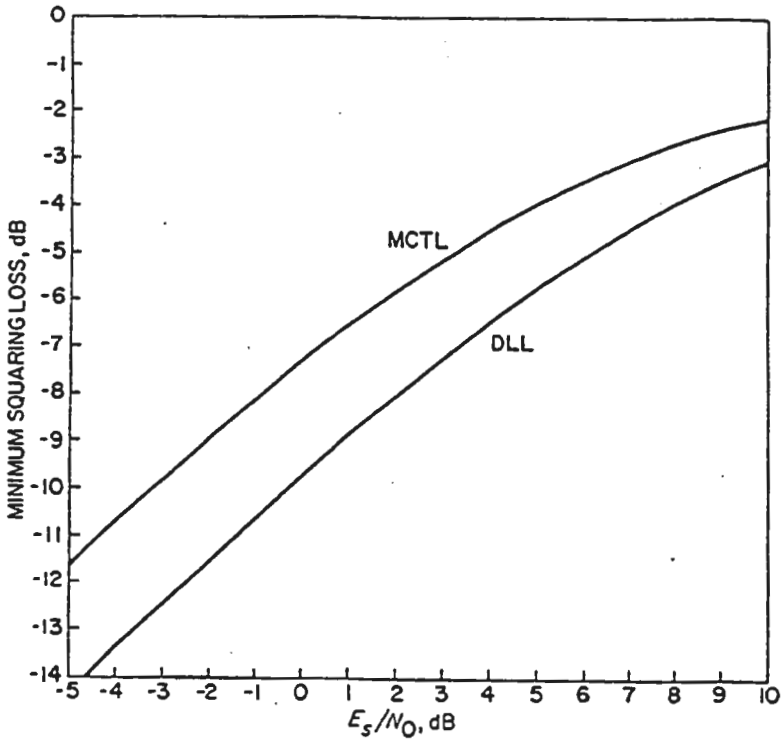

Figure 2.28. Minimum squaring loss comparison for Manchester data modulation (reprinted from [11]).

- Regarding acquisition behaviour of MCTL, it has been shown that for equal RMS

tracking jitter $\sigma_{MCTL} = \sigma_{DLL}$), the max normalized search rate is

$$\dot{y} = 0.6 \frac{S_L\Big|_{MCLT}}{S_L\Big|_{DLL}} = 0.6 \frac{M_4 + K_L \frac{2B_H/R_s}{E_s/N_o}}{M_4 + K_L \frac{B_H/R_s}{E_s/N_o}} \tag{2.91}$$

- This is compared with $\dot{y} = 1$ for the "one delta" DLL.

- Figure 2.29 gives $\dot{y}$ as function of E_s/N_o for NRZ and Manchester data, and 2 pole Butterworth BPF's.

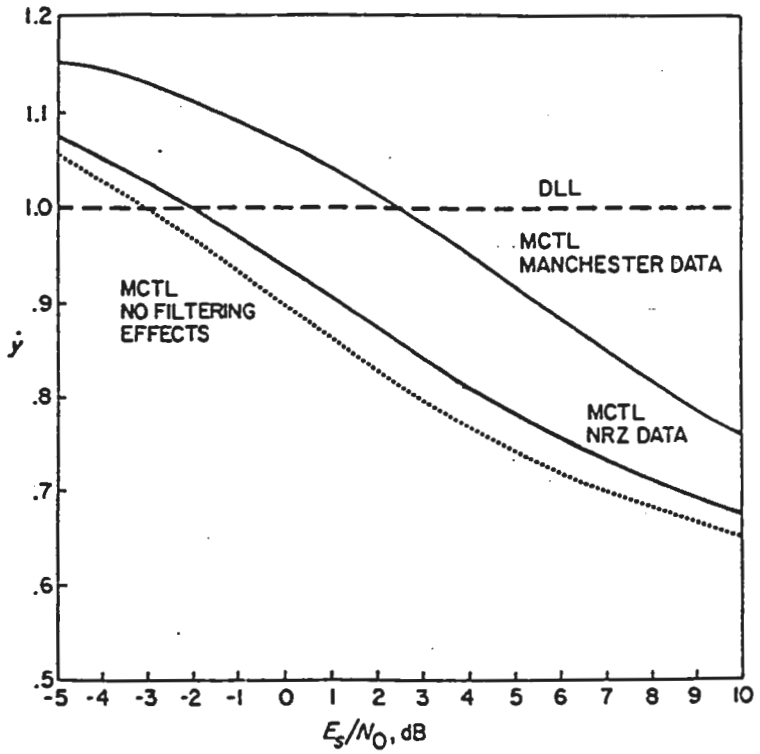

Figure 2.29. Normalized search rate comparison (reprinted from [11]).

- Also shown is curve corresponding to ignoring the arm filter band limiting effects (i.e., $M_2 = M_4 = K_L = 1$, and $B_H = R_s$).

- We see that for small E_s/N_o, the MCTL has a higher search rate capability than the DLL.

- For large E_s/N_o, it asymptotically approaches a max decrease of 40% in search rate capability.

- When compared with the $\Sigma\Delta$ DLL, the MCTL is significantly less sensitive to gain imbalances at low values of predetection signal to noise ratio, ρ_H, resulting in lower tracking bias errors.

- At high ρ_H values, the gain imbalance sensitivities of $\Sigma\Delta$ DLL and MCTL are nearly equivalent (both being much less sensitive than the DLL).

8. The Complex Sums Loop (Phase Sensing DLL)

- This is the least conventional loop discussed so far.

- It requires a spread spectrum signal where the PN code is phase modulated on the transmitted carrier rather than the usual amplitude modulation.

- The complex sums loop is the phase modulation analog of the amplitude sensing $\Sigma\Delta$ DLL.

- The input signal plus noise is correlated with the sum and difference of quadrature carriers, phase modulated respectively by the advanced and retarded versions of the locally generated PN code. See Figure 2.30.

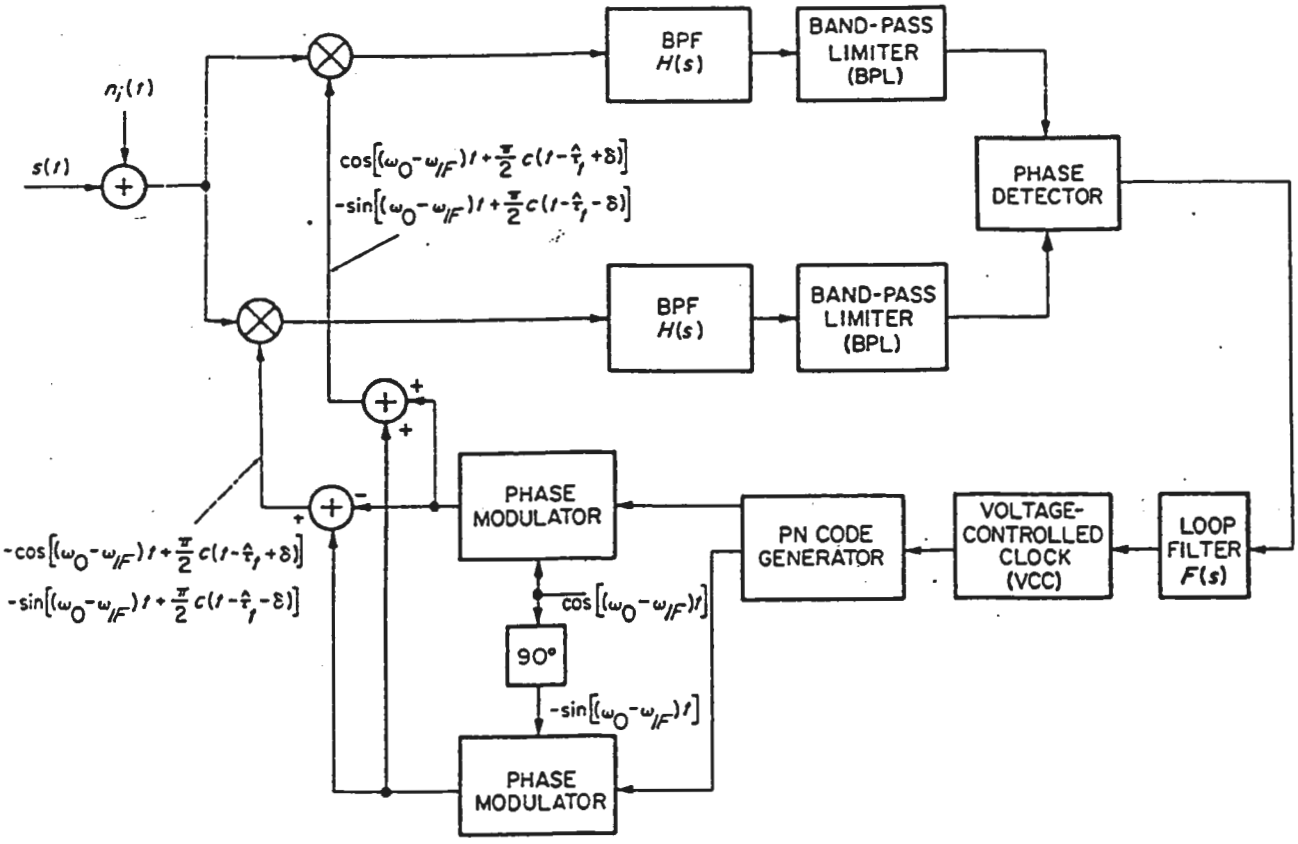

Figure 2.30. The complex sums PN tracking loop.

- The resultant correlations are BPFed and then BPLed (band pass limited) to remove

the AM.

- The relative phase between the two BPL outputs represents a measure of PN code delay error.

- The complex sums loop offers theoretically a factor of 4 improvement in RMS tracking error, and a factor of 2.67 improvement in max search velocity when compared with amplitude sensing correlation receivers such as DLL.

- However, virtually all DS/SS systems in use employ an amplitude modulated PN code. Hence, complex sums loop is not widely employed.

9. Quadriphase PN Tracking

- We have assumed up to now that the PN code is superimposed on a suppressed carrier binary data modulation.

- We will now investigate applicability of previous PN tracking techniques to various forms of quadriphase PN modulation (QPN).

A - Simplest form of QPN is obtained by spreading a quadriphase shift keyed (QPSK) modulation with a single PN code.

- The transmission delayed signal is

$$s(t) = \sqrt{S}\, c(t-\tau_t)\Big\{ m_1(t-\tau_t)\sin\left[\omega_o t + \theta(t)\right] + m_2(t-\tau_t)\cos\left[\omega_o t + \theta(t)\right] \Big\} \tag{2.92}$$

where $m_1(t)$ and $m_2(t)$ are unit power, statistically independent binary data modulations of the same data rate.

- If the DLL of Figure 2.1 is used to PN track the sum of $s(t)$ and $n_i(t)$ (given by equation (2.2)), then analogous to equation (2.7), the error signal $e(t)$ is:

$$e(t) = \frac{1}{2} S K_m^2 \left[\hat{m}_1^2(t-\tau_t) + \hat{m}_2^2(t-\tau_t)\right] D(\epsilon_t) + K_m^2 n_e(t,\epsilon_t) \tag{2.93}$$

where

$$\begin{aligned} n_e(t,\epsilon_t) = {} & \hat{N}_{c\_}^2(t) - \hat{N}_{c+}^2(t) + \hat{N}_{s\_}^2(t) - \hat{N}_{s+}^2(t) \\ & + \sqrt{2S}\,\hat{m}_2(t-\tau_t)\left\{R_{PN\_}(\epsilon_t)\hat{N}_{c\_}(t) - R_{PN+}(\epsilon_t)\hat{N}_{c+}(t)\right\} \\ & - \sqrt{2S}\,\hat{m}_1(t-\tau_t)\left\{R_{PN\_}(\epsilon_t)\hat{N}_{s\_}(t) - R_{PN+}(\epsilon_t)\hat{N}_{s+}(t)\right\} \end{aligned} \tag{2.94}$$

- Now, since

$$< \overline{\hat{m}_1^2(t-\tau_t)} > = < \overline{\hat{m}_2^2(t-\tau_t)} > = M_2 \tag{2.95}$$

where M_2 is defined in (2.14).

- And since $m_1(t)$ and $m_2(t)$ are independent, the auto correlation function of (2.94) is given by (2.18).

- Hence, the equation of operation remains unchanged from (2.15).

- Therefore, the tracking and acquisition performance of the DLL with a QPN input is identical to that with a biphase PN input.

- Another form of QPN is obtained by spreading inphase and quadrature biphase modulated carriers with independent PN codes.

- This is typically used where separate addressing of each channel is required, such as for a multiple access type system.

- Here, the received signal is

$$\begin{aligned} s(t) = &\sqrt{S}\, c_1(t-\tau_t) m_1(t-\tau_t) \sin[\omega_o t + \theta(t)] \\ &+ \sqrt{S}\, c_2(t-\tau_t-\tau_\Delta) m_2(t-\tau_t) \cos[\omega_o t + \theta(t)] \end{aligned} \tag{2.96}$$

- If the two codes have identical chip rates, they are often staggered by half a chip (ie: $\tau_\Delta = T_c/2$).

- This is referred to as staggered quadriphase PN (SQPN) and is used on nonlinear satellite channels to reduce regeneration of sidelobes (removes by transmitter filtering prior to transmission).

- Also, from an implementation standpoint $c_2(t)$ is often a time shifted version of $c_1(t)$ where the time shift is a large number of code chips.

- Again consider using a DLL (figure 2.1) to PN track the sum of $S(t)$ and $n_i(t)$ (equation (2.2)).

- If the PN generator of the DLL is selected to match $c_1(t)$, then by the assumption of code independence

$$\overline{c_2(t-\tau_t-\tau_\Delta) c_1(t-\hat{\tau}_t \pm \delta)} = 0 \tag{2.97}$$

- Again assuming the inphase and quadrature self noise processes can be neglected, we get a loop error signal identical to (2.7), except that S is replaced by $\frac{S}{2}$ in its signal and noise components.

- Hence, the DLL tracks the channel corresponding to $c_1(t-\tau_t)$ (which contains half the total power) as if the other channel were absent.

- Therefore, a 3 dB penalty in SNR is paid relative to that for a PN spread binary data modulation.

- This 3 dB penalty does not translate directly into a 3 dB increase in mean squared tracking jitter due to the nonlinear dependence of the loop squaring loss on S/N_o (see (2.29) and (2.30).

- Once having proper code alignment for $c_1(t-\tau_t)$, the despreading code for $c_2(t-\tau_t-\tau_\Delta)$ can be derived by an appropriate shift of the local PN generator (provided the two codes are generated as delayed versions of each other).

- If the two codes are totally unrelated (generated by separate PN generators having different tap connections and code periods), then 2 separate DLL must be used, each having a local PN generator matched to one of the codes.

- If the 2 codes have different chip rates in addition to different code structures, separate DLL's must be employed where the loops have different PN generators and different VCC's. Quadriphase PN can also be applied to unbalanced QPSK.

Here,

$$\begin{aligned} s(t) = &\sqrt{2S_1}\, c_1(t-\tau_t)m_1(t-\tau_t)\sin[\omega_o t+\theta(t)] \\ &+\sqrt{2S_2}\, c_2(t-\tau_t-\tau_\Delta)m_2(t-\tau_t)\cos[\omega_o t+\theta(t)] \end{aligned} \tag{2.98}$$

- Here S_1, the power in channel 1 is unequal to S_2, the power in channel 2.

- Also, $1/T_2$, the data rate in channel 1 is not restricted to equal $1/T_2$, the data rate in channel 2.

- Examples of such PN spread signals include many of the transmission modes of TDRSS (Tracking and Data Relay Satellite System).

10. Further Discussion

- We will summarize some recent contributions to PN tracking.

- One idea for improvement in PN tracking loop performance, the improved DLL (IDLL) has an effective increased number of correlators. This allows one to shape the discrimina-

tor characteristic so as to expand the correlation range without affecting its lock range.

- This concept is applicable for both noncoherent DLL and coherent DLL.

- As an example, consider the noncoherent DLL in Figure 2.31 which for $N = 2$ is a slight modification of the loop in Figure 2.1.

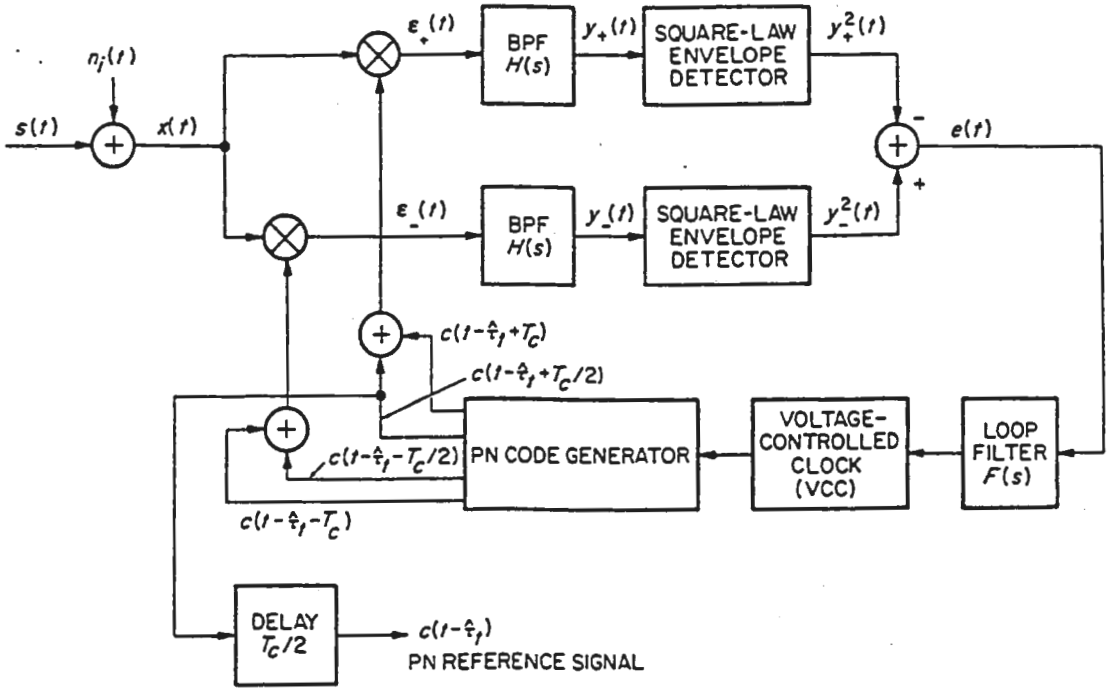

Figure 2.31. A non-coherent improved delay-locked loop (IDLL).

- Here, we have the effective addition of two correlations of the input signal with two new phase shifted PN reference signals which are advanced and retarded by 3/2 chips relative to the on-time PN reference.

- Although conceptually four correlations are being formed, the two delayed and two advanced signals are first summed so that for implementation only two correlators are needed.

- Figure 2.32 shows the component and resultant advanced and delayed correlation functions (analogous to Figure 2.2).

- Figure 2.33 gives the corresponding discriminator characteristic (analogous to Figure 2.3).

- Note that the lock range of the loop ($\pm T_c/2$) and its gain (positive slope of the discriminator) are unaffected by the modification, whereas the correlation range has been

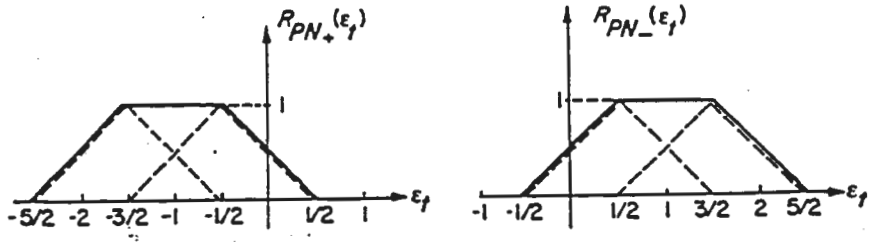

Figure 2.32. Autocorrelation functions of the advanced and retarded correlator outputs for a non-coherent IDLL.

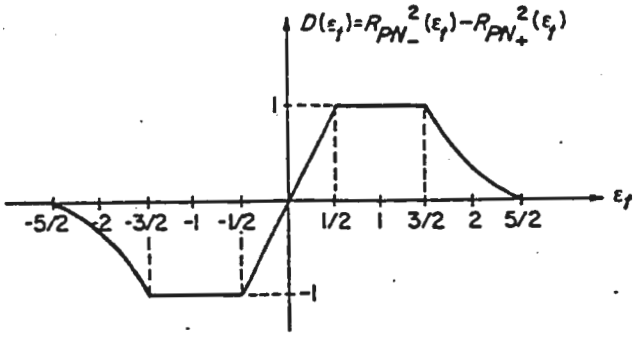

Figure 2.33. Discriminator characteristic.

extended from $\pm 3T_c/2$ to $\pm 5T_c/2$.

- The addition of more correlations with more phase shifted PN refence signals can increase the correlation region further.

- All previous discussion has assumed a transmission channel devoid of propagation disturbances.

a - Bogush et al have considered effect of frequency-selective fading (scintillation) such as produced by the ionosphere (where the coherence bandwidth is less than the signaling bandwidth) on the PN code correlation and tracking.

b - They considered both coherent and noncoherent DLL's and TDL's.

c - Several loop configurations were investigated having different bandwidths and order of tracking loop.

d - Also, the possibility of having the PN tracking loop Doppler aided from the carrier tracking loop was investigated. This involved using the Doppler estimate formed in the carrier tracking loop, appropriately scaled by the ratio of PN code chip rate to carrier frequency, to rate-aid the PN tracking loop.

e - Another configuration investigated was that of time sharing the single code loop for

PN receivers that are required to simultaneously track signals from several satellites.

- The following conclusions concerning the above configurations were reached:

1. A noncoherent code loop is less susceptible to losing lock than the equivalent coherent one, since the noncoherent loop does not depend on carrier phase lock which is difficult to maintain in scintillation conditions.
2. A dedicated (non time shared) loop is more robust than a time shared loop, since the former samples the code correlator output more frequently and thus does not suffer a loss of effective signal level produced by the reduced measurement rate of a time shared loop.

C - Finally, Meyr has applied theory of renewal (regenerative) Markov processes to nonlinear analysis of correlative tracking systems.

- This method is applicable to systems with periodic nonlinearities (PLL's) as well as non periodic nonlinearities (DLL's).

- The method allows characterization of cycle slipping for the former (PLL's) and of loss of lock for the latter.

- The " periodic extension solution" which is traditionally applied to such situations is shown to be identical to the "renewal process solution" only for first order loops.

- Significantly, the self noise (intrinsic noise) in the DLL, which is always present in the loop and which depends on the loop tracking error, is accounted for in the "renewal process solution."

- This intrinsic noise is dominant in many applications and cannot be neglected.

- The method has been developed for both coherent DLL and noncoherent DLL's.

Reference: Spread Spectrum Communications, Volume III, Chapter 3, by Marvin K. Simon, Jim K. Omura, Robert A. Scholtz, Barry K. Levitt, Computer Science Press, 1985, ISBN 0-88175-015-8 (Vol III) or 0-88175-017-4 (Set) TK5102.5.S6662.